CARBON DIOXIDE REMOVAL FROM COAL POWER PLANTS – A REVIEW OF CURRENT CAPTURE TECHNIQUES AND AN INVESTIGATION OF CARBON DIOXIDE ABSORPTION USING HYBRID SOLVENTS

Doctoral Thesis

By

Khalid Osman

MSc. Eng. (Chemical)

University of KwaZulu Natal, South Africa

Submitted in fulfilment of the academic requirements for the degree of Doctor of Philosophy in the School of Engineering, Discipline of Chemical Engineering, University of KwaZulu-Natal, Durban.

January 2014

Supervisor: Prof. D. Ramjugernath

Co-Supervisor: Prof. C. Coquelet

COLLEGE OF AGRICULTURE, ENGINEERING AND SCIENCE

DECLARATION 1 - PLAGIARISM

I, ……Khalid Osman…….……., declare that

1. The research reported in this thesis, except where otherwise indicated, is my original research.
2. This thesis has not been submitted for any degree or examination at any other university.
3. This thesis does not contain other persons' data, pictures, graphs or other information, unless specifically acknowledged as being sourced from other persons.
4. This thesis does not contain other persons' writing, unless specifically acknowledged as being sourced from other researchers. Where other written sources have been quoted, then:
   i. Their words have been re-written but the general information attributed to them has been referenced
   ii. Where their exact words have been used, then their writing has been placed in italics and inside quotation marks, and referenced.
5. This thesis does not contain text, graphics or tables copied and pasted from the Internet, unless specifically acknowledged, and the source being detailed in the thesis and in the References sections.

……

Khalid Osman

As the candidate's Supervisor I agree/do not agree to the submission of this thesis

……. …….

Prof. D. Ramjugernath Prof. C. Coquelet

January 2014

COLLEGE OF AGRICULTURE, ENGINEERING AND SCIENCE

DETAILS OF CONTRIBUTION TO PUBLICATIONS that form part and/or include research presented in this thesis (include publications in preparation, submitted, *in press* and published and give details of the contributions of each author to the experimental work and writing of each publication)

Publication 1
Title: "Review of Carbon Dioxide Capture and Storage With Relevance to the South African Power Sector"
Accepted for publication in the South African Journal of Science. Currently in press.
Authors: Khalid Osman (Research on all aspects of the manuscript and main write-Up, formatting and editing)
Deresh Ramjugernath (Formatting and editing)
Christophe Coquelet (Research on cryogenic separation, CO_2 properties, formatting and editing)

Publication 2
Title: "Absorption of CO_2 and O_2 in Methyl Trioctyl Ammonium Bis (trifluoromethylsulfonyl) imide, 1-Butyl-3-Methyl Imidazolium Bis (trifluoromethylsulfonyl) imide, and 1-Butyl-3-Methyl Imidazolium Methyl Sulphate"
Submitted to Journal of Physical Chemistry B and under review.
Authors: Indra Bahadur (Providing of ionic liquids, formatting and editing, construction of molecular diagrams)
Khalid Osman (All experimental measurements and modelling of data, main write-up, formatting and editing)
Deresh Ramjugernath (Formatting and editing)
Christophe Coquelet (Formatting and editing)

Other publications

Signed:

……
Mr. Khalid Osman

…… ……
Prof. Deresh Ramjugernath Prof. Christophe Coquelet

ACKNOWLEDGEMENTS

The following deserve acknowledgement for their continued contribution, directly or indirectly, to this project:

i. Professor D. Ramjugernath of the University of KwaZulu Natal, South Africa, and Prof. C. Coquelet of Mines-Paristech, Fontainebleau, France, for their supervision, continued guidance and support.
ii. The University of KwaZulu Natal, Centre for Engineering Postgraduate Studies (CEPS) for financial assistance.
iii. Eskom Ltd. for financial assistance.
iv. Prof. N. Ijumba of the University of KwaZulu Natal for securing of financial assistance.
v. Dr P. Naidoo of the University of KwaZulu Natal for securing financial assistance.
vi. The laboratory staff of the Thermodynamics Research Unit, University of KwaZulu Natal, for their technical assistance in the experimental aspects of this work. This includes Mr. P. Ngema, Mr. A. Khanyile, Mr. L. Mkize and Mr. L. Augustine.
vii. Dr T. Surridge of the South African National Energy Research Institute (SANERI) for providing of information pertaining to carbon capture and storage in South Africa.
viii. Mr. H. Ibrahim of the School of Chemistry, University of KwaZulu Natal, for providing of information regarding ionic liquid synthesis.
ix. Mr. P. Paelink of Alstom Ltd., for providing information regarding pilot plant absorption processes.
x. Mr. D. Goodier of Hiden Analytical Ltd. for assistance in setting up of Intelligent Gravimetric Analyser (IGA) apparatus.
xi. Mr. K. Wickee of Shimadzu Ltd. for assistance in the setup of the FTIR Probe apparatus.
xii. Dr D. Kock of NECSA Ltd. for advice on the setup of the FTIR Probe apparatus.
xiii. Dr I. Bahadur of the University of KwaZulu Natal for providing [MOA][Tf_2N] and [Bmim][$MeSO_4$] ionic liquids, and for collaborative research.
xiv. Dr J. Rarey for invaluable assistance in the handling of ionic liquids in Aspen regression and simulations.
xv. And importantly, my mum, Zubaida Bibi Osman, dad, Essa Osman, and grandfather, Osman Mohammed Essop, for their unyielding love, support, encouragement, motivation, and belief in me even in the most difficult of times in this work, and in my life.
xvi. Finally, my Lord, Creator and Sustainer, Allah (Almighty and Glorious is He) and His exalted messenger, Muhammed (Upon whom be peace), who have made my life and continued success a reality.

ABSTRACT

The aim of this project was to identify and assess all possible solutions to reduce carbon dioxide (CO_2) emissions from coal power plants in South Africa, identify the most likely solution to be implemented industrially in the short to mid-term future, and contribute towards its development through lab measurement and further research.

This thesis thus contains a substantial literature review conducted on the current state of CO_2 emissions in South Africa, conventional and novel coal power plant processes, modes of CO_2 capture, criteria regarding the implementation of CO_2 capture techniques, and the various CO_2 capture techniques currently investigated with varying levels of development.

The study found gas absorption using solvents to be the most likely mid-term CO_2 capture technique to reach industrial implementation. However, certain challenges still need to be overcome, particularly due to numerous limitations of current solvents, to make this technique feasible for CO_2 capture.

In an attempt to overcome the main challenge of solvent absorption capacity, it was decided to investigate the use of ionic liquids for CO_2 absorption. An in-depth review of ionic liquids was conducted, as well as a review of measurement techniques and modelling of gas absorption in alkanolamine and ionic liquid solvents.

Four ionic liquids, namely methyl trioctyl ammonium bis(trifluoromethylsulfonyl)imide [MOA][Tf_2N], 1-butyl-3-methyl imidazolium bis(trifluoromethylsulfonyl)imide [Bmim][Tf_2N], 1-butyl-3-methyl imidazolium tetrafluoroborate [Bmim][BF_4], and 1-butyl-3-methyl imidazolium methyl sulphate [Bmim][$MeSO_4$] were tested for CO_2 and O_2 absorption by measuring equilibrium Pressure-Temperature-Liquid mole fraction (P-T-x) data. Measurements were conducted using an Intelligent Gravimetric Analyser (IGA-01) at 303.15, 313.15, and 323.15 K. CO_2 partial pressures of 0.05 to 1.5 MPa and O_2 partial pressures of 0.05 to 0.7 MPa were investigated. Furthermore, density and refractive index measurements were conducted for all solvents. The ionic liquids were benchmarked against other ionic liquids and conventional alkanolamine solvents for CO_2 absorption capacity and selectivity.

The study found that ionic liquids achieved higher CO_2 absorption capacity at high pressure than conventional alkanolamine solvents, but very low absorption capacity at low pressure. Of the ionic liquids studied, [Bmim][BF_4] and [Bmim][Tf_2N] achieved high CO_2 absorption and high CO_2 selectivity over O_2. Therefore, these two ionic liquids were selected to be combined with conventional alkanolamine solvents, namely Monoethanolamine (MEA), Diethanolamine (DEA), and Methyl Diethanolamine (MDEA), in order to form hybrid solvents.

P-T-x data was obtained for CO_2 absorption in alkanolamine-ionic liquid hybrid solvents containing various compositions of the above alkanolamines and ionic liquids, by gravimetric analysis, under temperature and pressure conditions as described above. CO_2 absorption in the hybrid solvents was analysed, compared, and benchmarked against absorption in pure ionic liquids and conventional alkanolamine solvents.

Absorption data for pure ionic liquid systems was modelled using the Redlich-Kwong equation of state (RK-EOS), while absorption in hybrid solvents was modelled using the RK-EOS for the ionic liquid components and the Posey-Tapperson-Rochelle model for the alkanolamine components of each hybrid solvent. All modelling was programmed using Matlab^{TM} R2012B engineering programming software.

Further composition analysis was intended using Fourier transform infrared (FTIR) spectroscopy. The design and development of this apparatus is described herein. The apparatus possessed limitations in achieving the desired measurements. Recommendations are described for future modifications to make the apparatus more applicable for the systems in this work.

The most important conclusion was that the hybrid solvents successfully achieved higher equilibrium CO_2 absorption than conventional alkanolamine solvents and pure ionic liquids, at low pressure. Absorption increased with higher temperature, lower pressure, and alkanolamine concentrations lower than 40wt%. Modelling of CO_2 absorption in hybrid solvents using the above stated model proved inadequate, with deviations nearly as high as 10% of measured data.

A process of CO_2 capture was simulated using the engineering software Aspen Plus V8.0. CO_2 absorption in the hybrid solvent containing MEA:DEA:[Bmim][BF_4] at 31.8:12.1:56.1 wt% was benchmarked against CO_2 absorption in a conventional alkanolamine solvent. The simulation revealed a significant improvement in CO_2 absorption using the hybrid solvent at low system pressure. However CO_2 selectivity and solvent recycle heat duty results were undesirable.

Finally, recommendations are listed for future research endeavours, simulation and apparatus development.

TABLE OF CONTENTS

SECTION **PAGE**

CHAPTERS

SECTION **PAGE**

SECTION **PAGE**

SECTION **PAGE**

LIST OF FIGURES

FIGURE **PAGE**

Chapter 1

Chapter 2

Chapter 7

FIGURE **PAGE**

FIGURE **PAGE**

LIST OF TABLES

TABLE **PAGE**

TABLE **PAGE**

Appendix A

TABLE **PAGE**

NOMENCLATURE

Symbols	Definitions
	Terms
H	Henry's law constant (MPa)
P	Pressure (MPa)
T	Temperature (K)
R	gas constant ($J \cdot mol^{-1} \cdot K^{-1}$)
x	liquid mole fraction
f	fugacity of the solute in the mixture (1 indicates solvent)
$\bar{v}^{\infty}$	Partial molar volume at infinite dilution
P^{O}	Vapour Pressure (MPa)
h	Molar enthalpy ($kJ \cdot mol^{-1}$)
$\Delta \bar{h}$	Molar enthalpy of absorption ($kJ \cdot mol^{-1}$)
$\Delta \bar{S}$	Molar entropy of absorption ($J \cdot mol^{-1} \cdot K^{-1}$)
K	Equilibrium constant
L_T	gas loading (mol gas/mole solvent)
C^{O}	Concentration
W	Weight reading (mg)
g	Acceleration due to gravity (m/s^2)
m	Mass (g)
V	Volume (cm^3)
MM	Molar mass (g/mol)

Symbols	Greek Letters
ρ	Density (g/cm^3)
ρ_{CO2}	Density of CO_2 in cylinder (g/cm^3)

Symbols	Subscripts
i,j	Components/species
f	Fluid
1	Solvent
2	Solute
gas	Absorbed gas
solvent	Absorbing solvent
T	Temperature (K)
CO_2	Carbon dioxide
N_2	Nitrogen

C	Critical point
c	Counterweight
s	Dry sample
a, as	Absorbed gas
I	Balance components on the sample side
II	Balance components on the counterweight side
b	Boiling point
M	mixture

Symbols	**Superscripts**
G	Gas phase
L	Liquid phase
∞	infinite dilution
O	initial state

CHAPTER 1: INTRODUCTION

The amount of carbon dioxide (CO_2) emitted into the atmosphere by various industries is of great concern due to the global warming effects of CO_2, and industries worldwide are faced with increasing pressure by environmentalists, and the public at large, to reduce their emissions of the gas. In 2008, nearly 30000 mega tonnes (Mt) of CO_2 was emitted into the atmosphere (IEA, 2010). This is nearly a 100% increase since 1971. From 1750 to 2011, 365 Gt of CO_2 were emitted into the atmosphere by fossil fuel and cement industries (IPCC, 2013).The increasing worldwide demand for relatively cheap electricity and the advances in coal-to-liquids technology has resulted in 42.9% of CO_2 emissions stemming from coal industries, with oil and gas industries accounting for 36.8% and 19.9% of CO_2 emissions respectively (IEA, 2010).

High CO_2 emissions are of great concern due to the fact that CO_2 is a greenhouse gas. Greenhouse gases trap heat in the earth's atmosphere, resulting in an overall global surface temperature increase known as global warming. The CO_2 concentration in the atmosphere at the beginning of 2013 was 391 ppm (IPCC, 2013).

Climate change, including global warming and cooling, is an inevitable natural process that has occurred regardless of human activity. However, since the industrial revolution, fossil fuel usage and resultant industrial CO_2 emissions have collectively contributed towards an increased rate and extent of climate change. This poses a threat to many forms of life, including people, who may not be able to adapt towards the changes caused by rapid climate change.

An increased global temperature caused by climate change results in an increased rate of melting of ice at freshwater mountain sources, resulting in overflowing rivers that may have the potential to cause significant flooding. This would also result in the depletion of drinking water at the source in the future. The melting of polar ice caps, at a current rate of 275 Gt ice per year (IPCC, 2013), results in changes in ocean salinity which affects marine life, and rising sea levels of 3.2 mm/year (IPCC, 2013) which threaten low lying countries and coastal communities. These potentially devastating implications have resulted in much focus on reducing greenhouse gas emissions and hence preventing or at least lowering the rate of global temperature increase.

South Africa contains abundant coal reserves. It is estimated that 53% of coal mined in South Africa is used to generate electricity, while 36% of electricity produced worldwide stems from the burning of coal (Eskom, 2011). It has also been determined that 78 to 83% of CO_2 emissions stem from the burning of fossil fuels to generate electricity (Figueroa et al., 2008). While the

industry is beneficial in providing relatively cost effective electricity, substantial CO_2 emissions occur.

On the international scale, South Africa mines 224 million tonnes of coal annually and 25% is exported, making South Africa the third largest coal exporting country. It is estimated that South African coal reserves amount to 53 billion tonnes, enough to meet the country's electricity needs for nearly 200 years to come (Eskom, 2011).

The primary electricity utility in South Africa is Eskom Ltd.. While the company harnesses energy from a diverse range of sources, nearly 77% of its electricity production stems from the burning of coal at its 14 coal-fired power plants (Eskom, 2011). South Africa enjoys cost effective electricity due to its abundant coal reserves, but coal energy also results in the country emitting substantial amounts of CO_2.

Eskom's coal operations have made it the second highest CO_2-emitting company in the world after Huaneng Power International, a Chinese power company. Due to coal power, South Africa's power sector has become the ninth highest CO_2-emitting sector in the world. South Africa is also the highest CO_2 emitter in Africa (CARMA, 2010), with higher emissions than the next nine countries combined (CARMA, 2010). Refer to Table 1-1 for an indication of South Africa's power sector in comparison to other countries.

Table 1-1: The 10 largest CO_2 emitting power sectors in the world by country (CARMA, 2010)

Country		CO_2 emitted (Mega Tonnes)	Energy produced (GWh)	Fossil fuel power (%)	Hydroelectric power (%)	Nuclear power (%)	Other Renewable power (%)
1	China	3120	3260000	82.51	14.51	2.02	0.12
2	United States	2820	4190000	68.79	6.57	18.4	4.39
3	India	638	719000	76.3	16	2.41	1.6
4	Russia	478	896000	63.38	19.66	15.65	0.63
5	Germany	429	636000	62.11	3.05	24.36	7.46
6	Japan	414	1030000	33.23	7.57	27.74	2.75
7	United Kingdom	227	370000	71.35	1.33	20.34	5.28
8	Australia	224	228000	90.04	6.82	0	1.53
9	**South Africa**	**218**	**215000**	**93.38**	**0.42**	**5.68**	**0.2**
10	South Korea	192	392000	44.29	1.24	35.57	0.11

Seven of Eskom's power plants are among the top 30 CO_2-emitting power plants in the world. These include Kendal in Witbank (28-million tons), Majuba in Volksrust (26.5-million tons), Matimba in Ellisras (25.5-million tons), Lethabo in Viljoensdrift (23.3-million tons), Tutuka in Standerton (22.8-million tons), Duvha in Witbank (22.4-million tons), and Matla in Bethal (22.4-million tons) (CARMA, 2007). While CARMA (2010) contains relatively accurate estimates of CO_2 emissions in South Africa for the year 2010, the 2011 Annual Report of South Africa's primary electricity utility reported that 127.4 Mt of coal was burned in the past year, producing an estimated 230.3 Mt CO_2 (Eskom, 2011). South Africa's percentage of fossil fuel-derived power shown in Table 1-1 includes coal, gas, and minor oil operations.

In order to establish a global effort towards the research and reduction of CO_2 emissions, many governments are considering implementing CO_2 emissions taxes and South Africa is no exception. National Treasury (2010) reported that discussions have begun on the implementation of a CO_2 emissions tax. Current cost proposals range between R75-R200/tonne CO_2, with the most current figure settled on being R120/tonne CO_2 (National Treasury, 2013).

Considering the amount of CO_2 emitted through the use of coal power in South Africa, this would ultimately result in significant increases in electricity tariffs and the overall cost of living in South Africa. Eskom Ltd. would hence require feasible solutions to reduce its CO_2 emissions and maintain inexpensive electricity production. The overall aim is to produce inexpensive electricity in an environmentally friendly manner in an attempt to reduce the rate of climate change.

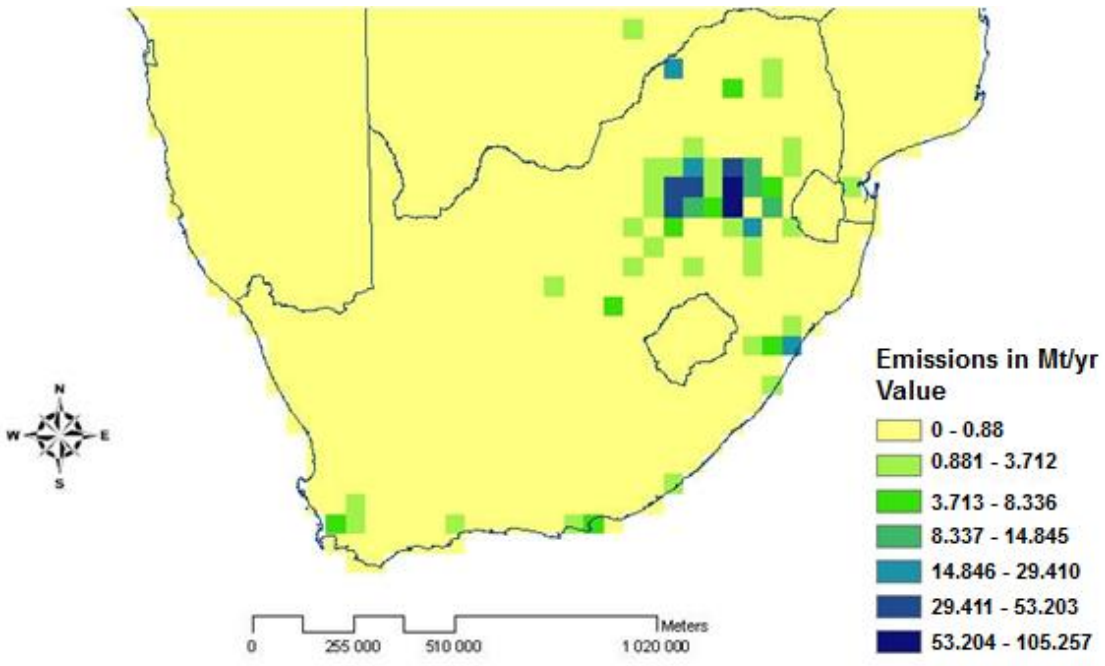

Figure 1-1: Main CO_2 Emission Point Sources in South Africa (edited from Surridge, 2005)

Refer to Figure 1-1. Most CO_2 emission sources in South Africa are situated in Mpumalanga, Gauteng and Free State regions. The map includes coal power plants, coal-to-liquids (CTL) industries, gas-to-liquids (GTL) industries, oil refining, and steel processes.

A promising mid-term solution to reducing CO_2 emissions and reducing the rate of climate change is a strategy called Carbon Capture and Storage (CCS). This involves capturing CO_2 from CO_2-emitting industries, compressing it, transporting it to a suitable sequestration site, and storing it underground. Refer to Figure 1-2 below:

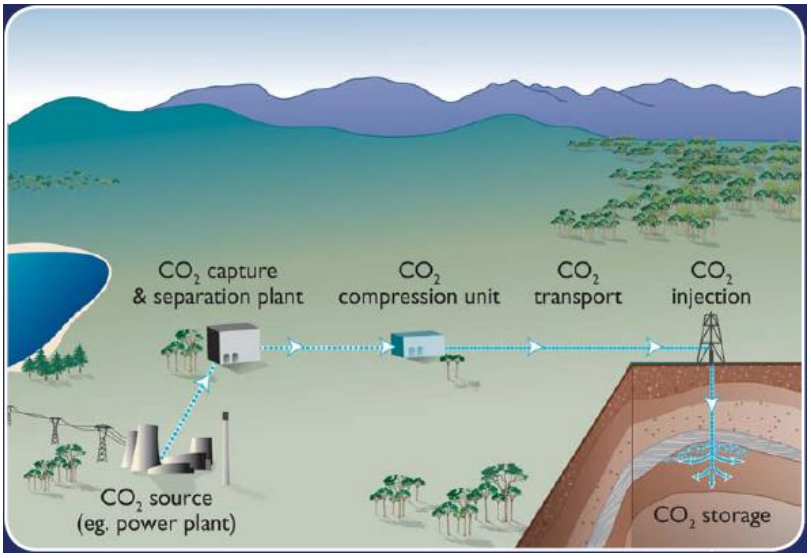

Figure 1-2: Illustration of Carbon Capture and Storage (CCS) (IPCC, 2005)

Well developed and feasible techniques of CO_2 compression, transportation, and injection exist currently (ADEME, 2007). However, an industrially feasible technique of CO_2 capture from industries remains to be found. CO_2 capture was found to be the most energy intensive and expensive component of the strategy of CCS. Significant research is thus being conducted worldwide to develop feasible solutions for CO_2 capture.

There are two main categories of approach towards finding these solutions. One method of approach is to modify processes to operate more efficiently and thus emit less CO_2. This approach provides solutions that are unique to the particular industry that is under investigation for modification. The second approach is to develop processes specifically for the separation and capture of CO_2. This includes the development of retrofit technology for application downstream of CO_2-emitting processes. While this solution is often unique to specific industrial processes, it provides greater possibility for use in a broader range of industries.

This study briefly investigated all CO_2 capture techniques that may be relevant to coal power plants. Coal power plant processes and constraints are identified and explained. There are two

main types of processes for coal power plants. These processes are pulverised coal (PC) power plants and integrated gasification combined cycle (IGCC) power plants.

The location in the power plant process where CO_2 capture can be implemented varies. Three main modes of CO_2 capture have been identified: post-combustion capture, pre-combustion capture, and oxy-fuel-combustion capture. These modes are explained in this study.

Focus was then made on CO_2 capture. Various concerns regarding the implementation of CO_2 capture at coal power plants were summarised and explained. There are many competing strategies of CO_2 capture. CO_2 capture techniques are designed to make use of the unique properties of CO_2, and account for the composition, temperature, and pressure of the flue gas to be treated. A technique that proves feasible for one industry may not necessarily be well suited to other industrial flue gas conditions.

This thesis addresses nine main CO_2 capture techniques, including gas absorption using solvents, CO_2 capture using membranes, cryogenic separation, hydrate formation, and sorbent usage, as well as newly emerging CO_2 capture techniques such as enzyme-based systems, metal organic frameworks, integrated gasification steam cycle (IGSC), and chemical looping combustion.

It was deduced by literature review that gas absorption using solvents had many advantages over other capture techniques. The main distinguishing advantages of the technique included the high level of development associated with industrial gas absorption, and the high potential for feasible CO_2 capture due to the number of possible solvents that may prove efficient for continuous industrial CO_2 absorption and desorption.

The most popular solvents studied for CO_2 capture are alkanolamines and carbonate-based solvents. These solvents result in high CO_2 absorption rate and capacity. However, they are also highly corrosive and can only be used if diluted with water. Water increases the heat capacity of the solvent, resulting in high amounts of energy being required for desorption. Alternative solvents need to be found that can either replace alkanolamine solvents, or be blended with alkanolamines to reduce desorption energy. This study focuses on the use of ionic liquids as a promising replacement of conventional alkanolamine solvents for gas absorption.

Ionic liquids are liquids which are composed entirely of ions. Cations and anions are present, while the ionic liquid as a whole remains a neutral liquid. There has been growing interest in the use of ionic liquids, either in their pure state or blended with other solvents such as alkanolamines, to capture CO_2, as shown in the work of Arshad (2009). Introductory information on ionic liquids was provided in this thesis. Ionic liquid synthesis, advantages and

disadvantages over other possible solvents, and types of ionic liquids are then presented. A review of the methods of analysis of ionic liquids and the resultant trends found, were also conducted. This included a review of equipment for absorption measurements and modelling of absorption in ionic liquids and alkanolamines.

This research focussed thereafter on hybrid solvents which combined ionic liquids with alkanolamines. CO_2 and O_2 absorption measurements were conducted by gravimetric analysis on four pure ionic liquids. The two most CO_2-selective ionic liquids were combined with alkanolamine solvents to create hybrid solvents. The alkanolamines used were Monoethanolamine (MEA), Diethanolamine (DEA), and Methyl Diethanolamine (MDEA), and they were combined with [Bmim][BF_4] and [Bmim][Tf_2N] ionic liquids. The measurements and modelling of gas absorption in ionic liquids and hybrid solvents is presented herein. Finally, the results of the measurements and modelling of CO_2 absorption in hybrid solvents is discussed and benchmarked against conventional solvents, and a simulation of CO_2 capture using a promising hybrid solvent was discussed and benchmarked against a conventional alkanolamine solvent using the engineering software Aspen Plus V. 8.0.

Recommendations for further research are also included.

CHAPTER 2: LITERATURE REVIEW

As mentioned in Chapter 1, many CO_2 capture techniques are currently under investigation throughout the world, to suite various industries. This project focused on CO_2 capture from coal power plants.

This chapter of the thesis consists of the theory of carbon dioxide capture from coal power plants. The chapter begins with an understanding of coal power plant operation. Two main types of power plant processes, namely the pulverised coal (PC) and integrated gasification combined cycle (IGCC) power plants, are explained and compared mainly on power plant efficiency and ease of CO_2 capture integration.

CO_2 capture modes are then introduced. These modes refer to the method of integration of CO_2 capture. There are three main modes of capture, namely post-combustion, pre-combustion, and oxy-fuel combustion.

Thereafter, the main overall criteria regarding CO_2 capture are explained. The main concerns found are capital expenditure, area constraints, disposable materials for CO_2 capture processes, solvent and other material properties, energy requirements, capture complexity, the level of development of CO_2 capture techniques, and the overall cost of applying the capture technique. These concerns are explained in detail.

A review of CO_2 capture techniques follows. This includes gas absorption using solvents, CO_2 capture using membranes, cryogenic separation, hydrate formation, and sorbent usage. Newly emerging CO_2 capture techniques are also explained, such as enzyme-based systems, metal organic frameworks, integrated gasification steam cycle (IGSC), and chemical looping combustion. All techniques are reviewed on their procedure, advantages, disadvantages, current challenges to implementation and significant studies made on the technique including pilot plant testing.

The review found that gas absorption using solvents was the most promising CO_2 technique that could be implemented in the near future. It was decided to investigate this technique further and attempt to contribute towards its implementation. The review found many challenges that need to be overcome for the use of solvents to be feasible for CO_2 capture. In order to overcome the disadvantages associated with conventional alkanolamine solvents, it was proposed to combine conventional solvents with ionic liquids.

A detail review of the study of ionic liquids for CO_2 absorption was conducted. This included analysis of CO_2 Henry's Law constants, CO_2 solubility, CO_2 mole fraction, enthalpy and entropy of absorption of CO_2 in ionic liquids. A review of ionic liquid density, viscosity and heat capacity was also conducted.

Finally, the chapter ends with establishing various trends and relationships between CO_2 absorption and the various properties of ionic liquids and system conditions.

2.1 Coal power plant operation

In order to find solutions to reducing CO_2 emissions at coal power plants, it is imperative that a complete understanding of coal power plant operation is realised. Eskom Ltd., South Africa's primary electricity utility, possesses 14 coal-fired power plants, all of which need to reduce CO_2 emissions.

There are currently two main types of coal power plants. The first and most abundant type of coal power plant is the pulverised coal (PC) power plant. The second and much newer type which is gaining interest in many countries is the Integrated Gasification Combined Cycle (IGCC) power plant.

This section discusses the operation of these two power plants.

2.1.1 Pulverised coal power plants

All of South Africa's coal power plants were found to be pulverised coal (PC) power plants. Figure 2-1 below illustrates the PC power plants process.

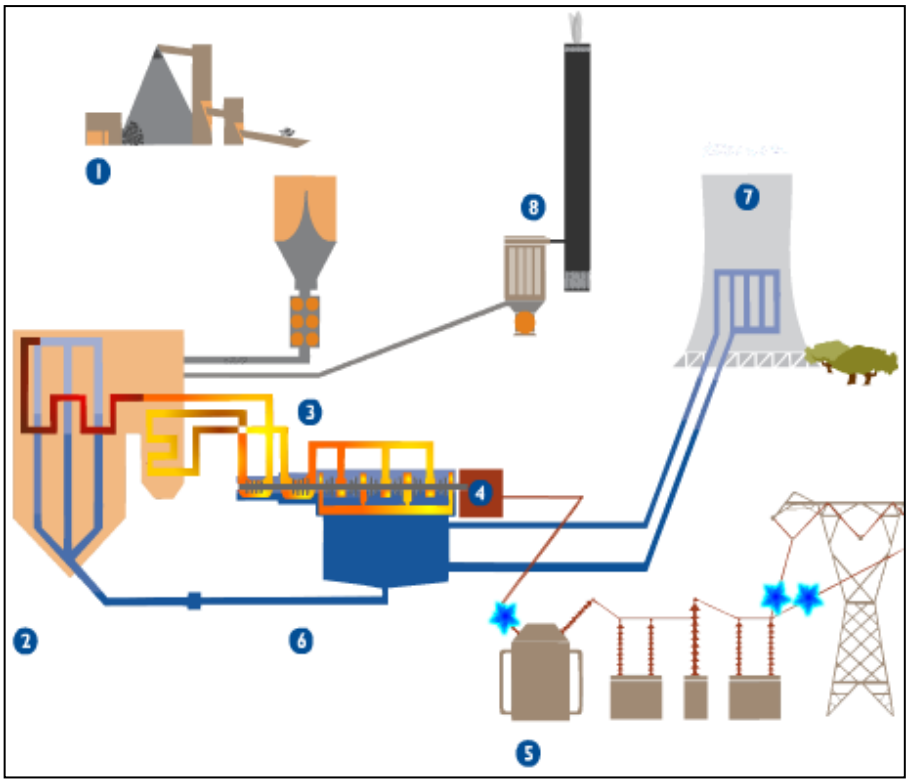

Figure 2-1: Pulverised Coal (PC) Power Plant (Eskom, 2011). 1- Coal heap; 2- Boilers; 3- Superheated steam in turbine; 4- Generator rotor; 5- Transmission lines; 6- Condensed H_2O; 7- Cooling tower; 8- Stack

Heaped coal is transported via conveyor belts to a pulveriser, which grinds the coal to 50 µm diameter. The coal is then transferred to a boiler via hot air blasts. The coal is burned in the boiler and the resulting heat energy that is generated is used to heat tubes that are filled with water. These tubes can be numerous kilometres long and filled with water (Eskom, 2011). The heat from the burning coal is enough to convert the water in the tubes into superheated steam at high pressure.

The steam moves to a turbine and is used to turn the turbine blades, spinning the turbine. The turbine shaft is linked to a generator rotor. The generator consists of an electromagnet which spins inside a large copper coil (Eskom, 2011). This generates electricity. Electricity flows through transmission lines and transformers to reach consumers at required voltages.

The steam that drove the turbines is cooled and condensed in cooling towers, enabling it to be pumped as water and recycled to the boilers for reheating.

The gases that are released during coal combustion are filtered using bag filters to remove ash. The efficiency is claimed to be at 99.8% ash removed (Eskom, 2011). The remaining gases are emitted through the stack as flue gas.

Depending on the quality of the coal (particularly sulphurous and nitrogenous content), emissions may contain harmful gases such as SO_2, H_2S and NO_X. If this is the case, then desulphurisation and denitrification processes are also installed to treat ash-free flue gas and then emit it into the atmosphere via a stack.

Brennecke and Gurkan (2010) and McColl (2011) noted that the typical composition of flue gas emitted from coal-fired power plants is 12-13 vol% CO_2, 68-77 vol% N_2, 6.2-16 vol% water, 3-4.4 vol% O_2, and lower concentrations of other components, 200-420 ppm SO_2, 60-420 ppm NO_X, 50 ppm CO, and 60 ppm hydrocarbons. The flue gas is typically emitted at 0.1-0.17 MPa and temperatures of 363.15 to 412.15 K (NETL, 2010, Eskom, 2011, McColl, 2011).

2.1.2 Integrated gasification combined cycle power plants

IGCC power plants are relatively new power plant processes which aim to ensure that flue gas emission composition and conditions are favourable for efficient CO_2 capture. Modifications of this process are the subject of ongoing research throughout the world. Figure 2-2 below illustrates the basic IGCC process.

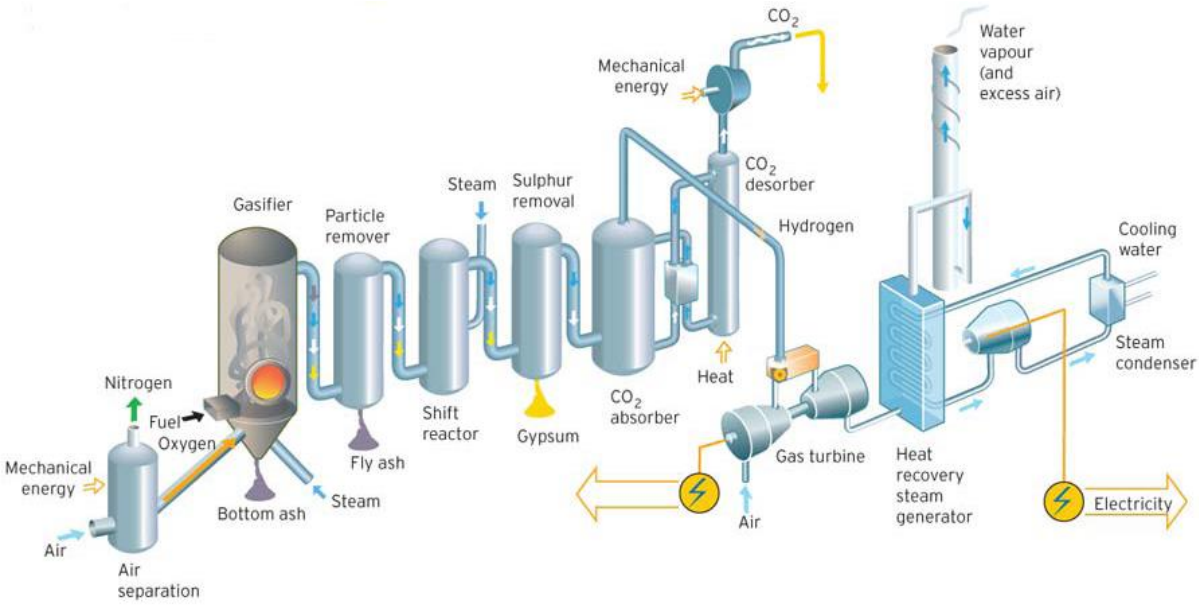

Figure 2-2: Integrated Gasification Combined Cycle (IGCC) Power Plant, including CO_2 Capture Unit (Arshad, 2009)

Air is sent through an air separation unit to obtain oxygen gas (O_2) as shown above. Nitrogen can be released into the atmosphere in this process, but it is often recovered and recycled in cryogenic processes as a cold source. The air separation unit may utilise membrane technology or cryogenic separation.

O_2 at 95 % purity (NETL, 2010) is sent to a gasifier. Coal is sent to the gasifier and burned in the presence of nearly pure O_2. Coal is partially oxidised to produce syngas, which is a mixture of CO, CO_2, and H_2 (Kanniche and Bouallou, 2007), in the gasifier. The gasifier operates at 3.5-7.0 MPa and 1255-1644 K. The necessary temperature is maintained using high pressure steam. The reactions occurring in the gasifier are (Steeneveldt et al., 2006):

$$C_xH_y + xH_2O \rightarrow xCO + (x+ y/2)H_2 \text{.....(R2-1)}$$

$$C_xH_y + (x/2)O_2 \rightarrow xCO + (y/2)H_2 \text{.....(R2-2)}$$

The syngas is treated for particulate removal and is sent to a shift convertor to undergo a water gas shift reaction:

$$CO + H_2O \rightarrow CO_2 + H_2 \text{ .....(R2-3)}$$

(393.15 – 623.15 K; 15 MPa) (Font et al., 2006)

Steam is added to the convertor as a reactant. A gas mixture of CO_2, H_2, sulphurous and nitrogenous compounds leave the convertor. Although not shown in Figure 2-2, the syngas is usually cooled to remove unreacted steam as water. The gas is then treated to remove sulphur and sometimes nitrogenous compounds, depending on their concentration.

The result is a gas mixture containing approximately 50 vol% H_2, 40 vol% CO_2, 2 vol% CO and other trace elements. The gas occurs at 2.7 MPa and 310 K (NETL, 2010).

At this point in the process, CO_2 may be removed using a feasible CO_2 capture technique. CO_2 may then be compressed and stored. After CO_2 capture, H_2 is burned to generate high pressure steam which is used to drive turbines and hence produce electricity. The design of the turbine system varies, but all are aimed at achieving an efficient system using recyclable steam.

The electricity generated by the turbine is used to heat steam for the gasifier and shift convertor, as well as achieve desired pressure and temperature for the air separation unit and CO_2 compression. The remaining electric energy is used commercially.

Gielen (2003) has estimated that IGCC power plants with CO_2 capture can be 25-40% more cost effective than PC power plants. This study took into account the energy required for air separation, compression and other energy requirements. The decrease in operating cost is due to the fact that the gas mixture to be treated for CO_2 capture possesses CO_2 in comparatively higher concentrations and at higher pressure. Separation is thus easier and compression costs are lower.

2.1.3 Comparison between PC and IGCC power plants

The Intergovernmental Panel on Climate Change (IPCC) had summarised emissions, energy increases and cost estimates for PC and IGCC power plants. The values are presented in Table 2-1.

Table 2-1: Estimated Performance and Cost Comparison between PC and IGCC Power Plants (IPCC, 2005)

Performance and cost measures	PC Plant		IGCC Plant	
	Range Low-High	Rep. Value	Range Low-High	Rep. Value
Emission rate without capture (kg CO_2/kWh)	0.736 – 0.811	0.762	0.682 – 0.846	0.773
Emission rate with capture (kg CO_2/kWh)	0.092 – 0.145	0.112	0.065 – 0.152	0.108
Percentage CO_2 reduction per kWh (%)	81 – 88	85	81 – 91	86
Plant efficiency with capture, LHV basis (%)	30 – 35	33	31 – 40	35
Capture energy requirement (% increase input/kWh)	24 – 40	31	14 – 25	19
Total capital requirement without capture (US$/kW)	1161 – 1486	1286	1169 – 1565	1326
Total capital requirement with capture (US$/kW)	1894 – 2578	2096	1414 – 2270	1825
Percent increase in capital cost with capture (%)	44 – 74	63	19 – 66	37
COE* without capture (US$/kWh)	0.043 – 0.052	0.046	0.041 – 0.061	0.047
COE with capture only (US$/kWh)	0.062 – 0.086	0.073	0.054 – 0.079	0.062
Increase in COE with capture (US$/kWh)	0.018 – 0.034	0.027	0.009 – 0.022	0.016
Percent increase in COE with capture (%)	42 – 66	57	20 – 55	33
Cost of net CO_2 captured (US$/tonne CO_2)	29 – 51	41	13 – 37	23

*Cost of electricity

There are many important conclusions that can be made from Table 2-1. Firstly, it is indicated that IGCC power plants without CO_2 capture may result in higher CO_2 emissions than PC power plants. However, if CO_2 capture is integrated into IGCC, less CO_2 emissions occur than for PC power plants. The IGCC plant would also be more efficient, require less capture energy in relation to plant energy output and result in a lower cost of electricity (COE) than PC plants with CO_2 capture.

IGCC plants are more expensive to construct than PC plants but if CO_2 capture is integrated, then IGCC plants require less capital investment overall. This is due to the fact that CO_2 capture is expensive when integrated with PC plants, since the flue gas to be treated for CO_2 capture is emitted at low pressure.

Overall the cost of CO_2 captured in terms of US$/tonne CO_2, is lower for IGCC plants than PC plants.

The International Energy Agency (IEA) had tabulated results comparing standard IGCC plants with CO_2 capture integrated thereafter, to IGCC plants built with CO_2 capture. The results prove

that it is not beneficial to set up an IGCC plant without CO_2 capture and then try to add a CO_2 capture process. Designing an IGCC plant with CO_2 capture from the beginning can potentially provide higher power, higher CO_2 capture and lower capture costs, than if CO_2 capture was added to an already existing IGCC plant. The resultant cost of electricity is also lower.

Table 2-2: Comparison of IGCC Plants with and without CO_2 Capture (IEA,2007)

Performance	Standard IGCC Plant (no capture)	Standard IGCC Plant Retrofitted for CO_2 Capture	Pre-investment IGCC Plant Retrofitted for CO_2 Capture
Net power, kW	509.28	424.83	448.85
Efficiency, %HHV	35.4	29.5	29.5
Heat rate, Btu/kWh HHV	9.653	11.569	11.55
CO_2 captured, kg/hr	N/A	380.73	401.60
Cost			
Total plant cost, $k	589.896	678.196	682.953
Total plant cost, $/kW	1.158	1.596	1.522
Fixed operating, $k/y	10.806	11.56	11.586
Variable operating, $k/y	13.837	14.878	15.173
Fuel @$1.35/MMBtu	51.157	51.144	53.947
COE, $/MW.ha	45.74	59.32	57.23

*Cost of electricity

There were some conflicting reports stated by IEA (2007), which suggested a higher CO_2 capture efficiency in PC power plants and a higher net plant efficiency of 35 % in PC plants, as opposed to 31% in IGCC plants. IEA (2004) estimated IGCC plant efficiency to be as high as 41%. The relatively small inconsistencies prevalent when comparing PC power plants to IGCC power plants, is evidence of the uncertainty in emissions, cost, and energy estimates pertaining to IGCC processes.

In terms of CO_2 capture and energy penalties, PC power plants suffer a high energy penalty for CO_2 capture, due to the flue gas being available at undesirable conditions of low CO_2 partial pressure and high flue gas temperature.

CO_2 capture in IGCC power plants incurs a lower energy penalty since the syngas that needs treatment for CO_2 capture, occurs at relatively high CO_2 partial pressure. However, high amounts of energy are needed for air separation to produce O_2 for the gasifier. Jones et al. (2011) noted that air separation that is required to produce O_2 at 95 mol% purity may account for 65% of the total auxiliary power and account for 16% of the gross power consumption of the plant. This is because the air separation unit (ASU) operates at 4 to 14 atm.

Jones et al. (2011) had summarised various studies towards optimising the ASU. Optimisation includes finding an ideal operating pressure, efficient integration of air products to the gasifier, gas and liquid handling, phase change behaviour of O_2 (O_2 may be produced as a gas or liquid depending on ASU conditions), and optimisation of gas turbine operating pressure.

In addition to the amounts presented in Table 2-1 and Table 2-2 above, it is important to also note that PC power plants are significantly more developed than IGCC power plants, for generating electricity worldwide. The integration of post combustion CO_2 capture into PC power plants is a more feasible short to mid-term solution. Cost estimates are available at greater certainty. However, although the IGCC process is not well developed for electricity production, Pre-combustion IGCC equipment and unit processes are well developed. Steeneveldt et al. (2006) stated that there are over 400 gasifiers in operation worldwide, that are used for the ultimate production of residual oils and high value liquid products such as petroleum. The IGCC process is a modification of the already well developed coal-to-liquids (CTL) process to produce electricity instead of liquid products.

While most industries see the modification of existing PC plants for CO_2 capture as a promising mid-term solution, it is becoming increasingly apparent that IGCC power plants are the best long term option for new coal power plant construction.

2.2 CO_2 capture modes

The modes of CO_2 capture refers to the location and manner in which CO_2 is captured. There are three main modes of CO_2 capture: post-combustion capture; pre-combustion capture; and oxy fuel-combustion capture. It is imperative that these modes be understood, since many capture techniques can only be feasibly applied in certain modes.

2.2.1 Post-combustion capture

Post-combustion CO_2 capture, in the context of coal power plants, refers to the capture of CO_2 after coal combustion.

Refer to Figure 2-1. In the case of post-combustion capture, a CO_2 capture unit would be installed after ash handling of the flue gas, and before the stack. The mode is referred to as post-combustion, because it is the flue gas emanating from the boiler where coal is combusted that is being treated for CO_2 removal.

The obvious advantage of post-combustion CO_2 capture is that the original process is not altered, since capture occurs downstream of coal combustion and other separation processes.

Modifications to the original process need not be necessary. A retrofit capture process may be installed after ash handling, desulphurisation and denitrification processes. Post-combustion capture is also applicable to other coal processes such as IGCC power plants and coal-to-liquids (CTL) processes.

An important disadvantage is that the flue gas that is available for treatment occurs at low pressure (often ambient pressure) and low CO_2 composition (Dias and Oliveira, 2010). As previously mentioned, flue gas emitted during coal combustion contains CO_2 at 13 vol%. At most, the CO_2 composition is 15 vol% (Descamps et al., 2008). The low CO_2 composition ultimately means that the CO_2 partial pressure is less than ambient. It is thus very difficult to separate CO_2 from flue gas at such conditions. Regardless of most CO_2 capture techniques, it is often proposed that the technique be applied in a complex multistage process to achieve desired CO_2 capture. And even once CO_2 is captured, there is a significant cost associated with the compression of CO_2 for transportation and storage.

2.2.2 Pre-combustion capture

Pre-combustion CO_2 capture involves capturing CO_2 before combustion (ie. upstream of combustion and turbine processes). In the context of coal power plants, this mode applies only to IGCC power plants. Refer to Figure 2-2. CO_2 capture occurs after shift conversion and sulphur removal. In Figure 2-2, CO_2 capture is shown to take place by gas absorption, using an absorber and stripping column. Although CO_2 capture is occurring after gasification and shift conversion, the mode is regarded as pre-combustion capture because CO_2 is being captured before H_2 gas is combusted and used to drive turbines.

The advantage of this mode is that the flue gas that is available for CO_2 capture treatment occurs at high pressure (approximately 2.7 MPa) (NETL, 2010). Moreover, CO_2 exists at compositions exceeding 40 vol%. These conditions are favourable as many CO_2 capture techniques are efficient only for flue gases with high CO_2 partial pressure. High CO_2 partial pressure increases the driving force for CO_2 separation, and results in CO_2 being isolated at relatively high pressure, reducing compression costs substantially (Dias and Oliveira, 2010).

The obvious disadvantage is that due to CO_2 capture occurring upstream, downstream combustion properties and conditions need to be re-evaluated. This is typically done with the aid of computer simulations. The change in downstream conditions requires a re-evaluation of operational and safety procedures, which may require additional equipment. Another obvious barrier to the implementation of pre-combustion capture in coal power plants is the fact that it is applicable only to IGCC power plants. There are comparatively few IGCC plants that are

presently in operation. The uncertainty and other barriers to implementing IGCC processes hence apply to pre-combustion capture as well. As Table 2-1 above shows, IGCC processes without CO_2 capture are expected to be less efficient than PC power plant processes. This further discourages investment in the construction of IGCC plants with pre-combustion CO_2 capture.

2.2.3 Oxy-fuel combustion capture

An innovative modification of the PC power plant is oxy-fuel combustion, which involves burning coal in nearly pure oxygen. This mode of combustion involves modifying a PC power plant process and introducing a specific CO_2 capture method in post-combustion mode. Figure 2-3 provides an illustration of the process.

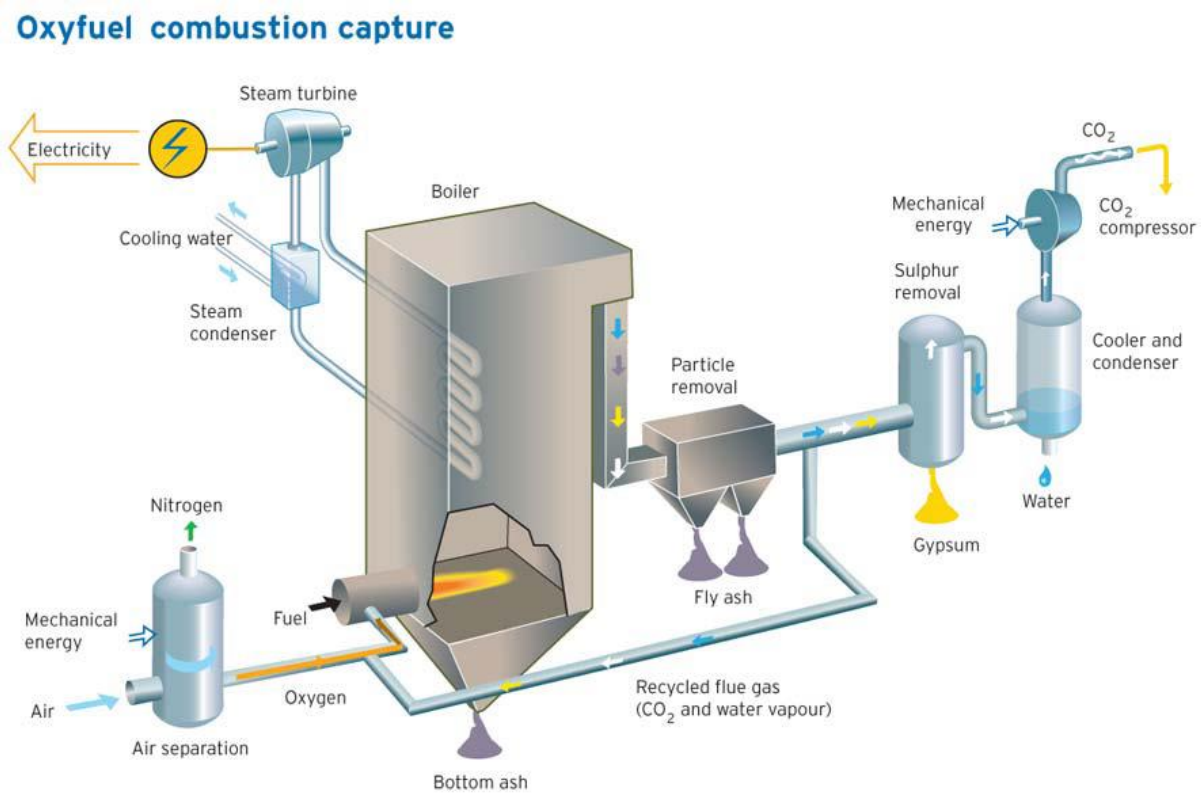

Figure 2-3: Oxy-fuel Combustion Capture (Arshad, 2009)

Air is first sent to an air separation unit (ASU), where oxygen is separated from nitrogen and other gases. Separation may be done using cryogenic methods. The nitrogen is either emitted into the atmosphere or recovered and sold or utilised, while oxygen is used in the boiler.

Coal is burned in the presence of nearly pure oxygen, generating heat which converts water to superheated steam, for use in steam turbines. The burning of coal in the presence of pure

oxygen results in a flue gas consisting mainly of CO_2 and water vapour. The flue gas is treated for ash and trace amounts of sulphurous products, producing a flue gas stream comprising exclusively of CO_2 and H_2O as water vapour.

The flue gas is then treated for CO_2 capture using ammonia scrubbing, cryogenic separation or newer methods such as CO_2 anti-sublimation explained in Section 2.4.3.

There are numerous advantages of oxy-fuel combustion. The main advantage is that the flue gas available to be treated for CO_2 capture is of high CO_2 partial pressure (Figueroa et al., 2007 and Davison, 2007). Moreover, the flue gas is composed mainly of CO_2 and H_2O. Aside from complete cryogenic separation and CO_2 anti-sublimation, even ammonia or NaOH scrubbing or partial condensation under recycle can separate these two components. CO_2 can be separated and made available at high pressure, reducing compression costs. Aside from the benefits in terms of CO_2 capture, there is an increased possibility of integrating oxy-fuel combustion into PC power plants. This is an attractive option compared to constructing entirely new IGCC power plants. An ASU may be retrofitted at the beginning of a PC power plant process and CO_2 capture technique retrofitted at the end. Davison (2007) estimated oxy-fuel combustion to result in lower CO_2 emissions than IGCC processes.

There are some disadvantages however. Coal burns at a high flaming temperature in the presence of pure oxygen, which puts much strain on the material of construction (Arshad, 2009). Flue gas is often recycled to enable some control over temperature changes, as shown in Figure 2-3. Cooled CO_2 streams after CO_2 capture may also be used to lower the temperature of the boiler to protect boiler material. Feasible air separation is also a challenge. ASUs often require high amounts of energy either in terms of refrigeration or high pressure, or both, resulting in high operating costs. The flue gas composition also limits the number of possible CO_2 capture techniques that may be feasibly used. Cryogenic methods for air separation are presently accompanied with high energy penalties and hence less commercially available power generation. Efforts are made however to improve the efficiency of cryogenic methods, as explained in Section 2.4.3.

2.3 Criteria regarding the introduction of CO_2 capture techniques in coal power plants

In order to identify a feasible solution for CO_2 capture at coal power plants, various constraints needed to be identified. Thereafter, a CO_2 capture technique could be judged on its applicability based on these constraints. Davison (2006), GPA (2004), and Osman (2011) have summarised a

few factors that affect the implementation of CO_2 capture, not only in coal power plants but in industry in general.

2.3.1 Capital expenditure

The immediate factor of concern for any company to introduce CO_2 capture is the initial capital investment that is required for the CO_2 capture process. When creating a new process or applying radical modifications to an existing process to achieve greater efficiency and inherently less CO_2 emissions, the capital expenditure is often comparatively high and is less likely to be accurately estimated because new downstream conditions may be created. Moreover, while energy requirements in some sections of the new process may be lowered, new energy requirements may emerge in other sections.

On the other hand, applying retrofit technologies downstream of an existing process offer potentially lower capital expenditure, greater accuracy and certainty of capital cost predictions, better energy requirement predictions and stream conditions.

Capital expenditure can also be justified depending on the expected operating expenditure that would result once all new modifications are in operation. If the operating expenditure, energy requirements, and stream results are expected to be promising, then it would encourage capital investment.

2.3.2 Area constraints

The area available for process modification or retrofit introduction is of inescapable concern. CO_2 capture technologies can only be safely incorporated into a process if there is enough space available to accommodate the additional equipment required. If there is not enough space, then the plant faces serious concerns and may have to scale down to accommodate CO_2 capture and keep within emissions regulations, or alternatively close and relocate to larger premises.

The application of retrofit technology requires space that is more accurately predictable. If an existing coal power plant has abundant free area, then retrofit CO_2 capture technology may be a better option to pursue. But if there is not enough space, then radical process modification, or decommissioning of the old process to build a new process, would be two options aside from relocating. There is however, comparatively higher uncertainty in terms of cost, process design and equipment setup associated with process modifications and new process development, as previously mentioned.

2.3.3 The cost of disposable components of CO_2 capture technologies

Some CO_2 capture technologies involve the use of solvents, membranes, sorbents, catalysts, and other additives to increase efficiency. The cost of these components can affect the feasibility of CO_2 capture, particularly if such components are not regenerable and have to be replaced or replenished often. Some ionic liquid solvents, zeolites and porous membranes are also of high cost.

Feasibility is greatly increased and costs are justified if such components can be regenerated and recycled over a substantial number of times.

2.3.4 The properties of solvents and other components

The properties of components affect the operating efficiency and cost. Solvents that degrade easily upon absorption or under high temperature make the CO_2 capture process unsustainable. Ionic liquid solvents have the problem of being of high viscosity generally, which increases circulation costs. Alkanolamine solvents are corrosive and have to be diluted with H_2O, increasing energy costs.

Many solid sorbents suffer low attrition resistance, hindering their use. Membrane stability under high pressure, as well as porosity and permeability influence its performance as a CO_2 separating unit.

Flammability and toxicity of components also introduce safety concerns under continuous operation.

2.3.5 Energy requirements of a capture process

All capture processes require energy in the form of heat or refrigeration, as well as pressure and circulation. Capture processes also specifically require energy for the compression of CO_2 after capture for storage and transportation. The amount of energy required forms a large portion of operating costs. Heat energy is typically applied using superheated steam. High energy requirements thus also translate into high water usage.

In the case of preserving an existing process and adding a retrofit CO_2 capture technology, the energy requirement of the process increases overall. The high increase in energy requirements is one of the main reasons why CO_2 capture has not been implemented on an industrial scale yet (IPCC, 2005). Pinch analysis and other energy integration methods to minimise energy costs, are in important concern in CO_2 capture pilot plant study (VNS, 2008 and Knudsen et al., 2008).

Modifying a process or replacing it with a new process that is more efficient and environmentally friendly, results in a lower energy requirement overall, lowering operating costs. This can only be realised if the high capital investment of new processes and process modifications can be overcome.

2.3.6 The complexity of CO_2 capture techniques

Complex techniques generally result in higher investment costs, higher energy usage, larger space, high maintenance costs, and high probability of malfunction. Depending on the mode of CO_2 capture, there may also be substantial changes to downstream conditions and efficiency, particularly in the case of pre-combustion capture.

2.3.7 Level of development of capture techniques

There are many techniques under evaluation as possible candidates for feasible CO_2 capture. Some are highly developed techniques that are already in use in other processes for the capture of other gases. Other techniques are new, having reached only pilot plant or lab stages of development.

A low level of development of capture techniques poses a hindrance to commercialisation in the near future. While many CO_2 capture techniques seem to be successful on a lab scale, there is much uncertainty associated with implementing a technique on a commercial scale (NETL, 2010). This is because of the associated low certainty of estimates such as capital and operating costs, safety aspects and maintenance costs required for commercial operation. New, highly complex processes and process modifications also possess substantial doubt in cost estimates and thus the success of the venture, deterring investors.

2.3.8 Overall cost of applying the capture technique

In light of the above factors, the overall operating cost is ultimately the deciding factor as to whether the CO_2 capture technique is feasible or not. High energy penalties, high costs of solvents or other components, and high maintenance costs reduce feasibility substantially, making CO_2 reduction an expensive process. High safety measures also increase costs due to the extra precaution and monitoring by extra personnel required. In the case of power plants, high energy penalty for CO_2 capture will substantially reduce the amount of power that the plant can produce for commercial use.

In the case of other industries, high operating costs of CO_2 capture result in more expensive product, which makes a company less competitive.

All of the above factors need to be addressed and optimised to ensure feasible CO_2 capture.

2.4 CO_2 capture techniques

The various CO_2 capture techniques that are currently being studied worldwide are explained in this section. This includes a theoretical explanation of each technique, its level of development, advantages, disadvantages, and barriers to implementation of these techniques.

2.4.1 Gas absorption using solvents

The use of solvents for gas separation and recovery is a mature technology that is already used for processes such as flue gas desulphurisation and denitrification (Su et al., 2013). As Figure 2-4 illustrates, the process involves passing a flue gas mixture through an absorber counter-currently with an initially unloaded or lean liquid solvent. Gases that are soluble in the solvent get absorbed, while insoluble gases pass through the absorber and are recovered at the stack.

The loaded solvent, now rich in absorbed gases, is then heated and sent to a stripper where the gases are desorbed from the solvent. The gases are recovered at the top of the stripper while the lean solvent leaves the stripper as bottoms. The lean solvent is then recycled to the absorber.

Desorption in the stripper is facilitated by increased temperature. Increasing the temperature of the loaded solvent, results in a reversal of the absorption mechanism. In the case of chemical solvents, the reverse reaction occurs producing the initial absorbed gas.

There are other methods to facilitate desorption in the stripper, such as temperature swing absorption (TSA) or pressure swing absorption (PSA). The operating temperature of the stripper may be increased as in TSA, or the operating pressure of the stripper may be decreased.

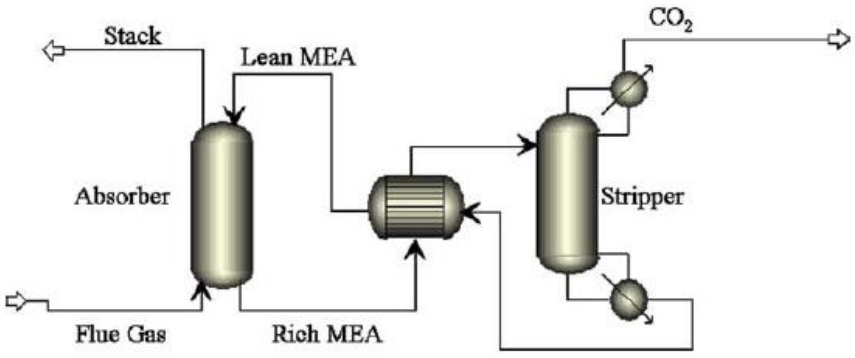

Figure 2-4: A Typical Solvent Absorption Process (Figueroa et al., 2008)

Many solvents have been studied for their applicability to CO_2 absorption from flue gases emanating from coal, oil, steel and natural gas industries worldwide. The solvents are grouped into different categories: chemical solvents, physical solvents, hybrid solvents, and blended

solvents. Other compounds are also emerging and have the potential to be used as feasible solvents, such as ionic liquids.

2.4.1.1 Chemical solvents

Chemical solvents are solvents which undergo a reaction with the gases that they absorb. In the treatment of flue gas for CO_2 removal, CO_2 may undergo a multistage reaction mechanism with the solvent. The mechanism is known as reactive absorption. Desorption of CO_2 entails increasing the temperature of the solvent, to facilitate the reverse reaction and hence obtain CO_2 gas.

Many chemical solvents are studied for CO_2 absorption. Ammonia (NH_3) was the first chemical solvent under investigation. Alstom Ltd has made much progress in researching the use of aqueous ammonia. The advantage is that it is much less sensitive to contaminants such as NO_X, SO_X and O_2, and can even simultaneously absorb these gases along with CO_2. There is also less degradation during regeneration, which means that the solvent can be used over more cycles than alkanolamine solvents such as MEA (Steeneveldt et al., 2006). Ammonia however proved to be too corrosive for use in industrial equipment. Moreover, a high saturation pressure was required for solvent loading (Figueroa et al., 2008)

Currently, the most popular chemical solvents are alkanolamines, due to their high CO_2 absorption rate. The reactive absorption mechanism between CO_2 and alkanolamines is as follows (Mamun et al., 2005, and Austgen et al., 1991):

CO_2 phase change: $CO_2\ (g) \leftrightarrow CO_2\ (aq)$…….(R2-4)

Dissociation of H_2O: $2H_2O \leftrightarrow OH^- + H_3O^+$ ……..(R2-5)

Dissociation of CO_2: $2H_2O + CO_2 \leftrightarrow H_3O^+ + HCO_3^-$ ……(R2-6)

Dissociation of Bicarbonate ion: $H_2O + HCO_3^- \leftrightarrow CO_3^{2-} + H_3O^+$ ……. (R2-7)

Reactions (R2-4) to (R2-7) are common for all alkanolamines. Thereafter, the reaction mechanism differs according to the type of amine that is being used. Primary amines are organic molecules containing an amine group attached to a single carbon atom. Secondary amines and tertiary amines are molecules possessing an amine group attached to two and three alkyl groups respectively. In terms of reaction mechanisms with CO_2, primary and secondary amines undergo Zwitterion formation mechanisms, while tertiary amines undergo alternative reaction mechanisms. Reaction mechanisms for primary and secondary amines with CO_2 are as follows:

Zwitterion formation: $CO_2 + R^1R^2NH \leftrightarrow R^1R^2NH^+COO^-$……...(R2-8)

Zwitterion deprotonation by a base: $R^1R^2NH^+COO^- + B \leftrightarrow R^1R^2NCOO^- + BH^+$…….(R2-9)

The mechanism for tertiary amines differs from secondary amines as tertiary amines cannot react with CO_2 directly. The tertiary amine acts as a base for CO_2 to react with hydroxide in solution according to the following reaction mechanism (Mamun et al., 2005):

Dissociation of Amine: $R^1R^2R^3N + H_2O \leftrightarrow R^1R^2R^3NH^+ + OH^-$ ……(R2-10)

Hydroxide reaction: $CO_2 + OH^- \leftrightarrow HCO_3^-$ ……(R2-11)

Overall reaction ((R2-26) and (R2-27) combined):

$CO_2 + R^1R^2R^3N + H_2O \leftrightarrow R^1R^2R^3NH^+ + HCO_3^-$ …….. (R2-12)

The above reactions were also documented in Osman (2011). Mamun et al. (2005) claimed that other reactions also occur, such as formation of dicarbamate and dissociation of diprotonated amine, but these are minor.

Since an exothermic reaction mechanism occurs, desorption of CO_2 is facilitated by heating the CO_2-rich solvent thus reversing the reaction in the stripper. Manuel et al. (1998) provides kinetics for (R2-8) to (R2-12). Table 2-3 presents popular alkanolamine solvents and their abbreviated representation (GPA, 2004, Mamun et al., 2005).

Table 2-3: Alkanolamine Solvents and Abbreviated Name

Alkanolamine Solvent	Abbreviation
Mono-ethanolamine	MEA
Di-ethanolamine	DEA
Methyl-di-ethanolamine	MDEA
Di-Glycol Amine	DGA
Tri-ethanol Amine	TEA
Methyl Mono-ethanol Amine	MMEA
Amino-Ethyl-Ethanol Amine	AEEA
Ethyl Amino-ethanol	EMEA
Butyl Amino-ethanol	BEA

The advantage of chemical solvents, particularly alkanolamine solvents, is that absorption can occur at a relatively high rate and achieve high absorption capacity even at low CO_2 composition of the flue gas (< 15 wt%). This is a particularly attractive solution especially for CO_2 capture being applied in post-combustion mode, which possesses flue gas with low CO_2 partial pressure. A lead additive can be added for greater efficiency when high CO_2 concentrations prevail in the flue gas.

The primary disadvantage of alkanolamines is that they are corrosive towards industrial equipment, which are generally metal alloys of various composition. Due to their corrosive nature, alkanolamines are heavily diluted with H_2O resulting in a solvent consisting of 50-70 wt% H_2O. Such solvents have very limited absorption capacity, requiring an absorption process to utilise and recycle high volumes of solvent. H_2O also possesses a relatively high heat

capacity, which contributes towards a high overall heat capacity of the solvent. This is undesirable during regeneration since substantial amounts of heat energy are required to heat the loaded solvent for desorption of CO_2. Another disadvantage of alkanolamine solvents is their sensitivity to contaminants in the flue gas such as NO_X, SO_X, and O_2. Contaminants either result in the decomposition of the solvent over extended periods of time, or the solvent may absorb the contaminants along with CO_2, making pure CO_2 recovery difficult.

Not all alkanolamine solvents suffer the same drawbacks. Secondary and tertiary amines such as DGA, MDEA, and DEA are less corrosive and have higher CO_2 loading and regeneration properties than primary amines such as MEA (GPA, 2004). However, secondary and tertiary amines provide significantly lower absorption rates of CO_2. Some secondary and tertiary solvents also have high selectivities towards other components such as SO_2, COS and other pollutants present in flue gas. In some cases, the amine degrades upon contact with such pollutants. This degradation is reversible with some solvents such as MDEA and DEA however. A regenerator unit may be used.

Another class of chemical solvents that receive much attention are sterically hindered amines, which are organic compounds with a primary amine functional group attached to a tertiary carbon atom (a carbon atom which is linked to three other carbon atoms). Hindered amines are also formed with secondary amine groups attached to secondary carbon atoms. Exxon (Nerula and Ashraf, 1987) and Mitsubishi Heavy Industries (Steeneveldt et al., 2006) are at the forefront of this study. Steric hindrance causes unstable carbamate ions to form upon reaction with CO_2, contrary to normal alkanolamines which form stable carbamate ions. This alternative reaction mechanism increases the absorption capacity of the solvent by 20-40 % for hindered amines (Steeneveldt et al., 2006).

Popular hindered amine solvents are KS-1, which is a product of MHI, as well as Flexsorb (R) and 2-amine-2-methyl-1-propanol (AMP), which are products of Exxon-Mobil (Figueroa et al., 2008).

IFP Energies Nouvelles developed a solvent consisting mainly of amines together with other compounds. This solvent is known as the DMX^{TM} solvent. Upon absorption of CO_2, the solvent separates into two liquid phases. One phase is a CO_2 rich phase while the other is a CO_2 lean phase. The presence of several amine functional groups creates a chance for hydrogen bonding to occur. After absorption and heat exchange, the bonds are broken at high temperature and facilitate demixing. The solvent may pass into a decanter to remove the CO_2 lean phase and recycle it to the absorber. Only the CO_2 rich phase is passed into the stripper for regeneration. This reduces the energy cost of the capture process since a lower amount of solvent needs to be

regenerated. Regenerator reboiler duty is reduced by 43% in comparison to conventional alkanolamine solvent containing 30 wt% MEA diluted in water (Raynal et al., 2011).

Aside from alkanolamines, carbonate based solvents (Knuutila et al., 2008) are also gaining popularity as chemical solvents for CO_2 absorption. Carbonate solvents are already in use for other gas absorption processes. Sodium carbonate is already used for flue gas desulphurisation. The high level of development of this technology is advantageous since equipment and systems may be optimised to allow for efficient CO_2 capture as well. Carbonate solvents are reported to be less corrosive than alkanolamines and they can absorb CO_2 and SO_2 simultaneously (Knuutila et al., 2008). The reaction with CO_2 is as follows:

$$CO_3^{2-} + H_2O + CO_2 \rightarrow 2HCO_3^- \quad \text{(R2-13)}$$

Another popular carbonate solvent is potassium carbonate, which was studied extensively by Mamun (2005). Mamun (2005) presents absorption rates and CO_2 loading for potassium carbonate. This solvent is particularly useful when combined with other solvents, forming hybrid or blended solvents.

The disadvantage of carbonate solvents is the comparatively low CO_2 absorption rate that they achieve, particularly with flue gases of low CO_2 concentration. Mamun (2005) suggests that the use of carbonate solvents is limited to pre-combustion mode, where the CO_2 concentration is relatively high in the syngas. The use of carbonate solvents also requires regular cleaning and inspection of equipment to prevent damage, as carbonate based solvents have a relatively high tendency to precipitate. This results in extra capital and labour costs to account for this.

2.4.1.2 Physical solvents

The absorption of gases such as CO_2 in physical solvents occurs without any chemical reaction. CO_2 absorption entails a rearrangement and reconfiguration of solvent molecules, to accommodate CO_2 molecules. Industrially, gas absorption using solvents is carried out in the same manner, using absorbers and strippers for absorption and desorption respectively.

Common physical solvents are Selexol® (Union Carbide), Rectisol (utilising mainly methanol) and Sulfinol® (Shell) (Gielen, 2003).

Selexol, a product of the Union Carbide Corporation, is made up of a polyethylene glycol derivative and has many advantages. Selexol solvent can absorb CO_2, water and sulphur compounds. The solvent is reported to be applicable and efficient at ambient pressure, producing relatively high absorption rates. The solvent also does not degrade appreciably and is thus stable and recyclable (IEA, 2004).

The disadvantage is that the solvent possesses low selectivity of CO_2 over other components of the flue gas. The solvent can also absorb valuable paraffins, olefins, and aromatics. The operating temperature is also limited, from 255.15 K to ambient. This is an undesirable condition since flue gas is available at higher than ambient temperature.

Methanol can also be used as a physical solvent. However, its operating conditions are demanding and undesirable for flue gas treatment. Due to the high volatility of methanol, the absorption process can only run efficiently between 200.15 and 238.15 K (GPA, 2004), with an operating pressure of 2 MPa (IEA, 2004).

The latest investigations on physical solvents are that of ionic liquids for CO_2 absorption, which are discussed in detail in Section 2.5.

2.4.1.3 Hybrid solvents

In an attempt to combine the best features and advantages of chemical and physical solvents, and minimise their flaws, researchers have tried to mix chemical and physical solvents together to create hybrid solvents. This is done in an attempt to produce a solvent that possesses the high absorption rates and capacities of chemical solvents, and low regeneration energy, low corrosiveness, and high stability of physical solvents.

A well-studied and promising hybrid solvent is the Sulfinol® solvent (IEA, 2004). The solvent contains a mixture of sulfolane, water, and either MDEA or Di-Isopropanol Amine (DIPA), which enables the solvent to absorb CO_2 physically and chemically. This solvent can absorb H_2S, CO_2, COS and CS_2 simultaneously, which is advantageous for flue gas treatment, but also undesirable during CO_2 recovery (Osman, 2010). Low corrosiveness and high CO_2 capacity is claimed by Nerula and Ashraf (1987). It is also claimed to reduce CO_2 concentration in flue gas to as low as 50 ppm. Regeneration may be done using a flash vessel rather than a stripper, hence the energy penalty is lower (Nerula and Ashraf, 1987).

The solvent also results in co-absorption of hydrocarbons, which could mean loss of product or reactants if the process has entrainment problems, which is a disadvantage. A reclaimer may also be needed to recover degraded solvent and the CO_2 entrained in it, making the absorption process more complex and likely more expensive. A further disadvantage mentioned in IEA (2004) is that the solvent only operates efficiently and produces high absorption rate and capacity for flue gases at 0.5 MPa or more.

Another popular hybrid solvent is the Amisol® solvent (IEA, 2004), which was researched and developed in the 1960s by Lurgi Ltd. The most developed Amisol® solvent is a mixture of diethyl amine (DETA), aliphatic alkyl amines, and di-isopropyl amine (DIPAM). Previous

mixtures also incorporated MEA and DEA as well. Optimum absorption with this solvent occurs at 308.15 K and regeneration is typically done at 353.15 K. The advantage of this close temperature range is that a lean/rich heat exchanger is not needed. The optimum pressure is 1 MPa (IEA, 2004). However, the exiting gas from the stripper has to undergo water washing after CO_2 desorption and the water needs to undergo distillation to retrieve entrained volatile methanol, since methanol may easily be lost to the gas stream during stripping (Nerula and Ashraf, 1987).

The Amisol® solvent was reported by Nerula and Ashraf (1987) to be non-corrosive. The solvent can also absorb sulphurous compounds such as COS, mercaptans, and HCN, and can reduce CO_2 concentration in the flue gas to as low as 5 ppm.

A disadvantage common to Amisol® and Sulfinol® solvents is that they also absorb hydrocarbons which occur in trace quantities in many flue gases. This amounts to a loss of valuable products. The flue gas needs to be treated for this before CO_2 absorption, making CO_2 capture a complicated procedure overall.

Duc et al. (2007) also noted the low selectivity of hybrid solvents as one of the main disadvantages of the solvent. In terms of absorbing multiple pollutants such as SO_X and NO_X along with CO_2, the solvent seems like an attractive operation. But CO_2 recovery and disposal in a relatively pure composition becomes difficult, requiring additional separation processes (Chatti et al., 2005).

Another class of hybrid solvents that are currently receiving much attention and study, are functionalised ionic liquids, which are physical solvents than contain functional groups such as amines, which result in chemical absorption of gases as well. Ionic liquids containing functional groups are discussed in later Section 2.5.5 of the thesis.

2.4.1.4 Blended solvents

Aside from combining physical solvents with chemical solvents, another initiative is to combine two or more chemical solvents to achieve a superior chemical solvent. This can also be done with physical solvents, where two or more physical solvents may be combined to create a more advantageous solvent mixture.

This strategy is popular particularly for alkanolamine solvents. Alkanolamine blends usually incorporate primary, secondary, and tertiary amines, in order to obtain a solvent that provides the high CO_2 absorption rates of primary amines, together with the low corrosiveness and high CO_2 absorption capacity of secondary and tertiary amines (Nerula and Ashraf, 1987). The blending of secondary and tertiary amines with primary amines also enables the solvent to

possess higher quantities of alkanolamine and lower quantities of H_2O. This is advantageous as high amounts of water contribute to a high overall heat capacity of the solvent, which results in exorbitant energy requirements for desorption. Water has a relatively high specific heat capacity (4.187 kJ/kg.K (IEA, 2004)), which is why it is better if less of it is incorporated into the solvent.

Blending of alkanolamines and creating solvents with higher alkanolamine concentrations also reduces the corrosiveness of the solvents, since tertiary amines such as MDEA are less corrosive than primary amines. Moreover, blending of different alkanolamines also enables the solvent to absorb other pollutants such as H_2S, SO_2 and other sulphurous compounds (Coquelet and Richon, 2007). There are thus numerous advantages to blending different alkanolamines.

The challenge of blending alkanolamines is that a compromise has to be made. The resulting solvent usually produces trade-off results. A blend may not produce an absorption rate that is as high as what a single primary amine can produce, or it may not possess an absorption capacity that is as high as what secondary and tertiary amines produce. An optimum blend ratio needs to be found, as with hybrid solvents.

Studies have found that MEA+MDEA blends were the most popular blends researched (Osman, 2010). Ritter et al. (2006) found that the energy required to capture CO_2 using MEA alone, was 3.14 GJ/ton CO_2. When MEA was used in combination with MDEA, the energy required was 2.2 GJ/ton CO_2. MEA:MDEA blend ratios are suggested by Chakravarti et al. (2001) to be 10 to 20% MEA with 20 to 40 % MDEA.

The same investigations were attempted with other alkanolamines. Absorption curves for MDEA blended with MEA, AEEA, and PZ were produced in a study by Mamun et al. (2005). MDEA + PZ, as well as MDEA + AEEA provided superior performance than MDEA + MEA blends. However, none of these blends produced higher CO_2 absorption rates than unblended MEA solvent. Mamun et al. (2006) blended MDEA with MMEA and piperazine additives. MMEA and piperazine were reported to increase the reaction rate between MDEA and CO_2. 5 to 10 mol% concentrations of piperazine and MMEA were used. The study found 10 mol% MMEA and 5 mol% piperazine to be particularly successful in increasing the solubility and rate of absorption of CO_2 in MDEA compared to simply using diluted MDEA solvent.

Solvent blending is not limited to amine-based solvents. Chemical solvents such as carbonate based solvents may also be blended with each other and with alkanolamines. The blending of potassium carbonate with MEA was studied by Mamun et al. (2005). Absorption data were tabulated for various concentrations of MEA. The study did not produce promising results

however. The performance of such a blend in terms of CO_2 loading and absorption rate was found to be comparatively lower to that of other alkanolamine blends, and even that of single alkanolamines.

The relatively high level of development of absorption processes is advantageous to CO_2 capture, since this technique possesses accurate estimates for good design and decision making. There is much potential for the process to be retrofitted in post-combustion mode, and can hence have little or no effect on the rest of the process, with the exception of energy requirements. Installation at post-combustion mode may require preparation of the flue gas before CO_2 capture however. Flue gas may need to undergo compression and refrigeration processes to bring it to optimum system conditions for efficient CO_2 capture. Such requirements may not be necessary if an ideal solvent is found. And on the other hand, it can be used in pre-combustion mode and achieve greater efficiency since syngas possesses higher CO_2 concentrations.

Mass transfer kinetics are well researched for the absorption of gases in solvents. The Two-Film theory of gas absorption is explained in the work of Lewis and Whitman (1924) and well investigated for physical and chemical absorption in the work of Danckwerts (1965). Film and Surface Renewal models applicable to physical and chemical absorption are stated and explained.

Gas absorption using solvents is also a highly flexible method. Two or more solvents may be combined to increase efficiency. There are different possibilities to create hybrid solvents, blended solvents, and investigate newly emerging solvents such as ionic liquids. The process is relatively simple and requires a comparatively smaller space, unless multistage operation involving two or more absorbers and strippers is employed. Many solvents are recyclable, which saves on operating costs.

The current disadvantage and primary barrier to implementation is the high energy penalty associated with gas absorption as a capture method. Energy is required in the form of heat for regeneration, as well as cooling of the solvent, since the absorption rate decreases with increasing temperature (Osman, 2010). Energy is also required for compression of CO_2 during recovery, and perhaps also for compression of the flue gas in order to ensure high CO_2 partial pressures and efficient CO_2 absorption. Absorption processes of this nature can account for up to 40% of the total plant energy requirements (Kanniche and Bouallou, 2007), making operating costs significantly high. Moreover, many solvents, especially physical solvents, are only feasible when treating flue gas at high CO_2 partial pressure, and hence can only be applied to

pre-combustion (IEA, 2004). Some solvents are also particularly expensive, contributing towards an increased capital cost.

Figure 2-5 below indicates the general trend between CO_2 absorption achieved and the desorption energy required for various types of solvents.

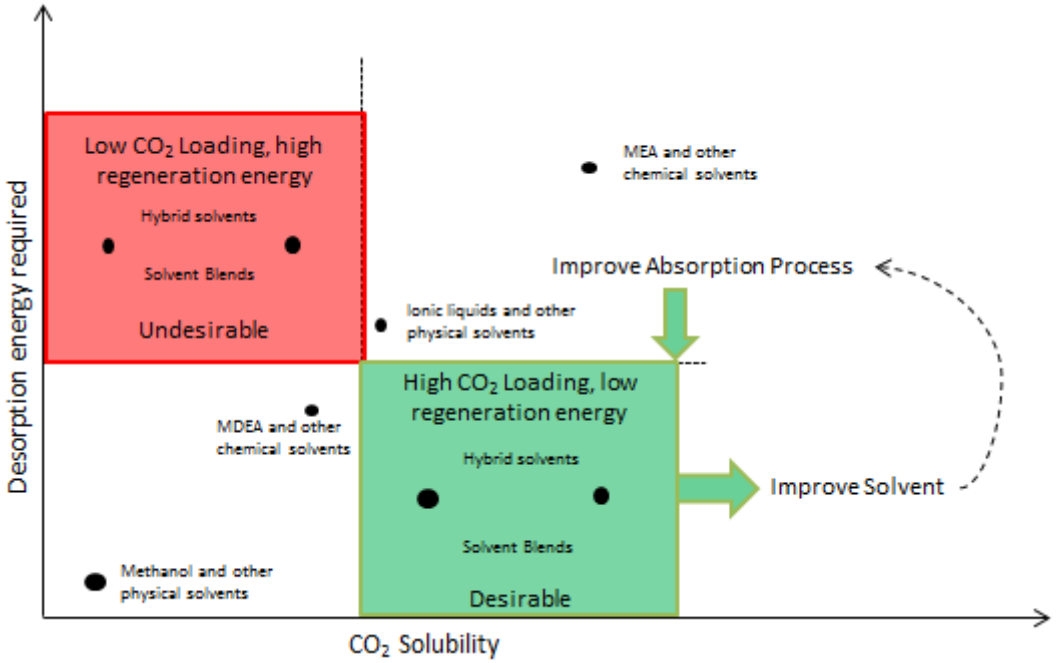

Figure 2-5: General Qualitative Trends of CO_2 Solubility and Desorption Energy Required for Various types of Solvents

It has been established by extensive literature review that no single solvent compound would achieve high CO_2 solubility and require low desorption energy, which is the desired result. Pure physical or chemical solvents offer either low CO_2 solubility with low desorption energy, or high CO_2 solubility and high desorption energy. Hybrid and blended solvents achieve mixed results, from highly desirable to highly undesirable. Nevertheless, these categories of solvents possess the most potential for high CO_2 solubility and it is thus worth pursuing research into hybrid solvents and solvent blends to increase the CO_2 solubility achieved. Higher CO_2 solubility in a solvent implies less solvent needs to be used, thereby reducing desorption energy required. However, desorption energy can also be reduced through pursuing process optimisation.

As mentioned previously, absorption processes have received the most attention for CO_2 capture and are currently the most researched and closest to commercialisation of all CO_2 capture techniques. Austria and Netherlands have managed to set up pilot plants in 2008 (VNS, 2008 and Knudsen et al., 2008). Studies towards the industrial implementation of solvents aim to find an ideal solvent, which may be defined to include a high CO_2 absorption capacity, high CO_2

absorption rate, high CO_2 selectivity, low viscosity, low volatility, low heat capacity, low corrosivity, low toxicity, and low cost.

2.4.2 CO_2 capture using membranes

In principle, the capture of CO_2 using membranes involves passing flue gas through a membrane contactor. CO_2 selectively permeates through the membrane. Other components of the flue gas do not. CO_2 is isolated on the other side of the membrane, compressed and recovered, while the treated flue gas leaves through an outlet on the entry side of the membrane. Refer to Figure 2-6 for an illustration.

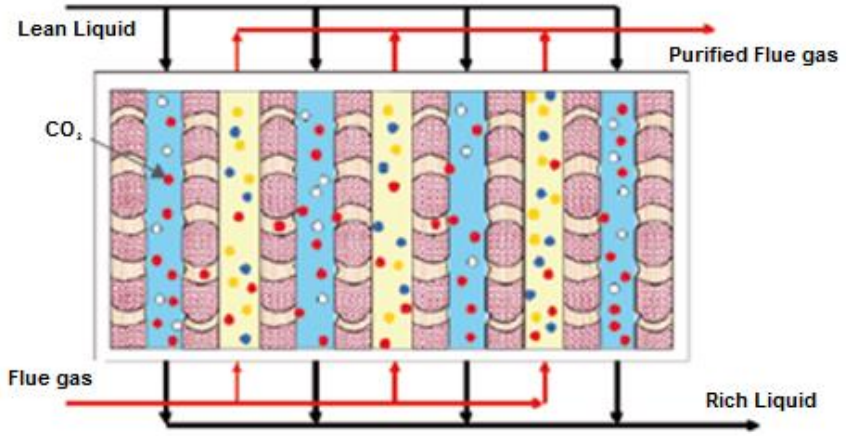

Figure 2-6: An Illustration of a Membrane Contactor with Solvent (NETL, 2007)

Membranes are often used in combination with solvents to increase CO_2 capture rate and yield. Figure 2-6 above shows a plate-and-frame filter containing multiple membranes, with a solvent present in the CO_2 recovery side of each membrane. The solvent facilitates quick CO_2 recovery, and increases the permeability and selectivity of CO_2 through the membrane (Figueroa et al., 2008).

There are many methods of implementing membranes as a CO_2 capture technique. Membranes may be applied as a sole CO_2 capture technique, in combination with solvents as shown above, as a flue gas pre-treatment step for the removal of other impurities before CO_2 capture, or as a polishing step to complement other capture techniques which may not achieve the desired CO_2 purity (Figueroa et al, 2008 and NETL, 2007).

Figure 2-6 above shows a plate-and-frame filter. The advantage of using plate-and-frame membrane filtration equipment is that there are no moving parts. The unit is less likely to fail and require constant maintenance. If solvents are not used, then regeneration energy is not needed. However, plate-and-frame filters require relatively higher downtime to remove membranes and unplug membrane pores of other gas molecules which may have condensed or

precipitated in the membrane. This disadvantage can theoretically be overcome by applying the membranes in a rotary filter, which provides continuous operation of membrane filtration and cleaning.

Many types of membranes have been studied for CO_2 capture. Common membrane material includes polymer, silica, zeolite, and ceramic material. Alumina support is used for more fragile membranes to achieve high selectivity for continuous operation.

Zeolite membranes are quite popularly investigated since the study of zeolites is well developed. This is due to its application in Fischer-Tropsch processes, and as molecular sieves. Figueroa et al. (2008) recorded zeolites to be useful in the isolation of CO_2 from CO_2-N_2 gas streams. An important advantage of zeolite membranes is their resistance to degradation, even at operating temperatures up to 673.15 K. This enables zeolite membranes to be reused over numerous cycles. Figueroa et al. (2008) stated that their use is safe and effective over 400 days before membrane replacement.

Steeneveldt et al. (2006) conducted studies on the use of ceramic porous membranes and Pd-ceramic membranes. The membrane was reported to isolate H_2 from a CO_2-H_2 gas stream, which is advantageous for IGCC and oxy-fuel combustion processes, which require separation of CO_2 and H_2. The membrane can also withstand high temperature. IEA (2004) reported however, that ceramic membranes have low CO_2 selectivity. Recovery of CO_2 can be as low as 7 %, thereby necessitating multistage membrane filtration. Ceramic membranes were also reported to be expensive.

Silica membranes were reported to isolate CO_2 from gas streams containing CH_4, O_2, N_2, and SO_2 (Figueroa et al., 2008). The use of inorganic silica can also be accompanied with alkanolamine solvents to increase CO_2 selectivity, and can be used to remove CO_2 even from flue gas containing CO_2 composition lower than 15wt%. Pore blockage however, is a fundamental drawback when using silica membranes. Significant downtime is required.

Polymer membranes are advantageous since this type of membrane has comparatively high selectivity to CO_2 (Figueroa et al., 2008), resulting in a comparatively high CO_2 recovery of 57%. Membrane filtration processes thus require fewer cycles to obtain a CO_2 stream of high purity and yield. Polymer membranes are also comparatively thin, which result in a smaller filtration apparatus. The disadvantage however, is that thin polymer membranes are weaker than zeolite or ceramic membranes and have a high risk of damage and breakage when operating under high pressure. Meisen and Shuai (1997) noted that mounting polymer membranes on strong alumina supports effectively mitigated this problem. Figueroa et al. (2008) stated that

polymer membranes are suited for pre-combustion and post-combustion CO_2 capture, even at low CO_2 flue gas compositions.

Apart from the challenge of membrane selectivity for CO_2 alone, another key disadvantage of membrane usage for CO_2 capture is the high energy penalty associated with gas compression. Membranes will only result in efficient CO_2 removal if the flue gas is at high pressure. There is also a relatively low level of development regarding the use of membranes for CO_2 capture. A balance between permeability and CO_2 selectivity needs to be found. Current membrane simulations include multistage operation, which introduce further compression costs and result in high capital expenditure. It is for these reasons that membranes are suggested mostly as a polishing step to increase CO_2 purity (Teng and Tondeur, 2006).

While the use of membranes alone is discouraged and not well researched, the combining of solvents onto membranes is receiving much attention as a feasible CO_2 capture solution. Teng and Tondeur (2006) reported that membranes combined with solvents are estimated to have the lowest energy penalty: capture rate ratio. Solvents are either combined with the membrane through a binding process, or used as a sweep fluid for easy recovery of CO_2. General efficiency results on combining MEA solvent with membranes are provided by Teng and Tondeur (2006). A similar study was done by Steeneveldt et al. (2006), which focussed on combining a polymeric membrane with DEA solvent. The use of solvents increases CO_2 recovery and enables smaller construction of membrane filtration processes (Meisen and Shuai, 1997). However, the excessive use of solvents increase energy penalty substantially, since CO_2 ultimately has to be recovered from the solvent by heating the loaded solvent in a regenerating column. A correct balance between the usage of membranes and solvents needs to be determined.

General data on membranes and membrane-solvent combinations, in comparison to other CO_2 capture techniques and strategies, are tabulated by IEA (2004).

Of particular interest currently, is the development of supported ionic liquid membranes (SILMs). Conventional membranes, such as polymer or ceramic material, are combined with ionic liquids to increase the permeability and selectivity of the membrane. Ionic liquids can also be used as liquid membranes suspended between two porous supports. The gas dissolves and diffuses into the ionic liquid through the pores of the solid supports and through the ionic liquid itself. Gas diffusion into the ionic liquid is faster than diffusion into a solid state, as with conventional membranes (Scovazzo et al., 2009).

The high viscosity of ionic liquids allows them to be well suspended in the pores of membranes. The solvent is used as an actual CO_2 capture and separation medium in the pores of the membrane, in contrast to conventional alkanolamine solvents which are typically used as sweep fluids for CO_2 recovery on the downstream side of the membrane. A further advantage of SILMs is that the contact area between gas and ionic liquid is increased (Hasib-ur-Rahman et al. 2010). Hasib-ur-Rahman et al. (2010) suggested that the mass ratio of ionic liquid:membrane material be 0.5-2:1. The disadvantage of high viscosity however is still noted, as high viscosities impede diffusion. Slow kinetics are thus achieved when using SILMs.

SILM studies include the combining of ionic liquids with poly-ether sulphone, hydrophobic poly-vinylidene fluoride (PVDF), and hydrophilic PVDF membranes. Studies on SILMs possessing conventional ionic liquids were also done by Scovazzo et al. (2009), Scovazzo (2009), Luebke et al. (2007), Park et al. (2009), and Baltusa et al. (2005).

While the idea of SILMs seems promising, they also face many of the same challenges to its application as any other membrane combined with any other solvent. The key issue is finding an optimum balance of CO_2 permeability and CO_2 selectivity over other components of flue gas. Increasing permeability often results in a decrease in selectivity, since more type of molecules can permeate through the membrane. While this remains an issue, the improvement over conventional membranes is significant due to the selectivity of ionic liquids (Seeberger et al., 2007). Moreover, Luebke et al. (2007) and Hanioka et al. (2008) noted that higher system temperature increases CO_2 permeability but decreases selectivity. The change in permeability was found to be more pronounced in larger imidazolium-based ionic liquids than smaller ones. However, small imidazolium-based ionic liquids encountered greater decreases in CO_2 selectivity. There is evidence to suggest also that membrane porosity increases at higher temperature.

The decision to use hydrophilic or hydrophobic membranes is also of high importance. Hydrophilic membranes result in higher CO_2 selectivity than hydrophobic membranes (Luis et al., 2009). However, there is a potential problem of creating water micro-environments within the membrane, causing pore blockage and ionic liquid displacement if a hydrophilic membrane is used (Lozano et al., 2011). This decreases SILM performance and selectivity, due to the increase of non-selective environments for solute transport. Moreover, hydrophobic membranes have to be used in combination with hydrophobic ionic liquids and the same applies to hydrophilic membranes and hydrophilic ionic liquids. Combining ionic liquids with membranes that possess a different affinity to water produces self-defeating results.

Knudsen et al. (2008) reported that a pilot plant in the Netherlands was constructed in 2008 which accommodates CO_2 capture using membranes combined with solvents.

2.4.3 Cryogenic separation

Cryogenic separation involves the separation of gases by a phase change. In the case of CO_2 capture from flue gas, flue gas will be cooled until CO_2 exists as a liquid or solid phase. If the process involves the precipitating of CO_2 as a solid, then the process is also popularly referred to as CO_2 anti-sublimation.

Burt et al. (2009) investigated processes that would be applicable as retrofit CO_2 capture technology for post-combustion CO_2 capture. Figure 2-7 provides an illustration of the process.

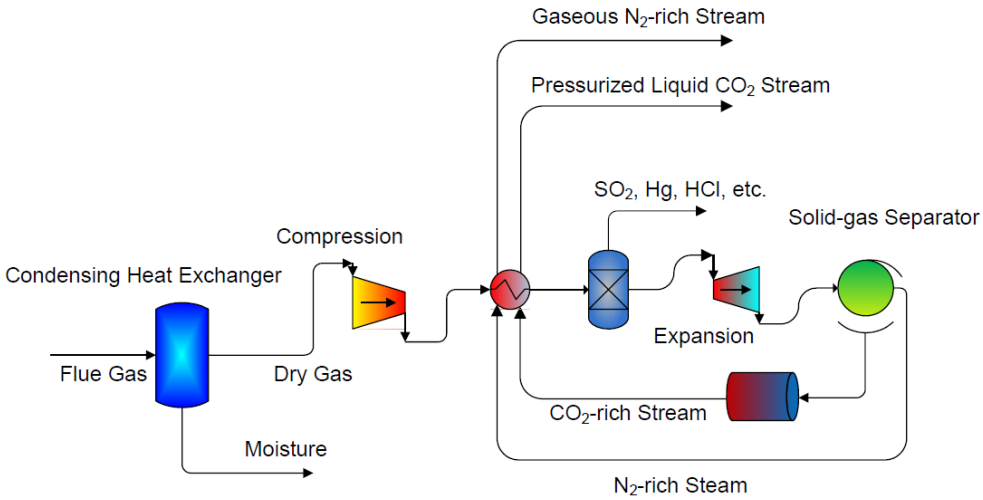

Figure 2-7: Cryogenic CO_2 Capture (Burt et al., 2009)

Flue gas is first cooled in a heat exchanger, where moisture (H_2O) is removed. The resultant dry gas is composed of N_2, O_2, CH_4, CO_2, and trace components such as SO_2, Hg, and HCl. The dry flue gas is moderately compressed and sent to a heat exchanger where the flue gas is cooled to a temperature just above the CO_2 solidification point. This temperature varies depending on the operating pressure, which needs to be optimised based on the flue gas conditions of any particular process.

A flash unit separates SO_2 and other trace compounds from the flue gas, and thereafter the flue gas passes through an expander. The further cooling caused by expansion results in the partial precipitation of CO_2. In this way, CO_2 is separated from the flue gas, which at this point consists primarily of N_2 gas. The CO_2 rich stream is further pressurised and recycled, in conjunction with the N_2 rich stream, to the heat exchanger to cool incoming dry flue gas. The temperature increase of the CO_2 rich stream during heat exchange results in CO_2 being produced in the liquid phase at elevated pressure. N_2 remains in the gaseous phase and is recovered as well.

Burt et al. (2009) claimed 99% CO_2 recovery at a freezing temperature of 138.15 K, and 99% CO_2 recovery at 153.15K. Clodic et al. (2005) concluded that a temperature of 194.65 K is required for flue gases containing 100 vol% CO_2, while 136.45 K is needed to remove CO_2 from flue gas containing 0.1 vol% CO_2.

Burt et al. (2009) did not indicate the method of refrigeration, while Clodic et al. (2005) suggested a refrigerant blend of n-butane, propane, ethane, and methane.

Burt et al. (2009) cited many advantages of cryogenic separation. Cryogenic separation can be used as a retrofit technology, which is less capital intensive than constructing IGCC and oxy-fuel combustion processes. The technology also operates in less demanding temperatures and pressures than what is required by air separation units of IGCC and oxy-fuel combustion processes. Cryogenic separation is also not sensitive to contaminants in the flue gas. Contaminants can be removed as explained in Figure 2-7 above. There is also the potential to save water and energy by utilising nitrogen as a cooling fluid.

In terms of energy comparisons, Clodic et al. (2005) claimed a 17-27% lower energy penalty than alkanolamine absorption retrofit technology. Baltus et al. (2004) stated that the cost of energy for cryogenic separation is lower than IGCC, alkanolamine absorption, oxy-fuel combustion with air separation, and membrane separation. The cost of CO_2 removal is 40% less than with alkanolamine absorption. Clodic et al. (2005) stated that the energy penalty is 647.7-1248.6 kJ/kg CO_2 depending on the composition of CO_2 in the flue gas. The energy required increases exponentially with decreasing CO_2 composition in the flue gas. At low CO_2 compositions in the flue gas of 2 vol% CO_2, the energy penalty for cryogenic separation could account for 21.95% of the total plant operational energy requirements. But for CO_2 flue gas compositions of 10 vol% or higher, the energy penalty may be as low as 11.39%. In either case, the process incurs a lower energy penalty compared to conventional alkanolamine absorption, which may account for 37.83% of the total plant energy requirements.

Not all estimates are promising however. Gottlicher and Pruschek (1997) performed estimations of electrical energy requirements of cryogenic separation in comparison to other CO_2 capture techniques. It was estimated that the energy required for cryogenic separation would be 0.6 to 1.0 kWh/kg CO_2, while solvent absorption (including physical and chemical solvents) was estimated to cost 0.09 to 0.34 kWh/kg CO_2. Gottlicher and Pruschek (1997) also estimated a relatively low efficiency of 39% for cryogenic separation in IGCC power plants, in comparison to membrane processes which achieved 42% plant efficiency. The design of the particular cryogenic separation system however, was not specified.

The benefits of high CO_2 composition makes cryogenic separation a good option especially for pre-combustion CO_2 capture, which possesses higher CO_2 compositions in the flue gas.

Different designs of cryogenic processes have been postulated and simulated. Valencia and Victory (1990) proposed two distillation column designs for cryogenic distillation enabling the recovery of solid CO_2 from the flue gas. Simulation results are presented, including compositions, temperature, pressure and flows on each tray in the designed column. Additional, older designs are also presented in McGalliard and Larrabee (1980).

The CATO programme, commissioned in Netherlands, has developed a pilot plant that also accommodates the study of cryogenic separation (VNS, 2008).

2.4.4 CO_2 capture by the formation of gas hydrates

A relatively new technique of gas separation is gas hydrate formation. The technique involves passing a flue gas mixture through chilled water. At particular optimum temperature and pressure conditions, some components of the flue gas freeze together with water molecules to form ice-like crystals where the gas molecules are trapped inside a cage of water molecules, formed through hydrogen bonding. It is for this reason that gas hydrates are known as crystalline inclusion compounds (Figueroa et al., 2008). Figure 2-8 below provides a pictorial explanation of gas hydrates.

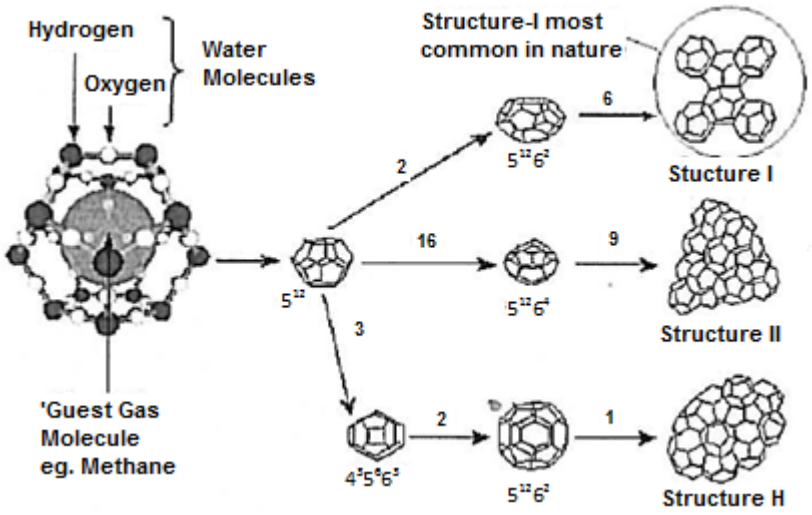

Figure 2-8: Guest Molecule Trapped inside Water Molecule, forming Hydrates (Jadhawar et al., 2006)

Hydrate formation occurs typically at low temperatures of 268.15-298.15 K, and very high pressures of 3-50 MPa (Jadhawar et al., 2006). Theoretically, CO_2 and H_2O are frozen together, forming a slurry of ice crystals in liquid water with other un-trapped gas components.

It is only certain gas molecules, of a certain size and form that may be trapped as hydrates and CO_2 is fortunately one of them. Other molecules that can form hydrates are CH_4 and to a lesser extent, N_2 (Duc et al., 2007). Other gas molecules can either be trapped in substantially different temperature and pressure conditions, or not at all, since their size is not applicable to H_2O cage cavities.

The hydrates containing CO_2 molecules can be separated from the other components of the flue gas. Thereafter, CO_2 recovery entails heating the slurry and breaking the ice cages, thereby releasing CO_2 molecules.

The use of hydrates is also being investigated in combination with membranes. Linga et al. (2007) conducted simulations using three hydrate-forming units which can collectively recover 98% of the CO_2 in the flue gas, with a final membrane filtration unit which can recover the final 2%. Membranes can also assist in removing other flue gas impurities which may be difficult for hydrate processes to separate.

The primary advantage of hydrate formation as a CO_2 capture technique is that water is used as a recyclable solvent. There are significantly fewer hazards compared to other solvents such as alkanolamines, carbonates or ionic liquids. In the event of H_2O becoming contaminated with other dissolved flue gas components, it can be disposed of and replaced at significantly lower expense compared to other solvents. Chatti et al. (2005) also noted that hydrate formation is efficient at recovering CO_2 even if CO_2 concentration in the flue gas is low. 99 % CO_2 recovery can be achieved.

One volume of hydrate is capable of accommodating 35 volumes of CO_2 (Duc et al., 2007). While this may seem advantageous in volume terms, the sheer amount of CO_2 emitted in molar terms would require large hydrate process units to completely remove all CO_2.

The main disadvantage is the demanding conditions at which this technique operates. A high energy penalty is incurred in achieving compression of up to 50 MPa, and refrigeration to as low as 268.15 K, in order to achieve hydrate formation conditions. Additives are introduced into the slurry to mitigate this problem. Duc et al. (2007) studied the use of tetra-n-butyl ammonium bromide (TBAB) and tetrahydrofuran (THF) in reducing the hydrate formation pressure. The additives reduced hydrate formation pressure to as low as 0.3 MPa, and caused hydrates to form more quickly. This was confirmed by Linga et al. (2007), who also investigated propane as an additive for flue gas containing significant H_2 together with CO_2. Park et al. (2006) noted the same effect using silica gel porous beads as an additive.

Studies into the use of ionic liquids, particularly 1-butyl 3-methylimidazolium tetrafluoroborate, were done by Chen et al. (2008). The study produced mixed results. The ionic liquid increased

the hydrate formation pressure, which was completely undesirable and counterproductive to the aim of reducing hydrate formation pressure. On the other hand, the CO_2 absorption rate increased, as more CO_2 was absorbed into the ionic liquid.

Another disadvantage is that the handling of hydrates may require substantial maintenance. Hydrate slurries can lead to pipeline plugging, a problem which requires downtime and pipeline inspection gauges to restore optimum flow. Duc et al. (2007) noted that methanol or glycol can inhibit pipeline plugging by hydrate slurries. The study also postulated and simulated multistage hydrate operation, a process which possesses much complexity. Significant studies on pipeline plugging by hydrate formation were done by Dholabal et al. (1993). Prevention of hydrate formation in offshore pipelines is a significant challenge and pilot plant studies were done to investigate methods to prevent this. Circulation loops provided better temperature control to prevent hydrate formation conditions from occurring.

The level of development of hydrate formation as a CO_2 capture solution is relatively low compared to other techniques such as solvents and membrane usage. There have however been attempts to take the technique into the phase of pilot plant study. Tam et al. (2000) planned setting up an IGCC pilot plant in the U.S.A. which caters for the study of CO_2 capture by hydrate formation. Gnanendren and Amin (2004) conducted kinetic studies on a small scale pilot plant hydrate reactor operating in semi-batch mode. Generally though, present research into the commercialisation of hydrates for CO_2 capture is done primarily through computer simulation, rather than practical trials (Duc et al., 2007 and Linga et al., 2007).

2.4.5 CO_2 capture using dry regenerable sorbents

Another method of CO_2 removal is the use of dry solid sorbents to absorb, or at least adsorb CO_2 molecules. The sorbent is then sent to a regenerator for CO_2 desorption. Refer to Figure 2-9 below. Flue gas is cooled and sent to a carbonation reactor where CO_2 is absorbed or adsorbed into the sorbents. This is a reactive process. The loaded sorbent is then transferred to a regenerator where it is heated to extract the CO_2. Sorbent is then transferred back to the carbonation reactor (Green et al., 2004).

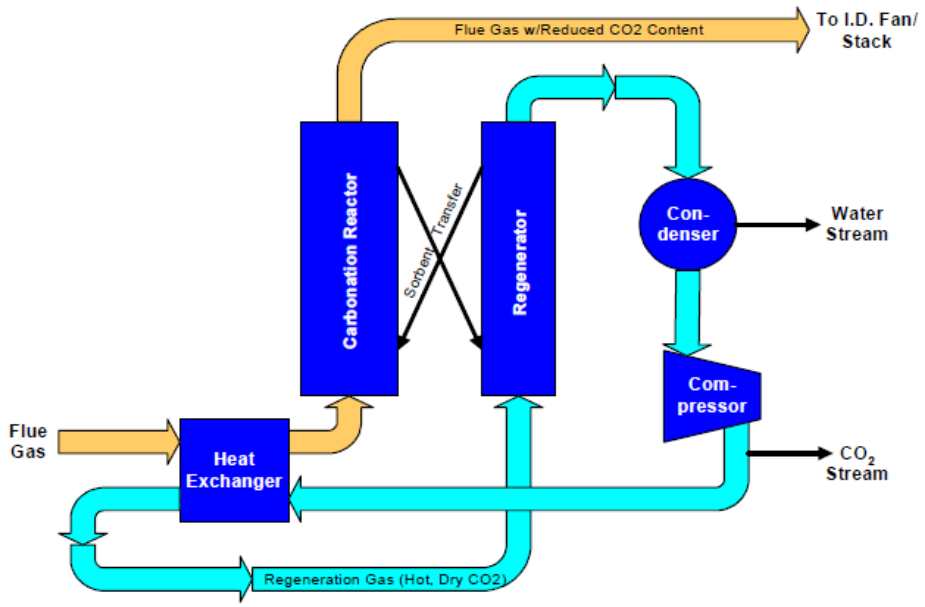

Figure 2-9: Sorbent Capture Process (Green et al., 2004)

Sorbents may occur in the carbonation reactor as a packed bed or fluidised bed. Packed bed reactors are popular for inherently porous sorbents. Sorbents occur as pellets, flakes or fine particulate matter for fluidisation processes. The process operates in batch or continuous mode, depending on the efficiency of solids handling for the sorbent.

There are many sorbents under investigation for CO_2 capture. Common sorbents include activated coal, sodium carbonate, potassium carbonate, and calcium carbonate. Green et al. (2004) studied novel sorbents for CO_2 capture such as Trona T-50, sodium bicarbonate, SBC#1, SBC#2, and SBC#3. Sorbent properties were recorded. Lee et al. (2008) investigated the use of different additives to sorbents such as inorganic binders, organic dispersants, supports, defoamers, and organic binders. Common additives in sorbents are varied amounts of sodium carbonate and sodium hydrogen carbonate. Modified sorbents such as Sorb N2A, N2B, N2C, NX, NH, and NX30 were developed in an attempt to reduce the energy penalty of the process and make sorbents more recyclable. Various properties were measured as a result, including attrition resistance. Surfactant additives were studied by Chen et al. (2011), who noted an increase in CO_2 absorption on calcium based sorbents. CO_2 recovery was 95%.

The most popularly studied sorbents are sodium carbonate and potassium carbonate. Details of their operation and associated reactions are contained in Green et al. (2004), and Zhao et al. (2008). Green et al. (2004) reported 90% CO_2 recovery in a single cycle using sodium carbonate sorbent at carbonation temperatures of 333.15-353.15 K and regeneration temperatures of 393.15-473.15K, while Zhao et al. (2008) reported 85% CO_2 recovery using potassium carbonate sorbent at a carbonation temperature of 383.15 K. While these results are

encouraging, the main problem with these sorbents is their low attrition resistance. Green et al. (2004) reported significantly reduced mass of sodium carbonate sorbent after 5 cycles of operation. While studies on potassium carbonate show good attrition resistance for 5 cycles, the sorbent began to cake due to the presence of H_2O in the flue gas (Lee et al., 2008). Irreversible reactions with contaminants such as SO_X and NO_X were also reported.

Another disadvantage of sodium and potassium carbonate is the low CO_2 capture rate. Green et al. (2004) reported a 30 minute cycle time to obtain 50% CO_2 recovery.

With conventional carbonate based sorbents being well studied, calcium based sorbents are receiving much attention in recent years. Fernández et al. (2010) studied CO_2 adsorption in ten sorbents containing varying concentrations of calcium oxide and calcium hydroxide on mesoporous molecular sieve supports. While the adsorption occurred at a very slow rate, the sorbents have been proven to be recyclable, maintaining a constant adsorption rate for over 5 cycles. Abanades (2008) studied calcium oxide sorbents. The study showed a marked decrease in adsorption over ten to fifty cycles. Three calcium based sorbents were studied under fixed bed configurations by Gray et al. (2004). The study combined alkanolamine solvents onto the sorbents at 298.15-333.15 K, and this strategy proved to be beneficial in increasing adsorption rate. A study by Chen et al. (2011) showed that a high pressure adsorption process, exceeding 0.5 MPa, increases the recyclability of calcium based sorbents.

The advantages of sorbents are their high CO_2 recovery and at relatively high operating temperatures in comparison to conventional alkanolamine solvent scrubbing. CO_2 capture can be efficient even at low CO_2 concentrations in the flue gas. Depending on the sorbent and the design of the process, the use of sorbents can have a potentially lower regeneration energy requirement than alkanolamine scrubbing (Green et al., 2004).

The main challenge facing the use of many sorbents is their low attrition resistance, which as explained above, substantially reduces efficiency and feasibility in multi-cycle operation. If the flue gas contains high amounts of water vapour, further attrition and sorbent caking may also occur. Another challenge is the expensive nature of solids handling. Some sorbent processes operate as fluidised beds and the solids thereafter need regeneration and recycle, which requires conveyor belts or compressed air blast loops. Such equipment requires relatively high maintenance.

Despite the current challenges, sorbent processes still possess enormous potential, especially with the introduction of additives and sorbent supports, as well as hybrid processes which combine sorbents with solvents. Manovic et al. (2008) explains the set up and operation of a pilot plant using sorbents for CO_2 capture. The sorbents in that particular study were able to

operate at temperatures up to 1123.15 K in a fixed bed reactor. Small scale fluidised bed pilot projects have been considered in Korea and Canada (Yi et al., 2007 and Lu et al., 2008).

2.4.6 New ideas of CO_2 capture

This section briefly explains newer, more recent strategies of CO_2 capture and recovery. Some are retrofit CO_2 capture techniques, while others are power plant modifications that can greatly improve the conditions of CO_2 capture and lower the overall energy penalty of CO_2 recovery. Some of these strategies are being actively investigated experimentally, while others are still theoretical, with any quantitative analysis being done using simulation software.

2.4.6.1 Enzyme based systems

The use of enzymes in the capture of CO_2 forms part of a wider strategy of CO_2 bio-processing. In the capture of CO_2, enzymes are used as a liquid membrane suspended between two hollow fibre supports. The flue gas passes through the liquid membrane. CO_2 is hydrated and permeates through the membrane as carbonic acid (HCO_3) much faster than O_2, N_2 and other flue gas constituents. CO_2 is recovered on the other side using a sweep gas (Figueroa et al., 2008). Figure 2-10 provides an illustration of the process.

Carbonic Anhydrase (CA) is used as a popular enzyme for CO_2 capture. Figueroa et al. (2008) reported a theoretical 90% potential CO_2 recovery using CA.

The enzyme is regenerated at ambient conditions, which is highly advantageous since it results in a significantly reduced regeneration energy penalty. This is due to the relatively low heat of absorption of CO_2 in CA. The dissolution rate of CO_2 into CA is limited by the rate of CO_2 hydration to carbonic acid. It was reported by Trachtenberg et al. (1999) that 600 000 molecules of CO_2 are hydrated by one molecule of CA.

Ge et al. (2002) performed elaborate studies on the permeability and selectivity of CO_2 in CA. The results were highly encouraging, showing CO_2 selectivities of 100 to 900 over O_2 and N_2. Studies on permeance were done, as well as the effect of different sweep gas conditions. Trachtenberg et al. (2009) reported 85.3% CO_2 removal from flue gas containing 15.4 wt% CO_2. CO_2 could be recovered with 81% purity using CA.

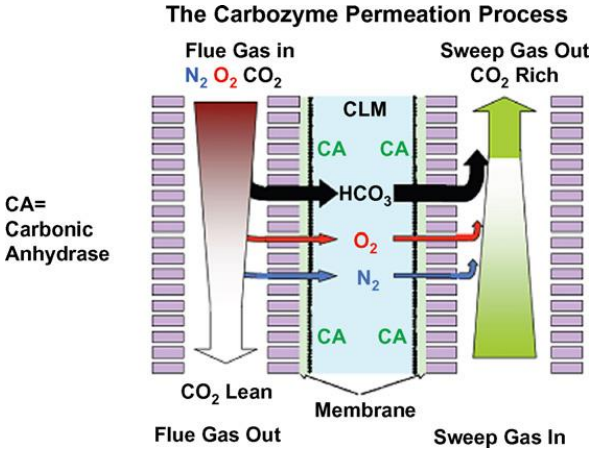

Figure 2-10: CO_2 Separation using Carbonic Anhydrase Enzyme (Figueroa et al., 2008)

The technique is relatively underdeveloped. The disadvantages are the limitations at membrane boundary layers due to pore wetting and surface fouling, scale up uncertainties, and uncertainty in long term operation. Trachtenburg et al. (2009) stated that a further disadvantage is that the enzymes are destroyed by flue gas containing high amounts of SO_X. Enzyme permeators can only operate on flue gases containing SO_X concentrations lower than 7 ppmv, which is a very demanding constraint, prompting further advancement in flue gas desulphurisation methods, or alternatively searching for more robust enzymes.

2.4.6.2 Metal organic frameworks

Metal organic frameworks (MOFs) are hybrid organic/inorganic structures containing metal ions geometrically co-ordinated and bridged with organic bridging ligands (Plasynski et al., 2008). This arrangement results in a structured system of molecules designed to increase surface area for efficient adsorption. Refer to Figure 2-11 for an illustration of metal organic frameworks.

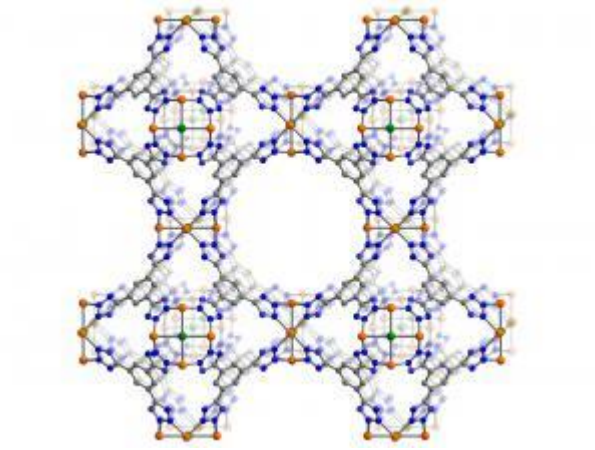

Figure 2-11: Structure of a Typical MetalOrganic Framework (MOF) (Long, 2010)

Figueroa et al. (2008) states that MOFs possess high CO_2 adsorption capacity and the regeneration energy required is lower than for conventional sorbents and solvent processes.

There are hundreds of possible MOFs that can be developed using various metal ions and organic ligands, and that can be tailor-made to suit various applications such as CO_2 capture. MOFs are used as nanoporous membranes or sorbents.

While the technology is still fairly new, studies are underway to investigate CO_2 adsorption in MOFs. Yazaydin et al. (2009) studied the adsorption of CO_2 in 14 metal organic frameworks. It was reported that MOFs containing magnesium and zinc ions provided higher CO_2 adsorption than other metal ions. This was confirmed in Simmons et al. (2011) who compared 7 different MOFs for CO_2 capture. MOF's containing zinc ions were shown to have a higher adsorption capacity and higher selectivity to CO_2 as a porous material.

Despite these few attempts, the study of metal organic frameworks is still in its infancy. However, there is great potential in this field, as the MOF possibilities are vast and this makes it highly possible that an ideal MOF can be found that would achieve feasible CO_2 capture and recovery.

2.4.6.3 Integrated gasification steam cycle

A U.S. consortium consisting of Jacobs Consultancy, Siemens, M.A.N., CO_2 Global, and Imperial College London have conducted research into a modified IGCC coal combustion process named Integrated Gasification Steam Cycle (IGSC). This process was developed in an attempt to minimise the energy penalty associated with power plants containing CO_2 capture. Waste energy is put to good use through a relatively complex system of recycle streams and turbines of varying pressure. Refer to Figure 2-12 below.

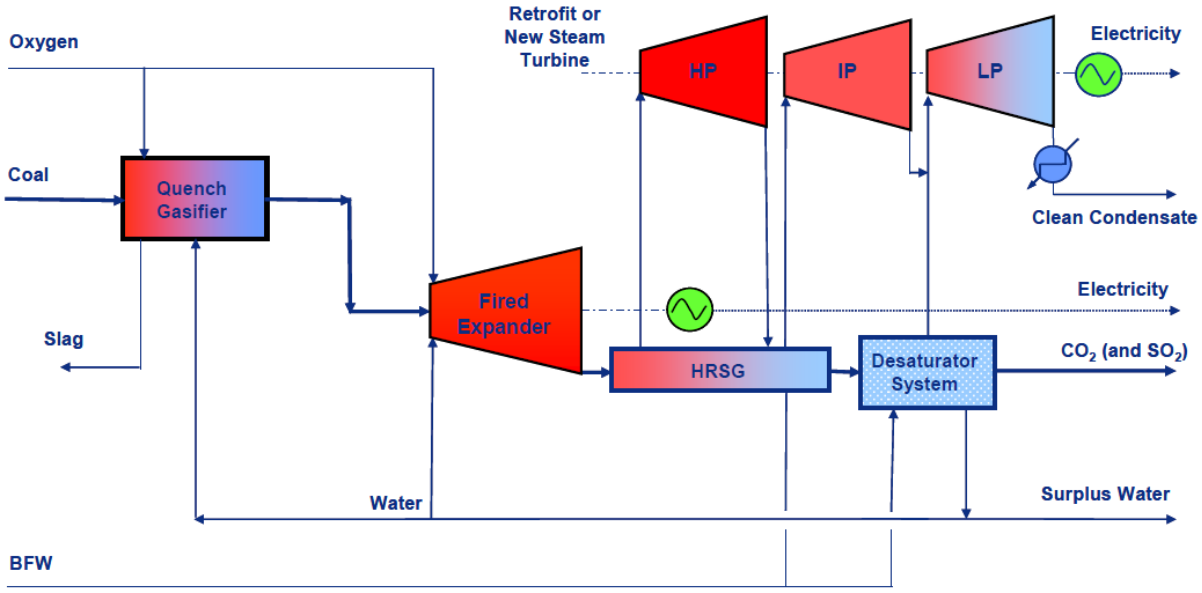

Figure 2-12: Integrated Gasification Steam Cycle (Karmarkar et al., 2009)

The process consists of a two-stage combustion system. Coal is gasified in a quench gasifier, which utilises water for the maintenance of temperature. The resultant syngas contains carbon monoxide, hydrogen gas, and oxygen gas. Combustion occurs at 1573.15-1773.15K and at high pressure (Griffiths, 2008). Combustion gases are passed through an expander to generate power. Combustion is completed in the expander, which consists of a burner connected to a gas turbine.

The exhaust heat is efficiently used to raise high pressure steam in a heat recovery steam generation (HRSG) system. This steam is then used to power an additional conventional condensing steam turbine, which can be retrofitted to the process.

Thereafter, gases are cooled in a desaturator. Water is condensed, leaving a gas stream containing primarily CO_2 with trace amounts of SO_2. The desaturator utilises recycled cooling water and if further optimised, can drive an additional low-pressure turbine (Karmarkar et al., 2009).

The process has the potential to obtain 100% CO_2 recovery and an increase in power plant output by nearly 60% (Kent, 2009). The drawback however, is the capital cost of IGSC processes. Kent (2009) estimated a capital cost for IGSC processes of $4235/kW. Most of the cost is attributed to air separation units which provide oxygen to the gasifier, without which the cost is $1801/kW. However, an internal rate of return on such an investment is claimed to range from 8% to 12%.

The process can be constructed using conventional turbines. It is claimed that the flue gas stream is available at high pressure, which would reduce CO_2 compression costs. If sulphur

content is too high, a solvent would be needed for desulphurisation. The process is designed for coal input but there are claims that it can be applied to natural gas processing as well.

The process is novel and research is being done solely by the consortium that invented it. There is hence no possibility of finding data from other independent sources. There is however, abundant information available from the consortium (Karmarkar et al., 2009).

2.4.6.4 Chemical looping combustion

This technology is not specifically a CO_2 capture technique, but rather a modification of the traditional oxy-fuel combustion concept. While oxy-fuel combustion utilises pure oxygen gas, chemical looping combustion utilises oxygen derived from metal oxides, during redox reactions. The process is shown in Figure 2-13 below.

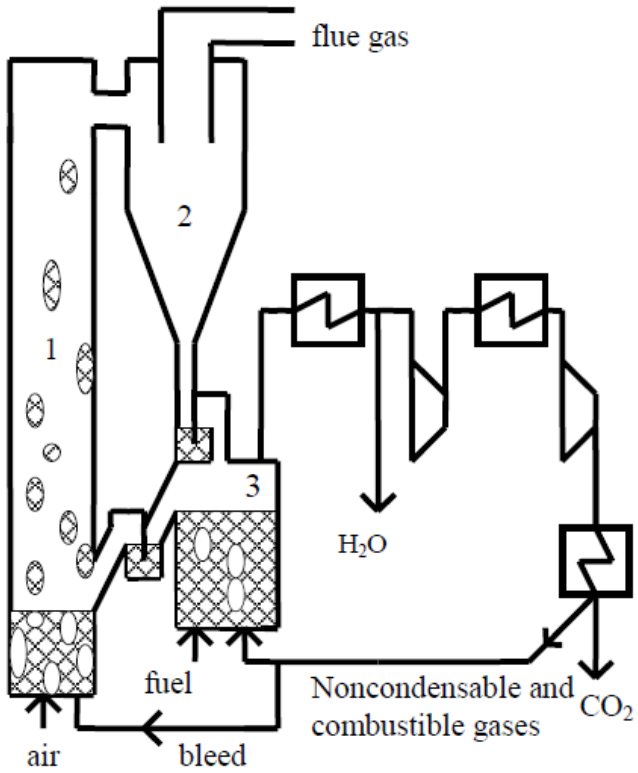

Figure 2-13: An illustration of Chemical Looping Combustion (Mattisson and Lyngfelt, 2001)

This process typically uses two fluidised bed reactors, namely the air reactor (1) and fuel reactor (3). Particulate metal or metal oxide is oxidised in the air reactor using air. The metal oxide now acts as an oxygen carrier. The oxygen carrier is then separated from unreacted components of air in a cyclone (2). The air, containing N_2, unreacted O_2 and inherent CO_2, is emitted as flue gas into the atmosphere, while the particulate oxygen carrier is transferred into the fuel reactor (3).

The metal oxide is reduced during a combustion reaction with hydrocarbon fuel. The reduced metal oxide is recycled to the air reactor. The resulting hot flue gas from the fuel reactor contains mainly CO_2 and H_2O and can be used to drive turbines or alternatively heat a separate steam cycle loop which would be used to drive turbines.

The metal oxides are transferred between reactors using conveyor belt systems or more popularly using compressed air blasts. The pressurised air acts as a medium of transfer while also oxidising the metal simultaneously before separation and entry into the fuel reactor. Since the oxidation reaction is exothermic, the compressed air also heats the oxide while transferring it to the fuel reactor, thereby assisting in efficient reduction.

The general reactions of the air and fuel reactor are:

Air reactor: $O_2 + 2Me \rightarrow 2MeO$.....(R2-14)

Fuel reactor: $C_nH_{2m} + (2n + m)MeO \rightarrow nCO_2 + mH_2O + (2n+m)Me$.....(R2-15)

The reactions in the chemical looping combustion process occur typically at 1173.15-1573.15 K (Mattisson, 2007). Different metal oxides can be used as the oxygen carrier, such as Fe_2O_3/CuO and $MgAl_2O_4$ (Wang et al., 2010). More recently studied oxygen carriers include nickel, manganese and calcium oxides (Fang et al., 2009). In order to maintain consistency in particulate size and shape, Mattisson (2007) investigated the use of support material such as Al_2O_3, TiO_2, SiO_2, sepiolite, and $MgAl_2O_4$.

The advantage of chemical looping combustion, as with oxy-fuel combustion, is that the flue gas contains primarily CO_2 and H_2O, which can be separated by cryogenic means or multistage condensation as shown in Figures 2-12 or 2-13 with simultaneous driving of turbines. NETL (2007) reported that CO_2 can be available in the flue gas at 31 wt%, which is significantly higher than CO_2 concentrations in flue gases emitted by conventional pulverised coal (PC) power plants. Aside from cryogenic separation or simple condensation, other post-combustion CO_2 capture techniques can also be used in this process, such as physical or chemical absorption (Figueroa et al., 2008).

The benefit of chemical looping over oxy-fuel combustion is that there is no need for an air separation unit (ASU) to provide pure oxygen to the combustion reaction. Current ASU technologies have high operating costs and are a major challenge to the implementation of oxy-fuel combustion. Chemical looping eliminates this challenge.

The current disadvantage of chemical looping is the lack of development and high cost of the technology. Chemical looping is a new coal combustion process. It is not a retrofit CO_2 capture

technique. Significant capital investment would be required to replace old existing power plant processes with chemical looping. The technology is highly promising for the construction of new power plants, but the feasibility of replacing conventional power plants with chemical looping remains uncertain.

Another challenge to implementation is choosing an ideal oxygen carrier. The main drawback to the process is the formation of side reactions in the air and fuel reactor, as a result of oxygen being supplied through a carrier as well as impurities that can enter during introduction of the metal oxides. A carrier is yet to be found, which ensures efficient oxidation and transfer of oxygen and the burning of fuel without producing undesirable products due to side reactions (Wall and Liu, 2008). Fang et al. (2009) provides a summary of the common oxygen carriers that are currently under investigation. Mattisson and Lyngfelt (2001) studied the reactivity and conversion rates of various oxygen carriers at temperatures of 873.15-1473.15 K.

Chemical looping also has potential applications in Fischer-Tropsch (FT) processes such as coal-to-liquids (CTL) and gas-to-liquids (GTL) processes (Mattisson and Lyngfelt, 2001). Cost estimates were done by NETL (2007), which found that chemical looping may have lower capital costs than conventional CTL and GTL processes. IEA (2004) also conducted capital and operating cost estimates. The study found chemical looping to be more efficient and cost effective than IGCC processes.

Wall and Liu (2008) state that most of the research on chemical looping that is currently underway is in the finding of a suitable oxygen carrier. Despite this drawback, a pilot plant has been developed in Sweden to investigate the industrial operation of chemical looping (Mattisson, 2007 and Mattisson and Lyngfelt, 2001).

All CO_2 capture techniques, as well as power plant operations and the potential for Carbon Capture and Storage in South Africa have also been documented in a manuscript titled "Review of Carbon Dioxide Capture and Storage With Relevance to the South African Power Sector" recently published in the South African Journal of Science. A copy is available electronically in the attached CD.

2.5 The choice of CO_2 capture technique to investigate

It is of great urgency that the reduction of CO_2 emissions be achieved, in order to contribute towards the realisation of the goal to reduce the rate of climate change, particularly global temperature increase.

The principle, advantages, and disadvantages of each CO_2 capture strategy have been explained in previous sections. While this study requires a review of all techniques, a decision was made regarding which technique to investigate with greater depth. The primary purpose of this study was to investigate a CO_2 capture technique that has high potential for industrially feasible CO_2 capture from South African coal power plants in the near future.

Despite the numerous advantages of many other CO_2 capture techniques, gas absorption using solvents still remains the most promising solution for CO_2 capture and recovery. Absorption and stripping are industrially developed technologies which are implemented in other gas treatment processes such as denitrification and flue gas desulphurisation. Process constraints, principles, parameters, equipment design and optimisation models are hence well developed and easily adaptable to the purpose of CO_2 capture.

In addition to this distinction, there are many possible solvents that are under investigation for CO_2 capture. The most studied solvents are alkanolamine and carbonate based solvents. However, there is also high potential for the use of hybrid and blended solvents. The concept of utilising ionic liquids as solvents for CO_2 capture further emphasises the potential that gas absorption using solvents has, as a CO_2 capture technique.

This study shall consider the use of ionic liquids, as well as hybrid solvents containing alkanolamines and ionic liquids, as possible solvents for feasible CO_2 capture. A review of ionic liquids was conducted, including introductory information, ionic liquid synthesis, advantages, disadvantages, and types or classification of ionic liquids, such as room temperature ionic liquids (RTILs) and task-specific ionic liquids (TSILs).

Thereafter, a review of the study of ionic liquids for CO_2 absorption was conducted. This included analyses of CO_2 Henry's Law constants, CO_2 solubility, CO_2 mole fraction, enthalpy and entropy of absorption of CO_2 in ionic liquids. A review of ionic liquid density, heat capacity, and viscosity was also conducted.

2.5.1 Ionic liquids

Ionic liquids are solvents composed of organic cations and inorganic or organic anions. While the liquid is composed entirely of ions, it is a neutral liquid overall. Ionic liquids differ from ionic solutions, which are solutions of a salt in a molecular solvent such as water, as shown in Figure 2-14 below. Ionic liquids contain no molecules, only ions.

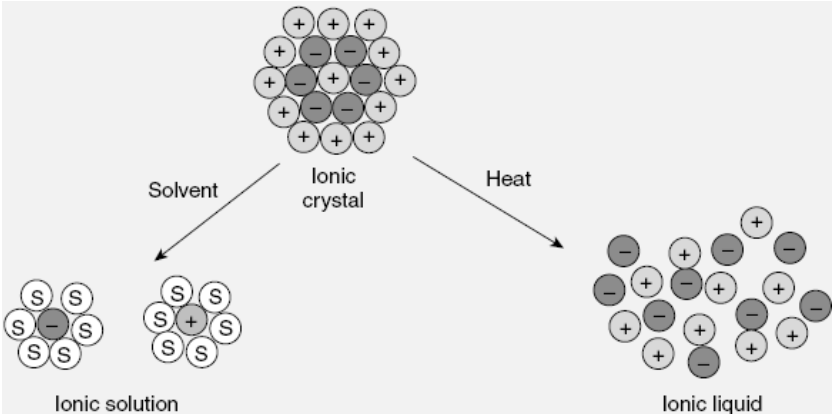

Figure 2-14: Difference between Ionic Solutions and Ionic Liquids (Othmer, 2008)

Molten salts are also regarded by some as ionic liquids since the heating of a salt produces a liquid comprised entirely of ions. However, others argue this claim since molten salts exist as liquids only at high temperatures, whereas other ionic liquids are in the liquid phase for a wide temperature range, including room temperature (Arshad, 2009). Older names for ionic liquids include liquid organic salts, fused salts, ionic melts, non-aqueous ionic liquids (NAILs), ionic fluids, and room temperature molten salts (Othmer, 2008).

The concept of ionic liquids was first developed in the early 20th century, but interest in them only rose in the 1950's, due to their theoretical potential as solvents and extractants (Welton, 1999). The first stable ionic liquids over a broad range of temperatures were created in the 1990's (Sen and Paolucci, 2006). Since then, hundreds of stable ionic liquids were discovered, containing different cation-anion combinations. Arshad (2009) conducted a study on the development of ionic liquids. The study found an exponential increase in publications and patents on ionic liquids and ionic liquid handling processes as shown in Figure 2-15 below.

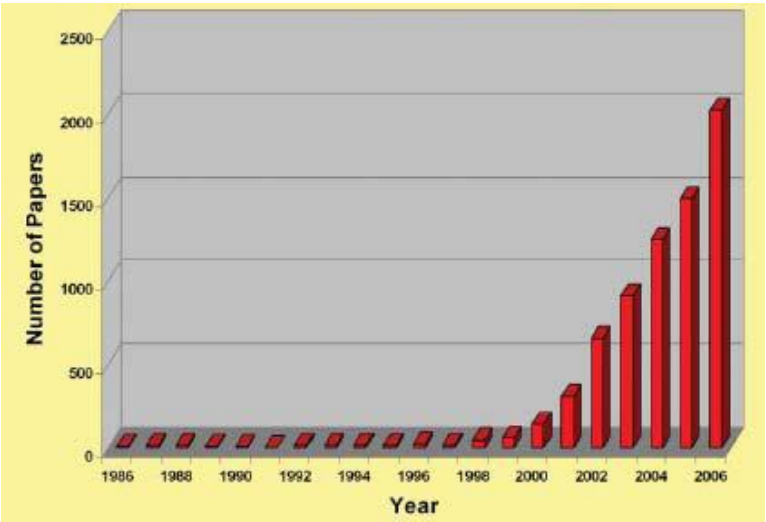

Figure 2-15: Number of Ionic Liquid Publications over the Period: 1986-2006 (Arshad, 2009)

The common cations currently under investigation are imidazolium (im), pyridinium (py), tetraalkylammonium, and tetraalkylphosphonium based cations as shown in Figure 2-16 (Anderson et al., 2007):

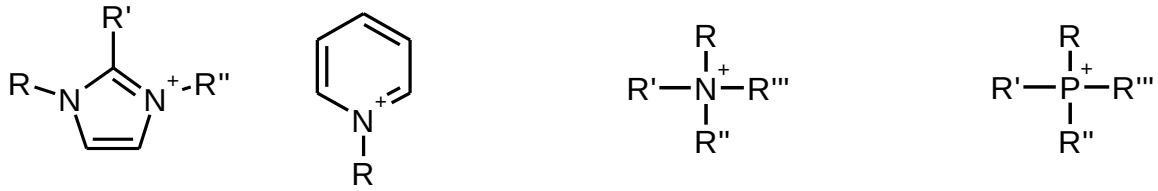

Imidazolium Pyridinium Tetraalkylammonium Tetraalkylphosphonium

Figure 2-16: Common Ionic Liquid Cation Precursors

Cations include 1-hexyl-3-methylimidazolium (hmim), 1-hexyl-2,3-dimethylimidazolium (hmmim), 1-butyl-3-methylimidazolium (bmim), 1-pentyl-3-methylimidazolium ($p_5$mim), 1-n-ethyl-3-methylimidazolium (emim), 1-hexyl-3-methylpyridinium (hmpy), and tetrabutyl ammonium (N_{4444}), as shown in Figure 2-17 below (Muldoon et al., 2007, Fredlake et al., 2004).

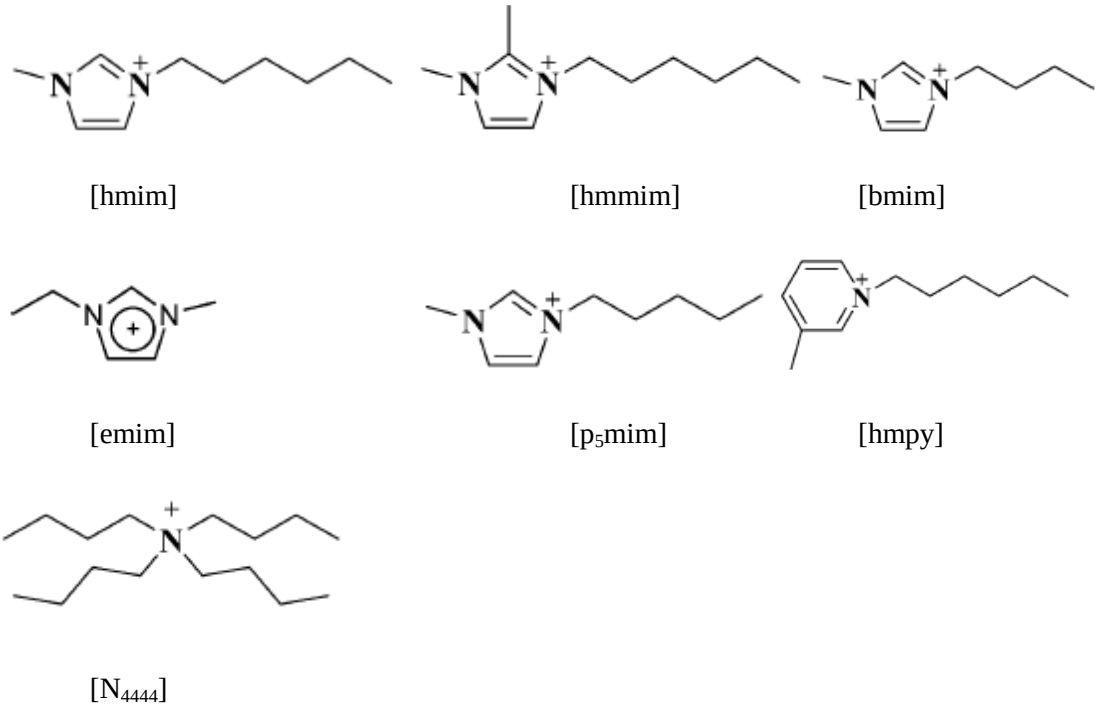

[hmim] [hmmim] [bmim]

[emim] [$p_5$mim] [hmpy]

[N_{4444}]

Figure 2-17: Common Ionic Liquid Cations

Common anions are Cl^-, Br^-, NO_3^-, dicyanimide (DCA^-), as well as fluorinated anions such as hexafluorophosphate (PF_6^-), bis(trifluoromethylsulphonyl) imide (Tf_2N^-), tetrafluoroborate (BF_4^-), tris(pentafluoroethyl) trifluorophosphate (eFAP), tris(heptafluoropropyl) trifluorophosphate

(pFAP), and tris(nonafluorobutyl) trifluorophosphate (bFAP) as shown in Figure 2-18 below (Sen and Paolucci, 2006, Muldoon et al., 2007, Fredlake et al., 2004):

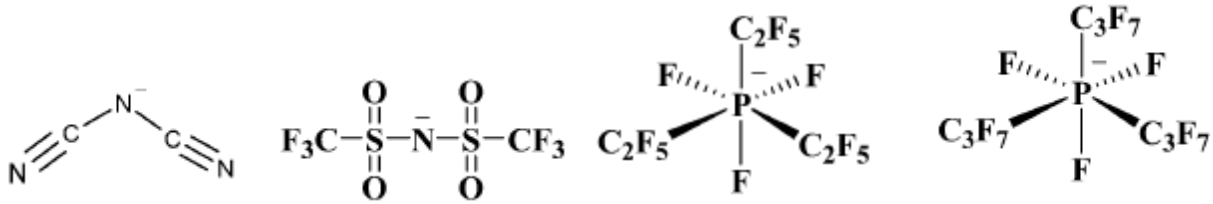

[DCA] [Tf_2N] [eFAP] [pFAP]

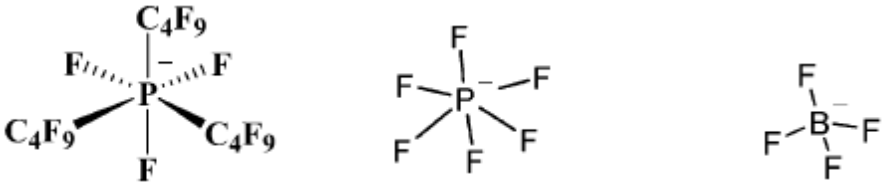

[bFAP] [PF_6] [BF_4]

Figure 2-18: Common Ionic Liquid Anions

While the above cations and anions are commonly studied and form conventional ionic liquids, there are many other cations and anions being synthesized to form optimised ionic liquids for particular applications (Anderson et al., 2007). Wappel et al. (2009) and Anderson et al. (2007) explained that there are millions of ionic liquids that can be synthesized and studied for various uses.

Arshad (2009) summarised the potential uses of ionic liquids. They may be used for obtaining the recovery of biofuels, liquid extractions, desulphurisation processes, heat storage, solar cell applications, membrane technology and catalysis. This study however, focuses on the use of ionic liquids in gas absorption, particularly the absorption of CO_2 from coal power plant flue gas. Arshad (2009) also provided a table citing the main companies that are synthesising and researching ionic liquids for various potential uses.

2.5.2 Synthesis of ionic liquids

While some ionic liquids, such as fluorinated, imidazolium based ionic liquids are available commercially, most ionic liquids are presently still synthesized in laboratories. While the method of synthesis is becoming increasingly unique due to various functionalisations, two conventional methods were found to be most prominent.

Abdul-Sada et al. (1997) and Holbrey and Seddon (1999) outlined the method of ionic liquid synthesis as shown in Figure 2-19. In the case of imidazolium based ionic liquids, which are of particular interest for gas absorption, ionic liquid synthesis first begins by the alkylation of 1-methyl-imidazole using an alkyl halide. A 1-alkyl-3-methylimidazolium precursor is the product. Currently, this precursor is becoming increasingly available from commercial suppliers, eliminating the need for the first step (Holbrey and Seddon, 1999). The temperature of the reaction for the first step varies depending on the ionic liquid that is intended to be synthesized. Holbrey and Seddon (1999) stated that the preparation temperature for the first step may be as low as 273 K, while Arshad (2009) suggested temperatures up to 363.15 K. The reaction is usually carried out at room temperature for most ionic liquids.

Physically, the alkyl halide is added drop-wise to stirred 1-methyl-imidazole. Depending on the quantity (laboratory or commercial), stirring may be done using a stirrer and beaker or using an autoclave. Ibrahim (2011) recommended a magnetic stirrer be used. Depending on the ionic liquid that is to be produced, the reaction is carried out in an ice bath since the reaction is highly exothermic. 3-5 drops of alkyl halide may be added every 5 minutes.

For other ionic liquids, the first step is the same, but starts with different reactants. To produce a 1-alkylpyridinium or 1-alkyl-2,3-dimethylimidazolium derivative, pyridine or 1,2-dimethylimidazole is reacted with an alkyl halide respectively (Arshad, 2009). Ibrahim (2011) however stated that imidazolium-based ionic liquids are the easiest and cheapest to synthesize, while pyridinium-based ionic liquids require more advanced equipment such as an autoclave and microwave reactor for synthesis of the precursor.

The ionic liquid precursor is then purified either by vacuum filtration, or by repeated washing with organic solvents such as ether. The ionic liquid precursor is then dried in a dessicator. The precursor may exist in liquid form, or as a solid salt which requires heating (Ibrahim, 2011).

Thereafter there are two reaction and separation paths for synthesising and purifying the ionic liquid. The ionic liquid precursor can undergo ion-exchange, where the precursor is exchanged with a Group I metal anion or an anion of a silver (I) salt (Holbrey and Seddon, 1999), represented as M[Y] in Figure 2-18. Alternatively, the precursor may undergo acid treatment (represented by H[Y] in Figure 2-18). Arshad (2009) stated that both of these methods are carried out at room temperature and in water, or other organic solvents, to produce the ionic liquid and halide products. Ibrahim (2011) suggested an ethanol:water solvent ratio of 4:1. Ethanol is used to dissolve the precursor, while water is present to dissolve M[Y] as shown in Figure 2-19.

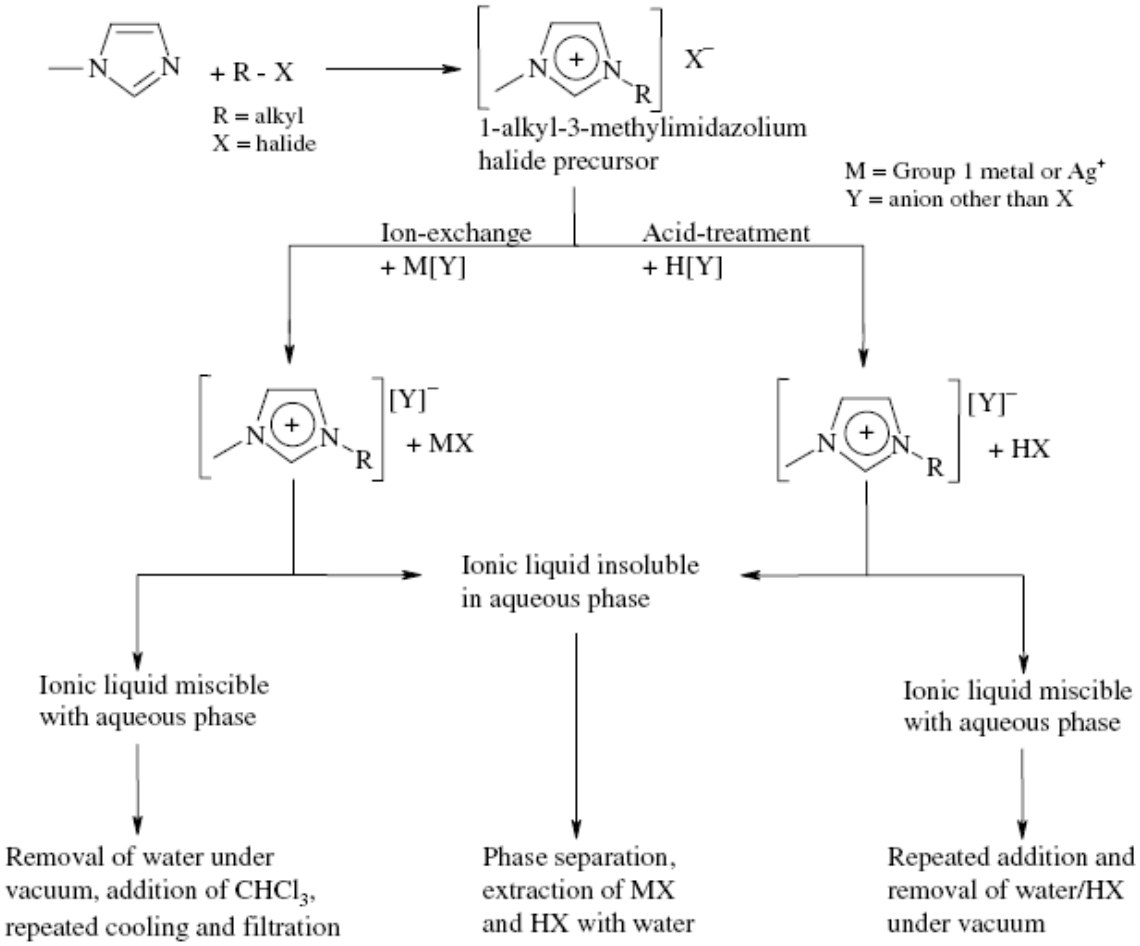

Figure 2-19: Synthesis of Ionic Liquids (Arshad, 2009)

Product separation differs depending on the ionic liquid produced. If the ionic liquid is insoluble in the solvent it was produced in (usually water), then phase separation by liquid-liquid extraction may be applied, removing the solvent and excess halide derivatives. The extraction may be conducted at room temperature and pressure conditions. However, Holbrey and Seddon (1999) noted easier separation if temperatures up to 343 K and vacuum were applied.

If the ionic liquid is water miscible, then the method of separation varies according to whether ion-exchange or acid treatment was the method of ionic liquid synthesis. If the ionic liquid was produced by ion exchange, then separation entails the removal of water under reduced pressure and cooling to 278.15 K to precipitate MX (Arshad, 2009). Trichloromethane additive facilitates precipitation. Ionic liquids produced by acid treatment require repetitive washing with water to eventually remove the water together with HX. This is done at elevated temperatures up to 343.15 K (Holbrey and Seddon, 1999 and Arshad, 2009). It is also possible to determine a

solvent that would selectively absorb unreacted compounds in order to purify the ionic liquid (Ibrahim, 2011).

Thin layer chromatography (TLC), gas chromatography mass spectrometry (GCMS), and high performance liquid chromatography (HPLC) are used to test the purity of the ionic liquid product. The method of purity testing depends on how high the viscosity of the ionic liquid is, and if the boiling point of the ionic liquid is lower than its decomposition temperature (Ibrahim, 2011).

While the above methods form the basis of ionic liquids synthesis, various other unique techniques are applied by other sources in the production of functionalised ionic liquids.

2.5.3 Advantages of ionic liquids

There is a myriad of different structures and variation possibilities of cations and anions (Wappel et al., 2009), which can result in literally millions of ionic liquids. The potential for finding ionic liquids that provide feasible operation in different processes is hence very high. Functional groups can be added to ionic liquids to optimise physicochemical properties such as the melting point, viscosity and thermal conductivity of the liquid (Huang and Rüther, 2009, Anderson et al., 2007). The addition of a functional group can result in the ionic liquid behaving as a chemical solvent rather than a physical one (Anderson et al., 2007). Desirable absorption rates and capacity can also be achieved in this way. Anderson et al. (2007) stated that ionic liquids could also be tuned to be hydrophobic or hydrophilic, depending on the intended use. The acidity of the ionic liquid, electrochemical stability, electrical conductivity, and ion mobility were also reported to vary with different cations and anions (Dias and Oliveira, 2010).

Ionic liquids have low volatility, low melting point and high thermal stability (Maginn, 2005, Anderson et al., 2007, and Sen and Paolucci, 2006). Many ionic liquids were reported to have decomposition temperatures greater than 573 K (Hasib-ur-Rahman et al., 2010). Anderson et al. (2007) reported ionic liquid decomposition temperatures ranging from 473 to 673 K. Dias and Oliveira (2010) found that some ionic liquids remain liquid even at temperatures above 573 K. Their low volatility was reported to result from strong interaction of ions due to Coulombic forces (Dias and Oliveira, 2010). This is an advantage in absorption processes as there would be negligible solvent losses during regeneration, through evaporation and entrainment (Anderson et al., 2007, Brennecke and Gurkan, 2010, Huang and Rüther, 2009). This provides little risk of the CO_2 gas stream being contaminated with solvent during regeneration, making ionic liquid solvents applicable to absorption, scrubbing, and even membrane processes (Zhao et al., 2005).

There is also little risk of ionic liquids causing air pollution, due to their low volatility (Maginn, 2005).

The low melting point and non-flammable nature of ionic liquids also enables their use in refrigeration and various other studies at room temperature (Sen and Paolucci, 2006, Huang and Rüther, 2009).

The low corrosivity of ionic liquids enables their use as undiluted solvents (Maginn, 2005, Anderson et al., 2007, and GovMonitor, 2010). This is a crucial advantage in CO_2 absorption processes. Alkanolamines are corrosive towards industrial equipment, and thus require dilution with water, to be used as solvents for CO_2 absorption. Generally, alkanolamine solvents are composed of 50 to 70 wt% H_2O, with 30 to 50 wt% alkanolamine. This increases the cost of solvent regeneration, since H_2O has a relatively high heat capacity. Moreover, solvent losses occur during regeneration because H_2O has relatively high volatility. Ionic liquids on the other hand don't need to be diluted. In their pure state, many ionic liquids are not corrosive (Brennecke and Gurkan, 2010, Wappel et al., 2009). In addition to this, many ionic liquids such as [bmim][PF_6], [C_8mim][BF_4], and [C_8mim][PF_6] are hydrophobic, which results in H_2O from flue gases being selectively rejected during absorption (Hasib-ur-Rahman et al., 2010).

Ionic liquids generally possess heat capacities which are three times lower than alkanolamine solvents (Hasib-ur-Rahman et al., 2010, Sen and Paolucci, 2006). Regeneration of the solvent is less energy intensive. GovMonitor (2010) estimates a regeneration energy reduction of up to 60%, in comparison to conventional alkanolamine solvents (GovMonitor, 2010). Hasib-ur-Rahman et al. (2010) suggested that pressure sweep and vacuum treatment processes can even be used when regenerating ionic liquid solvents. Solvents can be regenerated by adding heat or using N_2 gas to change pressure.

The low solvent regeneration required is also due to the fact that ionic liquids are physical solvents. CO_2 undergoes a physical absorption mechanism. Enthalpy of CO_2 absorption is typically 10 to 20 kJ/mol in ionic liquids, which is comparatively four times lower than the energy required to remove CO_2 from alkanolamine solvents (Huang and Rüther, 2009).

Huang and Rüther (2009) reported that ionic liquids are generally chemically stable, and resistant to oxidation and reaction with impurities. This and other factors mentioned above, make ionic liquids more easily recyclable than alkanolamine solvents (Anderson et al., 2007, Sen and Paolucci, 2006).

Solvent absorption is a well developed technique involving gas and liquid handling. Ionic liquids can be easily integrated into absorption processes, to take the place of less efficient and less feasible solvents. No novel processes and equipment designs may be necessary.

GovMonitor (2010) and Anderson et al. (2007) reported ionic liquids to be of high CO_2 selectivity. This is advantageous for CO_2 disposal processes. On the other hand, many ionic liquids have good solvation properties for other gases such as H_2S, SO_2 and CH_4 (Anderson et al., 2007). This introduces the possibility of absorbing multiple harmful gases from flue gas streams at the same time.

2.5.4 Disadvantages of ionic liquids

The main disadvantage of the ionic liquids studied so far, is their high viscosity (Wappel et al., 2009, Bates et al., 2002). Hasib-ur-Rahman et al. (2010) reported ionic liquid viscosities to be up to 40 times higher than alkanolamine solvents. Ionic liquid viscosity generally ranges from 20-2000cP. Anderson et al. (2007) reported ionic liquid viscosities of up to 10000 cP. The high viscosity of ionic liquids is attributed to strong molecular interaction between cations and anions (Huang and Rüther, 2009). This restricts the use of ionic liquids in industry, due to the high circulation energy that would be required for its application. Regarding fluid mechanics, high viscosity decreases the Reynold's number, a conclusive reflection of flow patterns and regimes. Absorption kinetics is also lowered due to lower diffusion coefficients. This reduces the rate of absorption/desorption of CO_2 and other gases (Huang and Rüther, 2009, Wappel et al., 2009). A further issue is that the density and viscosity of ionic liquids increases upon absorption of CO_2 and other gases (Brennecke and Gurkan, 2010, Zhang et al., 2009, Huang and Rüther, 2009).

There is uncertainty and disagreement on the effects of combining alkanolamines and other functional groups to ionic liquids. Hasib-ur-Rahman et al. (2010) suggested combining ionic liquids with alkanolamines to reduce viscosity. However, Huang and Rüther (2009) claimed that attaching amine functional groups to ionic liquids may increase the viscosity of the solvent. Viscosities of ionic liquids containing amines are reported to be 13 to 15 times higher than pure ionic liquids. On the other hand, adding primary amines such as mono-ethanolamine (MEA), by means of attaching amine functional groups to cations, were also reported to increase CO_2 absorption capacity (Huang and Rüther, 2009). The same effect can be achieved with secondary and tertiary amines but absorption capacity is not increased as significantly as when primary amines are combined. Liu et al. (2011) investigated the effect of attaching Zn to ionic liquids. The viscosity was reported to be 43 times higher than conventional room temperature ionic liquids.

The addition of H_2O to the ionic liquid also produces mixed results. Hasib-ur-Rahman et al. (2010) suggested that H_2O can be added to reduce viscosity. However, it is uncertain what effect H_2O has on CO_2 solubility of the ionic liquid. Some sources note a decrease in solubility and others note an increase, while some sources note a negligible effect (Huang and Rüther, 2009).

The use of ionic liquids is a relatively new development and ionic liquids are currently very expensive (Wappel et al., 2009). Many companies are currently producing lab quantities of ionic liquids rather than industrial quantities, bringing the cost of many ionic liquids to approximately $1-10/g ionic liquid (Arshad, 2009, Baltusa et al., 2005). Arshad (2009) also stated that the technology also lacks reliable physical data due to pure ionic liquids being made available only recently.

A further consequence of the lack of experience of working with ionic liquids is that there is a lack of toxicological data on most ionic liquids (Arshad, 2009, Hasib-ur-Rahman et al., 2010).

There have been some studies on the toxicity of ionic liquids. Fluorinated ionic liquids are found to be toxic and have low biodegradability (Muldoon et al., 2007). Increasing fluorination of anions and cations increases toxicity. Due to the low volatility of ionic liquids, there is minimal risk of air pollution. It is for this reason that many sources refer to ionic liquids as "green solvents", posing no air pollution hazard. However, water pollution can be caused by toxic ionic liquids, if leakages and spillages occur (Hasib-ur-Rahman et al., 2010). Lozano et al. (2011) also reported that fluorinated anions such as PF_6 could degrade to form HF, with is an environmental hazard.

Like many other physical solvents, ionic liquids have low CO_2 absorption capacity at low pressure, in comparison to alkanolamine solvents which are chemical solvents (Brennecke and Gurkan, 2010, Huang and Rüther, 2009). This is a drawback particularly for post-combustion CO_2 capture, which produces flue gas with low CO_2 partial pressure, less than ambient pressure (Huang and Rüther, 2009). CO_2 absorption using ionic liquids are optimised at high pressure and low temperature, but the flue gas in coal industries is available at low pressure and high temperature (Huang and Rüther, 2009). Increasing flue gas pressure and lowering temperature increases operational costs and hence decreases feasibility.

A popular solution to increasing the CO_2 solubility and absorption rate, is to increase fluorination of the anion, and to a secondary extent the cation (Anderson et al., 2007). Increasing the length of alkyl chains in the cation also improves absorption capacity. However, this also increases viscosity and toxicity of the solvent (Hasib-ur-Rahman et al., 2010).

Brennecke and Gurkan (2010) suggested the addition of an amine functional group to the cation of ionic liquids, in order to increase absorption capacity. The use of non-fluorinated ionic liquids results in low CO_2 solubility in comparison to fluorinated ionic liquids. Muldoon et al. (2007) suggested the addition of ethers and flexible alkyl chains to increase free volume of the liquid and hence have a high affinity and absorption rate for CO_2.

The industrial implications of flue gas water content produce conflicting results. While many ionic liquids are hydrophobic, many others are hydrophilic and this is a disadvantage for the treatment of flue gas which contains H_2O. H_2O gets absorbed into the ionic liquid in the absorber, thereby increasing the energy required for solvent regeneration in the stripper. However, ionic liquids containing low water content are claimed to provide higher CO_2 solubility (Huang and Rüther, 2009, Wappel et al., 2009). Although the hydrophilicity of ionic liquids poses a disadvantage, the regeneration energy required is still lower than for alkanolamine solvents, which contain 50-70 wt% H_2O (Brennecke and Gurkan, 2010).

While ionic liquids are highly selective towards CO_2, they are not exclusively selective to this gas. Many ionic liquids also absorb SO_2, H_2S, CH_4, and SO_2 along with CO_2 (Anderson et al., 2007, Shokouhi et al., 2010, Huang and Rüther, 2009). Some literature sources present this as an advantage. However, problems arise regarding the disposal of these absorbed gases, which ultimately need to be separated from each other.

2.5.5 Types of ionic liquids

On an atomic level, ionic liquids consist of anions and cations. They are categorised according to the structure of different anions and cations, the conditions at which their performance is measured, or the purpose for which they were synthesised. This categorisation is informal and not standardised, but offers convenient grouping when comparing different ionic liquids, especially since there are thousands of possible ionic liquids that may be synthesized and have potential uses commercially.

This section addresses two relevant categories of ionic liquids.

2.5.5.1 Room temperature ionic liquids (RTILs)

Room temperature ionic liquids (RTILs) refer to ionic liquids that are tested for their absorption performance as solvents, under room temperature or near room temperature conditions. These ionic liquids form the bulk of what is considered conventional ionic liquids. They are generally available commercially, albeit in laboratory scale quantities and at relatively high cost.

The RTILs investigated for CO_2 capture generally consist of imidazolium based cations with fluorinated anions, although there are exceptions to this. CO_2 absorption is studied at temperatures of 293.15 K to 313.15 K, at CO_2 partial pressures up to 2 MPa. There are exceptions and variations in opinion of the maximum pressure and temperatures that constitute RTIL studies.

Bara et al. (2010) investigated the use of RTILs for CO_2 capture. Three imidazolium-based RTILs were synthesized and CO_2 absorption measurements were done at ambient temperature and a CO_2 partial pressure of 0.101325 MPa. A review of RTILs was done by Hasib-ur-Rahman et al. (2010), including CO_2 absorption measurements using a thermo-gravimetric microbalance. CO_2 mole fraction and Henry's Law constants were recorded for CO_2 at various partial pressures up to 1.5 MPa, mainly at 298.15 K but with some measurements done at temperatures up to 323.15K. Results are presented in Table 2-4 and Table 2-6.

Palgunadi et al. (2009) investigated absorption of CO_2 in fluorine-free phosphate RTILs at temperatures of 313 to 333 K and CO_2 partial pressures of up to 5 MPa. This was done based on the RTIL's performance within general RTIL measurement ranges. Measurements were then taken further with higher system pressure. The synthesis of these ionic liquids and the experimental apparatus is discussed. Table 2-4 and Table 2-6 present some results of the measurements.

CO_2 Henry's Law constants in nine fluorinated imidazolium-based ionic liquids were measured by Baltus et al. (2004) using a quartz crystal microbalance. Measurements were done at 298.15K and at CO_2 partial pressures up to 0.1 MPa. Results are included in Table 2-4.

RTIL viscosity and molar volume at 298.15 K were recorded by Scovazzo (2009). This includes imidazolium, ammonium, phosphonium and functionalised RTILs. The functionalising of RTILs is given much caution however, since solvent-solvent interactions are presently not well understood. Results are recorded in Table 2-11. Condemarin and Scovazzo (2009) recorded CO_2 solubility in 20 ammonium-based RTILs, together with RTIL viscosity and molar volume. Table 2-5 and Table 2-11 present a summary of the results. Properties such as density and viscosity, as well as synthesis methods for imidazolium based RTILs are contained in Scovazzo et al. (2009), while styrene and acrylate-based RTILs are presented in Bara et al. (2007).

The modelling of CO_2 absorption in RTILs was elaborately presented in Scovazzo (2009), as well as Lozano et al. (2011). The popular models for CO_2 absorption in imidazolium based RTILs are the Camper Molar Volume Model and the Kilaru Viscosity Model. COSMO-RS,

UNIFAC, group contribution models and LFER/Abraham also provide gas solubility predictions. The accuracy of each model is addressed.

The study of ionic liquids at low temperatures often produces promising results. Relatively high CO_2 solubilities are noted, either directly or by inference of Henry's Law constants. This suggests a high suitability of ionic liquids for CO_2 capture. However, problems arise when studying the suitability of these ionic liquids for CO_2 capture on an industrial level. For coal combustion in particular, temperatures are high, at least over 373.15 K, and CO_2 partial pressure may be below atmospheric pressure, which substantially reduces CO_2 absorption in the ionic liquid. Refrigeration and compression units may be utilised to bring flue gas to ideal conditions for CO_2 absorption, but this contributes towards a higher energy penalty. Viscosity of the RTIL is also high at room temperature, which contributes towards high circulation costs in terms of energy.

Room temperature absorption also results in a higher energy penalty during desorption, as high temperature is required for CO_2 desorption from the ionic liquid.

2.5.5.2 Task-specific ionic liquids (TSILs)

These ionic liquids are categorised as such, simply due to the purpose for which they are being synthesized and investigated. As previously mentioned in Section 2.5.1, ionic liquids have many potential uses including CO_2 absorption. Research has thus been pursued to develop ionic liquids that are specifically suited to capturing CO_2 at conditions that would minimise energy penalty and improve efficiency.

These ionic liquids are usually novel, and are synthesized in the lab. Due to their specific rather than multiple potential uses, these ionic liquids are not typically available from commercial chemical companies.

Novel developments include the use of non-fluorinated anions, cations or both. Non-imidazolium based cations such as phosphate cations are also included in task-specific ionic liquid (TSIL) studies. An ongoing development of functionalised ionic liquids also forms part of the study on TSILs.

Bates et al. (2002) synthesized a TSIL which possessed an imidazolium-based cation of novel structure. The structure is presented, along with the method of synthesis. The TSIL was simply termed TSIL 1 and CO_2 solubility studies were done. The results are presented in Table 2-5. Compared to other ionic liquids, it is easily noted that TSIL 1 resulted in the highest CO_2 solubility even at higher temperature and lower partial pressure. The TSIL was also noted to be

recyclable. Bates et al. (2002) notes however that the main drawback to the industrial implementation of TSIL 1 is its high viscosity.

Zhao et al. (2005) studied the uses of various ionic liquids, including TSILs. TSILs are reported to be potentially useful as versatile solvents and catalysts, for extraction purposes, solid phase synthesis, and the production of liquid emulsions such as liquid Teflon.

Gurkan et al. (2010) and Brennecke and Gurkan (2010) have investigated TSILs containing phosphate cations with phosphate and sulphate anions. TSIL structure is shown, including $[P_{66614}]$[Met] and $[P_{66614}]$[Pro]. CO_2 solubility measurements were taken. This was presented in Gurkan et al. (2010). Table 2-5 shows CO_2 solubility in these TSILs to be relatively high at room temperature. However, Henry's Law constant results shown in Table 2-4 were not as encouraging as CO_2 Henry's Law constant in other conventional ionic liquids.

An elaborate literature study on TSILs was done by Hasib-ur-Rahman et al. (2010). It was noted that CO_2 solubility in TSILs can be up to 3 times higher than RTILs. Table 2-4 and Table 2-5 confirm this. CO_2 solubility can be comparable with conventional alkanolamine solvents. However, Hasib-ur-Rahman et al. (2010) also notes that TSIL viscosities can be extremely high, up to 2000 cP as shown in Table 2-11 for fluorinated TSILs. This is one of the main drawbacks to the industrial implementation of TSILs. In addition to this, Hasib-ur-Rahman et al. (2010) also notes that equilibrium and TSIL regeneration time can be very high, with some requiring a period of 24 hours to regenerate. TSILs such as [Am-im][BF_4], [Am-im][DCA], and [Pabim][BF_4] were considered. CO_2 solubility and Henry's Law constants are presented in Table 2-4 and Table 2-5, while viscosity of these TSILs are presented in Table 2-11. The high viscosity of TSIL has led to other strategies such as blending TSILs with low-viscosity RTILs to maintain high CO_2 solubility while reducing viscosity.

A more detailed investigation into the amine-functionalised TSIL [Pabim][BF_4] was done by Arshad (2009). Experimental procedures regarding CO_2 absorption, as well as reaction mechanisms between [Pabim][BF_4] and CO_2, are presented. A significantly more elaborate study on amine-functionalised TSILs was done by Zhang et al. (2009), which included density, viscosity and CO_2 mole fraction data for twenty amine-functionalised TSILs. Results of this study are presented in Table 2-6, Table 2-10 and Table 2-11 for comparison. Significantly higher viscosity and density are easily noted, compared to conventional ionic liquids.

Novel TSILs will only be available commercially if they are proven to be successful on an industrial level.

2.5.6 Gas absorption using ionic liquids as solvents

There has been increasing interest in the potential use of ionic liquids as solvents for gas absorption as previously explained and shown in Figure 2-4. Arshad (2009) notes an exponential increase in the study of ionic liquids in recent years, with over 6000 papers being published between 1999 and 2006 investigating the absorption of different gases. The interest in ionic liquids has resulted in over 700 ionic liquid patents.

Gases of particular interest include: carbon dioxide (CO_2), sulphur dioxide (SO_2), hydrogen sulphide (H_2S), nitrogen gas (N_2), methane (CH_4), and nitrogenous gases (NO_X) (Cserjesi et al., 2010, Scovazzo, 2009, Luis et al., 2009). These compounds form components of coal, steel and petrochemical process flue gas. The gas receiving the most attention particularly for coal industries is CO_2, due to its relative abundance in flue gas emissions and overall impact on climate change.

Current studies have shown the gas absorption process to be energy intensive, since a solvent with high CO_2 absorption rate, high absorption capacity, low heat capacity, and low viscosity, is yet to be found. Brennecke and Gurkan (2010) summarised the energy requirements of gas absorption using solvents. The main energy consumption occurs during the regeneration of the solvent for recovery of CO_2 and reuse of the solvent. This is due to the high heat capacity of the solvent. Most solvents, particularly alkanolamine and carbonate solvents are diluted with water to lower their corrosiveness. Water has a relatively high heat capacity which contributes to the high regeneration energy required. Secondly, circulation energy is required to pump the solvent between absorbers and strippers. The relatively high viscosity of solvents contributes to this energy penalty. Thirdly, energy is needed to compress CO_2 once it is recovered from stripping. Depending on the desired requirements, the required compression pressure could be up to 14 MPa (Brennecke and Gurkan, 2010).

Elaborate studies of ionic liquid properties have been undertaken. The main properties that are studied include: gas solubility (mol gas/mol ionic liquid), mole fraction of gas absorbed in the ionic liquid, Henry's Law constants of gases absorbed in the ionic liquid (MPa), ionic liquid viscosity (cP), ionic liquid density (g/cm^3), diffusivity of gases into the ionic liquid (m^2/s), the heat capacity of the ionic liquid ($J.mol^{-1}.K^{-1}$), the enthalpy of absorption of a gas into the ionic liquid (kJ/ mol gas), and the entropy of absorption of a gas into the ionic liquid ($J.mol^{-1}.K^{-1}$). Zhang et al. (2006) presented all of the above mentioned properties, as well as other properties of 588 ionic liquids, including combinations of 276 cations and 55 anions. Less frequently measured properties of ionic liquids are also contained such as ionic liquid decomposition

temperature, conductivity, melting point, glass transition temperature, polarity and electrochemical window.

One of the most popular measurements of gas absorption using physical solvents, and the most conclusive, is the measurement and calculation of the Henry's Law constant (MPa). Henry's law states that the solubility of a gas in a liquid at a particular temperature is proportional to the partial pressure of that gas above the liquid.

The Henry's Law constant is given by:

$$H_{2,1,T} = H_{gas,solvent,T} = \frac{P_{gas}}{x_{gas}} \quad \text{.....(E2-1)}$$

where:

$H_{gas,solvent,T}$ = Henry's Law constant (bar) of a particular gas (2) at a particular temperature in a particular solvent (1)

P_{gas} = Partial pressure of gas above the solution (MPa)

x_{gas} = Mole fraction of gas in solution.

More accurate methods of finding Henry's Law constants from solubility data at high pressure, have been developed by Krichevski and Kasarnovski (1935). The Krichevski-Kasarnovski equation is given as follows (Carroll and Mather, 1992):

$$\ln(f_2 / x_2) = \ln H_{21} + \bar{v}_2^{\infty}(P - P_1^O)/RT \quad \text{……(E2-2)}$$

where f_2 = fugacity of the solute in the mixture (1 indicates solvent)

$\bar{v}_2^{\infty}$ = Partial molar volume at infinite dilution

P_1^O = vapour pressure of the solvent

For most ionic liquids, which possess negligible vapour pressure, P_1^O can be assumed to be zero. The above equation also assumes that the concentration of the solute is sufficiently small for activity coefficients to be unity. A plot of $\ln(f_2 / x_2)$ vs $(P - P_1^O)$ for a set of solubility data at constant temperature would yield a straight line with $\ln H_{21}$ as the intercept.

For activity coefficients expected to be less than unity, the equation may be modified in a number of ways to incorporate activity coefficient models of varying complexity. Details are available in the work of Carrol and Mather (1992).

A lower Henry's Law constant for a particular temperature suggests that a gas is more soluble in a solvent. This is the reason why its measurement and calculation has become so useful in studying ionic liquids for gas absorption, particularly CO_2 absorption.

Numerous sources have investigated the Henry's Law constant of CO_2 in various ionic liquids. Maginn (2005), Shiflett and Yokozeki (2005), Condemarin and Scovazzo (2009), and Cadena et al. (2004) obtained Henry's Law constants for CO_2 in a variety of fluorinated ionic liquids, within temperatures of 283.15-333.15 K. The effect of humidity on Henry's Law constants was addressed by Hasib-ur-Rahman et al. (2010) and Baltus et al. (2004). Ionic liquids with imidazolium-based cations were studied by Anderson et al. (2007), Palgunadi et al. (2009), Chen et al. (2006) and Huang and Rüther (2009), to establish the effect of cation chain length on Henry's Law constants. Comparatively few non-fluorinated ionic liquids were studied for CO_2 Henry's Law constants. The most significant study was that of Palgunadi et al. (2009), which investigated Henry's Law constants for seven non-fluorinated phosphate-based ionic liquids at temperatures of 313.15-333.15 K. The study produced comparatively high Henry's Law constants to that of fluorinated ionic liquids of the same temperature, confirming that CO_2 is more soluble in fluorinated ionic liquids. Arshad (2009), Zhang et al. (2009), and Anderson et al. (2007) have studied CO_2 Henry's Law constants in non-fluorinated ionic liquids to a very limited extent. However, their results also confirm higher solubility in fluorinated ionic liquids. Table 2-4 contains Henry's Law constant data for CO_2 in ionic liquids, measured by various literature sources.

Table 2-4: CO_2 Henry's Law Constant Measurements by Numerous Literature Sources

Ionic Liquid	Henry's Constant/MPa	Temperature/K	References
[bmim][BF_4]	0.35-1.02	281.69-392.16	Shiflett and Yokozeki (2005)
	4.19-8.4	283.15-323.15	Hasib-ur-Rahman et al. (2010)
	4.18-8.86	283.15-323.15	Anderson et al. (2007)
	4.08-8.89	283.15-323.15	Cadena et al. (2004)
	1.71-2.35	307.15-322.15	Chen et al. (2006)
	5.57	298.15	Huang and Rüther (2009)
[BMIM][Bu_2PO_4]	4.98-6.85	313.15-333.15	Palgunadi et al. (2009)
[BMIM][$BuHPO_3$]	6.3-8.52	313.15-333.15	Palgunadi et al. (2009)
[BMIM][$MeHPO_3$]	8.68-11.29	313.15-333.15	Palgunadi et al. (2009)
[bmim][PF_6]	0.35-1.01	281.69-392.16	Shiflett and Yokozeki (2005)
	5.34-8.13	298.15-323.15	Muldoon et al. (2007)
	5.34	298.15	Hasib-ur-Rahman et al. (2010)

Table 2-4 (Contd.): CO_2 Henry's Law Constant Measurements by Numerous Literature Sources			
Ionic Liquid	Henry's Constant/MPa	Temperature/K	References
	3.88-8.13	283.15-323.15	Anderson et al. (2007)
	3.87-8.13	283.15-323.15	Anthony et al. (2002)
	5.34	298.15	Huang and Rüther (2009)
	3.87-8.13	283.15-323.15	Cadena et al. (2004)
	3.88-8.13	283.15-323.15	Arshad (2009)
[bmim][Tf_2N]	3.3-4.87	298.15-323.15	Muldoon et al. (2007)
	2.8-1.5	283.15-323.15	Hasib-ur-Rahman et al. (2010)
	2.53-4.87	283.15-323.15	Anderson et al. (2007)
	3.7	300.65	Baltus et al. (2004)
[bmim][Tf_2N] with 2.7 wt % polyethylenimine	3.8	300.65	Baltus et al. (2004)
	3.8	298.15	Hasib-ur-Rahman et al. (2010)
[bmmim][BF_4]	4.57-9.22	283.15-323.15	Cadena et al. (2004)
[bmmim][PF_6]	4.73-8.85	283.15-323.15	Cadena et al. (2004)
[bmpy][Tf_2N]	1.27-5.86	293.1-493.2	Kumelan et al. (2010)
	2.6-4.6	283.15-323.15	Arshad (2009)
[$C_6H_4F_9$mim][Tf_2N]	2.84-4.85	298.15-333.15	Anderson et al. (2007)
[C_8F_{13}mim][Tf_2N]	0.6	298.15	Baltusa et al. (2005)
[$C_8H_4F_{13}$mim][Tf_2N]	2.73-4.47	298.15-333.15	Muldoon et al. (2007)
[DMIM][Me_2PO_4] Non Fluorinated	10.64-15.22	313.15-333.15	Palgunadi et al. (2009)
[DMIM][$MeHPO_3$]	11.48-16.35	313.15-333.15	Palgunadi et al. (2009)
[emim][BF_4]	0.7-1	298.15-310.15	Shokouhi et al. (2010)
	8.12-16.21	298.15-333.15	Arshad (2009)
[EMIM][Et_2PO_4]	6.99-9.66	313.15-333.15	Palgunadi et al. (2009)
[EMIM][$EtHPO_3$]	9.18-12.36	313.15-333.15	Palgunadi et al. (2009)
[emim][PF_6]	5.2	298.15	Hasib-ur-Rahman et al. (2010)
[emim][Tf_2N]	3.7	298.15	Hasib-ur-Rahman et al. (2010)
	3.9	298.15	Bara et al. (2007)
	2.53-5.15	283.15-323.15	Cadena et al. (2004)
[emmim][Tf_2N]	2.86-6.05	283.15-323.15	Cadena et al. (2004)
	2.86-6.05	283.15-323.15	Arshad (2009)
[Et_3NBH_2mim][T_2N]	3.31	298.15	Anderson et al. (2007)
[hemim][BF_4]	1.08-1.98	303.15-353.15	Shokouhi et al. (2010)
[hexafluoroimid][Tf_2N]	2.85-4.85	298.15-323.15	Maginn (2005)
[hmim][ACE]	11.31	333.15	Muldoon et al. (2007)
	11.31	333.15	Anderson et al. (2007)
[hmim][BF_4]	1.59-2.19	307.15-322.15	Chen et al. (2006)
[hmim][eFAP]	2.53-4.29	298.15-323.15	Maginn (2005)
	2.52-4.2	298.15-333.15	Arshad (2009)
[hmim][pFAP]	2.16-3.6	298.15-333.15	Muldoon et al. (2007)
[hmim][SAC]	13.22	333.15	Anderson et al. (2007)
[hmim][Tf_2N]	2.42-4.56	283.15-323.15	Maginn (2005)
	3.5	298.15	Hasib-ur-Rahman et al. 2010

Table 2-4 (Contd.): CO_2 Henry's Law Constant Measurements by Numerous Literature Sources			
Ionic Liquid	Henry's Constant/MPa	Temperature/K	References
	2.42-4.56	283.15-323.15	Anderson et al. (2007)
	3.4	298.15	Bara et al. (2007)
	3.5	300.65	Baltus et al. (2004)
	3.16-4.56	298.15-323.15	Muldoon et al. (2007)
[hmpy][Tf_2N]	2.53-4.61	283.15-323.15	Maginn (2005)
	3.28-4.62	298.15-323.15	Muldoon et al. (2007)
[mmim][$MeSO_4$]	13.17-26.34	298.15-333.15	Arshad (2009)
[$N_{(1)444}$][Tf_2N]	5.07	303.15	Condemarin and Scovazzo (2009)
[$N_{(1)888}$][Tf_2N]	2.84	303.15	
[$N_{(10)111}$][Tf_2N]	4.46	303.15	
[$N_{(10)113}$][Tf_2N]	4.26	303.15	
[$N_{(4)111}$][Tf_2N]	6.08	303.15	
[$N_{(4)113}$][Tf_2N]	6.38	303.15	
[$N_{(6)111}$][Tf_2N]	4.36	303.15	
[$N_{(6)113}$][Tf_2N]	5.17	303.15	
[$N_{(6)222}$][Tf_2N]	5.88	303.15	
[octafluoroimid][Tf_2N]	2.61	298.15	Maginn (2005)
[omim][BF_4]	1.5-2.06	307.15-322.15	Chen et al. (2006)
[omim][Tf_2N]	3	298.15	Hasib-ur-Rahman et al. (2010)
[omim][Tf_2N]	3	300.65	Baltus et al. (2004)
	3	298.15	Baltusa et al. (2005)
[omim][Tf_2N] (58 mol%)/[C_8F_{13}mim][Tf_2N] (42 mol%)	1.5	298.15	Hasib-ur-Rahman et al. (2010)
[omim][Tf_2N] with 20% relative humidity	3	298.15	Hasib-ur-Rahman et al. (2010)
	3	300.65	Baltus et al. (2004)
[omim][Tf_2N] with 40% relative humidity	2.7	298.15	Hasib-ur-Rahman et al. (2010)
	2.7	300.65	Baltus et al. (2004)
[$P_{(14)444}$][DBS]	3.04	298.15	Arshad (2009)
[$P_{(14)666}$][Cl]	3.546	298.15	Arshad (2009)
[$P_{(14)666}$][DCA]	2.969	298.15	Arshad (2009)
[$P_{(14)666}$][Tf_2N]	3.344	298.15	Arshad (2009)
[P_{2444}][DEP]	6.991	298.15	Arshad (2009)
[$p_5$mim][bFAP]	2.02-3.29	298.15-333.15	Muldoon et al. (2007)
[P_{66614}][Met]	15.7	298.15	Gurkan et al. (2010)
[P_{66614}][Pro]	5.7	298.15	Gurkan et al. (2010)
[perfluoro-hmim][Tf_2N]	2.55-4.2	283.15-323.15	Hasib-ur-Rahman et al. (2010)
[pmim][PF_6]	5.2	298.15	Baltusa et al. (2005)
	5.2	300.65	Baltus et al. (2004)
[pmim][Tf_2N]	3.7	300.65	Baltus et al. (2004)
[pmim][Tf_2N] with constant-density gas	3.9	300.65	Baltus et al. (2004)
[pmmim][Tf_2N]	2.96-5.3	283.15-323.15	Hasib-ur-Rahman et al. 2010

Table 2-4 (Contd.): CO_2 Henry's Law Constant Measurements by Numerous Literature Sources			
Ionic Liquid	Henry's Constant/MPa	Temperature/K	References
1,4-Dibutyl-3-phenylimidazolium bis(trifluoromethylsulfonyl)imide	6.3	298.15	Hasib-ur-Rahman et al. (2010)
	6.3	300.65	Baltus et al. (2004)
1-Butyl-3-phenylimidazolium bis(trifluoromethylsulfonyl)imide	18	298.15	Hasib-ur-Rahman et al. (2010)
	18	300.65	Baltus et al. (2004)
58 mol % C_8mimTf_2N/42 mol % C_8F_{13}mimTf_2N	1.5	300.65	Baltus et al. (2004)
C_8F_{13}mimTf_2N	0.45	300.65	Baltus et al. (2004)
	0.45	298.15	Hasib-ur-Rahman et al. (2010)
TEGO IL K5	2.71-10.43	300.15-500.15	Heintz et al. (2009)

CO_2 solubility data is comparatively more difficult to find, since it is more difficult to measure and easily compare ionic liquid performance for CO_2 absorption. This is due to the fact that CO_2 solubility in ionic liquids is dependent on temperature and pressure, while CO_2 Henry's Law constants in ionic liquids are dependent only on temperature. Brennecke and Gurkan (2010), Condemarin and Scovazzo (2009), and Wilkes (2004) obtained CO_2 solubility data in a variety of ionic liquids. Condemarin and Scovazzo (2009) investigated CO_2 solubility in nine fluorinated ionic liquids at 0.101325 MPa and 323.15 K. Bara et al. (2007) and Brennecke and Gurkan (2010) focussed on non-fluorinated ionic liquids, obtaining higher CO_2 solubilities but at lower temperatures of 293.15-298.15 K. CO_2 solubility data in various ionic liquids measured by numerous sources are presented in Table 2-5 below.

Table 2-5: CO_2 Solubility in Ionic Liquids Measured by Numerous Sources

Ionic Liquid	CO_2 loading/ mol CO_2·mol IL^{-1}	Pressure/MPa	Temperature/K	References
[Am-im][BF_4]	0-2 mol CO_2/dm^3 IL	0-1	303.15	Hasib-ur-Rahman et al. (2010)
[Am-im][DCA]	0-1.8 mol CO_2/dm^3 IL	0-1	303.15	Hasib-ur-Rahman et al. (2010)
[bmim][BF_4]	0-0.8	0-1	303.15	Hasib-ur-Rahman et al. (2010)
[bmpy][Tf_2N]	0.028-6.151 mol CO_2/dm^3 IL	1.365-10.8	413.12-293.15	Kumelan et al. (2010)
[emim][$MDEGSO_4$]	0.065-0.959	0.85-6.2	343.15-303.15	Hasib-ur-Rahman et al. (2010)
[emim][Tf_2N]	0.026	0.101325	298.15	Bara et al. (2007)
[hmim][Tf_2N]	0.05	0.1	298.15	Brennecke and Gurkan (2010)
	0.029	0.101325	298.15	Bara et al. (2007)
[$N_{(1)444}$][Tf_2N]	0.02	0.101325	303.15	Condemarin and Scovazzo (2009)
[$N_{(1)888}$][Tf_2N]	0.037	0.101325	303.15	Condemarin and Scovazzo (2009)
[$N_{(10)111}$][Tf_2N]	0.023	0.101325	303.15	Condemarin and Scovazzo (2009)
[$N_{(10)113}$][Tf_2N]	0.024	0.101325	303.15	Condemarin and Scovazzo (2009)
[$N_{(4)111}$][Tf_2N]	0.018	0.101325	303.15	Condemarin and Scovazzo (2009)
[$N_{(4)113}$][Tf_2N]	0.016	0.101325	303.15	Condemarin and Scovazzo (2009)
[$N_{(6)111}$][Tf_2N]	0.024	0.101325	303.15	Condemarin and Scovazzo (2009)
[$N_{(6)113}$][Tf_2N]	0.02	0.101325	303.15	Condemarin and Scovazzo (2009)

Table 2-5 (Contd.): CO_2 Solubility in Ionic Liquids Measured by Numerous Sources

Ionic Liquid	CO_2 loading/ mol CO_2·mol IL^{-1}	Pressure/MPa	Temperature/K	References
$[P_{66614}][Met]$	0.9	0.12	298.15	Gurkan et al. (2010)
$[P_{66614}][Met]$	0.9	0.1	298.15	Brennecke and Gurkan (2010)
$[P_{66614}][Pro]$	0.85	0.1	298.15	Brennecke and Gurkan (2010)
butyl acrylate	0.204 mol CO_2/dm^3 IL	0.101325	293.15	Bara et al. (2007)
butyl styrene	0.2 mol CO_2/dm^3 IL	0.101325	293.15	Bara et al. (2007)
General	0.4-0.7	0.0005-0.016	383.15	Wappel et al. (2009)
hexyl styrene	0.177 mol CO_2/dm^3 IL	0.101325	293.15	Bara et al. (2007)
MDEA + $[MDEA][BF_4]$ + H_2O + PZ	100-180e-3 mol CO_2 in 180min	0.5-2.5	298.15-338.15	SuoJiang et al. (2010)
methyl acrylate	0.163 mol CO_2/dm^3 IL	0.101325	293.15	Bara et al. (2007)
methyl styrene	0.1815 mol CO_2/dm^3 IL	0.101325	293.15	Bara et al. (2007)
TSIL 1	0.45 in 180min	-	-	Bates et al. (2002)
	0.4-0.95	0.0005-0.016	313.15	Wappel et al. (2009)

Another approach is to simply record the CO_2 mole fraction that was ultimately achieved in an ionic liquid at a particular temperature. This is more popular than CO_2 solubility measurements, but less popular than Henry's Law constant investigations, since the mole fraction of CO_2 is also dependent on the pressure and temperature of the ionic liquid. Mole fraction measurements are useful if such data are accompanied by the partial pressure that they were measured in, as Henry's Law constants may easily be calculated using such data. Anderson et al. (2007) and Muldoon et al. (2007) measured CO_2 mole fractions in a variety of fluorinated and non-fluorinated ionic liquids at temperatures of 283.15-333.15 K and pressures up to 9 MPa. Palgunadi et al. (2009) and Zhang et al. (2009) focussed on CO_2 mole fraction measurement in non-fluorinated ionic liquids, at atmospheric pressure and temperatures of 298.15-334.15 K. Shiflett and Yokozeki (2005), Arshad (2009), and Hasib-ur-Rahman et al. (2010) considered fluorinated imidazolium-based ionic liquids in their studies, at temperatures of 298.15-348.15 K and 0.1-80 MPa.

Table 2-6: CO_2 Mole Fraction in Ionic Liquids Measured by Numerous Sources

Ionic Liquid	CO_2 mole fraction	Pressure/MPa	Temperature/K	Reference
$[aP_{4443}][Ala]$	0.155-0.17	0.1013	298.15	Zhang et al. (2009)
$[aP_{4443}][Gly]$	0.16-0.19	0.1013	298.15	Zhang et al. (2009)
$[aP_{4443}][Leu]$	0.08-0.1	0.1013	298.15	Zhang et al. (2009)
$[aP_{4443}][Val]$	0.12-0.14	0.1013	298.15	Zhang et al. (2009)
$[b_2\text{-Nic}][Tf_2N]$	0.2-0.71 at 12-88 bar	1.2-8.8	333.15	Anderson et al. (2007)
$[b_2\text{-Nic}][Tf_2N]$	0.3-0.7	2-9	333.15	Muldoon et al. (2007)
$[bmim][BF_4]$	0.02-0.36	0.01-2	283-348	Shiflett and Yokozeki (2005)
	0.15-0.45	2-8.5	333.15	Anderson et al. (2007)
	0.25-0.115, 0.25	0.2-1.3	323.15, 283.15	Cadena et al. (2004)
	0-0.2	0-1.3	298.15	Arshad (2009)

Table 2-6 (Contd.): CO_2 Mole Fraction in Ionic Liquids Measured by Numerous Sources

Ionic Liquid	CO_2 mole fraction	Pressure/MPa	Temperature/K	Reference
[BMIM][Bu_2PO_4]	0.021-0.015	0.1	314.15-334.15	Palgunadi et al. (2009)
[BMIM][$BuHPO_3$]	0.016-0.012	0.1	314.15-334.15	Palgunadi et al. (2009)
[bmim][$C_7F_{15}CO_2$]	0.2-0.75	1.5-8	333.15	Muldoon et al. (2007)
	0.2-0.78	1.5-8	333.15	Anderson et al. (2007)
[bmim][DCA]	0.1-0.5	1.5-11.5	333.15	Anderson et al. (2007)
	0.18-0.5	1.2-6	298.15	Arshad (2009)
[BMIM][$MeHPO_3$]	0.011-0.009	0.1	314.15-334.15	Palgunadi et al. (2009)
[bmim][methide]	0.25-0.65	1.5-8	333.15	Muldoon et al. (2007)
	0.3-0.75	2-9	333.15	Anderson et al. (2007)
	0.38-0.74	1.2-6.2	298.15	Arshad (2009)
[bmim][NO_3]	0.08-0.45	1.5-9	333.15	Anderson et al. (2007)
	0.23-0.55	1.8-9	313.15	Arshad (2009)
[bmim][PF_6]	0-0.2	0-1.3	298.15	Anderson et al. (2007)
	0.01-0.31	0.01-2	283-348	Shiflett and Yokozeki (2005)
	0-0.21	0-1.3	298.15	Hasib-ur-Rahman et al. (2010)
	0-0.2, 0.55	0-1.3,13.5	298.15	Anderson et al. (2007)
	0.02-0.27, 0.7	0.2-1.3,9	323.15-283.15, 323.15	Anthony et al. (2002)
	0.063-0.492	0.26-4	298.15	Kim et al. (2011)
	0.04-0.13, 0.26	0.2-1.3	323.15, 283.15	Cadena et al. (2004)
	0.02-0.26	0.2-1.3	323.15-283.15	Arshad (2009)
[bmim][Tf_2N]	0.15-0.65	1.5-9	333.15	Muldoon et al. (2007)
	0.3-0.75	2-13	333.15	Anderson et al. (2007)
	0-0.3, 0.52	0-1.3	298.15, 279.15	Arshad (2009)
	0.09-0.59	0.5-14	333.15-453.15	Raeissi et al. (2008)
[bmim][TFA]	0.1-0.6	1-9	333.15	Muldoon et al. (2007)
[bmim][TFA]	0.1-0.55	1-9	333.15	Anderson et al. (2007)
[bmim][TfO]	0.1-0.5	1.5-11	333.15	Anderson et al. (2007)
	0.2-0.64	1-6.4	298.15	Arshad (2009)
[bmmim][BF_4]	0.25-0.11, 0.21	0.2-1.3	323.15, 283.15	Cadena et al. (2004)
[bmmim][PF_6]	0.03-0.12, 0.22	0.2-1.3	323.15, 283.15	Cadena et al. (2004)
[$C_6H_4F_9$mim][Tf_2N]	0-0.34	0-1.3	298.15	Anderson et al. (2007)
	0-0.33	0-1.3	298.15	Anderson et al. (2007)
	0.25-0.75, 0-0.8	1-9	333.15, 298.15	Muldoon et al. (2007)
[$C_8H_4F_{13}$mim][Tf_2N]	0-0.35	0-1.3	298.15	Anderson et al. (2007)
	0-0.35, 0.65	0-1.3,4	298.15	Muldoon et al. (2007)
	0-0.35	0-1.3	298.15	Anderson et al. (2007)
[C_9mim][PF_6]	0.186-0.554	0.89-3.4	293-298	Kim et al. (2011)
[choline][Tf_2N]	0.15-0.6	1-8	333.15	Muldoon et al. (2007)
[DMIM][Me_2PO_4]	0.009-0.006	0.1	314.15-334.15	Palgunadi et al. (2009)
[DMIM][$MeHPO_3$]	0.008-0.006	0.1	314.15-334.15	Palgunadi et al. (2009)
[EMIM][Et_2PO_4]	0.014-0.011	0.1	314.15-334.15	Palgunadi et al. (2009)
[EMIM][$EtHPO_3$]	0.011-0.008	0.1	314.15-334.15	Palgunadi et al. (2009)
[emim][$EtSO_4$]	0.1-0.3	1.8-9	313.15	Arshad (2009)
[emim][PF_6]	0.12-0.6	0-10	298.15	Hasib-ur-Rahman et al. (2010)
[emim][Tf_2N]	0.12-0.6	0-80	298.15	Hasib-ur-Rahman et al. (2010)
	0.026	0.101325	298.15	Bara et al. (2007)
	0.09, 0.17	0.55	323.15, 283.15	Cadena et al. (2004)

Table 2-6 (Contd.): CO_2 Mole Fraction in Ionic Liquids Measured by Numerous Sources

Ionic Liquid	CO_2 mole fraction	Pressure/MPa	Temperature/K	Reference
[EMIM][TFSI]	0-0.05	0-0.1	313.15	Liu et al. (2011)
[emmim][Tf_2N]	0.08, 0.16	0.55	323.15, 283.15	Cadena et al. (2004)
[Et_3NBH_2mim][Tf_2N]	0-0.3	0-1.3	298.15	Muldoon et al. (2007)
[$H_2NC_3H_6$mim][Tf_2N]	0.21	0.2	333.15	Anderson et al. (2007)
[hemim][BF_4]	0.0004-0.102	0.153-1.102	353-303	Shokouhi et al. (2010)
[hmim][eFAP]	0-0.36, 0.8	0-1.3, 9	298.15	Anderson et al. (2007)
	0.15-0.8	1-9.2	333.15	Muldoon et al. (2007)
	0-0.36	0-1.3	298.15	Anderson et al. (2007)
[hmim][PF_6]	0.1-0.5	1-7	333.15	Muldoon et al. (2007)
[hmim][pFAP]	0-0.4	0-1.3	298.15	Anderson et al. (2007)
	0-0.4	0-1.3	298.15	Muldoon et al. (2007)
	0-0.4	0-1.3	298.15	Anderson et al. (2007)
[hmim][Tf_2N]	0-0.39	0-1.3	283.15	Anderson et al. (2007)
	0-0.31	0-1.3	298.15	Anderson et al. (2007)
	0-0.21	0-1.3	323.15	Anderson et al. (2007)
	0-0.3, 0.7	0-1.3, 9	298.15	Anderson et al. (2007)
	0-0.3	0-1.3	313.15	Brennecke and Gurkan (2010)
	0-0.3	0-1.3	298.15	Anderson et al. (2007)
	0.25-0.75	1.5-12	313.15	Arshad (2009)
	0.2-0.7, 0-0.75	2-9.5	333.15, 298.15	Muldoon et al. (2007)
[hmpy][Tf_2N]	0-0.29	0-1.3	298.15	Anderson et al. (2007)
	0-0.2	0-0.7	298.15	Anderson et al. (2007)
	0-0.3	0-1.3	298.15	Arshad (2009)
	0-0.3	0-1.4	298.15	Muldoon et al. (2007)
[N_{4111}][Tf_2N]	0.15-0.7	1.5-8	333.15	Muldoon et al. (2007)
[N_{4444}][doc]	0.2-0.79 at 20 - 90 bar	2-9	333.15	Anderson et al. (2007)
[N_{4444}][docusate]	0.2-0.8	2-9	333.15	Muldoon et al. (2007)
[Nbupy][BF_4]	0.22-0.57	1.8-9	313.15	Arshad (2009)
[omim][BF_4]	0.23-0.7	1.8-9	313.15	Arshad (2009)
[omim][PF_6]	0.24-0.75	1.8-9	313.15	Arshad (2009)
[omim][Tf_2N]	0.25-0.80	1.5-12	313.15	Arshad (2009)
[$p_5$mim][bFAP]	0-0.42	0-1.3	298.15	Anderson et al. (2007)
	0.25-0.82	1.5-9	333.15	Muldoon et al. (2007)
	0-0.42	0-1.3	298.15	Anderson et al. (2007)
Ecoeng 41M	0.1-0.5 at 20-90 bar	2-9	333.15	Anderson et al. (2007)
	0.1-0.5	2-9	333.15	Muldoon et al. (2007)
Ecoeng 500	0.2-0.7 at 15-90 bar	1.5-9	333.15	Anderson et al. (2007)
	0.2-0.7	1.5-10	333.15	Muldoon et al. (2007)
EM(Zn)TFSI 1-1	0-0.82	0-0.1	313.15	Liu et al. (2011)
TEGO IL K5	0.05-0.6	0.5-3	500-300	Heintz et al. (2009)

Henry's Law constants, CO_2 solubility, and CO_2 mole fraction are obtained either by vapour-liquid equilibrium (VLE) measurement, or by analysis of infinite dilution activity coefficients using a dilutor cell apparatus. Equipment for measurements on ionic liquids were designed to use as little ionic liquid sample as possible, due to the high cost of ionic liquids.

Anderson et al. (2007) utilised an Intelligent Gravimetric Analyser (IGA) for low pressure VLE measurement (0-2 MPa). Shiflett and Yokozeki (2005) explain the operation of this apparatus. Desorption under high temperature can also be conducted. Anderson et al. (2007) utilised a Rubotherm for high pressure VLE measurement. The apparatus required 0.075-1.5g ionic liquid samples.

Henry's Law constant measurement using a dilutor cell apparatus was presented in Richon et al. (1980), with a view to increase accuracy and speed of measurement in Richon (2011).

Another method of measuring CO_2 mole fractions and calculating CO_2 solubility and Henry's Law constant, is to test the loaded ionic liquid solvent using nuclear magnetic resonance (NMR) spectrometry (Zhang et al., 2009). Chromatography analysis is not always recommended due to the high viscosity of the ionic liquid. Zhang et al. (2009) successfully utilised NMR spectrometry for measuring CO_2 absorption in 20 amine-functionalised non-fluorinated ionic liquids.

Other imperative measurements in the study of ionic liquids for CO_2 absorption are the ionic liquid heat capacity, entropy and enthalpy of absorption of CO_2 into the ionic liquid. These measurements provide an indication of the energy that would be required to release CO_2 from the ionic liquid, and recycle the ionic liquid. Heat capacity measurements are not popular regarding CO_2 absorption since it is only the minimum amount of energy necessary for desorption that is of interest. Fredlake et al. (2004) and Liu et al. (2011) conducted heat capacity measurements for imidazolium-based ionic liquids at 298.15-323.15 K.

Table 2-7: Heat capacity of Ionic Liquids Recorded by Different Sources

Ionic Liquid	Heat Capacity/J·mol^{-1}·K^{-1}	Temperature/K	References
[bmim][BF_4]	351.5-358	298.15-323.15	Fredlake et al. (2004)
[bmim][Br]	316.7-323.6	298.15-323.15	Fredlake et al. (2004)
[bmim][Cl]	322.7-333.7	298.15-323.15	Fredlake et al. (2004)
[bmim][dca]	364.6-370	298.15-323.15	Fredlake et al. (2004)
[bmim][methide]	782.8-802.4	298.15-323.15	Fredlake et al. (2004)
[bmim][Tf_2N]	536.3-543.9	298.15-323.15	Fredlake et al. (2004)
[bmim][TfO]	417.2-423.1	298.15-323.15	Fredlake et al. (2004)
[bmmim][BF_4]	375.3-406.5	298.15-323.15	Fredlake et al. (2004)
[bmmim][PF_6]	397.6-405.1	298.15-323.15	Fredlake et al. (2004)
	433.6-449.1	298.15-323.15	Fredlake et al. (2004)
[emim][Tf_2N]	524.3-532.2	298.15-323.15	Fredlake et al. (2004)
[EMIM][TFSI]	1.242-1.795 J.g^{-1}.K^{-1}	300-479.73	Liu et al. (2011)
[emmim][Tf_2N]	492.7-498.8	298.15-323.15	Fredlake et al. (2004)
[pmmim][Tf_2N]	554.5-558.7	298.15-323.15	Fredlake et al. (2004)
EM(Zn)TFSI 1-1	1.077-2.043 J.g^{-1}.K^{-1}	300-479.73	Liu et al. (2011)

Enthalpy of absorption for non-volatile solvents such as ionic liquids may be expressed by the following equation (Prausnitz et al., 1999, Pg. 597):

$$\Delta\bar{h}_2\left[kJ.mol^{-1}\right] = \bar{h}_2^L - h_2^G = -R\left(\frac{\partial \ln x_2}{\partial 1/T}\right)_P \quad \text{.....(E2-3)}$$

Where $\bar{h}_2^L$ is the enthalpy of the gas absorbed in the liquid, h_2^G is the enthalpy of the pure gas in the gas phase, x_2 is the liquid mole fraction of the absorbed gas, R is the gas constant in [J.mol^{-1}.K^{-1}] and T is the system temperature in [K].

Enthalpy of absorption is also an indication of the temperature dependence of absorption of particular gases in particular solvents. Solubility of a gas in some solvents decreases more substantially upon increasing temperature than for solubility in other solvents (Prausnitz et al., 1999, Pg. 598).

Table 2-8: Enthalpy of Absorption of CO_2 in Ionic Liquids Recorded by Different Sources

Ionic Liquid	Enthalpy of Absorption (kJ/mol CO_2)	References
[bmim][BF_4]	-15.9	Cadena et al. (2004)
	-13.9	Arshad (2009)
	-15.8	Chen et al. (2006)
[bmim][PF_6]	-16.1	Anthony et al. (2002)
	-16.1	Cadena et al. (2004)
	-14.3	Arshad (2009)
[bmim][Tf_2N]	-12.5	Arshad (2009)
[bmmim][BF_4]	-14.5	Cadena et al. (2004)
[bmmim][PF_6]	-13	Cadena et al. (2004)
[bmpy][Tf_2N]	-10.4	Arshad (2009)
[emim][BF_4]	-13	Arshad (2009)
[emim][Tf_2N]	-14.2	Cadena et al. (2004)
[emmim][Tf_2N]	-14.7	Cadena et al. (2004)
[hemim][BF_4]	-22.9--10.6 at 303-353K	Shokouhi et al. (2010)
[hmim][BF_4]	-17.3	Chen et al. (2006)
[hmim][Tf_2N]	-11.8	Maginn (2005)
	-12	Anderson et al. (2007)
	-11.8	Anderson et al. (2007)
[hmpy][Tf_2N]	-11.1	Maginn (2005)
	-12	Anderson et al. (2007)
	-11.5	Anderson et al. (2007)
[mmim][$MeSO_4$]	-12	Arshad (2009)
[omim][BF_4]	-18.3	Chen et al. (2006)
[P_{66614}][Met]	-64	Gurkan et al. (2010)
[P_{66614}][Pro]	-80	Gurkan et al. (2010)
[pmmim][Tf2N]	-11	Arshad (2009)
TEGO IL K5	-11.92--15.05 at 300-500K	Heintz et al. (2009)

Maginn (2005), Sen and Paolucci (2006), and Anderson et al. (2007) studied the comparison between imidazolium-based ionic liquids and pyridinium- based ionic liquids, showing a miniscule difference in enthalpy of absorption. Anderson et al. (2007) recorded no difference, while Maginn (2005) and Sen and Paolucci (2006) recorded the enthalpy of absorption to be 0.3-0.7 kJ/mol lower in pyridinium-based ionic liquids. Chen et al. (2006) studied the effect of increasing cation chain length on enthalpy of absorption. Smaller chain length resulted in lower enthalpy of absorption. Cadena et al. (2004) and Arshad (2009) summarised enthalpy of absorption for fluorinated ionic liquids, while Heintz et al. (2009) and Gurkan et al. (2010) measured enthalpy of absorption for non-fluorinated ionic liquids. Enthalpy of absorption was much higher for non-fluorinated ionic liquids, ranging from [-64 – -80 kJ/mol] CO_2 at 298.15 K.

Another method of quantifying the temperature dependence of solubility is the entropy of absorption. This is expressed by the following equation (Prausnitz et al., 1999, Pg. 597):

$$\Delta\bar{s}_2\left[J.mol^{-1}.K^{-1}\right] = \bar{s}_2^{L} - s_2^{G} = R\left(\frac{\partial \ln x_2}{\partial \ln T}\right)_P \quad \text{.....(E2-4)}$$

Where, $\bar{s}_2^{L}$ is the entropy of the gas absorbed in the liquid, s_2^{G} is the enthalpy of the pure gas in the gas phase, x_2 is the liquid mole fraction of the absorbed gas, R is the gas constant in [$J.mol^{-1}.K^{-1}$] and T is the system temperature in [K].

Table 2-9: Entropy of Absorption of CO_2 in Ionic Liquids Recorded by Different Sources

Ionic Liquid	Entropy of Absorption ($J \cdot mol^{-1} \cdot K^{-1}$)	References
[bmim][BF_4]	-52.4	Cadena et al. (2004)
	-55.8	Chen et al. (2006)
[bmim][PF_6]	-53.2	Anthony et al. (2002)
	-53.2	Cadena et al. (2004)
[bmmim][BF_4]	-47.7	Cadena et al. (2004)
[bmmim][PF_6]	-42.8	Cadena et al. (2004)
[emim][Tf_2N]	-46.9	Cadena et al. (2004)
[emmim][Tf_2N]	-48.7	Cadena et al. (2004)
[hemim][BF_4]	-104--66.4 at 303-353	Shokouhi et al. (2010)
[hmim][BF_4]	-60	Chen et al. (2006)
[hmim][Tf_2N]	-38.4	Maginn (2005)
	-48.2	Anderson et al. (2007)
[hmpy][Tf_2N]	-36	Maginn (2005)
	-38.1	Anderson et al. (2007)
[omim][BF_4]	-63	Chen et al. (2006)

A negative value for entropy of absorption indicates that absorption decreases with increasing temperature, which prevails for substantially soluble gases. However, for negligibly soluble gases, entropy of absorption may be positive, indicating that high temperature may increase

absorption. The increase however, will not be as substantial as soluble gases in solvents (Prausnitz et al., 1999, Pg. 598).

Apart from measurements pertaining to absorption, the most important properties that were measured were the viscosity and density of the ionic liquid. Numerous sources have measured the density of fluorinated imidazolium-based ionic liquids at temperatures of 283.15-344 K. The density of novel ionic liquids containing phosphorous and cobalt anions was studied by Arshad (2009) and Palgunadi et al. (2009), at temperatures up to 353 K. Zhang et al. (2009) has studied 20 novel ionic liquids for CO_2 absorption, recording densities at temperatures of 298.15-348.15 K. Maginn (2005), Shiflett and Yokozeki (2005), Fredlake et al. (2004), Palgunadi et al. (2009), and Nishi et al. (2006) used a pycnometer to measure ionic liquid density of ionic liquids of all types. Zhang et al. (2009) used an Anton Paar DMA 5000 for non-fluorinated ionic liquid density measurement. Ignat'ev et al. (2005) used an Anton Paar Viscosimeter SVM 3000 in conjunction with a Mettler Toledo TG-SDTA 851 for the density measurement of ionic liquids containing highly fluorinated FAP anions. Gan et al. (2006) produced accurate ionic liquid density measurements using an Anton Paar DMA 4500 U-tube density meter for conventional fluorinated imidazolium-based ionic liquids.

Table 2-10: Density of Ionic Liquids at Different Temperatures Measured by Various Sources

Ionic Liquid	Density/g·cm^{-3}	Temperature/K	References
[aP$_{4443}$][Ala]	0.9859-0.9564	298.15-348.15	Zhang et al. (2009)
[aP$_{4443}$][Arg]	0.9943-0.9942	298.15-348.15	Zhang et al. (2009)
[aP$_{4443}$][Asn]	1.0458-1.0167	298.15-348.15	Zhang et al. (2009)
[aP$_{4443}$][Asp]	0.9963-0.9908	338.15-348.15	Zhang et al. (2009)
[aP$_{4443}$][Cys]	1.0496-1.0195	298.15-348.15	Zhang et al. (2009)
[aP$_{4443}$][Gln]	1.0571-1.0265	298.15-348.15	Zhang et al. (2009)
[aP$_{4443}$][Glu]	1.0161-0.9889	298.15-348.15	Zhang et al. (2009)
[aP$_{4443}$][Gly]	0.9973-0.9682	298.15-348.15	Zhang et al. (2009)
[aP$_{4443}$][His]	0.9993-0.9720	298.15-348.15	Zhang et al. (2009)
[aP$_{4443}$][Ile]	0.9742-0.9444	298.15-348.15	Zhang et al. (2009)
[aP$_{4443}$][Leu]	0.9661-0.9363	298.15-348.15	Zhang et al. (2009)
[aP$_{4443}$][Lys]	0.9991-0.9696	298.15-348.15	Zhang et al. (2009)
[aP$_{4443}$][Met]	1.0167-0.9874	298.15-348.15	Zhang et al. (2009)
[aP$_{4443}$][Phe]	1.0220-0.9923	298.15-348.15	Zhang et al. (2009)
[aP$_{4443}$][Pro]	1.0047-0.9754	298.15-348.15	Zhang et al. (2009)
[aP$_{4443}$][Ser]	1.0262-0.9958	298.15-348.15	Zhang et al. (2009)
[aP$_{4443}$][Thr]	1.0126-0.9824	298.15-348.15	Zhang et al. (2009)
[aP$_{4443}$][Trp]	1.0596-1.0318	298.15-348.15	Zhang et al. (2009)
[aP$_{4443}$][Tyr]	1.0429-1.0138	298.15-348.15	Zhang et al. (2009)
[aP$_{4443}$][Val]	0.9750-0.9453	298.15-348.15	Zhang et al. (2009)
[bmim][BF$_4$]	1.21-1.17	283-348	Shiflett and Yokozeki (2005)
	1.2048-1.1737	295.45-343.85	Fredlake et al. (2004)
	1.21-1.17	293.15-363.15	Arshad (2009)

Table 2-10 (Contd.): Density of Ionic Liquids at Different Temperatures Measured by Various Sources

Ionic Liquid	Density/g·cm^{-3}	Temperature/K	References
[BMIM][Bu_2PO_4]	1.0400-1.0271	313.15-333.15	Palgunadi et al. (2009)
[BMIM][$BuHPO_3$]	1.0661-1.0535	313.15-333.15	Palgunadi et al. (2009)
[bmim][CF_3COO]	1.209	298.15	Arshad (2009)
[bmim][Cl]	1.08	298.15	Arshad (2009)
[bmim][dca]	1.0580-1.0258	297.15-355.85	Fredlake et al. (2004)
[bmim][I]	1.44	298.15	Arshad (2009)
[BMIM][$MeHPO_3$]	1.1352-1.1226	313.15-333.15	Palgunadi et al. (2009)
[bmim][methide]	1.5630-1.5288	297.65-333.25	Fredlake et al. (2004)
[bmim][PF_6]	1.38-1.33	283-348	Shiflett and Yokozeki (2005)
	1.366	298.15	Kim et al. (2011)
	1.360-1.324	298.15-343.15	Cadena et al. (2004)
	1.3739	298.15	Arshad (2009)
[bmim][Tf_2N]	1.4386-1.4054	296.45-333.75	Fredlake et al. (2004)
	1.4337	298.15	Arshad (2009)
	1.44	293.15	Gan et al. (2006)
[bmim][triflate]	1.3013-1.27	295.75-342.95	Fredlake et al. (2004)
[bmmim][BF_4]	1.0935-1.0634	300.15-323.15	Fredlake et al. (2004)
[bmmim][PF_6]	1.2416-1.2055	295.65-323.15	Fredlake et al. (2004)
	1.242-1.174	295.65-343.15	Cadena et al. (2004)
[bmpy][Tf_2N]	1.4043-1.3885	209-309.1	Kumelan et al. (2010)
[C_9mim][PF_6]	1.198-1.194	293.15-298.15	Kim et al. (2011)
[dmim][BF_4]	1.07-1.03	293.15-363.15	Arshad (2009)
[DMIM][Me_2PO_4] Non Fluorinated	1.251-1.2380	313.15-333.15	Palgunadi et al. (2009)
[DMIM][$MeHPO_3$]	1.2332-1.2222	313.15-333.15	Palgunadi et al. (2009)
[dmim][Tf_2N]	1.2746	293.15	Gan et al. (2006)
[emim][BF_4]	1.305-1.264	293-343	Shokouhi et al. (2010)
	1.25-1.21	293.15-363.15	Arshad (2009)
[emim][CF_3SO_3]	1.29	298.15	Arshad (2009)
[EMIM][Et_2PO_4]	1.1386-1.1255	313.15-333.15	Palgunadi et al. (2009)
[EMIM][$EtHPO_3$]	1.1492-1.1363	313.15-333.15	Palgunadi et al. (2009)
[emim][OTf]	1.39	295.15	Arshad (2009)
[emim][Tf_2N]	1.5213-1.4858	296.15-333.65	Fredlake et al. (2004)
[emmim][Tf_2N]	1.4913-1.4572	296.15-333.65	Fredlake et al. (2004)
[hemim][BF_4]	1384-1369	300-314	Shokouhi et al. (2010)
[hexafluoroimid][Tf_2N]	1.7-1.64	283.15-343.15	Maginn (2005)
[hmim][$(CF_3SO_2)_2N$]	1.377	293.15	Ignat'ev et al. (2005)
[hmim][BF_4]	1.15-1.1	293.15-363.15	Arshad (2009)
	1.15	293.15	Ignat'ev et al. (2005)
[hmim][Cl]	1.05	293.15	Ignat'ev et al. (2005)
	1.03	293.15	Arshad (2009)
[hmim][eFAP]	1.58-1.5	283.15-343.15	Maginn (2005)
	1.56	293.15	Ignat'ev et al. (2005)
[hmim][PF_6]	1.297	293.15	Ignat'ev et al. (2005)
	1.29	298.15	Arshad (2009)
[hmim][pFAP]	1.62	293.15	Ignat'ev et al. (2005)

Table 2-10 (Contd.): Density of Ionic Liquids at Different Temperatures Measured by Various Sources

Ionic Liquid	Density/g·cm^{-3}	Temperature/K	References
[hmim][Tf_2N]	1.4-1.34	283.15-343.15	Maginn (2005)
[hmpy][Tf_2N]	1.4-1.35	283.15-343.15	Maginn (2005)
[N8881][Tf_2N]	1.0823	293.15	Gan et al. (2006)
[omim][BF_4]	1.11-1.06	293.15-363.15	Arshad (2009)
[omim][Cl]	1	298.15	Arshad (2009)
[omim][PF_6]	1.22	298.15	Arshad (2009)
[ompy][Tf_2N]	1.3327	293.15	Gan et al. (2006)
[P_{66614}][BF_4]	0.93	303.15	Arshad (2009)
[P_{66614}][Cl]	0.88	303.15	Arshad (2009)
[$PC_6C_6C_6C_{14}$][bis-dicarbollylcobalt(III) (CoCB)]	1-0.96	293.15-353.15	Arshad (2009)
[$PC_6C_6C_6C_{14}$][$Co(NCS)_4$]	0.96-0.925	293.15-353.15	Arshad (2009)
[$PC_6C_6C_6C_{14}$][$Co(NCSe)_4$]	1.02-0.97	293.15-353.15	Arshad (2009)
[$PC_6C_6C_6C_{14}$][dithiomaleonitrile (dtmn)]	0.945-0.905	293.15-353.15	Arshad (2009)
[$PC_6C_6C_6C_{14}$][methylxanthate (xan)]	0.92-0.88	293.15-353.15	Arshad (2009)
[$PC_6C_6C_6C_{14}$][$N(CN)_2$]	0.905-0.87	293.15-353.15	Arshad (2009)
[$PC_6C_6C_6C_{14}$][Tf_2N]	1.07-1.035	293.15-353.15	Arshad (2009)
[pmmim][Tf_2N]	1.4567-1.4155	295.15-344.65	Fredlake et al. (2004)
[TBA][BEHSS]	0.993	298.15	Nishi et al. (2006)
[TH_pA][BEHSS]	0.961	298.15	Nishi et al. (2006)
[TH_xA][BEHSS]	0.968	298.15	Nishi et al. (2006)
[THxA][C_1C_1N]	1.186	298.15	Nishi et al. (2006)
[TOA][BEHSS]	0.952	298.15	Nishi et al. (2006)
[TP_nA][BEHSS]	0.978	298.15	Nishi et al. (2006)
1-Pentyl-3-methylimidazolium [bFAP]	1.693	293.15	Ignat'ev et al. (2005)
bmim][acetate]	1.09-1.04	283.15-343.15	Maginn (2005)

While the density of ionic liquids is an important indication of industrial flow rate, the viscosity of ionic liquids receives more attention, since ionic liquids are generally of high viscosity which would certainly contribute towards high circulation costs in an absorption process. The study of viscosity of non-fluorinated ionic liquids was pursued by Nishi et al. (2006), Zhang et al. (2009), and Scovazzo (2009), at temperatures of 298.15-348.15 K. The viscosity was significantly higher for non-fluorinated ionic liquids than for fluorinated ionic liquids, which were studied by numerous sources including Arshad (2009), Scovazzo (2009) and Hasib-ur-Rahman et al. (2010). Nishi et al. (2006) used an oscillation type viscometer (VM-10A-M) for ionic liquid viscosity measurement. Ignat'ev et al. (2005) used an Anton Paar Viscosimeter SVM 3000 for measuring viscosity of imidazolium-based ionic liquids. Zhang et al. (2009) utilised an Anton Paar AMVn for the same measurement on non-fluorinated ionic liquids.

Table 2-11: Viscosity of Ionic Liquids Measured at Different Temperatures by Various Sources

Ionic Liquid	Viscosity (cP)	Temperature (K)	References
[1-C_3NH_2-2,3-$(mim)_2$][Tf_2N]	2307	303.15	Scovazzo (2009)
[1-Pentyl-3-(mim)][bFAP]	594 mm^2/s	293.15	Ignat'ev et al. (2005)
[aP_{4443}][Ala]	758-54.3	298.15-348.15	Zhang et al. (2009)
[aP_{4443}][Arg]	1429.3-124.8	308.15-348.15	Zhang et al. (2009)
[aP_{4443}][Asn]	1700.7-447.1	328.15-348.15	Zhang et al. (2009)
[aP_{4443}][Asp]	1632.5-481.8	338.15-348.15	Zhang et al. (2009)
[aP_{4443}][Cys]	1543.6-775.5	338.15-348.15	Zhang et al. (2009)
[aP_{4443}][Gln]	1653.3-377.7	328.15-348.15	Zhang et al. (2009)
[aP_{4443}][Glu]	1417.5-434.9	328.15-348.15	Zhang et al. (2009)
[aP_{4443}][Gly]	713.9-54.2	298.15-348.15	Zhang et al. (2009)
[aP_{4443}][His]	1094.9-313.7	328.15-348.15	Zhang et al. (2009)
[aP_{4443}][Ile]	1408.1-73.8	298.15-348.15	Zhang et al. (2009)
[aP_{4443}][Leu]	1193.8-66.3	298.15-348.15	Zhang et al. (2009)
[aP_{4443}][Lys]	1432.2-81.8	298.15-348.15	Zhang et al. (2009)
[aP_{4443}][Met]	766.8-55.10	298.15-348.15	Zhang et al. (2009)
[aP_{4443}][Phe]	1985.0-88.3	298.15-348.15	Zhang et al. (2009)
[aP_{4443}][Pro]	1772.8-81.9	298.15-348.15	Zhang et al. (2009)
[aP_{4443}][Ser]	1341.7-71.7	298.15-348.15	Zhang et al. (2009)
[aP_{4443}][Thr]	1790.5-84.6	298.15-348.15	Zhang et al. (2009)
[aP_{4443}][Tyr]	1291	348.15	Zhang et al. (2009)
[aP_{4443}][Val]	888.2-56.3	298.15-348.22	Zhang et al. (2009)
[bmim][BETI]	77	303.15	Scovazzo et al. (2009)
[bmim][BF_4]	5-100	282.48-383.15	Shiflett and Yokozeki (2005)
	219	298.15	Hunt et al. (2007)
[bmim][CF_3CO_2]	753-37	283.15-343.15	Maginn (2005)
	73	298.15	Arshad (2009)
	1630-43	283.15-343.15	Maginn (2005)
[bmim][Cl]	40890	293.15	Hunt et al. (2007)
	1534	323.15	Arshad (2009)
[bmim][I]	1110	298.15	Arshad (2009)
[bmim][PF_6]	176	303.15	Scovazzo (2009)
	10-200	282.48-383.15	Shiflett and Yokozeki (2005)
	450	298.15	Arshad (2009)
[bmim][Tf_2N]	52	303.15	Scovazzo (2009)
	70	298.15	Hasib-ur-Rahman et al. (2010)
	52	298.15	Hunt et al. (2007)
	52	293.15	Gan et al. (2006)
[bmim][Tf_2N], PTFE	70	298.15	Hanioka et al. (2008)
[Bu_2Nic][Tf_2N]	1830-49	283.15-343.15	Maginn (2005)
[C_3NH_2mim][CF_3SO_3]	3760	298.15	Hasib-ur-Rahman et al. (2010)
	3760	298.15	Hanioka et al. (2008)
[C_3NH_2mim][Tf_2N]	2180	298.15	Hasib-ur-Rahman et al. (2010)
	2.18E+03	303.15	Scovazzo (2009)
[C_3NH_2mim][Tf_2N], PTFE	2180	298.15	Hanioka et al. (2008)
[C_3NH_2mim][TfO]	3760	303.15	Scovazzo (2009)

Table 2-11 (Contd.): Viscosity of Ionic Liquids Measured at Different Temperatures by Various Sources

Ionic Liquid	Viscosity (cP)	Temperature (K)	References
[desmim][TfO]	554	303.15	Scovazzo (2009)
[despyrrol][Tf_2N]	1743	303.15	Scovazzo (2009)
[dmim][Tf_2N]	142	293.15	Gan et al. (2006)
[dumbbell][Tf_2N]	2420	303.15	Scovazzo (2009)
[emim][BF_4]	38	303.15	Scovazzo (2009)
	67	298.15	Arshad (2009)
	34	303.15	Scovazzo et al. (2009)
[emim][CF_3SO_3]	45	303.15	Scovazzo et al. (2009)
	90	298.15	Arshad (2009)
[emim][dca]	21	303.15	Scovazzo et al. (2009)
	21	303.15	Scovazzo (2009)
[emim][TfO]	50	293.15	Arshad (2009)
	45	303.15	Scovazzo (2009)
[emim][PF_6]	23	343.15	Arshad (2009)
[emim][Tf_2N]	28	298.15	Arshad (2009)
	26	303.15	Scovazzo et al. (2009)
	26	303.15	Scovazzo (2009)
[EMIM][TFSI]	7-55	313.15	Liu et al. (2011)
[Et_2Nic][$EtSO_4$]	19610-130	283.15-343.15	Maginn (2005)
[hmim][$(CF_3SO_2)_2N$]	44 mm^2/s	293.15	Ignat'ev et al. (2005)
[hmim][BF_4]	314	293.15	Arshad (2009)
	195 mm^2/s	293.15	Ignat'ev et al. (2005)
[hmim][Cl]	7453 mm^2/s	293.15	Ignat'ev et al. (2005)
	716	298.15	Arshad (2009)
[hmim][eFAP]	74 mm^2/s	293.15	Ignat'ev et al. (2005)
[hmim][lactate]	3350-54	283.15-343.15	Maginn (2005)
[hmim][PF_6]	548 mm^2/s	293.15	Ignat'ev et al. (2005)
	585	298.15	Arshad (2009)
[hmim][pFAP]	227 mm^2/s	293.15	Ignat'ev et al. (2005)
[hmim][Tf_2N]	148-16	283.15-343.15	Maginn (2005)
	55	303.15	Scovazzo et al. (2009)
	55	303.15	Scovazzo (2009)
[hmmim][Tf_2N]	317-23	283.15-343.15	Maginn (2005)
[hmpy][Tf_2N]	197-17	283.15-343.15	Maginn (2005)
[$N_{(1)444}$][Tf_2N]	386	303.15	Scovazzo (2009)
[$N_{(1)888}$][Tf_2N]	532	303.15	Scovazzo (2009)
[$N_{(10)11}$(i-3)][Tf_2N]	183	303.15	Scovazzo (2009)
[$N_{(10)111}$][Tf_2N]	173	303.15	Scovazzo (2009)
[$N_{(4)11}$(i-3)][Tf_2N]	85	303.15	Scovazzo (2009)
[$N_{(4)111}$][Tf_2N]	71	303.15	Scovazzo (2009)
	71	303.15	Condemarin and Scovazzo (2009)
[$N_{(6)11}$(i-3)][Tf_2N]	126	303.15	Scovazzo (2009)
[$N_{(6)111}$][Tf_2N]	100	303.15	Scovazzo (2009)
[$N_{(6)222}$][Tf_2N]	167	303.15	Scovazzo (2009)
[N_{8881}][Tf_2N]	589.3	293.15	Gan et al. (2006)

Table 2-11: Viscosity of Ionic Liquids Measured at Different Temperatures by Various Sources

Ionic Liquid	Viscosity (cP)	Temperature (K)	References
[omim][Cl]	337	298.15	Arshad (2009)
[omim][PF_6]	682	298.15	Arshad (2009)
[ompy][Tf_2N]	26.7	293.15	Gan et al. (2006)
[$P_{(14)444}$][DBS]	3011	303.15	Scovazzo (2009)
[$P_{(14)666}$][Cl]	919	303.15	Scovazzo (2009)
[$P_{(14)666}$][Cl]	1316	303.15	Scovazzo (2009)
[$P_{(14)666}$][dca]	213	303.15	Scovazzo (2009)
[$P_{(14)666}$][Tf_2N]	243	303.15	Scovazzo (2009)
[$P_{(2)444}$][DEP]	207	303.15	Scovazzo (2009)
[P_{66614}][Cl]	1500	298.15	Arshad (2009)
[PP-13][Tf_2N]	94.3	303.15	Scovazzo (2009)
[$S_{(1)22}$][Tf_2N]	42	303.15	Scovazzo (2009)
[$S_{(2)22}$][Tf_2N]	38.9	303.15	Scovazzo (2009)
[TBA][BEHSS]	373	298.15	Nishi et al. (2006)
[TH_pA][BEHSS]	690	298.15	Nishi et al. (2006)
[TH_xA][BEHSS]	639	298.15	Nishi et al. (2006)
[THxA][C_1C_1N]	388	298.15	Nishi et al. (2006)
[TOA][BEHSS]	759	298.15	Nishi et al. (2006)
[TP_nA][BEHSS]	517	298.15	Nishi et al. (2006)
Ecoeng 41M	4065-97.9	283.15-343.15	Maginn (2005)
Ecoeng 500	10244-186.10	283.15-343.15	Maginn (2005)
EM(Zn)TFSI 1-1	148-2000	313.15	Liu et al. (2011)
General	14.6-388.4*	298.15	Wappel et al. (2009)
General	7.6-54.6	323.15	Wappel et al. (2009)
tri-iso-butyl(methyl) phosphonium tosylate (TSIL)	1.65-1320**	298.15	Hasib-ur-Rahman et al. (2010)

*Viscosity recorded at 50-70 wt% H_2O **Viscosity recorded at 100-0 wt% H_2O

A study into the absorption kinetics of some novel ionic liquids has been done by Wappel et al. (2009), which found that ionic liquid regeneration is less energy intensive than conventional alkanolamine solvents. The study also found that the addition of water at 30-40wt% provides better absorption performance and contributed towards a significantly lower solvent viscosity than if pure undiluted ionic liquid was used. While the required regeneration energy is elevated by the dilution with water, there are potentially significant savings in circulation energy for the solvent.

2.5.7 Trends exhibited in the study of CO_2 absorption in ionic liquids

The study of ionic liquids by various sources has provided many general observations. It is necessary to note these observations in order to commence further research into finding an ionic liquid which is advantageous for CO_2 absorption.

The solubility of CO_2 in ionic liquids increases with increasing CO_2 partial pressure, and decreasing temperature. Muldoon et al. (2007) explained that high pressures introduce

secondary interactions of CO_2 with the cation, increasing CO_2 solubility. SuoJiang et al. (2010) identified trends between temperature and CO_2 solubility. It was found that high temperatures reduce absorption capacity, while very low temperatures reduce absorption rate. An optimum temperature of 318.15 K was found. Temperature also affects the significance of various functional groups attached to cations and anions, but no standard trend has been identified (Cadena et al., 2004).

The addition of hydrogen instead of methyl functional groups are reported to provide increased CO_2 solubility. Methyl functional groups possibly result in steric hindrance. The effect is more pronounced at low temperatures (Cadena et al., 2004). Lower enthalpy of absorption was also reported.

In order to optimise CO_2 solubility, it was observed that changing or modifying the anion provided far more significant changes than changing or modifying the cation, which provided a secondary change in results (Anderson et al., 2007, Anderson et al., 2007, Arshad, 2009). Cadena et al. (2004) and Huang and Rüther (2009) explained that CO_2 molecules are absorbed and interact strongly about the anions, occurring in a tangent like arrangement. CO_2 molecules occur diffusely around cations.

Huang and Rüther (2009) discovered that a Lewis-acid type interaction occurs between CO_2 and anions, with CO_2 acting as a Lewis acid and anions acting as a Lewis base. The absorption mechanism of CO_2 in ionic liquids was studied. Coulombic interactions cause the cations and anions to organize themselves to form a more rigid packing than in molecular solvents. As a result, thermal expansion coefficients are lower than molecular solvents. CO_2 absorption does not significantly perturb the arrangement of ions. The ionic arrangement contains a large amount of free volumes for CO_2 absorption. The ions experience an angular displacement to accommodate CO_2 during absorption. CO_2 exists above and below ions, particularly near imidazolium rings and near long alkyl chains on the rings. Greater interaction occurs between CO_2 and anions, which causes CO_2 molecules to remain in close proximity to the anions. CO_2 diffuses throughout the IL, without significant disturbance to the rigid cation-anion arrangement.

While cations were found to provide secondary interactions with CO_2, research has shown by observation that imidazolium based cations are the best cations for ionic liquids used in CO_2 absorption. Arshad (2009) has compared ionic liquids containing different cations with the same anions. The chain length of cations was kept constant. The study found imidazolium cations to provide the highest CO_2 solubility. Baltus et al. (2004) compared CO_2 solubilities in ionic liquids containing imidazolium cations with phenol based cations. CO_2 solubility was higher in

imidazolium cations. Huang and Rüther (2009) found diffusion coefficients of CO_2 in ionic liquids with imidazolium cations to be less affected by high viscosity. Less interaction between cations and anions occur, resulting in less viscosity and higher diffusion coefficients.

It was observed that increasing fluorination of the ionic liquid increases absorption rate and capacity. The effect was more pronounced when fluorinating the anion (Muldoon et al., 2007, Brennecke and Gurkan, 2010, Arshad, 2009, Baltus et al., 2004). Arshad (2009) stated that increasing the number of CF_3 groups on the anion greatly increases CO_2 solubility. Increasing fluorination of the cation increased CO_2 solubility but not as significantly as anion fluorination. Huang and Rüther (2009) explained that during interaction with hydrocarbons, CO_2 molecules act as a weak Lewis base. The oxygen atom in CO_2 interacts with the C–H bond. But when electronegative fluorine atoms are present, the C–F bond may interact with the Lewis acidic carbon atom on the CO_2 molecule. It is this difference in interaction or possibly the combination of these interactions that causes higher CO_2 solubility in fluorinated ionic liquids.

While increased fluorination of the ionic liquid provides increased absorption rate and capacity, it was also found to contribute to increasing toxicity of the ionic liquid (Anderson et al., 2007, 25). Arshad (2009) reported fluorinated ionic liquids to be of poor biodegradability and are persistent in the environment.

Non-fluorinated ionic liquids are more environmentally friendly but provide lower CO_2 solubility than fluorinated ionic liquids. Arshad (2009) reported ideas to mitigate this problem, with the addition of ester, ether and carbonyl groups to enhance the CO_2-philicity of the ionic liquid. Palgunadi et al. (2009) suggested the introduction of alkyl phosphate and dialkyl phosphate anions, which were also found to increase CO_2 solubility in non-fluorinated ionic liquids.

Huang and Rüther (2009) suggested limiting fluorination of ionic liquids to reduce toxicity. Fluorination of the cation is not necessary and may be omitted, since this does not significantly impact on CO_2 solubility compared to fluorination of anions. CO_2 was reported to interact with anions and with the C-2 position of cations.

The longer the alkyl chain length of cations and anions, the higher the solubility of CO_2 observed (Muldoon et al., 2007, Brennecke and Gurkan, 2010, Baltus et al., 2004). The increased chain length provides increased gas permeability and diffusivity. Anderson et al. (2007) noted that the effect is more pronounced when the system is operating at high pressure. Longer alkyl chains are reported to provide smaller ionic liquid density and larger free volume between ions to accommodate CO_2 molecules (Huang and Rüther, 2009). However, Hasib-ur-

Rahman et al. (2010) noted that too long alkyl chains can result in steric hindrance, which ultimately reduces absorption capacity of the solvent. Palgunadi et al. (2009) confirmed the effects of increasing chain length and suggested this practice as an environmentally friendly alternative to fluorination for increasing CO_2 solubility.

The effect of increasing chain length is not as significant as increasing fluorination of the ionic liquid, particularly the anion (Brennecke and Gurkan, 2010, Gonzalez et al., 2011).

The disadvantage of increasing chain length of cations and anions is that the viscosity of the ionic liquid increases (Gan et al., 2006). This is an important issue as ionic liquids generally possess high viscosities of up to 2000 cP (Scovazzo, 2009) and some over 2000 cP. Increased viscosity was also reported to result in lower diffusion coefficients. Huang and Rüther (2009) observed the diffusion coefficient (D) of CO_2 into ionic liquids with imidazolium based cations to decrease with increasing viscosity (μ) according to the proportion: $D\alpha\mu^{-0.6}$. Branched cations increased viscosity further (Gan et al., 2006). For phosphonium based cations, the proportion is $D\alpha\mu^{-0.35}$. These proportionalities indicate that in attempts to increase chain length, it must be ensured that the increased chain length must increase diffusivity by a higher proportion than which the viscosity is increased. If this criterion is not met, then increasing chain length would have reached its limits.

Additionally, Lozano et al. (2011) provided evidence of increasing toxicity of the ionic liquid, with increasing alkyl chain length.

Cadena et al. (2004) reported a 10% increase in density of ionic liquids upon absorption of CO_2, while Huang and Rüther (2009) noted increases in ionic liquid volume of 18%. This result differs greatly to organic solvents which undergo volume increases of up to 103% with no significant change in density upon CO_2 absorption.

The functionalising of ionic liquids produces varying results. Brennecke and Gurkan (2010) noted that the addition of amine groups to imidazolium cations provided increased absorption capacity. Simply adding alkanolamines to ionic liquids resulted in a hybrid solvent in which physical and chemical absorption occurs. This was beneficial in terms of heat requirements, when compared to conventional alkanolamine solvents which contain high quantities of water. The energy requirement of ionic liquid-alkanolamine mixtures is dictated by the heat of reaction between CO_2 and the alkanolamine. Heterocyclic anions are used for hybrid solvents to simplify the reaction mechanism to provide lower increases in solvent viscosity.

In addition to amines, the use of ether functional groups also increased CO_2 solubility (Anderson et al., 2007). Liu et al. (2011) investigated the addition of zinc (Zn) to cations. CO_2

solubility was 21 times higher than conventional ionic liquids, but viscosity increased, resulting in diffusivity values 3 times lower than conventional ionic liquids. Huang and Rüther (2009) noted that when adding a functional group, it needs to be ensured that CO_2 binds with the functional group in a thermodynamic sense and kinetics should be sufficient for fast absorption rate. Absorption must not be too exothermic, as required regeneration energy will be high. The addition of carboxylate groups to ionic liquids improved absorption capacity but not as much as that of conventional alkanolamines. Heat of absorption was lower than conventional alkanolamines however.

Huang and Rüther (2009) also investigated the prospect of combining ionic liquids with more than one functional group. Amines and acid groups such as SO_3 were added. The study found that this prospect increased solvent viscosity substantially. Hence, much consideration needs to be taken upon the addition of functional groups to alkyl chains of cations and anions.

CHAPTER 3: REVIEW OF EQUIPMENT FOR MEASURING CO_2 ABSORPTION IN SOLVENTS

As previously mentioned in Section 2.5 of Chapter 2, it was determined by literature review that gas absorption using solvents showed very high potential as an industrial CO_2 capture technique in the near future. Many advantages and challenges were found regarding the implementation of gas absorption using solvents for CO_2 capture. The main challenge was to find a suitable solvent that would selectively capture CO_2 at low pressure and high temperature, to avoid significant flue gas pre-treatment costs.

Alkanolamines were found to be abundantly investigated while many ionic liquids received comparatively little attention for CO_2 capture. It was thus explained in Section 2.5 of Chapter 2 that this research would investigate the use of ionic liquids as solvents to selectively absorb CO_2. Chapter 6 further explains that suitable ionic liquids would be combined with alkanolamines to create novel hybrid solvents that were also investigated for CO_2 absorption.

This chapter contains a concise review of various apparatus for measuring equilibrium gas absorption in various solvents, including systems containing CO_2, alkanolamines, and ionic liquids.

Equilibrium gas absorption in alkanolamines was successfully measured using a static analytic apparatus by Osman (2011) and Dicko et al. (2010). The apparatus was constructed using sapphire tube for high pressure and temperature conditions. Gas and liquid composition analysis was achieved using gas chromatography and sampled using ROLSI^{TM} samplers. The use of ROLSI^{TM} samplers resulted in minimal disturbance in equilibrium due to the sample size being in the order of magnitude of microliters. Systems containing H_2O, CO_2, N_2, MEA, DEA, and MDEA were investigated. The setup is completely sealed, thereby allowing measurement of systems with volatile components. P-T-x-y measurements were obtainable to establish equilibrium absorption capacity of the solvent.

Absorption measurements were obtained using a dynamic still by Austgen and Rochelle (1991). A presaturator and diluter cell were used and gas composition was measured using Fourier Transform Infrared (FTIR) spectroscopy. Measurements were reported to be relatively quicker than when using a static analytic apparatus. As previously mentioned, the use of a diluter cell apparatus to measure absorption by calculation of infinite dilution activity coefficients and Henry's Law constants, was investigated by Richon et al. (1980) and Richon (2011). In these cases, analyses were done using gas chromatography.

Previous sources in literature have successfully used Fourier Transform Infrared (FTIR) spectroscopy for composition analysis in absorption measurements by analysing the spectra of samples before absorption and then after absorption at different equilibrium conditions. An FTIR spectrometer measures the composition of a sample by passing infrared light of multiple frequencies through the sample, detecting the infrared light, and establishing which frequencies were absorbed by the sample and which were not. Each compound vibrates at a unique frequency due to the vibrations that occur between different atoms in a molecule. This gives each compound in a mixture a unique frequency signature. When light of multiple frequencies passes through a sample, certain frequencies of light match the frequency of molecules and are hence absorbed while frequencies not matching the vibration frequencies of the compounds in the sample pass through unaffected (Thermo Nicolet, 2001).

Archane et al. (2008) utilised FTIR spectroscopy to measure CO_2 absorption in aqueous DEA solutions. An equilibrium cell with circulation to the spectrometer was employed and an accurate indication of the reaction mechanism was achieved, including the carbamate concentration. Further studies of a similar nature with CO_2 in DEA were completed by Diab et al. (2012). These studies differ from that of Austgen and Rochelle (1991) in that the liquid phase composition is analysed and an equilibrium cell is used instead of a diluter cell with gas phase composition analysis. Zhao et al. (2011) used FTIR spectroscopy to propose the absorption and desorption mechanism of CO_2 in amine-functionalised ionic liquids.

The advantages of using an FTIR spectrometer for composition analysis is that the technique is non-destructive, measurements are quick, and the in-situ analysis, as was intended in this study, is safe due to the FTIR probe possessing no moving parts. The technique is also non-invasive in comparison to the use of other apparatus for composition analysis such as gas chromatography. Species are not disturbed at all from equilibrium during composition analysis.

The disadvantage of using equilibrium cells with FTIR spectroscopy or gas chromatography is that the quantity of solvent that measurements require is substantial. This is because gas chromatography is an invasive measurement technique which would disturb equilibrium if solvent and gas quantity is too low. Although the use of FTIR is not invasive, in practise a significant amount of solvent is required to be circulated to the spectrometer or for the use of in-situ infrared probes. This disadvantage is particularly significant when measuring new solvents such as ionic liquids, which are of very high cost and very difficult to synthesize with high purity. Moreover, the solvent quantity results in higher equilibration time for temperature, pressure and gas absorption. In the work of Osman (2011), equilibrium took up to 12 hours for systems containing CO_2, H_2O, DEA, and MDEA.

Gravimetric analysis was used by numerous sources in the study of CO_2 absorption in ionic liquids and other non-volatile solvents and sorbents. This measurement technique utilises a high resolution microbalance to track the weight change of solvents or sorbents as they absorb a gas. Anthony et al. (2002) detailed measurements related to CO_2 absorption in ionic liquids by gravimetric analysis. Further measurements of CO_2 and other gases in ionic liquid solvents were done by Anderson et al. (2007), Cadena et al. (2004), and Shiflett and Yokozeki (2005). Measurements of mole fraction in the ionic liquid sample were taken for different isotherms at pressures of 0 – 2 MPa.

Anthony et al. (2001) obtained VLE and LLE measurements of various gases and water in ionic liquids. Henry's constant and infinite dilution activity coefficient were measured. Roper (2005) conducted measurements on the adsorption of CO_2 on activated carbon in order to establish the pore size distribution of activated carbon. In this case, a sample of solid activated carbon was inserted and CO_2 gas constituted the gas phase. The adsorption in terms of mass uptake was measured for different pressures at 273 K.

Accuracy in results can be established by conducting repeated absorption and desorption of the sample. The hysteresis gives an indication of species purity and resultant accuracy. Shao et al. (2004) stated that the apparatus is fully computer controlled and can be programmed so that experiments can continue for several days if necessary.

Absorption and desorption of H_2 was studied at various pressures, at 333.15 K by Shao et al. (2004). Accurate results were achieved due to gravimetric analysers being able to maintain a constant pressure throughout the measurement. This is advantageous over volumetric measurement which fails to adequately maintain system pressure during equilibration.

Shao et al. (2004) investigated the adsorption of H_2 on various surfaces such as activated meso-carbon microbeads. Methane was also investigated in the study. RSC (2011) also studied the adsorption of H_2 gas on CF and CF/Pd-Hg samples at a single isotherm of 298 K, at pressures of 0 – 2 MPa.

A particular advantage of gravimetric analysis is that very little ionic liquid needs to be used to obtain accurate measurements. Anthony et al. (2002) utilised 75 mg of ionic liquid during the measurements of Henry's constants for various flue gas components in ionic liquids, which is advantageous since ionic liquids are comparatively very expensive at present.

RSC (2011) found that due to the high resolution of the microbalance, buoyancy effects needed to be accounted for. Instead of adding extra equilibration time to account for this as Anthony et

al. (2001) did, the measurements were mathematically corrected based on Archimedes principle to account for buoyancy.

The disadvantage of gravimetric analysis is that it cannot be used for volatile solvents since the solvents may evaporate from the microbalance, resulting in erroneous absorption measurements. Moreover, simple gravimetric analysers do not encompass direct composition analysis for the liquid or gas phase, though this can be achieved by passing the gas phase through NMR or IR spectroscopy.

Due to the high cost of ionic liquids, it was decided that gravimetric analysis would be used to measure gas absorption in the ionic liquid and hybrid solvents studied in this work. In the case of hybrid solvents, solvents contained ionic liquids and alkanolamines as explained in Chapter 6. For each measurement the gas phase contained a single gas. The method of measurement is described in Section 5.3 of Chapter 5.

In order to understand the reaction mechanism between CO_2 and the hybrid solvents investigated, an equilibrium cell was developed using in-situ infrared spectroscopy to identify components in the liquid phase and measure liquid phase composition. The apparatus was found to be limited in measurement range. The details of this apparatus are presented in Appendix F.

CHAPTER 4: REVIEW OF THE MODELLING OF CO_2 ABSORPTION IN ALKANOLAMINES, IONIC LIQUIDS AND HYBRID SOLVENTS

It is important to model the CO_2 absorption data measured in this work in order to provide accurate interpolation and even extrapolation of data to wider system pressure and temperature ranges. Modelling saves not only time, but also resources, since absorption data can be calculated with fairly good accuracy using a model with parameters regressed from a reliable and comprehensive data set. This ensures that every single data point need not be measured, but can be calculated with fairly high accuracy instead.

Moreover, regressed model parameters can be programmed into simulation software to be used in process simulation, a task that requires data at many more conditions that couldn't possibly be achieved through measurement alone.

The modelling of CO_2 partial pressure in systems containing both ionic liquids and alkanolamines was highly challenging due to the presence of up to 5 components in a system, including CO_2, MEA, DEA, MDEA, and either [Bmim][BF_4] or [Bmim][Tf_2N]. Moreover, the chemistry of the systems containing hybrid solvents is unknown due to the absence of water in the systems. In the systems in this work, all diffusion occurs into the ionic liquid and alkanolamine directly. There is no water, thus no diffusion reactions between CO_2, HCO_3^- and water, as that shown conventionally in reactions R2-4 to R2-12 in Section 2.4.1.1.

Numerous models have been investigated for the prediction of CO_2 partial pressure and CO_2 mole fraction for systems containing CO_2 and alkanolamine solvents diluted with water. Accurate modelling of CO_2 solubility in alkanolamines was typically made possible by taking into account the Debye-Huckel limiting term which accounts for non-ideality of solutions containing ionic solutes, which is a result of long range electrostatic interactions between ions (Osman, 2011). Klyamer et al. (1973) used an activity coefficient approach for the excess Gibbs free energy. Chemical reaction equilibrium in the liquid phase was assumed. Species interaction was ignored and activity coefficients were assumed equal for each species (Weiland et al., 1993).

The Kent-Eisenberg model thereafter accounted for non-idealities in the system by including them in equilibrium constant (K) values, (Benamor and Aroua, 2005 and Osman, 2011). Activity coefficients and fugacity coefficients were taken to be unity, and the model was found

to be highly useful for single alkanolamine systems. The model assumes a 6 stage reaction mechanism between CO_2 and alkanolamines. Weiland et al. (1993) attempted to apply the model for alkanolamine blends and systems containing tertiary amines, with little success in accuracy. Lee et al. (2013) however successfully modelled systems containing mixtures of MEA and Benzoic Acid using the Kent-Eisenberg model. The model was successfully applied in steady state absorption simulations by Jayarathna et al. (2011) and more recently for absorption plant start-up by Jayarathna et al. (2013) for a solvent containing MEA and water.

Modelling of CO_2 absorption using the Elec-NRTL was investigated extensively in the work of Chen and Evans (1986), Austgen et al. (1989), and Austgen et al. (1991). Solution chemistry is included in the Elec- NRTL model, allowing for all liquid-phase molecular and ionic species to be determined (Osman, 2011). Up to 6 stage reaction mechanism is assumed, and interactions parameters are found by regressing solubility data. This model was successfully used in the simulation of gas absorption by Osman (2011). Systems involving single alkanolamines MEA and DEA with gases including H_2S and CO_2 were studied by Austgen et al. (1989) using this model at 298.15 to 393.15 K. Fairly accurate predictions were achieved. Systems containing CO_2 and SO_2 gas were modelled using the Elec-NRTL model by Wappel et al. (2008).

A less complex model that is also thermodynamically rigorous and accounts for long and short range species interactions, is the Deshmukh-Mather model. A 6 stage reaction mechanism including 3 diffusion reactions between CO_2 and H_2O are assumed. Model development is found in the work of Deshmukh and Mather (1981) and Weiland et al. (1993).The model was successfully modified and provided good predictions for alkanolamine blends, including tertiary amines such as MDEA (Benamor and Aroua, 2005, Osman et al., 2012). Weiland et al. (1993) also investigated alkanolamine blends. Modelling of CO_2 and H_2S was accurately achieved.

The Deshmukh-Mather model was used to model CO_2 solubility in a variety of alkanolamines and alkanolamine blends. CO_2 absorption in aqueous mixtures of MDEA and di-isopropanolamine (DIPA) was modelled using the Deshmukh-Mather model at 313 to 358 K, by Vahidi et al. (2013). Absolute deviations of 0.2 to 40.3% were observed, with particularly high inaccuracy at pressure below 500 kPa. Najibi and Maliki (2013) modelled CO_2 absorption in MDEA-Piperazine systems at 363 to 423 K and up to 204 kPa. High average absolute deviations were achieved at pressures below 70 kPa. Greater accuracy was achieved for systems containing AEEA at 313 to 368 K and pressure from atmospheric up to 4400 kPa (Zoghi et al., 2012). Systems containing MEA and TEA were also modelled well at 313 to 373 K and up to 120 kPa using the Deshmukh-Mather model (Cheng et al., 2010).

Posey et al. (1996) introduced a simple empirical model, assuming the entire reaction mechanism between CO_2 and alkanolamines to be a single absorption reaction. Posey et al. (1996) systems involved a gas mixture of CO_2 and H_2S in single alkanolamine solvents of MDEA: H_2O and DEA: H_2O at various concentrations.

The model was tested for systems using DEA solvent for CO_2 and H_2S. Dicko et al. (2010) confirmed the model to be relatively accurate for systems involving MDEA at concentrations of up to 50 wt%, despite its simplicity. Osman (2011) utilised the model for CO_2 absorption in blends of H_2O, DEA and MDEA. Inaccuracies of as low as 0.01% of the measured data were achieved.

The absence of H_2O in the systems in this research invalidated the complex reaction mechanisms assumed by more complex models. Moreover, infrared measurements were unsuccessful in determining liquid phase composition, due to technical limitations associated with the FTIR Probe apparatus as explained in Section F2 of Appendix F. It was thus decided to model CO_2 absorption in the alkanolamine component of the hybrid solvents using the Posey-Tapperson-Rochelle model. The extent of CO_2 absorption was estimated using data from measurements with CO_2 in pure ionic liquid systems, and noting the difference in absorption upon inclusion of the alkanolamines. The extent of absorption in each alkanolamine component however could not be determined by gravimetric analysis alone. The only option with such experimental circumstances was to assume a single reversible reaction and model the data based on this simplified case.

Model computation is very easy to apply to any P-T-x data. P-T-x data presented in Tables A-10 to A-21 of Appendix A were regressed. The following reaction is assumed for CO_2 with all alkanolamines in the hybrid solvent.

$$AmineH^+ + HCO_3^- \leftrightarrow Amine + CO_2(aq.) + H_2O \quad \text{.....(R4-1)}$$

Carbonate (CO_3^{2-}) and hydroxide (OH^-) ion concentration are assumed to be small and neglected. The assumed presence of H_2O does contribute to inaccuracy in prediction, since CO_2 diffusion is occurring in the ionic liquid instead of water. This is seen in Section 7.9.

The equilibrium constant for the above reaction is given by (Posey et al., 1996, and Dicko et al., 2010):

$$\text{Ln}(K_{CO2}) = a + \frac{b}{T} + cL_T C^O{}_{AMINE} + d(L_T C^O{}_{AMINE})^{0.5} \quad \text{.....(E4-1)}$$

with $C^O{}_{AMINE}$ = Amine concentration neglecting the presence of acid gases.

$$= \frac{\text{Amine}}{\text{Amine} + \text{Ionic Liquid}} \quad \text{.....(E4-2)}$$

Thereafter, P_{CO2} can be predicted using the following formula:

$$P_{CO2} = X_{CO2} K_{CO2} \frac{L_T}{(1 - L_T)} \quad \text{.....(E4-3)}$$

Parameter "a" in Equation E4-1 represents an overall correction factor, 'b' represents a temperature correction and "c" and "d" accounting for amine concentration in the solvent. Parameters a to d are found by regression of measured data. CO_2 partial pressure can then be calculated and compared to measured results.

Gas absorption in ionic liquids has been modelled by numerous sources in literature utilising various models. Semi-empirical models such as COSMO-RS were utilised by Mortazavi et al. (2012) to predict CO_2 partial pressure in ionic liquids containing imidazolium and pyridinium cations with fluorinated anions. The model did not provide good accuracy, with deviations from experimental data of up to 23%.

Statistical Associating Fluid Theory (SAFT) equations of state have also been used for the prediction of CO_2 partial pressure in CO_2-ionic liquid systems. The SAFT models cater for the asymmetry of ionic liquid molecules, the Lewis-base type interactions of CO_2 with ionic liquid molecules, as well as the presence of charges. Truncated Perturbed Chain- Statistical Associating Fluid Theory (tPC-SAFT) takes into account dipolar and quadrupolar interaction, as well as cross polar interactions between molecules of the system. Andreu and Vega (2007) successfully modelled CO_2 absorption in ionic liquids containing $[BF_4]$ and $[PF_6]$ anions using the soft-SAFT EOS. TPC-SAFT was employed by Kroon et al. (2006) for similar ionic liquids as in the work of Andreu and Vega (2007). Good agreement between experimental and calculated VLE data was achieved.

The drawback of SAFT equations of state is the complexity in computation and the resultant slow speed of computation (Andreu and Vega, 2007). Simpler equations of state could also be used to achieve fairly good accuracy with considerably less complexity and computation time.

CO_2 partial pressure was modelled by Yazdizadeh et al. (2011) using the Peng-Robinson equation of state (EOS) with Wong-Sandler mixing rules, for systems of CO_2 with various imidazolium based ionic liquids with fluorinated anions. The Van-Laar model for excess Gibbs energy was used. Average absolute deviations between experimental and calculated results were 3.9 to 4.9%.

A generic non electrolyte Redlich-Kwong EOS was employed by Shiflett et al. (2005) for CO_2 absorption in [Bmim][BF_4] and [Bmim][PF_6] ionic liquids, due to the presence of non-volatile components containing no known critical point conditions. Systems of this nature containing electrolytes have also been reported in literature to be successfully modelled using ordinary equations of state (Tillner and Friend, 1998 and Yokozeki, 2005).

Data at 283.15 to 348.15 K and up to 2 MPa were modelled by Shiflett et al. (2005). The simplicity and low computation time of the RK-EOS made it an attractive choice to model the data in this research. Moreover, the model was proven successful at temperature and pressure conditions similar to that measured in this research. CO_2 and O_2 absorption in [Bmim][BF_4] and [Bmim][Tf_2N] was thus modelled using the RK-EOS.

The RK-EOS is given by the following (Shiflett et al., 2005):

$$P = \frac{RT}{V-b} - \frac{a(T)}{V(V+b)} \quad \text{.....(E4-4)}$$

where $a(T)$ is a function of species mole fraction and temperature. The Van der Waals-Berthelot mixing formula was used for this research, as successfully applied for similar conditions (Yokozeki, 2001).

$$a(T) = \sum_{i,j=1}^{N} \sqrt{a_i a_j}\left(1+\frac{\tau_{ij}}{T}\right)\left(1-k_{ij}\right)x_i x_j \quad \text{.....(E4-5)}$$

where $k_{ij} = \dfrac{l_{ij} l_{ji}\left(x_i + x_j\right)}{l_{ji} x_i + l_{ij} x_j}$; $a_i = 0.427480 \dfrac{R^2 T_{ci}^2}{P_{ci}} \alpha_i(T)$

and where $\alpha_i(T) = \sum_{k=0}^{\leq 3} \beta_k \left(\frac{T_C}{T} - \frac{T}{T_C}\right)^k$

and $b = \frac{1}{2}\sum_{i,j=1}^{N}\left(b_i + b_j\right)\left(1-m_{ij}\right)\left(1-k_{ij}\right)x_i x_j$ where $b_i = 0.08664 \dfrac{RT_{ci}}{P_{ci}}$

$m_{ij} = m_{ji}$ and $m_{ii} = 0$ and l_{ij}, l_{ji}, τ_{ij}, and m_{ij} are binary interaction parameters. Coefficients β_k are treated as adjustable fitting parameters. l_{ij}, l_{ji}, τ_{ij}, m_{ij}, and β_k are obtained by regression of measured data P-T-x data. Critical temperature and pressure for the ionic liquids studied in this research could not be found due to the ionic liquids decomposing before reaching their critical point (Valderrama and Robles, 2007). Critical temperature and pressure were computed using a

modified Lydersen-Joback-Reid group contribution method (Alvarez and Valderrama, 2004 and Valderrama and Robles, 2007):

$$T_C = \frac{T_b}{A_M + B_M \sum n\Delta T_M - \left(\sum n\Delta T_M\right)^2} \quad \text{.....(E4-6)}$$

where $T_b = 198.2 + \sum n\Delta T_{bM}$

$$P_C = \frac{M}{\left[C_M + \sum n\Delta P_M\right]^2} \quad \text{.....(E4-7)}$$

where A_M = 0.5703, B_M = 1.0121, C_M = 0.2573, E_M = 6.75 (Valderrama and Robles, 2007). n is the number of occurrences of any particular functional group in the molecule. Group contributions for ΔT_{bM}, ΔT_M and ΔP_M are provided in the work of Alvarez and Valderrama (2004).

The absorption of CO_2 and O_2 in pure ionic liquids, as well as the absorption of CO_2 in the ionic liquid component of systems containing hybrid solvents were modelled using the RK-EOS. CO_2 absorption in alkanolamines was modelled using the Posey-Tapperson-Rochelle model, as was successfully applied in the work of Osman et al. (2012). All modelling was programmed in Matlab R2011b™. The modelling of CO_2 absorption in hybrid solvents is available under the file name "PhDModelling2.m", while the modelling of CO_2 and O_2 absorption is available under the file name "IL_Generic_RK_EOS_Modelling.m". These files and their supporting files are available electronically in the attached CD. Binary interaction and fitting parameters are presented in Table 7-4 and 7-5of Chapter 7, while calculated CO_2 partial pressure is presented in Tables A-1 to A-21 of Appendix A. The results of the modelling are discussed in Sections 7.6 and 7.9 of Chapter 7. Critical properties are presented in Table B-1 of Appendix B.

CHAPTER 5: APPARATUS AND EXPERIMENTAL PROCEDURE

5.1 Refractometer for sample purity tests

The purity of all chemicals was tested using an Atago RX-7000 CX refractometer. The refractometer contains an optical lense and requires approximately 1 ml of each sample to cover the lense. A conical design ensures even distribution of the sample over the lense. A base plate covers the sample to avoid contact with atmosphere, or any dust particles from invalidating the measurement.

The refractometer has an LCD display and measurement time takes 10 seconds for each sample. Refractive indices are recorded with a resolution of ±0.000001.

5.2 Density measurement apparatus

Density of all ionic liquids and alkanolamines were measured using an Anton Paar DMA 5000M vibrating U-tube densitometer. The densitometer was calibrated at each temperature using Ultra-pure water obtained using an Elga Purelab Option-Q Millipore Device, and dried air. Temperature was achieved using an internal heating and cooling mechanism within the device and controlled with a built-in thermostat controller with a temperature uncertainty of ±0.01 K.

5.3 Gas solubility apparatus

All gas solubility measurements for this research were conducted by gravimetric analysis using an Intelligent Gravimetric Analyser (IGA-01) designed and constructed by Hiden Analytical Ltd.

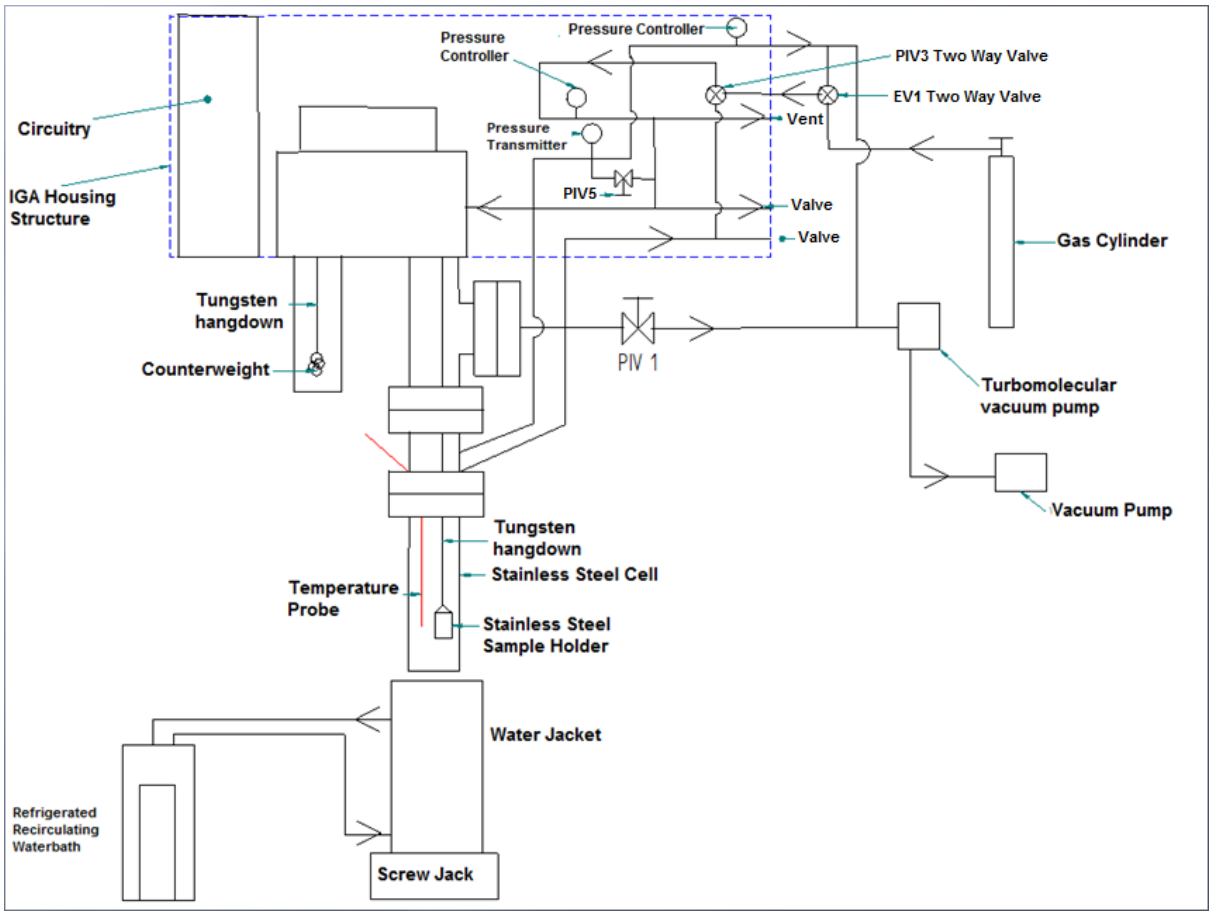

Figure 5-1: Diagram of Intelligent Gravimetric Analyser (IGA-01) for Gas Solubility Measurements

Figure 5-1 shows the setup of the gravimetric analyser. The IGA consists of a small sample reactor cell into which sorbents or solvents can be placed. The cell is very small, allowing for small volumes of material to be studied at a time. Sample size may be between 50 mg and 5 g in mass. The sample holder is suspended inside a stainless steel reactor by being attached to a tungsten and gold wire leading up to a microbalance which has a resolution of ±0.001 mg. The weight of the sample holder is countered using a counterweight so that only the weight of the sample may be tracked. The reactor is sealed using copper gaskets.

The reactor can be degassed using a Vacuubrand GMH-MD1 vacuum pump and an Edwards WRGS-NW35 turbomolecular pump to achieve high vacuum of $1x10^{-4}$ Pa.

Pressure was controlled using two pre-calibrated pressure controllers. One pressure controller controls flow out using the vacuum pumps, while the other controls gas flow and pressure into the reactor. The error in pressure reading was ±0.001 kPa. The control accuracy of the two pressure controllers was stated to be 0.025% of desired conditions.

Temperature is controlled using a Polyscience SD07R-20 refrigerated recirculating water bath and a Severn TF50/3/12/F furnace. A Pt100 probe with a resolution of ±0.01 K was located inside the reactor next to where the sample holder is suspended to read temperature. Temperature control accuracy was to 0.05% of desired conditions.

The apparatus can conduct measurements at a system pressure in the range of 0.005 MPa to 2 MPa. The apparatus can achieve a system temperature in the range of 273.15 to 353.15 K using the refrigerated recirculating water bath, and 263.15 to 773.15 K using the furnace (Roper, 2011 and Hiden Isochema, 2011).

The apparatus is connected to a personal computer and all measurements including temperature, pressure and sample weight are recorded using specialised software suited for the apparatus. Temperature and pressure control are set using the software as well. The apparatus is constructed for programmable operation. A programme of measurement for each desired equilibrium point may be set up and the apparatus records equilibrium points sequentially and automatically.

5.4 Refractive index measurement procedure

Equipment needed for measuring refractive indices using the refractometer included distilled water, acetone, compressed air, paper towels, gloves, vials and 5 ml syringes. The procedure below was followed:

1. The refractometer lense and reservoir were cleaned with distilled water and dried with a paper towel
2. The lense and reservoir were cleaned with acetone and dried with compressed air.
3. 1 to 2 ml of sample was poured into a vial
4. 1 ml of sample was drawn from the vial using a syringe and transferred to the lense.
5. The refractometer plate covering was closed and measurement was initiated
6. After approximately 10 seconds, the reading was displayed on the LCD screen.
7. The sample was wiped off using a paper towel, and discarded safely.
8. The lense and reservoir was cleaned according to step 1.

Measurements were repeated 3 times to ensure reproducibility. The results are presented in Table 7-1 in Section 7.1.

5.5 Density measurement procedure

Each density measurement was completed 3 times to ensure good repeatability. The uncertainty in density measurement was ±0.00004 $g \cdot cm^{-3}$. In addition to the sample itself, a larger beaker, distilled water, acetone, gloves, paper towels, and syringes were required for density measurements. The procedure was as follows:

1. The densitometer was set to 343.15 K, in case previous samples were of high viscosity.
2. The densitometer was cleaned twice using distilled water. Water was injected into the densitometer, and thereafter pumped out.
3. The densitometer was then cleaned using acetone. Acetone was injected into the densitometer once and pumped out.
4. The sample was injected using a syringed and readings were taken starting at 293.15 K.
5. Once the apparatus reached the set equilibrium temperature, density was recorded and a higher temperature was set.
6. Upon reaching 343.15 K, density measurements continued by decreasing the temperature. A second set of measurements were obtained.
7. Upon reaching 293.15 K again, sample was pumped out and fresh sample injected.

The above procedure confirmed repeatability and reproducibility of density measurements. Density measurements are presented and discussed in Section 7.2 of Chapter 7. Low standard deviations were exhibited and are shown in Table 7-2.

5.6 Sample preparation procedure for gas absorption measurements

Pure ionic liquid samples did not undergo any preparation and were simply loaded into the Intelligent Gravimetric Analyser (IGA). However, hybrid solvents were prepared in 1g solutions, by individually measuring appropriate masses for each component using a mettler balance. The procedure was as follows:

1. The following equipment was needed:
    a. Gloves
    b. Distilled water
    c. Acetone
    d. Compressed Air
    e. 2 ml syringes or droppers
    f. 2 ml sealable vials
    g. Mettler balance with ±1μg resolution

2. Vials were cleaned with distilled water and acetone, followed by compressed air. 1 ml of each component was added thereafter to each vial.
3. An empty 2 ml vial was placed on a mettler balance and the balance was zeroed. The balance has an accuracy in mass measurement of ±1μg.
4. Each component was added drop-wise into the 5ml vial using a syringe.
5. Once all components were added, the hybrid solvent was thoroughly mixed by manual agitation.
6. The vial was sealed and immediately taken for degassing using the gravimetric analyser.

Note that only 70 to 100 mg of solvent is needed for gravimetric analysis. However, 1g samples were prepared to ensure accurate mass measurement, effective mixing, and high solvent masses in the vial with low contact with the atmosphere.

The accuracy in mass measurement was ±1μg for each component. This resulted in a combined uncertainty of up to ±4μg in sample mass depending on the number of components in the hybrid sample. A further uncertainty of ±2 μg was added due to impurities stated by the suppliers of all solvents. In all cases, the impurity was stated to be water and removed by the gravimetric analyser upon degassing.

5.7 Loading and gas absorption measurement procedure by gravimetric analysis

Gas solubility measurements for CO_2 and O_2 in all ionic liquids, and CO_2 in alkanolamine-ionic liquid hybrid solvents, were conducted in this research. The systems investigated are presented in Tables 6-1 to 6-3 of Chapter 6. Initially, all balance components were weighed using a Mettler balance. This included the sample container, the hook and chain in the reactor, the hook and chain for the counter weight, and the counterweight itself. The results of these measurements are presented in Section 7.3 of Chapter 7. The following procedure was conducted for sample preparation and use of the gravimetric analyser:

1. All temperature and pressure control was switched off in the gravimetric analyser through use of IGA software on the PC.
2. The temperature controlled water jacket was switched off and detached from the reactor using a screw jack.
3. The reactor was then detached from the microbalance.
4. The sample container inside the reactor was removed. Any previous sample was discarded into waste bottles.
5. The sample container was cleaned using distilled water, acetone, and a paper towel, and finally dried using compressed air.

6. The sample container was re-attached to the microbalance and its weight reading was taken to ensure that its mass remained constant, indicating effective cleaning.
7. With the gravimetric analyser prepared for a new sample, the preparation of a new sample then followed, as explained in Section 5.6 above.
8. Immediately upon sample preparation, the sample was transferred from its vial to the gravimetric analysers sample container using a dropper. 70 to 100 mg of sample was loaded onto the sample container. The rough mass was checked by hooking the sample container to the microbalance and noting the weight reading.
9. Once the correct mass was loaded, the reactor was reattached and sealed using copper gaskets.
10. The temperature controlled water jacket was reattached to the reactor.
11. To achieve higher accuracy in sample mass and composition, the sample was first degassed using the vacuum pump and turbo molecular pump. This was achieved through commands prompted using the IGA software. Water and other volatile impurities which may have existed were thus removed from the sample.
12. Valve PIV1 as shown in Figure 5-1 above was opened to allow for stronger vacuum as low as $1x10^{-4}$ Pa, which was achieved.
13. Thereafter, a programme of measurement was set up, with each isothermal temperature and gas pressure being specified. The first isotherm was 303.15 K and the first equilibrium partial pressure was 0.05 MPa.
14. The measurement programme was then initiated and the gas was introduced and controlled at each desired equilibrium pressure and temperature. Sorption measurements were conducted by considering the measurement of weight change of the sample as it absorbed the gas. These changes and the equilibrium points were recorded in real time by the apparatus.
15. For each isotherm, absorption measurements were conducted, followed by desorption measurements, in order to ensure good repeatability of results. CO_2 Gas partial pressures of 0.05, 0.1, 0.4, 0.7, 1, 1.3, and 1.5 MPa were considered for all solvents. O_2 partial pressures of 0.05, 0.1, 0.4, and 0.7 MPa were considered due to limitations in gas regulation.
16. Due to the low quantity of sample being analysed, each equilibrium absorption and desorption point took 2 to 4 hours measure.
17. Once the absorption and desorption was complete for a particular isotherm, the temperature was increased for the next isotherm. Isotherms of 303.15 K, 313.15 K, and 323.15 K were considered.
18. Once all isotherms and all equilibrium points were measured, the temperature was reduced to 298.15 K and the apparatus pressure control ceased.

19. The vent valve as shown in Figure 5-1 above, was opened to achieve atmospheric pressure in the apparatus and temperature control was switched off. It was then safe to unload the sample as explained in points 1 to 4 above.

The systems investigated for CO_2 and O_2 absorption are explained in Chapter 6. The results were plotted to establish trends and draw conclusions, and are presented and discussed in Sections 7.3 to 7.7 of Chapter 7. Tabulated data for CO_2 and O_2 absorption and desorption are available in Tables A-1 to A-21 of Appendix A.

For all systems investigated by gravimetric analysis, measurements were also conducted using non-absorbing nitrogen gas, in order to correct buoyancy effects brought about by significant changes in the density of liquid samples upon gas absorption. This effect is discussed in greater detail in Section 7.3 of Chapter 7 and Appendix C. Buoyancy correction data for all systems are presented in Appendix D.

5.8 Liquid phase composition measurement using fourier transform infrared (FTIR) spectroscopy

It was intended to determine the chemistry of CO_2 absorption in pure ionic liquids and hybrid solvents containing alkanolamines and ionic liquids at a pressure range of 0.05 to 1.5 MPa and 303.15 to 323.15 K using infrared spectroscopy. Despite significant investigation and consultation with experts, the apparatus did not produce the desired results due to the infrared probe being limited to the near infrared region only. Further investigation and liaison with consultants for the development of this apparatus is on-going, requiring further investment and modification into achieving the desired measurements. Details of the development of the apparatus and its operation are however presented in Section F1 of Appendix F. Recommendations regarding the modification of this apparatus is presented in Chapter 10.

CHAPTER 6: SYSTEMS INVESTIGATED FOR ABSORPTION MEASUREMENTS

Upon conducting a significant review of ionic liquids, it was found that ionic liquids possess great potential in improving the technique of CO_2 absorption using solvents. However, it was also found that since ionic liquids are physical solvents, their CO_2 absorption capacity was low at low pressure. This was evident when comparing the CO_2 mole fractions in Table 2-6 with the performance of conventional alkanolamine solvents in literature (Jou et al., 1994).

Alkanolamine solvents on the other hand were found to be corrosive and need to be diluted for commercial use. In most cases, alkanolamines were diluted with water. While water assisted the alkanolamine in dissolving CO_2 for reaction between the alkanolamine and CO_2, water did not increase the absorption capacity of the alkanolamine. Moreover, dilution with water resulted in the solvent possessing a high heat capacity, which was undesirable due to high energy costs when regenerating the solvent.

It was thus found worthy to investigate the combining of alkanolamines with ionic liquids instead of water. From the perspective of the ionic liquid, an addition of alkanolamines could result in a hybrid solvent with a high CO_2 absorption capacity at low pressure. From the perspective of the alkanolamine, the addition of ionic liquids instead of water not only provides adequate dilution of the alkanolamine to reduce the corrosiveness of the solvent, but could also result in a solvent where all components in the solvent can absorb CO_2, thereby increasing the CO_2 absorption capacity across all pressure, especially at higher pressure.

Studies on mixing ionic liquids with alkanolamines have received very limited attention thus far. Zhang et al. (2009) modified the cation synthesis of ionic liquids to include alkanolamines in the cation itself. Table 2-6 presents some results of the study. The study did not achieve CO_2 absorption superior to that of imidazolium based fluorinated ionic liquids. Limited studies were conducted by Ma et al. (2011) on MDEA+Ionic Liquid+H_2O mixtures. Loading results were promising, yet overall absorption was low due to high H_2O dilution. Very encouraging results were obtained in the corrosion study of BF_4+MDEA hybrid solvents by SuoJiang et al. (2010), showing low solvent corrosiveness towards various steels. CO_2 absorption in hybrid solvents containing MEA and DEA with undisclosed RTILs were measured by Camper et al. (2008), indicating superior absorption over amine functionalised ionic liquids.

While the above results were promising overall, the area of hybrid solvents containing alkanolamines and ionic liquids was found to be relatively understudied. This research thus aimed to investigate the use of hybrid solvents further.

As previously mentioned, mass transfer theory of gas absorption was extensively covered by Lewis and Whitman (1924) and Danckwerts (1965). A more comprehensive and quantitative explanation, and analysis of gas absorption mass transfer theory, including reactive absorption, is available in Treybal (1981, pg 333). This research however, concerns a thermodynamic investigation into gas absorption rather than a kinetic analysis, which forms a good basis for research in the future.

From the review, it was observed that ionic liquids with fluorinated anions and imidazolium based cations were most suited for CO_2 absorption. For this research, four ionic liquids were first selected and tested to confirm these observations. The ionic liquids investigated are presented in Table 6-1:

Table 6-1: Ionic Liquids to be Investigated Experimentally

Ionic Liquid	Abbreviation
1-Butyl-3-methylimidazolium tetrafluoroborate	[Bmim][BF_4]
1-Butyl-3-methylimidazolium bis(trifluoromethylsulfonyl)imide	[Bmim][Tf_2N]
Methyl trioctyl ammonium bis(trifluoromethylsulfonyl)imide	[MOA][Tf_2N]
1-Butyl-3-methylimidazolium methyl sulphate	[Bmim][$MeSO_4$]

The above ionic liquids were selected to determine the effect of increasing fluorination of the anion, and the use of different cations. Imidazolium based cations were compared to ammonium based cations to observe the effect of cation type and chain length, and methyl sulphate anions were compared to intermediately fluorinated tetrafluoroborate anions and heavily fluorinated bis(trifluorosulphonyl)imide anions. Carbon dioxide (CO_2) and oxygen (O_2) absorption were measured in these ionic liquids to assess not only absorption capacity but also CO_2 selectivity.

A list of alkanolamines is presented in Table 2-3 of Section 2.4.1, along with an in depth explanation of chemical absorption in alkanolamines. The alkanolamine solvents that were investigated to combine with ionic liquids are presented in Table 6-2 below.

Table 6-2: Alkanolamine Solvents to be Investigated Experimentally

Alkanolamine	Abbreviation
Mono-ethanol amine	MEA
Di-ethanol amine	DEA
Methyl-di-ethanol amine	MDEA

The above alkanolamines were selected mainly because it was useful to determine the effect of combining primary, secondary, and tertiary amines with ionic liquids. MEA is a primary amine, DEA is a secondary amine, and MDEA is a tertiary amine. Moreover, the above alkanolamines

are well studied for CO_2 absorption (Jou et al., 1994, Mamun et al., 2005, and Austgen et al., 1991).

Four ionic liquids were studied and the two ionic liquids which were found to have a high CO_2 absorption capacity and be the most selective for CO_2 absorption over O_2 absorption were then blended with alkanolamines at different compositions. The two ionic liquids were [Bmim][BF_4] and [Bmim][Tf_2N], and they were blended with MEA, DEA, and MDEA in the following mass compositions shown in Table 6-3 below:

Table 6-3: Mass Composition (%) of Samples Measured for CO_2 Absorption

Sample	Mass Composition (wt%)				
	MEA	DEA	MDEA	[Bmim][BF_4]	[Bmim][Tf_2N]
1	0.0	0.0	0.0	100.0	0.0
2	29.3	0.0	0.0	70.7	0.0
3	33.0	16.2	0.0	50.8	0.0
4	31.8	12.1	0.0	56.1	0.0
5	31.6	0.0	10.4	58.0	0.0
6	30.3	0.0	21.8	48.0	0.0
7	29.8	11.7	12.8	45.7	0.0
8	0.0	0.0	0.0	0.0	100.0
9	32.8	0.0	0.0	0.0	67.2
10	32.55	21.29	0.00	0.00	46.2
11	30.28	10.53	0.00	0.00	59.2
12	29.9	0.0	12.6	0.0	57.5
13	30.4	0.0	19.3	0.0	50.3
14	29.1	10.1	12.5	0.0	48.3

The reason for the above compositions was to investigate the effects of different alkanolamine-ionic liquid compositions on CO_2 absorption. Conventional solvents utilise MEA at 30wt%, with 70wt% water (Jou et al., 1994, Mamun et al., 2005). The advantage of this alkanolamine is that it is a primary amine which reacts with CO_2 at a comparatively high absorption rate, with a reasonably high CO_2 absorption capacity (Figueroa et al., 2008). It was thus decided that all hybrid solvents studied must include 30wt% MEA.

Carbon dioxide (CO_2), nitrogen (N_2), and oxygen (O_2) gas were purchased from Afrox Ltd. (South Africa) with a stated minimum purity of 99.9 %. CO_2 and O_2 absorption was measured, while all solvents were also tested for absorption with N_2, in order to provide the correction for buoyancy effects described in Section 7.3 and Appendix C.

Methyltrioctyl ammonium bis(trifluoromethylsulfonyl)amide [MOA][Tf_2N] was purchased from Fluka Ltd. while 1-butyl-3-methyl imidazolium methyl sulphate [Bmim][$MeSO_4$] was

purchased from Sigma-Aldrich Ltd.. 1-butyl-3-methyl imidazolium bis(trifluoromethylsulfonyl)amide [Bmim][Tf_2N], 1-butyl-3-methyl imidazolium tetrafluoroborate [Bmim][BF_4], Monoethanolamine, Diethanolamine and Methyl Diethanolamine were purchased from DLD Scientific Ltd.

The purity of all ionic liquids was stated by the supplier to be ≥98% while the purity of all alkanolamines was stated to be ≥99%. The supplier's method of testing purity was stated to be H-NMR. The purity of all chemicals was tested in this research using an Atago RX-7000 CX refractometer, as explained in Sections 5.1 and 5.4 of Chapter 5. Table 7-1 in Section 7.1 shows the refractive indices of each compound in comparison to literature values.

Pure component densities of all ionic liquids and all alkanolamines were measured using an Anton Paar densitometer as explained in Sections 5.2 and 5.5 of Chapter 5. A discussion of the density data obtained is available in Section 7.2 of Chapter 7.

Blending the hybrid solvents began by considering 30wt% MEA with 70wt% ionic liquid. Hybrid solvents thereafter considered 30wt% MEA with the addition of the secondary amine DEA at 10wt% and 20wt%. The same compositions were studied for the tertiary amine MDEA, as shown above. Finally, an inclusion of all three alkanolamines was considered for the hybrid solvent. These compositions were studied for both ionic liquids, as shown in Table 6-3 above.

CO_2 absorption in the above pure ionic liquids and hybrid solvents was measured by gravimetric analysis. Previous studies on gas absorption in numerous ionic liquids by gravimetric analysis was successfully accomplished in numerous other literature sources, including Shiflett et al. (2005), Anderson et al. (2007), Brennecke and Gurkan (2010), and Cadena et al. (2004). The technique of measurement is explained in Chapter 5. Results are discussed in Chapter 7.

Liquid phase composition was expected to be complex due to chemical absorption occurring between CO_2 and alkanolamines in the hybrid solvents. It was thus also intended to test the liquid phase composition of hybrid solvents as in Table 6-3 at the same CO_2 absorption isotherms and CO_2 partial pressure using Fourier Transform Infrared (FTIR) spectroscopy. This was attempted using an in-situ infrared probe in a stainless steel equilibrium cell. Initial measurements with systems containing only CO_2 were successful in tracking CO_2 at different partial pressures. The apparatus was found to be limited however in the measurement of gas absorption in solvents and results were inconclusive. Details of this apparatus, preliminary measurements, potential advantages and measurement challenges, and recommendations on how to overcome these challenges are presented in Appendix F.

CHAPTER 7: RESULTS AND DISCUSSION OF MEASUREMENTS AND THERMODYNAMIC MODELLING

The objective of this research was to identify all methods of CO_2 capture that are under investigation throughout the world, and determine which method demonstrates the most promise in terms of mitigating CO_2 emissions on a commercial scale in the near future.

The technique of gas absorption using solvents was identified as the most promising CO_2 capture technique. Due to the numerous advantages of ionic liquids and alkanolamine solvents, it was ultimately decided to combine alkanolamines and ionic liquids in order to achieve novel hybrid solvents that may possess all the advantages of alkanolamines and ionic liquids while minimising their disadvantages.

CO_2 absorption measurements were conducted by gravimetric analysis as described in Chapter 3 and Section 5.7 of Chapter 5. This chapter discusses the results and implications of these measurements.

Four ionic liquids were first considered: [MOA][Tf_2N], [Bmim][BF_4], [Bmim][Tf_2N], and [Bmim][$MeSO_4$]. Purity and density of each ionic liquid was measured as explained in Chapter 5. Thereafter, CO_2 and O_2 absorption was measured in these four pure ionic liquids, in order to determine absorption capacity and CO_2 selectivity of the ionic liquids.

Thereafter two most CO_2 selective ionic liquids were chosen to be combined with alkanolamines at compositions shown in Table 6-3 of Chapter 6. Purity and density of each alkanolamine was also measured as explained in Chapter 5.

All absorption measurements were modelled. The RK-EOS was used to model physical absorption in ionic liquid components while the Posey-Tapperson-Rochelle model was used to model chemical absorption in alkanolamine components.

The results of the above are presented and discussed in this Chapter.

7.1 Purity of solvents used

It was imperative that the purity of all chemicals used in this research was verified. This was especially important in the combining of alkanolamines with ionic liquids to create hybrid solvents. Purity was confirmed by measuring refractive indices and pure component density. As mentioned in Chapter 5, a refractometer was used to obtain refractive indices, while an Anton

Paar densitometer was used to obtain pure component density. Table 7-1 below contains the measured refractive indices in comparison to literature values.

Table 7-1: Refractive Indices of Compounds used in this Research

Ionic Liquid	Measured Refractive index	Standard Deviation	Literature Refractive Index	Difference/%	Temperature /K	Reference
[Bmim][Tf_2N]	1.428413	9.43E-6	1.428	0.03	293.15	Tariq et al. (2009)
[Bmim][$MeSO_4$]	1.476930	8.49E-5	1.478	-0.07	293.15	Chemicalbook (2013)
[MOA][Tf_2N]	1.439710	4.71E-6	1.439	0.05	293.15	Chemicalbook (2013)
[Bmim][BF_4]	1.423200	1.25E-4	1.42475	-0.11	293.15	Lee et al. (2012)
MEA	1.454128	1.99E-4	1.4541	0.00	293.15	Weast et al. (1984), Pp. E-361
DEA	1.476998	9.12E-4	1.4776	-0.04	293.15	Weast et al. (1984), Pp. E-361
MDEA	1..469573	9.43E-6	1.469	0.04	293.15	Weast et al. (1984), Pp. E-361

The indices measured in this work compare quite favourably to those reported in the literature (ChemicalBook, 2012, Weast et al., 1984), as Table 7-1 above shows. Refractive indices measured in this research differed by as much as 0.11% from values obtained in previous literature sources. This suggests high purity of the supplied chemicals.

7.2 Pure component density of solvents

Density measurements were conducted as described in Section 5.5 of Chapter 5. Table 7-2 below presents the final results obtained. As mentioned in Section 5.5, density was measured 3 times to ensure repeatability and reproducibility. Temperature and density values are presented below along with the standard deviation obtained.

Table 7-2: Measured Density of All Compounds

Temperature/K	ρ/g·cm^{-3}		Literature ρ/g·cm^{-3}	Reference
	MEA			
293.15	± 0.0013	1.0157 ± 2.11E-05	-	-
303.15	± 0.0025	1.0077 ± 4.00E-06	1.0085	Estimated using Elec-NRTL
313.15	± 0.0031	0.9997 ± 4.23E-06	1.0009	Estimated using Elec-NRTL
323.15	± 0.0023	0.9917 ± 5.29E-06	0.9931	Estimated using Elec-NRTL
343.15	± 0.0019	0.9757 ± 3.16E-06	-	-
	MDEA			
293.15	± 0.0021	1.0386 ± 3.86E-05	-	-
303.15	± 0.0013	1.0306 ± 6.05E-06	1.0298	Estimated using Elec-NRTL
313.15	± 0.0035	1.0226 ± 2.43E-06	1.0198	Estimated using Elec-NRTL
323.15	± 0.0024	1.0146 ± 4.06E-06	1.0150	Estimated using Elec-NRTL
343.15	± 0.0014	0.9986 ± 6.16E-06	-	-

Table 7-2 (Contd.): Measured Density of All Compounds

Temperature/K		ρ/g·cm^{-3}			Literature ρ/g·cm^{-3}	Reference
		DEA				
293.150	±	0.0028	1.0972	± 5.39E-05	-	-
303.148	±	0.0015	1.0905	± 8.92E-05	1.0911	Estimated using Elec-NRTL
313.148	±	0.0021	1.0842	± 1.21E-05	1.0843	Estimated using Elec-NRTL
323.149	±	0.0021	1.0777	± 5.69E-06	1.0775	Estimated using Elec-NRTL
343.149	±	0.0015	1.0644	± 2.00E-06	-	-
		[Bmim][MeSO$_4$]				
293.152	±	0.0028	1.2074	± 1.84E-05	-	-
303.15	±	0.0000	1.2004	± 1.34E-05	1.2088	Pereiro et al. (2007)
313.149	±	0.0028	1.1937	± 7.07E-07	1.1920	Pereiro et al. (2007)
323.149	±	0.0014	1.1871	± 2.83E-06	1.1903	Pereiro et al. (2007)
343.15	±	0.0012	1.1739	± 2.43E-06	1.1722	Pereiro et al. (2007)
		[MOA][Tf$_2$N]				
293.149	±	0.0010	1.1097	± 3.41E-05	-	-
303.148	±	0.0012	1.1023	± 1.00E-06	1.1032	Deenadayalu et al. (2010)
313.148	±	0.0031	1.0947	± 3.21E-06	1.0957	Deenadayalu et al. (2010)
323.149	±	0.0026	1.0872	± 3.79E-06	-	-
343.148	±	0.0017	1.0723	± 4.16E-06	-	-
		[Bmim][Tf$_2$N]				
293.148	±	0.0032	1.4422	± 5.86E-05	-	-
303.152	±	0.0012	1.4319	± 6.35E-06	1.4316	Fredlake et al. (2004)
313.149	±	0.0025	1.4223	± 1.53E-06	1.4247	Fredlake et al. (2004)
323.149	±	0.0025	1.4128	± 5.57E-06	1.4122	Fredlake et al. (2004)
343.153	±	0.0007	1.3939	± 2.62E-05	-	-
		[Bmim][BF$_4$]				
293.149	±	0.0030	1.0440	± 1.44E-05	-	-
303.151	±	0.0022	1.0380	± 1.02E-05	1.2005	Fredlake et al. (2004)
313.15	±	0.0025	1.0320	± 1.07E-06	1.194	Fredlake et al. (2004)
323.148	±	0.0035	1.0260	± 1.76E-06	-	-
343.151	±	0.0011	1.0140	± 1.58E-06	-	-

The data shown for the ionic liquids above compares well with that measured by Deenadayalu et al. (2010), Jacquemin et al. (2006), and Pereiro et al. (2007). Density data for [Bmim][BF$_4$] and [Bmim][Tf$_2$N] also compares well with Baltus et al, (2004), Fredlake et al. (2004), and Shiflett et al. (2005) shown in Table 2-10. Pure component density was not easily avaialable in literature for MEA, DEA, and MDEA since these solvents are typically studied in diluted form with water. The measured pure component density data does however compare well with pure component density estimates using the Elec-NRTL model in Aspen Engineering Suite V 8.0 as shown. In addition to the refractive indices, this provides a supporting indication of the purity of the chemicals used in this research.

The above data could also be fitted to a 1st order equation for accurate interpolation of density data. The following 1st order equations apply to the pure component density of each solvent:

$$\rho_{MEA}[g \cdot cm^{-3}] = -0.0008 * T[K] + 1.2502 \quad \text{(E7-1)}$$

$$\rho_{DEA}[g \cdot cm^{-3}] = -0.0007 * T[K] + 1.2918 \quad \text{(E7-2)}$$

$$\rho_{MDEA}[g \cdot cm^{-3}] = -0.0008 * T[K] + 1.2731 \quad \text{(E7-3)}$$

$$\rho_{[Bmim][Tf_2N]}[g \cdot cm^{-3}] = -0.001 * T[K] + 1.7235 \quad \text{(E7-4)}$$

$$\rho_{[Bmim][BF_4]}[g \cdot cm^{-3}] = -0.0006 * T[K] + 1.2199 \quad \text{(E7-5)}$$

$$\rho_{[Bmim][MeSO_4]}[g \cdot cm^{-3}] = -0.0007 * T[K] + 1.4038 \quad \text{(E7-6)}$$

$$\rho_{[MOA][Tf_2N]}[g \cdot cm^{-3}] = -0.0008 * T[K] + 1.3300 \quad \text{(E7-7)}$$

It was also recommended by Roper (2011) to input the density of each sample into the IGA software at 298.15 K for the initial loading of the sample. Merely an estimate was stated to be recommended. Density of hybrid solvents was thus calculated by the following equation:

Density of Hybrid solvents: $\rho_{Hybrid}(g \cdot cm^{-3}) = \sum_{i=1}^{n} x_i \rho_i$ (E7-8)

Where n is the number of components in the solvent before absorption. The above equation was used for all hybrid solvents simply as initial density measurements for gravimetric analysis. While the above equation decreases in accuracy as the system departs from ideal gas conditions, the key estimates were needed at atmospheric conditions, where a high degree of ideal solution behaviour was assumed. Thus, excess volume was assumed to be negligible.

7.3 Buoyancy correction for gravimetric measurements

Gravimetric analysis produces a weight reading of the sample by taking into account all contributing forces in the reactor. This includes the dry sample m_s [g], the mass of gas absorbed m_a [g] the sample container and its associated attachments (hook and chains) represented by m_I [g], the mass of the counterweight m_c [g], the mass of associated attachments linking the counterweight to the microbalance together with the tungsten hook and gold chain linking the sample container to the microbalance, represented by m_{II} [g].

A buoyancy force is also caused by the surrounding gas displaced by the presence of the sample, the sample container and balance components in the reactor. These are represented by

V_I, V_C, and V_{II} accounting for the volume of the sample container and chain, the counterweight, and counterweight chain respectively. The force is dependent on the density of the gas at each equilibrium temperature and pressure condition. Table 7-3 below contains measured masses and calculated volumes of each of the components explained above. The density of each component was given by Hiden Analytical Ltd., the manufacturer of the gravimetric analyser used in this research.

Table 7-3: Measured Mass and Calculated Volume of Balance Components used in Gravimetric Analysis

Balance Component	Mass/g	Density/g·cm^{-3}	Volume/cm^3
Sample Container (m_{sc})	0.6194	7.9	0.078
Wire ($m_{I,1}$)	0.063	21	0.003
Chain ($m_{I,2}$)	0.1776	19.3	0.009
Counterweight (m_C)	0.8008	7.9	0.101
Hook ($m_{II,1}$)	0	0	0.000
Chain ($m_{II,2}$)	0.143	19.3	0.007

A significant source of error in weight reading, especially when studying liquid samples using gravimetric analysis, is that the density of the sample decreases significantly upon uptake of the absorbing gas. This term is represented by V_{as}, the volume of the sample and the absorbed gas.

The weight reading produced by the gravimetric analyser is thus given by the following equation:

$$W = g[m_s + m_a - m_c + m_I - m_{II} - \rho_f(V_{as} + V_I - V_{II} - V_c)] \quad \text{(E7-9)}$$

where W is the weight reading in [N], g is acceleration due to gravity in [m·s^{-2}], and ρ_f is the density of the absorbing gas [g·cm^{-3}].

The samples loaded into the apparatus were pure ionic liquids and alkanolamine-ionic liquid hybrid solvents, all in the liquid phase throughout the entire temperature and pressure range of operation. Upon absorption of a gas, the density of these samples significantly decreases, making the sample more buoyant and thus lowering the weight of the sample. Samples thus appear to have a lower mass than they actually have.

For example, the data for N_2 gas in MEA:[Bmim][Tf_2N] at 32.8:67.2 wt% at 313.15 K has been plotted below in Figure 7-1, simply for illustration of the buoyancy effect.

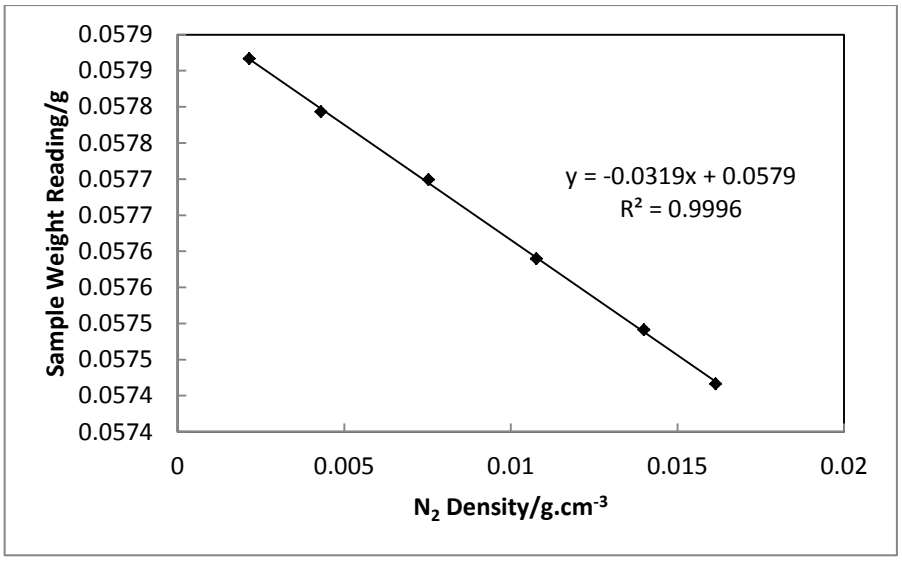

Figure 7-1: Bouyancy Measurements using N_2 gas for MEA:[Bmim][Tf_2N] at 32.8:67.2 wt% at 313.15 K

As shown in the figure above, for a constant temperature, an increase in equilibrium partial pressure resulting in an increase in N_2 density, has made the sample more buoyant and with increasing gas density, a decrease in sample weight reading is observed by the apparatus. In reality however, it is known that the sample is not volatile and the actual mass is not changing, but rather the weight reading changes. Another example containing pure [Bmim][BF_4] is shown in Figure C-1 in Appendix C.

The above effect has to be corrected to achieve accurate solubility results. To account for this buoyancy effect, all sample weight readings were taken at each equilibrium pressure and temperature using a non-absorbing gas. Nitrogen or helium is typically appropriate. Nitrogen was used in this research as it molecular weight is relatively more comparable to O_2 and CO_2 than the molecular weight of helium.

The calculation procedure for buoyancy correction and the obtaining of equilibrium CO_2 and O_2 liquid mole fraction by gravimetric analysis are provided in Appendix C. Further details of this method of correction for buoyancy effects was explained in the work of Macedonia et al. (2000).

This buoyancy correction was implemented for all solvents studied in this research, including pure ionic liquids and hybrid solvents. The buoyancy correction data, including pressure, weight reading, and density of N_2 is available in Tables D-1 to D-3 of Appendix D.

7.4 Test system proving the accuracy of technique in this research

It was necessary to confirm the accuracy of our technique in measurement of P-T-x data using gravimetric analysis. Thus, a test system was measured for CO_2 in [Bmim][BF_4] ionic liquid at 298.15 K and 323.15 K, comparing measured data with two independent literature sources and two isotherms.

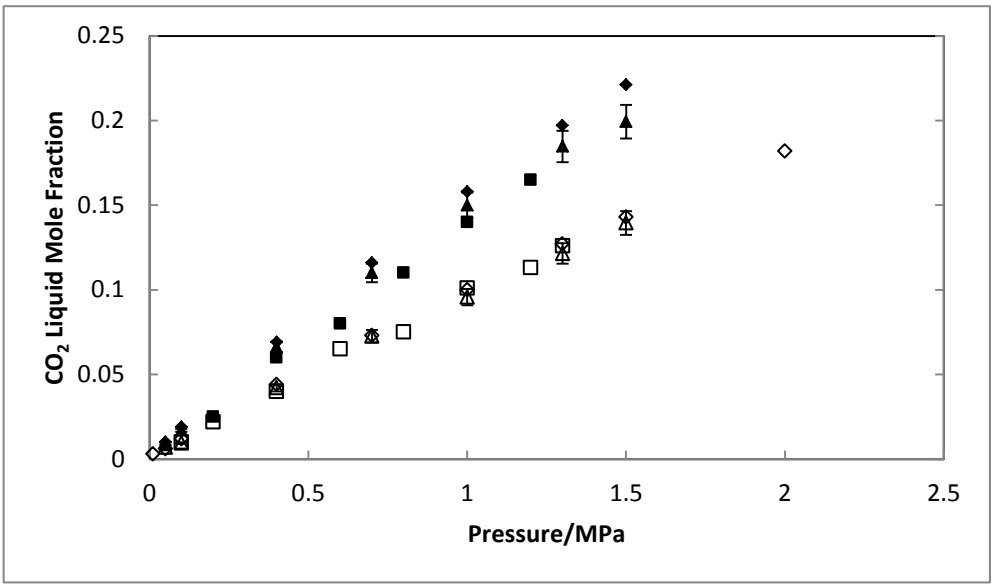

Figure 7-2: Test System - CO_2 Absorption in [Bmim][BF_4]. ▲- Measured data at 298.15 K; Δ - Measured Data at 323.15 K; ♦ - Shiflett et al. (2005) at 298.15 K; ◊ - Shiflett et al. (2005) at 323.15 K; ■ – Cadena et al. (2004) at 298.15 K; □ – Cadena et al. (2004) at 323.15 K.

It is evident from Figure 7-2 that data measured in this work compares quite favourably to data measured in the literature (Cadena et al., 2004 and Shiflett et al., 2005). At a temperature of 298.15 K, deviation of experimental was 4.04 to 16.2% of literature data, with deviations being greatest at low pressure and very high pressure of 1.5 MPa. At 323.15 K, experimental data deviated from literature data by 0.5 to 15.28% of literature data. It was also noted that the data from the two literature differed by up to 20.1% at low pressure and very high pressure.

7.5 CO_2 and O_2 absorption measurements in pure ionic liquids

CO_2 and O_2 absorption were measured in four pure ionic liquids: [MOA][Tf_2N], [Bmim][BF_4], [Bmim][Tf_2N] and [Bmim][$MeSO_4$] using the IGA-01 as explained in Sections 5.7 and Chapter 6. Temperature, pressure, O_2 and CO_2 mole fraction were measured at equilibrium and the data is provided in Tables A-1 to A-8 of Appendix A. The data was plotted to easily demonstrate trends and compare solvents, and are shown in Figures 7-3 to 7-10. Note that the axes were kept constant so that CO_2 liquid mole fractions for different solvents can be visually compared

conveniently. Absorption measurements were conducted and studied in depth, while desorption measurements were done merely to confirm the repeatability of the measurements. Figures 7-3 to 7-6 below show the absorption of CO_2 at various temperatures and pressures studied.

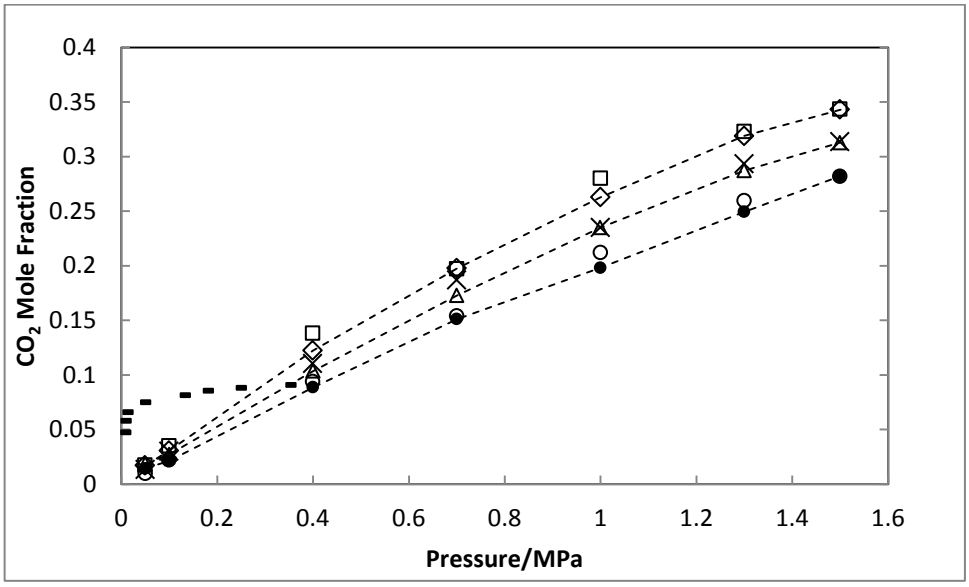

Figure 7-3: Isothermal Solubility of CO_2 in [MOA][Tf_2N]: (◊) absorption, (□) desorption at 303.15 K; (Δ) absorption, (x) desorption at 313.15 K; (●) absorption, (○) desorption at 323.15 K; - - CO_2 in MEA:H_2O at 30:70 wt%. *Dotted lines indicate model predictions

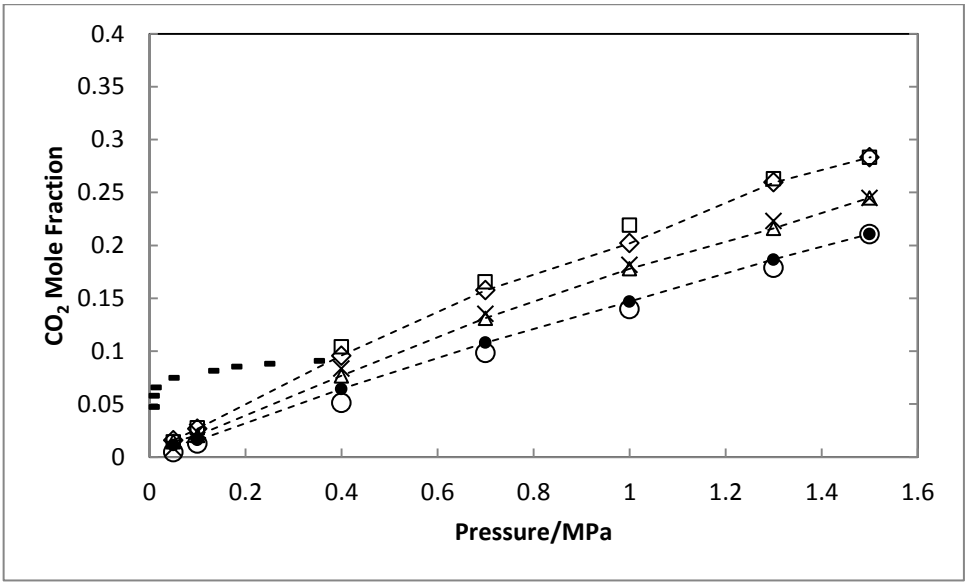

Figure 7-4: Isothermal Solubility of CO_2 in [Bmim][Tf_2N]: ◊ - absorption, □ - desorption at 303.15 K; Δ - absorption, x - desorption at 313.15 K; ● - absorption, ○ - desorption at 323.15 K; - - CO_2 in MEA:H_2O at 30:70 wt%. *Dotted lines indicate model predictions

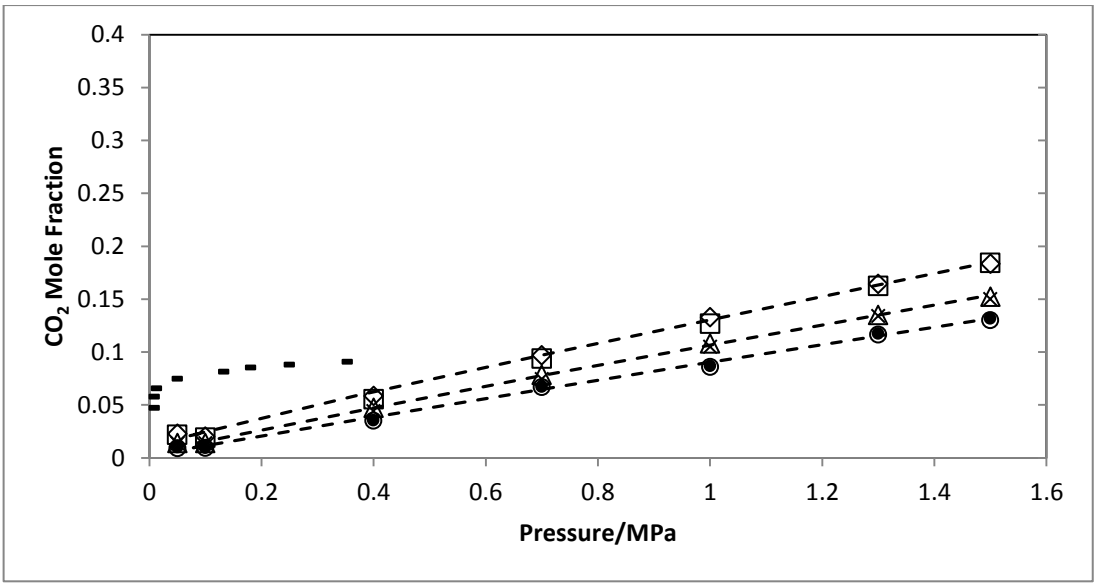

Figure 7-5: Isothermal Solubility of CO_2 in [Bmim][BF_4]: ◊ - absorption, □ - desorption at 303.15 K; Δ - absorption, x - desorption at 313.15 K; ● - absorption, ○ - desorption at 323.15 K; - - CO_2 in MEA:H_2O at 30:70 wt%. *Dotted lines indicate model predictions

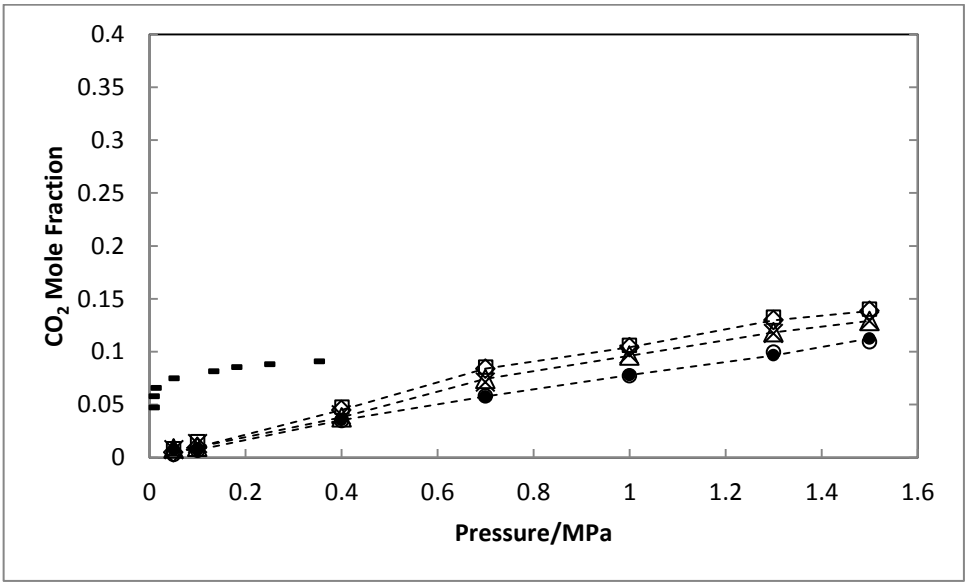

Figure 7-6: Isothermal Solubility of CO_2 in [Bmim][$MeSO_4$]: (◊) absorption, (□) desorption at 303.15 K; (Δ) absorption, (x) desorption at 313.15 K; (●) absorption, (○) desorption at 323.15 K; - - CO_2 in MEA:H_2O at 30:70 wt%. *Dotted lines indicate model predictions

Figures 7-3 to 7-6 indicate that the absorption of both gases was the highest at a lower temperature of 303.15 K, and lowest at a higher temperature of 323.15 K for each ionic liquid, measured at all equilibrium partial pressures. This behaviour is consistent with literature for other ionic liquids as well as other solvents, confirming gas absorption to be an exothermic process (Shiflett and Yokozeki, 2005).

Table E-1 of Appendix E contains enthalpy and entropy of absorption calculated by equations E2-3 and E2-4 of Section 2.5.6 respectively, using the absorption data measured in this work for pure ionic liquids. Enthalpy of absorption for CO_2 in [Bmim][BF_4] and [Bmim][Tf_2N] compare well with data obtained by Cadena et al. (2004) and Chen et al. (2006). Deviations in enthalpy and entropy of absorption calculated was consistent with those presented in Anthony et al. (2002). Enthalpy and entropy of absorption were negative, indicating that absorption decreases with increasing temperature.

As found in the works of Cadena et al. (2004), Arshad (2009), Heintz et al. (2009) and Gurkan et al. (2010), enthalpy of absorption was found to be higher in the non-fluorinated ionic liquid [Bmim][$MeSO_4$] than the other three ionic liquids which were fluorinated. This indicates a higher temperature dependence of CO_2 absorption in [Bmim][$MeSO_4$] which is confirmed by comparing Figure 7-6 to Figures 7-3, 7-4, and 7-5. The effect can also be noted by comparing selectivities in Tables A-5 to A-8 of Appendix A. Entropy of absorption for CO_2 is also highest in the case of [Bmim][$MeSO_4$], indicating high temperature dependence and the unsuitability of [Bmim][$MeSO_4$] to efficiently absorb CO_2.

Another observation consistent with literature (Tang et al., 2012, Rodriguez et al., 2006, Anthony et al., 2005) is that increased gas partial pressure resulted in increased gas absorption for each ionic liquid. The effect was quite significant particularly for CO_2 absorption in [MOA][Tf_2N] and [Bmim][Tf_2N] as shown in Figure 7-3 and 7-4. Higher partial pressure favoured absorption of the gas into the ionic liquid to reduce the pressure and maintain equilibrium.

The effect of ionic liquid anion fluorination could be seen when comparing Figures 7-4 to 7-6. All three ionic liquids contained the [Bmim] cation. By comparing the above mentioned figures, it was noted that [Bmim][$MeSO_4$] achieved the lowest CO_2 absorption, with [Bmim][BF_4] achieving higher absorption and [Bmim][Tf_2N] achieving the highest CO_2 absorption of all ionic liquids containing the [Bmim] cation. This is consistent with works done by Shiflett et al. (2005), Cadena et al. (2004) and Hasib-ur-Rahman et al. (2010).

Figure 7-3 and 7-4 showed the effect of increasing cation chain length. [Bmim][Tf_2N], containing the smaller [Bmim] cation achieved lower CO_2 absorption than [MOA][Tf_2N], which is consistent with literature findings (Hasib-ur-Rahman et al. 2010, Brennecke et al. 2010). [MOA][Tf_2N], [Bmim][Tf_2N], [Bmim][BF_4] and [Bmim][$MeSO_4$] possess molar masses of 648.85, 419.36, 226.03 and 250.32 $g \cdot mol^{-1}$ respectively. From the density measurements, the molar volume of each ionic liquid at 303.15 K was obtained. The molar volume of the ionic liquids was found to decrease in the following order: [MOA][Tf_2N] (588.64 $cm^3 \cdot mol^{-1}$) >

[Bmim][Tf_2N] (292.87 $cm^3 \cdot mol^{-1}$) > [Bmim][BF_4] (217.74 $cm^3.mol^{-1}$) > $[BMIM]^+[MeSO_4]^-$ (207.09 $cm^3 \cdot mol^{-1}$). The same trend applies at all isotherms studied. It was observed that the increased cation chain length, resulting in a higher molar volume for [MOA][Tf_2N], proved effective at increasing CO_2 absorption in comparison to [Bmim][Tf_2N]. Higher molar volume of the cation facilitated a higher amount of CO_2 molecules absorbing into the ionic liquid. This is consistent with other comparisons of cation chain length found in literature (Anderson et al., 2007, Shiflett and Yokozeki, 2007).

It can thus be proposed that ionic liquids with higher molar volumes would achieve greater absorption of a gas solute, possibly due to an increase in the void space (free volume) of the ionic liquid (Zhou et al., 2013, Shannon et al., 2012). Gases may occupy these free spaces available in ionic liquids. (Scovazzo et al., 2004, Huang et al., 2005).

Of the four ionic liquids studied for gas absorption, [MOA][Tf_2N] achieved the highest CO_2 absorption at all four isotherms and at each partial pressure studied due to high anion fluorination and cation chain length, followed by [Bmim][Tf_2N], [Bmim][BF_4], and lastly with [BMIM][$MeSO_4$] achieving the lowest CO_2 absorption. These findings are consistent with the effects of cation chain length and anion fluorination as claimed in numerous literature sources (Cadena et al. 2004, Shiflett and Yokozeki, 2007, and Brennecke et al., 2010).

The above four ionic liquids were benchmarked against a conventional solvent containing MEA:H_2O at 30:70 wt% at 313.15 K. It can be seen that at 313.15 K in Figures 7-3 to 7-6, the conventional solvent achieved significantly higher equilibrium CO_2 absorption at low pressure than all the ionic liquids studied. All ionic liquids achieved particularly low CO_2 absorption at low pressure of 0.05 to 0.4 MPa due to only physical absorption taking place. However, it is also noted from the trend that the conventional solvent tends to achieve low CO_2 absorption at higher pressure, due to the chemical solvent having limited absorption capacity. At high pressure the ionic liquids achieve higher CO_2 absorption. It can thus be concluded that if the above investigated ionic liquids were to be used as pure solvents for industrial CO_2 capture, the flue gas pressure would have to be increased for efficient CO_2 capture. If the energy cost of compressing flue gas is high, then the conventional solvent would be beneficial over the ionic liquid solvents.

The above ionic liquids were also benchmarked for CO_2 absorption against other ionic liquids measured in literature at 323.15 K. Figure 7-7 below shows the comparison.

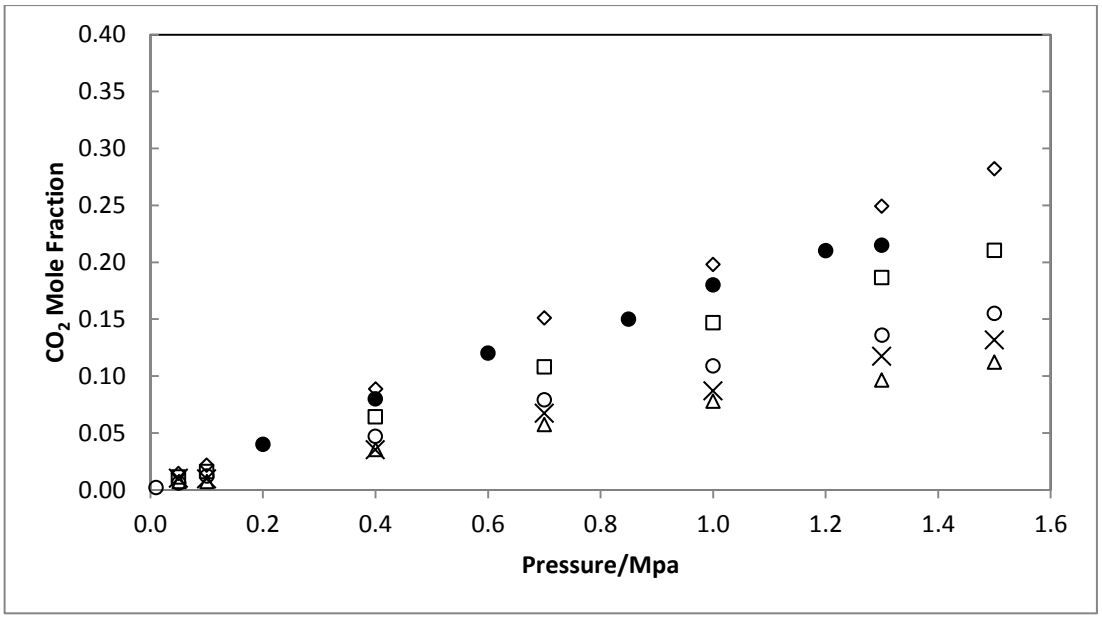

Figure 7-7: CO_2 Absorption in Ionic Liquids at 323.15K. ◊ - [MOA][Tf_2N]; ● – [Hmim][Tf_2N] (Anderson et al., 2007); □ – [Bmim][Tf_2N]; ○ – [Bmim][PF_6] (Shiflett and Yokozeki, 2005); X – [Bmim][BF_4]; Δ - [Bmim][$MeSO_4$].

It was found that [MOA][Tf_2N] achieved higher CO_2 absorption at 323.15 K than other more well studied ionic liquids such as [Bmim][BF_4], [Bmim][Tf_2N] and [Bmim][PF_6] and even [hmim][Tf_2N] as measured by Shiflett and Yokozeki (2005) and Anderson et al.(2007). A comparison of absorption in [Bmim][Tf_2N] can be compared with absorption in [Hmim][Tf_2N], indicating once again that increased cation chain length increases CO_2 absorption. The even longer [MOA] cation resulted in a further increase in CO_2 absorption. Anion fluorination can also be observed by comparing absorption in ionic liquids with [BF_4], [PF_6], and [Tf_2N] anions. Absorption in the ionic liquid [Bmim][PF_6] measured by Shiflett and Yokozeki (2005) is higher than absorption in [Bmim][BF_4] but lower than in [Bmim][Tf_2N], thereby neatly reconfirming the trend of increasing CO_2 absorption with increasing anion fluorination.

Additionally, [MOA][Tf_2N] also achieved higher CO_2 absorption than [bmmim][PF_6], [bmmim][BF_4], [emim][Tf_2N] and [emmim][Tf_2N] measured by Cadena et al. (2004), as well as ionic liquids with fluorinated cations such as [$C_6H_4F_9$mim][Tf_2N] and [$C_8H_4F_{13}$mim][Tf_2N] at 303.15 K, investigated by Arshad (2009). This indicates that it is cation chain length that is more influential on CO_2 absorption than cation fluorination.

The optimum conditions for CO_2 absorption in this study was a partial pressure of approximately 1.5 MPa, at a temperature of 303.15 K and using the [MOA][Tf_2N] ionic liquid to achieve a maximum CO_2 mole fraction of 0.343. However, studies concerning the

measurement of O_2 absorption which was also conducted in this work provided further information regarding the suitability of the four ionic liquids in capturing CO_2.

Although the primary focus of this research was to investigate solvents most suitable for CO_2 absorption, the measurement of other gases was also found to be of great concern since a solvent for CO_2 capture must not only possess a high CO_2 absorption rate and capacity but also a high selectivity for CO_2 above all other gases present in coal power plant flue gas. A review of the ionic liquids in this work confirmed that absorption of nitrogen in the above ionic liquids was negligible (Macedonia et al., 2000). The absorption of water vapour at the isotherms measured was not possible to accurately achieve by gravimetric analysis. However, another important constituent of coal power flue gas is oxygen (O_2), accounting for approximately 3% by volume, of a pulverised coal power plant flue gas. Thus, the absorption of O_2 was also measured for each of the four ionic liquids.

The absorption of O_2 in all ionic liquids is shown in Figures 7-8 to 7-11 below and presented in Tables A-5 to A-8 of Appendix A.

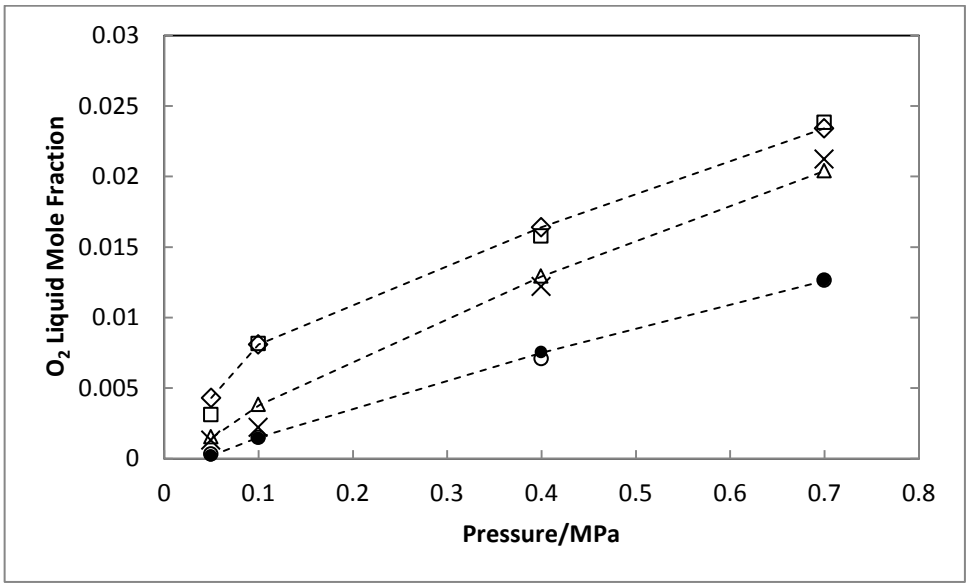

Figure 7-8: Isothermal Solubility of O_2 in [MOA][Tf_2N]: (◊) absorption, (□) desorption at 303.15 K; (Δ) absorption, (x) desorption at 313.15 K; (●) absorption, (○) desorption at 323.15 K
*Dotted lines indicate model predictions

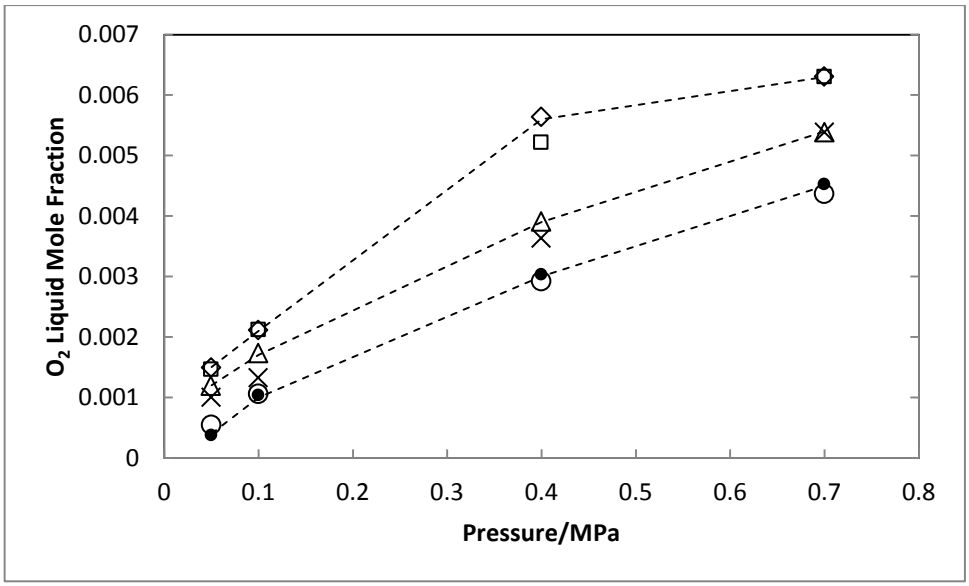

Figure 7-9: Isothermal Solubility of O_2 in [Bmim][Tf_2N]: (◊) absorption, (□) desorption at 303.15 K; (Δ) absorption, (x) desorption at 313.15 K; (●) absorption, (○) desorption at 323.15 K
*Dotted lines indicate model predictions

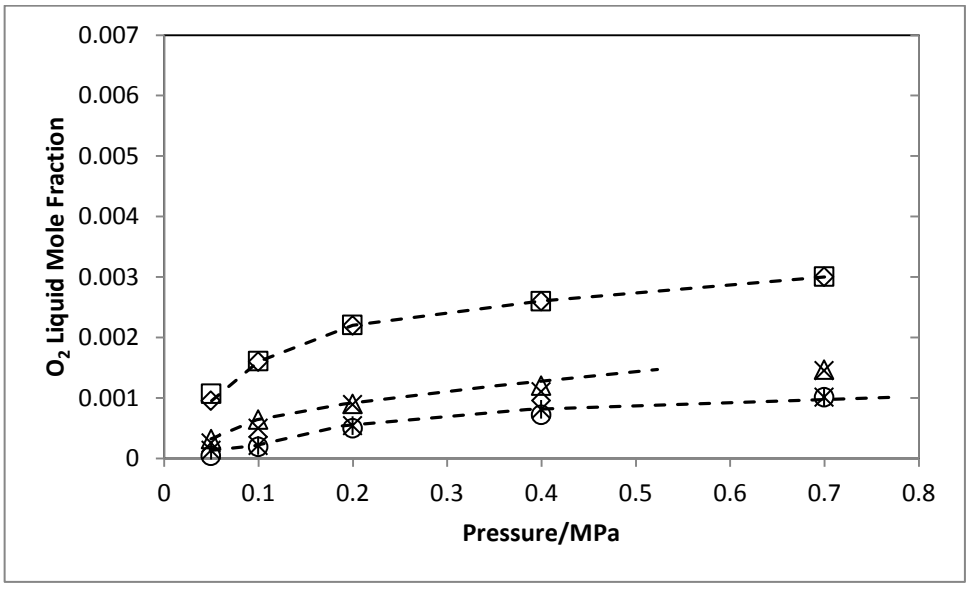

Figure 7-10 : Isothermal Solubility of O_2 in [Bmim][BF_4]: (◊) absorption, (□) desorption at 303.15 K; (Δ) absorption, (x) desorption at 313.15 K; (●) absorption, (○) desorption at 323.15 K
*Dotted lines indicate model predictions

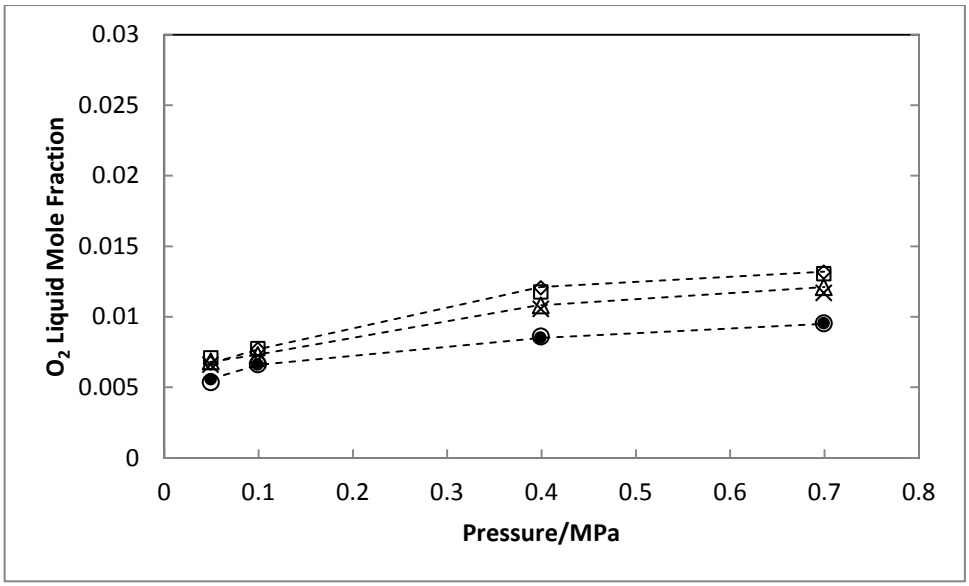

Figure 7-11: Isothermal Solubility of O_2 in [Bmim][$MeSO_4$]: (◊) absorption, (□) desorption at 303.15 K; (Δ) absorption, (x) desorption at 313.15 K; (●) absorption, (○) desorption at 323.15 K
*Dotted lines indicate model predictions

For all isotherms studied, O_2 absorption can be listed to occur in the following ionic liquids in the following order of magnitude: O_2 absorption in [MOA][Tf_2N] > [Bmim][$MeSO_4$] > [Bmim][Tf_2N] > [Bmim][BF_4].

The effect of anion fluorination on O_2 absorption was inconsistent regarding O_2 absorption data for [Bmim][$MeSO_4$], [Bmim][BF_4] and [Bmim][Tf_2N]. The comparison of Figures 7-9 and 7-11 shows that [Bmim][$MeSO_4$] achieved significantly higher O_2 absorption than [Bmim][Tf_2N], suggesting that anion fluorination may be recommended for lower O_2 absorption. However, [Bmim][BF_4] had lower anion fluorination and yet achieved even lower O_2 absorption as shown in Figure 7-10.

An analysis of enthalpy of absorption for O_2 in the ionic liquids also indicates that fluorinated ionic liquids are beneficial over non-fluorinated ones regarding higher CO_2 absorption and lower O_2 absorption. Data in Table E-1 of Appendix E shows enthalpy of absorption for O_2 in [Bmim][$MeSO_4$] to be substantially lower than for the other ionic liquids indicating lower temperature dependence for O_2 absorption, an undesirable result for CO_2 capture. There is no consistency when comparing enthalpy of absorption for [Bmim][BF_4] and [Bmim][Tf_2N] however.

It can thus only be concluded that fluorinated anions may be beneficial compared to non-fluorinated anions in achieving low O_2 absorption, but this study found no conclusive correlation between increasing the fluorination of the anion and decreasing O_2 absorption.

An undesirable result is that entropy of absorption was found to be negative for O_2 absorption in all ionic liquids, indicating that while O_2 absorption may be low for some of the ionic liquids in this work, it is not negligible. It implies that if any of the studied ionic liquids are used for flue gas treatment, some O_2 absorption is to be expected, which is an undesirable result. Calculation of entropy of absorption at each partial pressure did however find that at low pressure, entropy of absorption did not remain constant but tended to be less negative, which indicates that O_2 absorption would be negligible at low pressure.

A potentially more significant observation is that [MOA][Tf_2N] achieved higher O_2 absorption than [Bmim][Tf_2N], as shown in Figures 7-8 and 7-9. [MOA][Tf_2N] achieved the highest O_2 absorption at all isotherms and partial pressures of all ionic liquids studied, despite this ionic liquid containing a highly fluorinated anion. This suggests that the effect of cation chain length and type on O_2 absorption is greater than the effect of anion fluorination. The high O_2 absorption could be the result of a larger cation chain length, or the fact that an ammonium cation was used instead of an imidazolium cation.

The above observation also casts doubt on the applicability of [MOA][Tf_2N] as a solvent for CO_2 capture. Although this ionic liquid achieved the highest CO_2 absorption, it also achieved the highest O_2 absorption. This indicates low CO_2 selectivity, which is an undesirable result for CO_2 compression and disposal industrially.

Included in Tables A-5 to A-8 of Appendix A are values for x_{CO2}/x_{O2} for each equilibrium partial pressure from 0.05 to 0.7 MPa and all three isotherms, which may be used to quantitatively study and compare the CO_2 selectivity of each pure ionic liquid. The first observation when studying the data for each system at each isotherm is that the CO_2 selectivity of all ionic liquids appears highest at low pressures of 0.05 MPa, and high pressures of 0.7 MPa. This is due to the relatively very low O_2 absorption achieved by all ionic liquids at low pressure, and the relatively high CO_2 absorption achieved at high pressures of 0.7 MPa. CO_2 selectivity over intermediate pressures is fairly consistent and can be averaged and compared for each ionic liquid.

By comparing Tables A-5, A-6 and A-8, it can also be observed that in the case of the three fluorinated ionic liquids, CO_2 selectivity over O_2 increases with increasing temperature. This is due to a relatively greater drop in O_2 selectivity upon increasing temperature, for fluorinated ionic liquids. By contrast, CO_2 selectivity was fairly consistent over the temperature range in the case of [Bmim][$MeSO_4$]. An increase in temperature did not increase CO_2 selectivity. This can also be seen with the proportionate drop in CO_2 and O_2 absorption in Figures 7-3 to 7-11, with increasing temperature.

Another way of comparing gas absorption in physical solvents such as ionic liquids is the calculation of Henry's Law constants as explained using equation E2-2 in Section 2.5.6. Henry's Law constants as accurately obtained using the Krichevski-Kasarnovski equation are not pressure dependent. Thus, the ability of a solvent to absorb gases can be compared and benchmarked for each isotherm. Table A-9 in Appendix A presents CO_2 and O_2 Henry's Law constants obtained for each system at each isotherm. The magnitudes of Henry's Law constants also provide a consistent indication of the CO_2 selectivity of each ionic liquid at each temperature.

The x_{CO2}/x_{O2} values in Tables A-5 to A-8 and the Henry's Law constants presented in Table A-9 of Appendix A clearly show [Bmim][$MeSO_4$] to be the least CO_2 selective ionic liquid. While [MOA][Tf_2N] achieved the highest CO_2 absorption, it also achieved the highest O_2 absorption. A comparison of x_{CO2}/x_{O2} and Henry's Law constant values revealed [MOA][Tf_2N] achieved the 2nd lowest CO_2 selectivity. [Bmim][BF_4], while achieving the 3rd lowest CO_2 absorption, achieved the lowest O_2 absorption. The Henry's Law constants and x_{CO2}/x_{O2} values revealed [Bmim][BF_4] to achieve the highest CO_2 selectivity, with [Bmim][Tf_2N] achieving the 2nd highest CO_2 selectivity.

It was thus determined that the two ionic liquids which achieved the most desirable results for CO_2 capture were [Bmim][BF_4] and [Bmim][Tf_2N].

Other factors adding to the desirability of the above mentioned ionic liquids was their comparatively low molecular weight and viscosity, which made these ionic liquids more miscible with alkanolamine solvents than [MOA][Tf_2N] which would form LLE with undiluted alkanolamines as many higher molecular weight ionic liquids do (Chen et al., 2006).

It was therefore decided to investigate [Bmim][BF_4] and [Bmim][Tf_2N] further by including these ionic liquids in hybrid solvents containing conventional alkanolamines. The method of combining components to develop hybrid solvents for study, and the measurement of CO_2 absorption in hybrid solvents was described in Section 5.6. The results of these measurements are discussed in Section 7.7.

7.6 Modelling of CO_2 and O_2 absorption in pure ionic liquids

The dotted lines of Figures 7-3 to 7-11 are model predictions of CO_2 and O_2 partial pressure. The absorption data in pure ionic liquids was modelled using the RK-EOS as explained in Chapter 4 above.

The inaccuracy in model prediction was calculated by the following equation for each data point:

$$\text{Error (\%)} = \frac{P_{CO_2}(\text{exp}\,erimental) - P_{CO_2}(calculated)}{P_{CO_2}(\text{exp}\,erimental)} \times 100 \quad \text{.....(E4-1)}$$

All P_{CO2} values were recorded in MPa. In order to analyse the accuracy in prediction of absorption in each ionic liquid, a root mean square error was calculated by taking an average of the errors of each data point.

$$\text{Root Mean Square Error} = \frac{\sum_{i=1}^{n} \sqrt{Error_i^{\,2}}}{n} \quad \text{……..(E4-2)}$$

Where n = number of data points for each alkanolamine-ionic liquid hybrid system. n = 21, since each isotherm contained 7 points.

Figures 7-3 to 7-11 and Tables A-1 to A-8 indicate that model estimates compare quite favourably with measured data. Binary interaction and fitting parameters for each system are presented in Table 7-4 below, along with root mean square error values. Note that the root mean square error merely illustrates the deviation of model predictions from experimental results.

Table 7-4: Binary Interaction and Fitting Parameters for CO_2 and O_2 in Pure Ionic Liquid Systems

System	Temperature (K)	β_0	β_1	β_2	β_3	ℓ_{12}	ℓ_{21}	τ_{12}	m_{12}	Root Mean Square Error/%
(1) CO_2 + (2) [MOA][Tf_2N]	303.15 - 323.15	0.152	-0.0235	0	0	15.2265	$1.07x10^{14}$	-230.87	0.911	0.061
(1) CO_2 + (2) [Bmim][Tf_2N]	303.15 - 323.15	0.064	$8.41x10^{-4}$	0	0	-0.2244	12.3078	-880.24	2.928	0.354
(1) CO_2 + (2) [Bmim][$MeSO_4$]	303.15 - 323.15	0.172	-0.017	0	0	0.9997	0.9996	$7.25x10^{5}$	$7.18x10^{3}$	0.200
(1) CO_2 + (2) [Bmim][BF_4]	303.15 - 323.15	0.000	0.000	0	0	$7.278Ex10^{11}$	29.5388	-204.1327	1.151	0.235
(1) O_2 + (2) [MOA][Tf_2N]	303.15	-0.167	0.043	0	0	-6.4025	-87.5686	$-1.04x10^{-5}$	2.107	0.000
	313.15	1.194	-0.232	0	0	$7.27x10^{-8}$	$-3.49x10^{-6}$	67.72	0.973	0.984
	323.15	3.292	-0.487	0.694	-0.157	0.000	0.000	-36729	56.153	0.050
(1) O_2 + (2) [Bmim][Tf_2N]	303.15	5.496	-1.356	0	0	$6.33x10^{-10}$	$-9.98x10^{-8}$	-543.60	1.172	0.100
	313.15	1.213	-0.295	0	0	-0.0062	1.1451	-102.20	0.995	0.100
	323.15	118.969	-49.527	1	1	$-4.16x10^{-7}$	-6.0775	$-2.53x10^{4}$	39.420	0.075
(1) O_2 + (2) [Bmim][$MeSO_4$]	303.15	9.971	-3.050	0	0	-1.2135	-3.4655	-1.102	0.114	0.417
	313.15	3.432	-1.076	0	0	-0.0525	4.0805	-0.202	1.032	1.382
	323.15	1.027	-12.424	1	1	-518.57	$-3.13x10^{5}$	-325.088	1.004	0.208
(1) O_2 + (2) [Bmim][BF_4]	303.15	2.7632	-10.1738	1	1	$-7.56x10^{-7}$	0.0002513	-80217	790.265	0.100
	313.15	91.0967	-44.9777	1	1	191.6243	-941.3965	8541.9	4.746	4.965
	323.15	49.5208	-19.7845	1	1	101.0326	$2.45x10^{3}$	$2.93x10^{3}$	4.015	3.822

As can be seen in Table 7-4, systems containing CO_2 were regressed and are valid for all temperatures studied (303.15 to 323.15 K). Deviations of model predictions lower than 0.4% of measured partial pressure, was achieved for these systems.

Regarding O_2 absorption, it can be seen in Figures 7-8 to 7-11 above, that O_2 absorption in the studied ionic liquids is more sensitive to temperature effects than systems with CO_2. O_2 absorption decreases more significantly than CO_2 absorption with increasing temperature. This can also be seen with the sharp increase in Henry's Law constants as temperature is increased, in Table A-9 of Appendix A.

As a result, accurate modelling of measured O_2 absorption data for the temperature range was significantly more difficult. Isothermal data regression was thus conducted for systems containing O_2. Fairly accurate predictions can be achieved with regressed parameters for O_2 in each ionic liquid as shown in Table 7-4.

Modelling of CO_2 and O_2 absorption in the systems above are available electronically in the attached CD, as Matlab^{TM} files under the file name "IL_Generic_RK_EOS_Modelling.m".

The above measurements and modelling were also presented and discussed in a manuscript submitted to the Journal of Physical Chemistry B, titled "Absorption of CO_2 and O_2 in Methyl Trioctyl Ammonium Bis (trifluoromethylsulfonyl) imide, 1-Butyl-3-Methyl Imidazolium Bis (trifluoromethylsulfonyl) imide, and 1-Butyl-3-Methyl Imidazolium Methyl Sulphate". The manuscript is currently under review.

7.7 CO_2 absorption in hybrid solvents

CO_2 and O_2 absorption and desorption was measured in four ionic liquids as explained above. The two most CO_2-selective ionic liquids were [Bmim][BF_4] and [Bmim][Tf_2N]. These ionic liquids were combined with alkanolamines in order to create hybrid solvents, as explained in Section 5.6 and Chapter 6. CO_2 absorption measurements were conducted by gravimetric analysis for pressures of 0.05-1.5 MPa and isotherms of 303.15, 313.15, and 323.15 K. The results of these measurements are presented in Figures 7-12 to 7-17 below. The P-T-x data are presented in Tables A-9 to A-21 of Appendix A.

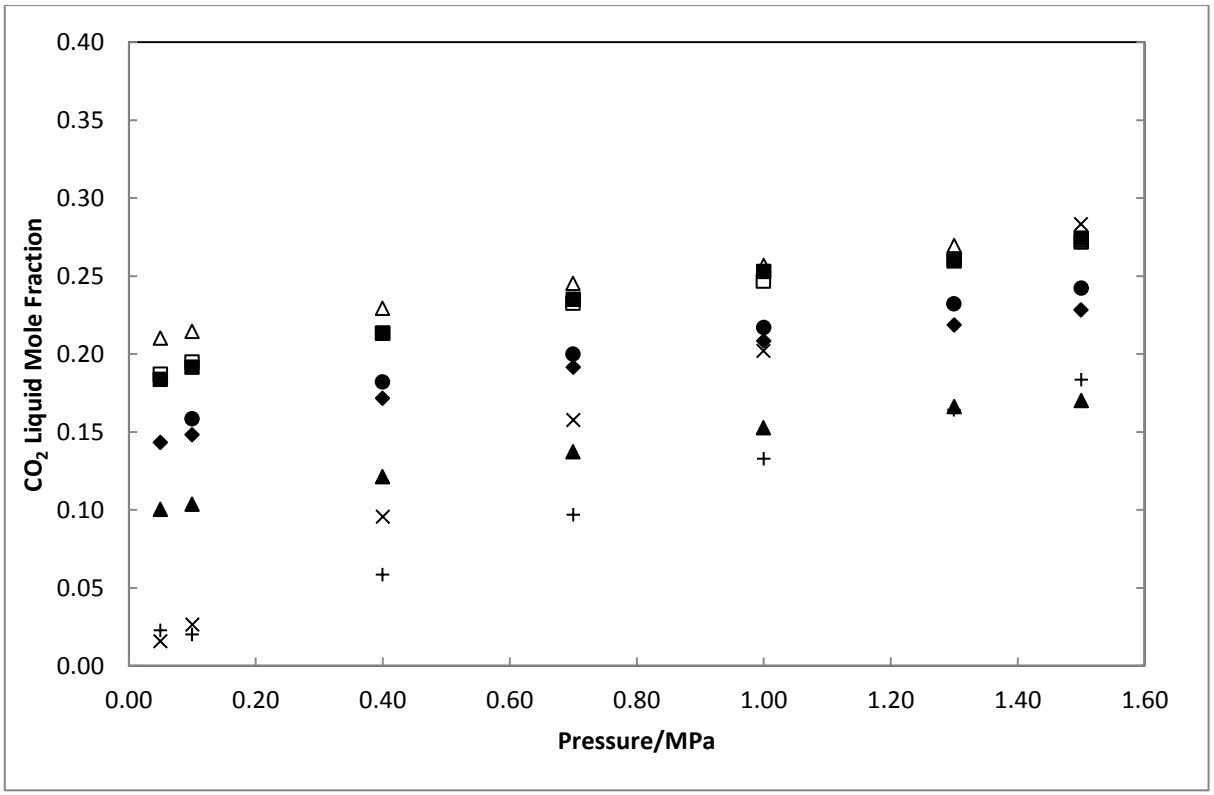

Figure 7-12: Absorption of CO_2 in [Bmim][BF_4]:Alkanolamine Hybrid Solvents at 303.15 K. ● – MEA:[Bmim][BF_4] at 29.3:70.7 wt%; □ – MEA:MDEA:[Bmim][BF_4] at 31.6:10.4:58 wt%; ■ – MEA:MDEA:[Bmim][BF_4] at 30.3:21.8:48 wt%; Δ - MEA:DEA:[Bmim][BF_4] at 31.8:12.1:56.1 wt%; ▲ – MEA:DEA:[Bmim][BF_4] at 33:16.2:50.8 wt% ♦ - MEA:DEA:MDEA:[Bmim][BF_4] at 29.8:11.7:12.8:45.7 wt%; + - Pure [Bmim][BF_4]; x- Pure [Bmim][Tf_2N]

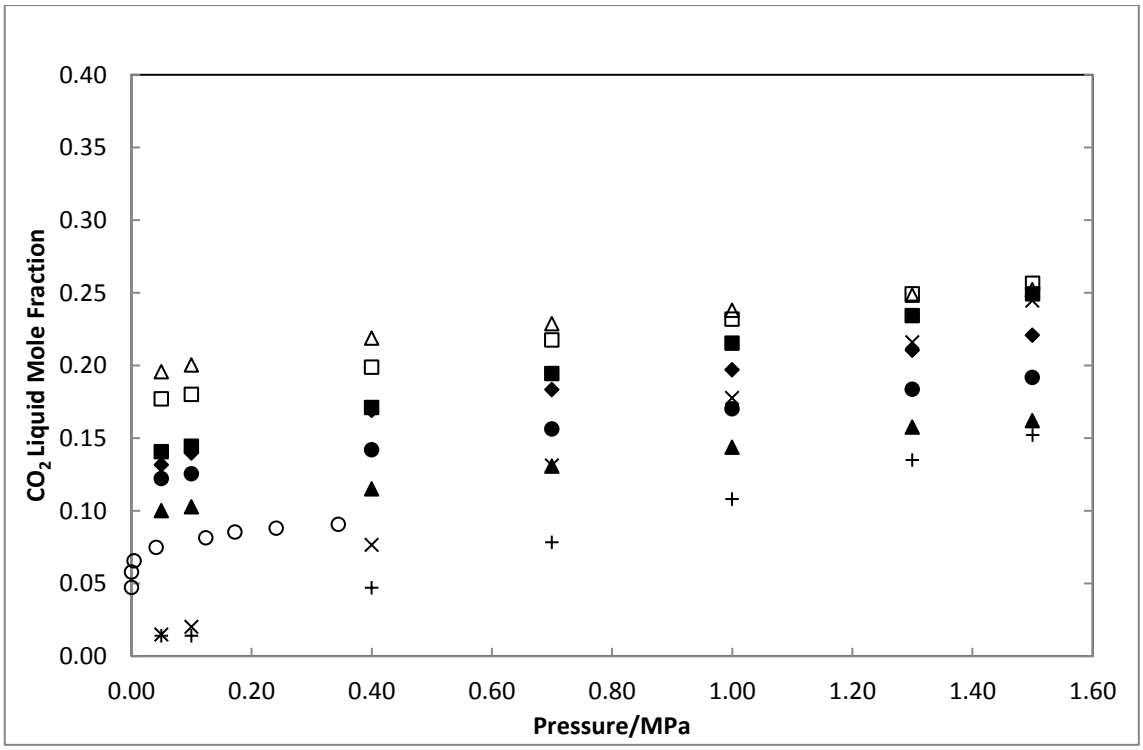

Figure 7-13: Absorption of CO_2 in [Bmim][BF_4]:Alkanolamine Hybrid Solvents at 313.15 K. ● – MEA:[Bmim][BF_4] at 29.3:70.7 wt%; □ – MEA:MDEA:[Bmim][BF_4] at 31.6:10.4:58 wt%; ■ – MEA:MDEA:[Bmim][BF_4] at 30.3:21.8:48 wt%; Δ - MEA:DEA:[Bmim][BF_4] at 31.8:12.1:56.1 wt%; ▲ – MEA:DEA:[Bmim][BF_4] at 33:16.2:50.8 wt% ♦ - MEA:DEA:MDEA:[Bmim][BF_4] at 29.8:11.7:12.8:45.7 wt%; + - Pure [Bmim][BF_4]; x- Pure [Bmim][Tf_2N]; ○ – MEA:H_2O at 30:70 wt% (Park et al., 2002)

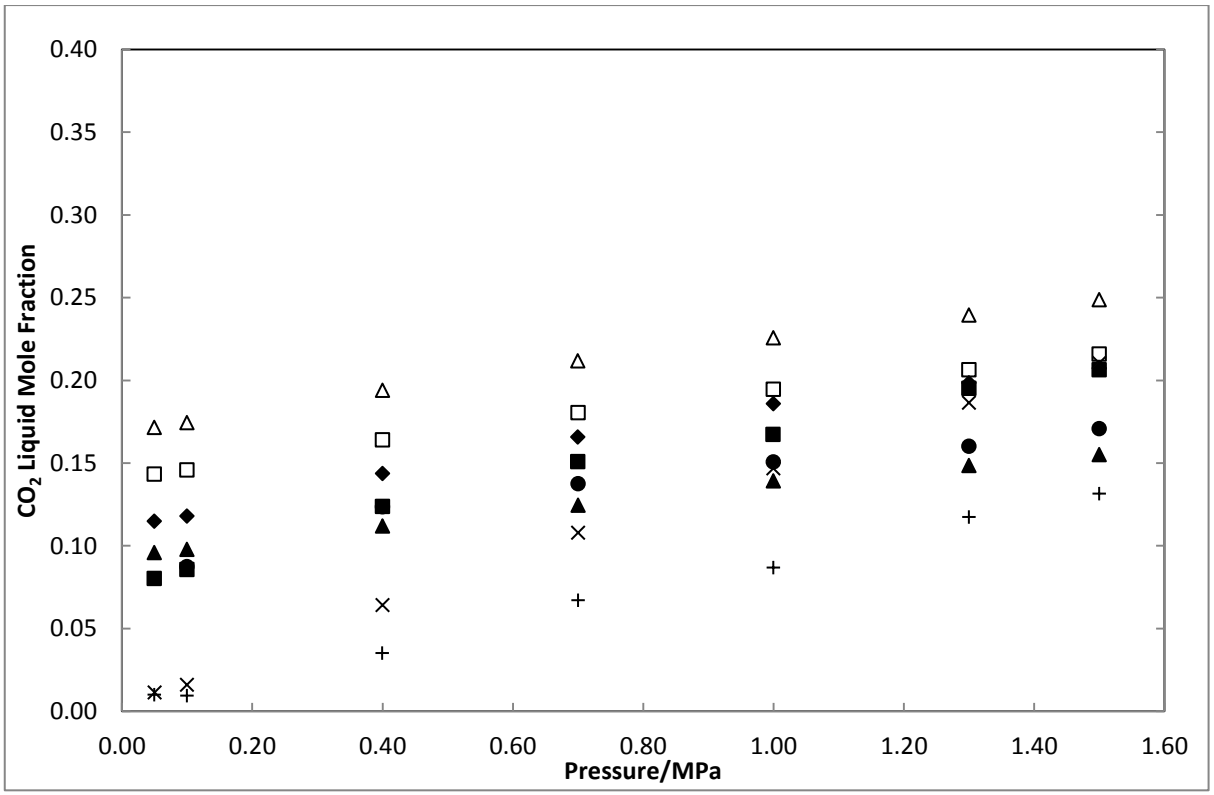

Figure 7-14: Absorption of CO_2 in [Bmim][BF_4]:Alkanolamine Hybrid Solvents at 323.15 K. ● – MEA:[Bmim][BF_4] at 29.3:70.7 wt%; □ – MEA:MDEA:[Bmim][BF_4] at 31.6:10.4:58 wt%; ■ – MEA:MDEA:[Bmim][BF_4] at 30.3:21.8:48 wt%; Δ - MEA:DEA:[Bmim][BF_4] at 31.8:12.1:56.1 wt%; ▲ – MEA:DEA:[Bmim][BF_4] at 33:16.2:50.8 wt% ♦ - MEA:DEA:MDEA:[Bmim][BF_4] at 29.8:11.7:12.8:45.7 wt%; + - Pure [Bmim][BF_4]; x- Pure [Bmim][Tf_2N]

The apparent and consistent finding with literature was that CO_2 absorption increased with increasing CO_2 partial pressure. This is evident in Figures 7-12 to 7-14 above for absorption in all solvents and is consistent with physical and chemical equilibrium. Regarding chemical absorption in alkanolamines, increasing pressure favours the primary, secondary and tertiary reaction mechanism between CO_2 and alkanolamines, thereby increasing CO_2 absorption. In the case of the ionic liquid in the solvent, increasing pressure favours CO_2 absorption.

A further observation is that while CO_2 absorption increased quite significantly with increasing pressure in the case of pure ionic liquids, there was a more gradual increase in the case of CO_2 absorption in alkanolamine-ionic liquid blends. Figures 7-12 to 7-14 above show that for absorption in pure [Bmim][BF_4] and [Bmim][Tf_2N], a great increase in CO_2 partial pressure resulted in a high increase in CO_2 absorption. For example, in Figure 7-12 the equilibrium CO_2 mole fraction increased from 0.023 to 0.283 in the case of [Bmim][Tf_2N] and from 0.027 to

0.183 in the case of [Bmim][BF_4] from 0.05 to 1.5 MPa at 303.15 K. By contrast, for hybrid solvents containing approximately 60% ionic liquid by mass, equilibrium CO_2 mole fraction increased by 0.064 across the same pressure range and for the same isotherm. This is likely due to the fact that amines are chemical solvents which react with CO_2 and have an ultimate absorption capacity which is lower than that of physical solvents. CO_2 reacts with the alkanolamine and once all the alkanolamine is converted to ensure equilibrium, there is not going to be any further absorption. This is observed in the works of Osman (2011) and Osman et al. (2012). Ionic liquids on the other hand are physical solvents. Absorption merely occurs through a rearrangement of solvent molecules to accommodate the solute. Pressure thus has a significant effect on the absorption of gases into the ionic liquid solvent.

It is also observed that higher amounts of alkanolamines in the hybrid composition results in increased pressure having a lower effect on CO_2 absorption. Figure 7-13 illustrates this. CO_2 mole fraction in the sample containing MEA:[Bmim][BF_4] at 29.3:70.7 wt% at 303.15 K increased by 0.1 when comparing results at 0.05 MPa and 1.5 MPa, a difference significantly higher than for hybrid solvents containing alkanolamines at 40 wt% composition as explained above. Measurements concerning [Bmim][Tf_2N] shown in Figures 7-15 to 7-17 below, reveal that for hybrid solvents 50 wt% alkanolamines, the difference in CO_2 mole fraction achieved is as low as 0.04 for pressures from 0.05 to 1.5 MPa.

The most encouraging observation is that all hybrid solvents achieved higher CO_2 absorption at low pressure than the pure ionic liquids, as well as the conventional alkanolamine solvent of 30 wt% MEA in H_2O (Jou et al, 1994, Mamun et al., 2005). This is shown in Figure 7-12 to 7-14 at all isotherms, with Figure 7-13 showing superior CO_2 absorption at 313.15 K compared to the conventional alkanolamine solvent. This is a very encouraging result with significant industrial implications. As mentioned in Section 2.1 of Chapter 2, pulverised coal power plant flue gas is available at 0.1 to 0.17 MPa (NETL, 2010). CO_2 is available at pressure lower than atmospheric pressure. Thus, it is beneficial if the solvent in the absorption process is able to absorb CO_2 at low pressure. And this is what was observed in the programme of measurement conducted.

The hybrid solvents also achieved higher CO_2 absorption than the pure [MOA][Tf_2N] ionic liquid. This can be seen when comparing Figures 7-12 to 7-14 with Figures 7-3. At all isotherms, all hybrid solvents achieved CO2 absorption than [MOA][Tf_2N] for pressures up to 0.4 MPa. The hybrid solvent containing MEA:DEA:[Bmim][BF_4] at 31.8:12.1:56.1 wt% achieved higher CO_2 absorption for pressures up to 1 MPa. However, at pressure higher than 1 MPa, [MOA][Tf_2N] achieved higher CO_2 absorption.

For absorption at pressure up to 1 MPa, hybrid solvents containing [Bmim][BF_4] are beneficial over conventional alkanolamine solvents and pure ionic liquids. Diluting the alkanolamines with [Bmim][BF_4] instead of water was found to be very beneficial in terms of CO_2 absorption achieved.

The purpose of diluting alkanolamines such as MEA with water is to reduce the overall corrosiveness of the solvent and facilitate diffusion of CO_2 into the solvent, as shown in Reaction R2-5 in Section 2.4.1.1. However as this research revealed, diluting alkanolamines with non-corrosive ionic liquids instead of water would not only lower the overall corrosiveness of the solvent and facilitate diffusion, but also increase absorption since the ionic liquid absorbs CO_2 as well.

Regarding the CO_2 mole fraction in systems containing [Bmim][BF_4] in Figures 7-12 to 7-14, it was found that the sample containing MEA:DEA:[Bmim][BF_4] at 31.8:12.1:56.1 wt% achieved the highest equilibrium CO_2 absorption across all three isotherms. However, the sample containing MEA:DEA:[Bmim][BF_4] at 33:16.2:50.8 wt% achieved the lowest CO_2 absorption from all hybrid solvents studied. This shows that while the addition of a secondary amine such as DEA in compositions of up to 10wt% increases CO_2 absorption, further increases in DEA compositions achieve lower CO_2 absorption, possibly due to the high viscosity of DEA which may impede diffusion. DiGuillo et al. (1992) conducted a density and viscosity measurements for many alkanolamines, including those which are studied in this work. At 303.15 K, DEA viscosity was measured to be 356 cP, while that of MEA and MDEA was 14.86 cP and 57 cP respectively, indicating a highly significant difference in viscosity.

Enthalpy and entropy of absorption measured for all hybrid solvent systems are presented in Table E-2 of Appendix E. It is shown that solvents containing approximately 20 wt% DEA had the lowest enthalpy and entropy of absorption, and also the lowest deviation of these values. While this may indicate relatively lower temperature dependence than other systems, absorption was low anyway. Low standard deviations suggest little effect of the chemical solvent in the hybrid solvent mixture, possibly due to low diffusion brought about by high DEA viscosity.

The same is noted for hybrid solvents containing MDEA. At 303.15 K, Figure 7-12 shows that the second highest CO_2 achieved in the sample containing MEA:MDEA:[Bmim][BF_4] at 31.6:10.4:58 wt%, yet an increase in MDEA composition resulted in slightly lower absorption for the sample containing MEA:MDEA:[Bmim][BF_4] at 30.3:21.8:48 wt%. The effect is more pronounced at higher temperatures of 313.15 and 323.15 K as shown in Figure 7-13 and Figure 7-14 respectively. One possible reason in the case of samples containing MDEA is that higher

temperatures significantly reduce the CO_2 absorption capacity of samples containing MDEA. The reaction mechanism between MDEA and CO_2 is different to primary and secondary amines, as discussed in Section 2.4.1.1. Another possibility is that in the case of systems containing only alkanolamines and ionic liquids, with no presence of water, the tertiary reaction mechanism does not occur, since MDEA needs to react directly with water, as shown in reaction R2-10 in Section 2.4.1.1.

A comparison between Figure 7-12, Figure 7-13 and Figure 7-14 confirms that absorption decreases with increasing temperature. This is consistent in literature for both chemical and physical solvents, since CO_2 absorption is an exothermic reaction. It is also noted that temperature has varying effects on different samples depending on their composition of alkanolamines and ionic liquid. It can be observed that samples containing higher amounts of MDEA achieved much lower CO_2 absorption when increasing the temperature from 303.15 to 323.15 K. CO_2 mole fraction in the sample containing MEA:MDEA:[Bmim][BF_4] at 30.3:21.8:48 wt% achieved the second highest CO_2 absorption at 303.15 K, yet by 323.15 K, it achieved the 3rd lowest CO_2 absorption of all hybrid solvents containing [Bmim][BF_4]. A significant reduction in CO_2 absorption is noted even in the sample containing a low composition of MDEA such as MEA:MDEA:[Bmim][BF_4] at 31.6:10.4:58 wt%. At 303.15 K, this sample achieved CO_2 absorption almost as high as the sample containing MEA:DEA:[Bmim][BF_4] at 31.8:12.1:56.1 wt%. Yet at 313.15 K and 323.15 K, a significant difference in absorption achieved between the two hybrid solvents is noted.

Figures 7-15 to 7-17 below present the CO_2 mole fraction results for systems containing [Bmim][Tf_2N].

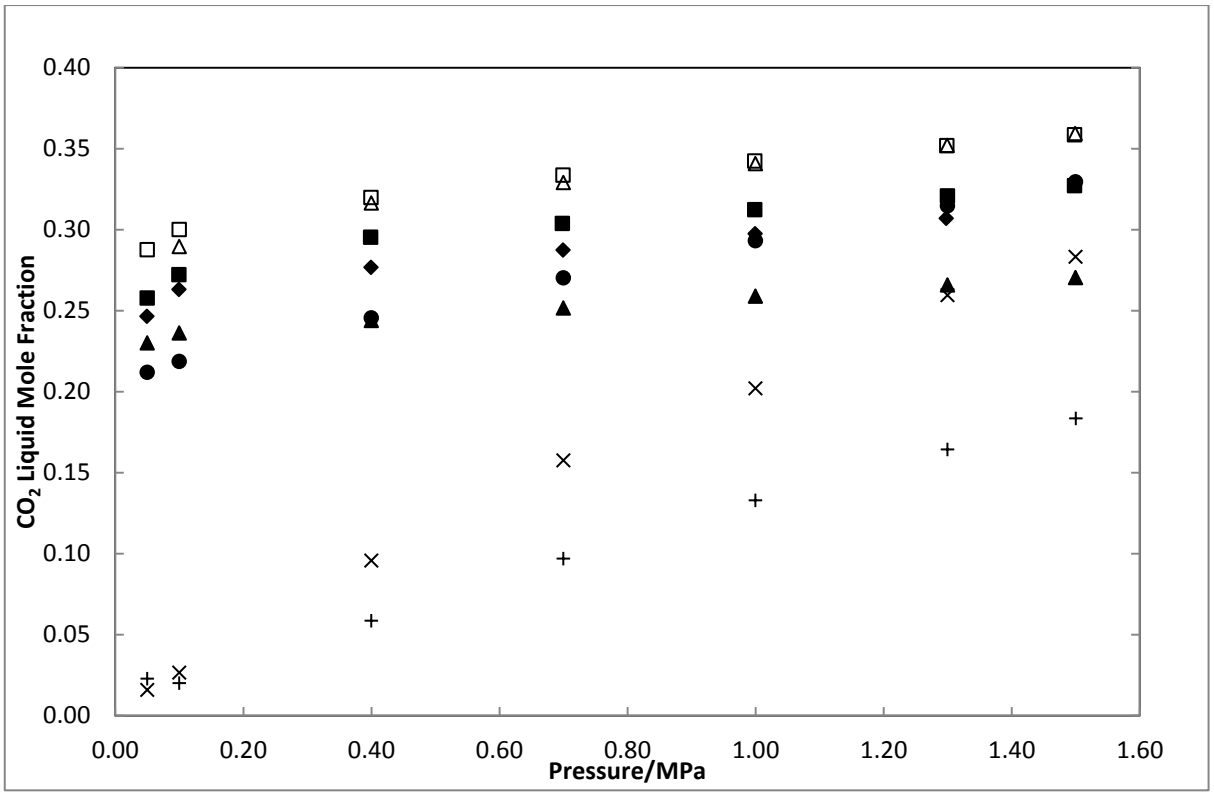

Figure 7-15: Absorption of CO_2 in [Bmim][Tf_2N]:Alkanolamine Hybrid Solvents at 303.15 K. ● – MEA:[Bmim][Tf_2N] at 32.8:67.2 wt%; □ – MEA:MDEA:[Bmim][Tf_2N] at 29.9:12.6:57.5 wt%; ■ – MEA:MDEA:[Bmim][Tf_2N] at 30.4:19.3:50.3 wt%; Δ - MEA:DEA:[Bmim][Tf_2N] at 30.3:10.5:59.2 wt%; ▲ – MEA:DEA:[Bmim][Tf_2N] at 32.6:21.3:46.2 wt% ♦ - MEA:DEA:MDEA:[Bmim][Tf_2N] at 29.1:10.1:12.5:48.3 wt%; + - Pure [Bmim][BF_4]; x- Pure [Bmim][Tf_2N]

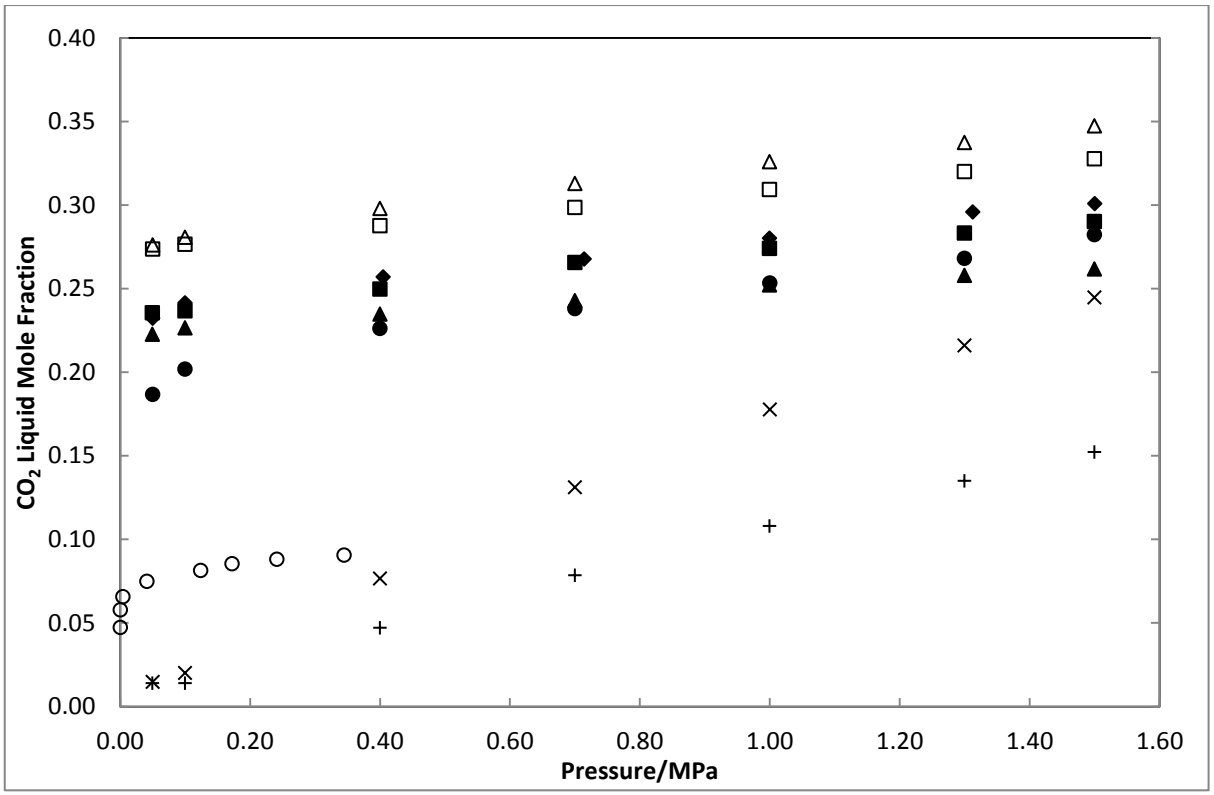

Figure 7-16: Absorption of CO_2 in [Bmim][Tf_2N]:Alkanolamine Hybrid Solvents at 313.15 K. ● – MEA:[Bmim][Tf_2N] at 32.8:67.2 wt%; □ – MEA:MDEA:[Bmim][Tf_2N] at 29.9:12.6:57.5 wt%; ■ – MEA:MDEA:[Bmim][Tf_2N] at 30.4:19.3:50.3 wt%; Δ - MEA:DEA:[Bmim][Tf_2N] at 30.3:10.5:59.2 wt%; ▲ – MEA:DEA:[Bmim][Tf_2N] at 32.6:21.3:46.2 wt% ♦ - MEA:DEA:MDEA:[Bmim][Tf_2N] at 29.1:10.1:12.5:48.3 wt%; + - Pure [Bmim][BF_4]; x- Pure [Bmim][Tf_2N]; ○ – MEA:H_2O at 30:70 wt% (Park et al., 2002)

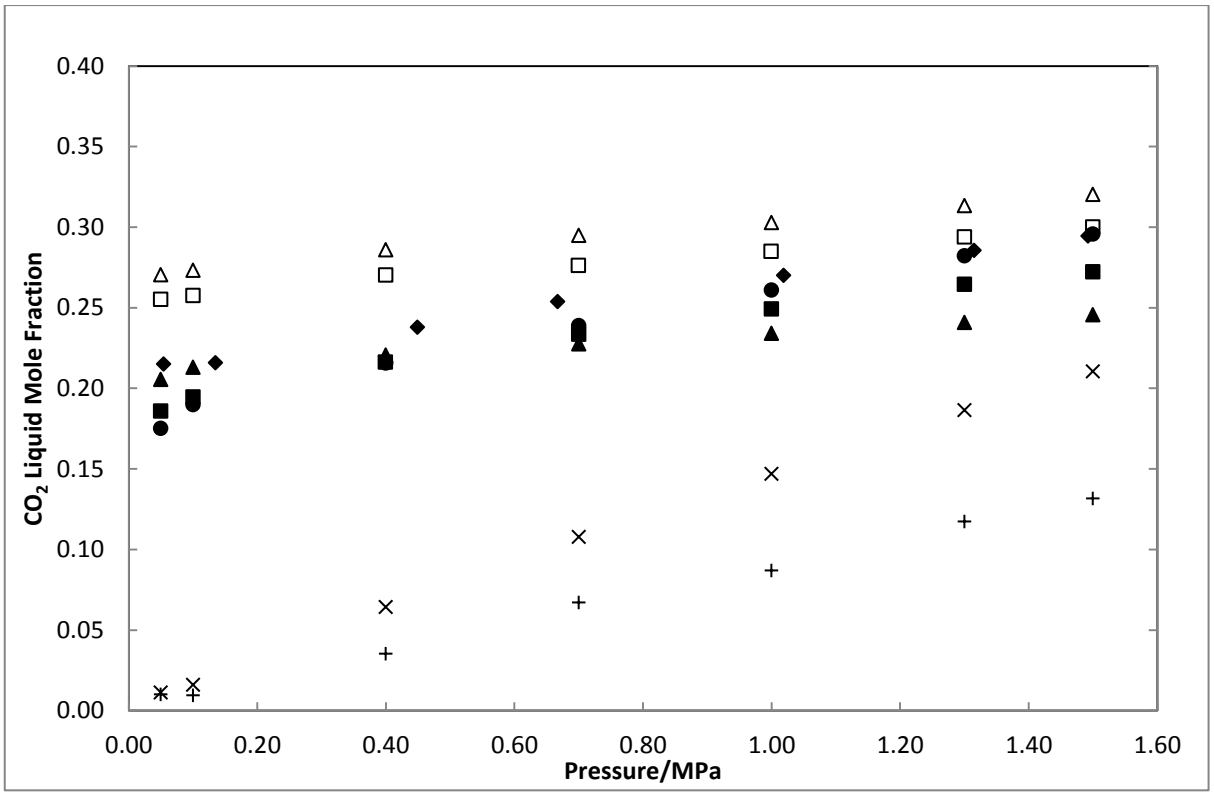

Figure 7-17: Absorption of CO_2 in [Bmim][Tf_2N]:Alkanolamine Hybrid Solvents at 323.15 K. ● – MEA:[Bmim][Tf_2N] at 32.8:67.2 wt%; □ – MEA:MDEA:[Bmim][Tf_2N] at 29.9:12.6:57.5 wt%; ■ – MEA:MDEA:[Bmim][Tf_2N] at 30.4:19.3:50.3 wt%; Δ - MEA:DEA:[Bmim][Tf_2N] at 30.3:10.5:59.2 wt%; ▲ – MEA:DEA:[Bmim][Tf_2N] at 32.6:21.3:46.2 wt% ♦ - MEA:DEA:MDEA:[Bmim][Tf_2N] at 29.1:10.1:12.5:48.3 wt%; + - Pure [Bmim][BF_4]; x- Pure [Bmim][Tf_2N]

It is immediately noted that samples containing [Bmim][Tf_2N] achieved significantly higher CO_2 absorption than samples containing equivalent compositions of [Bmim][BF_4], when comparing Figures 7-12 to 7-14 with Figures 7-15 to 7-17. This is also consistent with literature (Cadena et al. 2004, Anderson et al., 2007) that increased fluorination of the ionic liquid anion increases CO_2 absorption as explained in Section 2.5.7.

It is well noted that the effect of alkanolamine composition on CO_2 mole fraction in systems containing [Bmim][Tf_2N] was quite consistent with systems containing [Bmim][BF_4], thereby providing validation of the effect of alkanolamines in alkanolamine:ionic liquid hybrid solvents on equilibrium CO_2 mole fraction.

As with systems containing [Bmim][BF_4], it was observed for systems containing [Bmim][Tf_2N] that lower compositions of secondary and tertiary amines achieved higher CO_2 absorption. This is noted when comparing the samples containing MEA:DEA:[Bmim][Tf_2N] at

32.55:21.29:46.2 wt% and MEA:MDEA:[Bmim][Tf_2N] at 30.4:19.3:50.3 wt%, with MEA:DEA:[Bmim][Tf_2N] at 30.28:10.53:59.2 wt% and MEA:MDEA:[Bmim][Tf_2N] at 29.9:12.6:57.5 wt%. In the case of samples containing DEA, it is possible that the high viscosity of DEA undiluted with H_2O inhibits CO_2 absorption. Moreover, DEA is a secondary amine with a lower rate of CO_2 absorption than MEA, a primary amine. High concentrations of DEA are thus not effective at increasing CO_2 absorption.

High compositions of alkanolamines were not beneficial in achieving high CO_2 absorption. As mentioned previously, solvents containing approximately 20 wt% of MDEA or DEA achieved lower CO_2 absorption than solvents containing approximately 10 wt% MDEA or DEA. Moreover, as Figures 7-12 and 7-15 show, samples containing MEA:[Bmim][BF_4] at 29.3:70.7 wt% and MEA:[Bmim][Tf_2N] at 32.8:67.2 wt% achieved higher CO_2 absorption than samples containing approximately 20 wt% DEA. At pressures greater than 1 MPa, samples containing MEA:[Bmim][BF_4] at 29.3:70.7 wt% and MEA:[Bmim][Tf_2N] at 32.8:67.2 wt% achieved higher CO_2 absorption than samples containing approximately 20 wt% MDEA. However, these samples which only contained approximately 30 wt% MEA also achieved lower CO_2 absorption than samples containing approximately 30wt% MEA and approximately 10 wt% MDEA or DEA. It can thus be concluded that an alkanolamine composition of 40 wt% is the optimum alkanolamine composition to be included in a hybrid solvent with ionic liquids.

Regarding temperature, when comparing the sample containing MEA:DEA:[Bmim][Tf_2N] at 30.3:10.5:59.2 wt% with MEA:MDEA:[Bmim][Tf_2N] at 29.9:12.6:57.5 wt%, it was also observed that while both samples achieved high CO_2 absorption at 303.15 K as showed in Figure 7-15, as the temperature increases in Figures 7-16 and 7-17 , CO_2 absorption in the sample containing MDEA decreases more substantially and achieves the third lowest CO_2 absorption at 323.15 K, from all the hybrid solvents containing [Bmim][Tf_2N]. This is consistent with systems containing [Bmim][BF_4].

The same can be observed when comparing the sample containing MEA:MDEA:[Bmim][Tf_2N] at 30.4:19.3:50.3 wt% to the sample containing MEA:DEA:MDEA:[Bmim][Tf_2N] at 29.1:10.1:12.5:48.3 wt%. CO_2 absorption in the system containing a higher composition of MDEA decreased more substantially than in the case of systems with lower amounts of MDEA, with an increase in temperature.

The effect can be quantified by comparing the enthalpy and entropy of absorption for CO_2 in hybrid solvents, which is presented in Table E-2 of Appendix E. It is noted that the hybrid solvents containing high amounts of MDEA, particularly those containing

MEA:MDEA:[Bmim][Tf_2N] at 30.4:19.3:50.3 wt% and MEA:MDEA:[Bmim][BF_4] at 30.3:21.8:48 wt% had the highest enthalpies and entropies of absorption of all hybrid solvents studied. Even when comparing the solvents containing approximately 10 wt% MDEA with those containing approximately 10 wt% DEA, the solvents containing approximately 10 wt% MDEA had higher enthalpy and entropy of absorption, indicating higher temperature dependence and increased ordering of molecules upon absorption. This reflects the effect of the alternative reaction mechanism of MDEA, a tertiary alkanolamine, as opposed to MEA and DEA.

Another observation was that enthalpies and entropies of absorption measured for systems containing MDEA had the highest standard deviation as shown in Table E-2, indicating a varying effect on absorption due to the alternative, tertiary reaction mechanism.

Enthalpy and entropy of absorption was intermediate for systems containing only the primary alkanolamine MEA combined with either [Bmim][BF_4] or [Bmim][Tf_2N]. This suggests an intermediate temperature dependence and high ordering, possibly due to the high reactivity of MEA in comparison to DEA and MDEA.

Regarding the samples which contained [Bmim][BF_4], the sample which achieved the highest CO_2 absorption was MEA:DEA:[Bmim][BF_4] at 31.8:12.1:56.1 wt%, and regarding samples which contained [Bmim][Tf_2N] the sample which achieved the highest absorption was MEA:DEA:[Bmim][Tf_2N] at 30.18:10.53:59.2 wt%. The sample containing MEA:DEA:[Bmim][Tf_2N] at 30.18:10.53:59.2 wt% achieved the highest CO_2 absorption of all solvents studied, across all temperatures and pressures. This hybrid solvent also achieved higher CO_2 absorption than pure [MOA][Tf_2N] for the entire pressure range (0.05 to 1.5 MPa), as found when comparing Figures 7-15 to 7-17 with Figure 7-3. The hybrid solvent containing MEA:DEA:[Bmim][Tf_2N] at 30.18:10.53:59.2 wt% can thus be recommended by this study for further investigation into its potential as a solvent in a commercial CO_2 absorption process.

The most encouraging conclusion drawn from the measurements of CO_2 absorption in hybrid solvents is that hybrid solvents achieve significantly superior CO_2 absorption at low pressure than pure physical solvents such as pure ionic liquids, and conventional amine solvents such as MEA:H_2O at 30:70 wt%. The industrial implication of this is that flue gas from an industrial source does not need to be greatly compressed to increase the pressure and facilitate efficient CO_2 capture. CO_2 capture can occur at lower pressures from atmospheric to 0.5 MPa, rather than the higher pressures of 1.5MPa. The implication is ultimately lower compression costs.

Moreover, the high equilibrium CO_2 mole fractions achieved at low pressure also implies that less solvent may be used and the CO_2 capture process may be scaled down and require less energy. Further investigation is required to confirm this.

As with measurements concerning pure ionic liquids, absorption and desorption was measured for systems containing hybrid solvents. Absorption measurements were the key focus of study in this research, while desorption measurements were conducted merely to assess the repeatability and hence validity of equilibrium solubility data. Desorption data are available in Tables A-10 to A-21 of Appendix A. The data shows fairly good repeatability generally. However, for solvents containing MDEA, CO_2 equilibrium desorption data was reported to be 1-3% higher than absorption data, indicating that solvents containing MDEA may not be completely recyclable. Further investigation is however required for this, which is beyond the scope of this research.

7.8 Absorption analysis using the FTIR probe apparatus

As mentioned in Section 5.8 and Chapter 6, while the designed FTIR Probe apparatus could detect CO_2 at different concentrations, it did not produce the results necessary to determine liquid phase species concentrations of components participating in the reaction mechanism between CO_2 and the undiluted alkanolamines used in this research, which may have provided information for more accurate modelling of CO_2 absorption in hybrid solvents.

Details of the analyses attempted using the FTIR probe apparatus, and reasons for why the apparatus did not achieve the desired measurements, are discussed in Section F2 of Appendix F. Propositions for its further upgrade and development are also provided.

7.9 Modelling of CO_2 absorption in hybrid solvents

The modelling of CO_2 absorption in alkanolamine-ionic liquid hybrid solvents has proven to be challenging. As explained in Sections 7.8, Chapter 3, Chapter 6 and Appendix F, the FTIR Probe Apparatus was intended to provide insight into the chemistry of CO_2 absorption in hybrid solvents. The chemistry of such systems was expected to be complex due to the presence of physical solvents and multiple chemical solvents. Current models for chemical absorption assume the presence of water, with up to 4 diffusion reactions between CO_2 and water included in the assumed reaction mechanisms.

Due to setbacks in the development of this apparatus, the chemistry of the systems containing hybrid solvents remains unknown, thereby invalidating the use of more complex models for

chemical absorption such as the Deshmukh-Mather and Elec-NRTL models typically used by various sources in literature (Osman, 2011, Osman et al., 2012, Benamor and Aroua, 2005).

Due to the lack of information on the chemistry of these hybrid systems, simpler models were utilised to model the data. The RK-EOS was used to model CO_2 partial pressure in the ionic liquid component of the hybrid solvent, while the Posey-Tapperson-Rochelle model was used to model CO_2 partial pressure in the alkanolamine components of the hybrid solvent, as explained in Chapter 4. The model was previously applied successfully for alkanolamine mixtures of DEA and MDEA by Osman et al. (2012).

Figures 7-18 to 7-23 below provide the experimentally measured absorption data, together with model predictions for systems containing [Bmim][BF_4] at all isotherms (303.15 to 323.15 K).

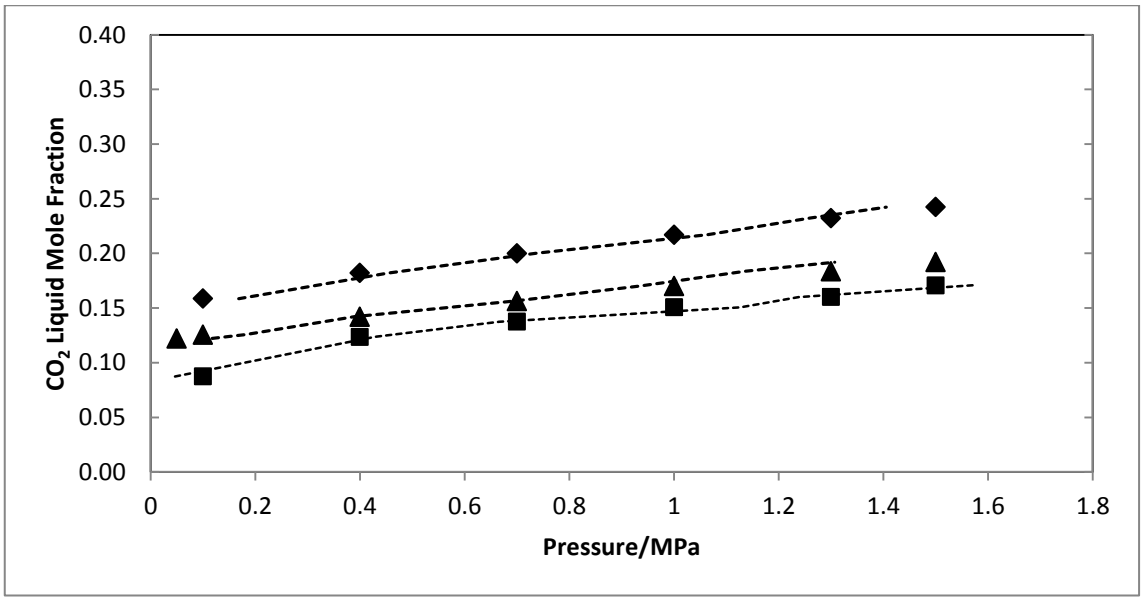

Figure 7-18: Experimental Results together with Posey-Tapperson-Rochelle and RK-EOS predictions for the System of CO_2 in [Bmim][BF_4]:MEA at 70.7:29.3 wt%. ■ – 303.15 K; ▲ – 313.15 K; ♦ - 323.15 K. *Dotted lines indicate model predictions

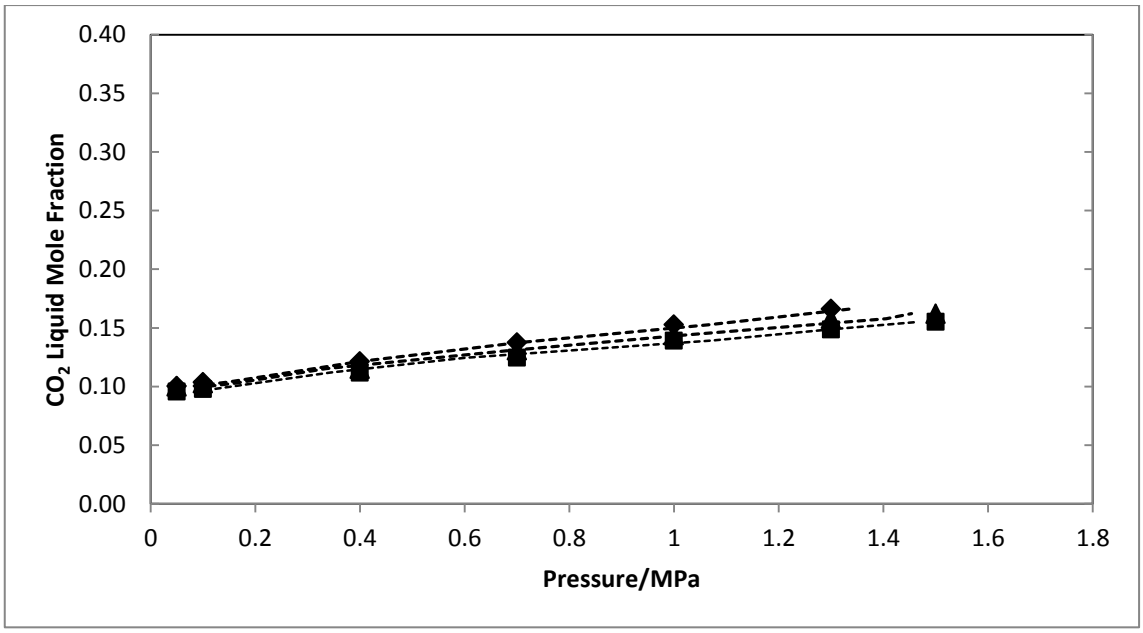

Figure 7-19: Experimental Results together with Posey-Tapperson-Rochelle and RK-EOS predictions for the System of CO_2 in in MEA:DEA:[Bmim][BF_4] at 33:16.2:50.8 wt%. ■ – 303.15 K; ▲ – 313.15 K; ♦ - 323.15 K

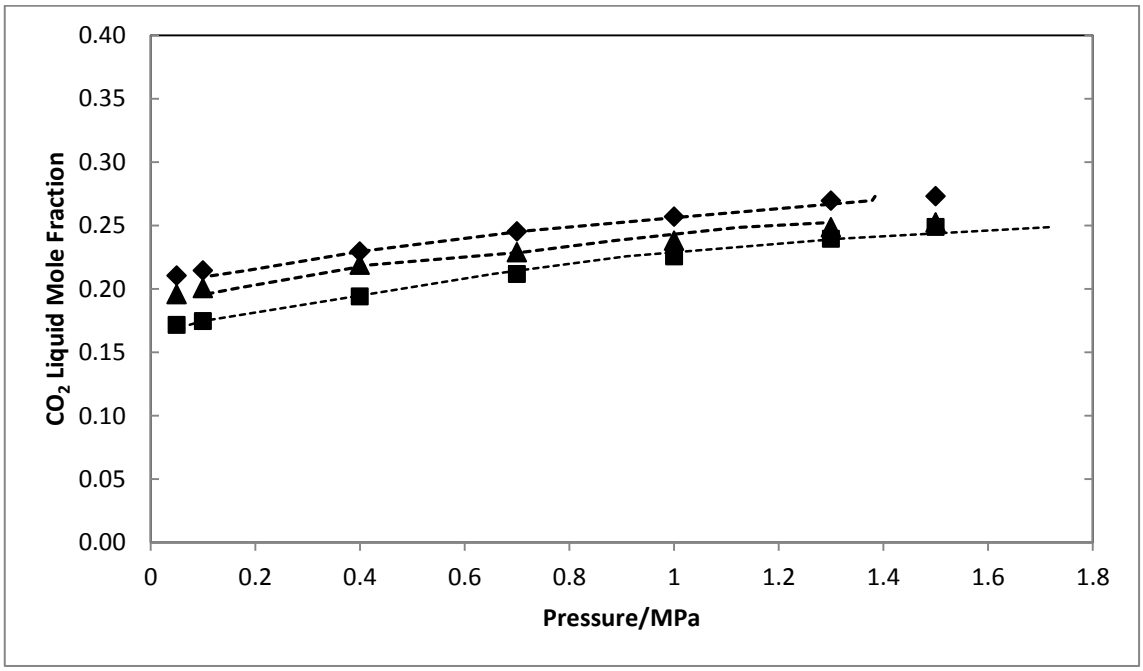

Figure 7-20: Experimental Results together with Posey-Tapperson-Rochelle and RK-EOS predictions for the System of CO_2 in in MEA:DEA:[Bmim][BF_4] at 31.8:12.1:56.1 wt%. ■ – 303.15 K; ▲ – 313.15 K; ♦ - 323.15 K*Dotted lines indicate model predictions

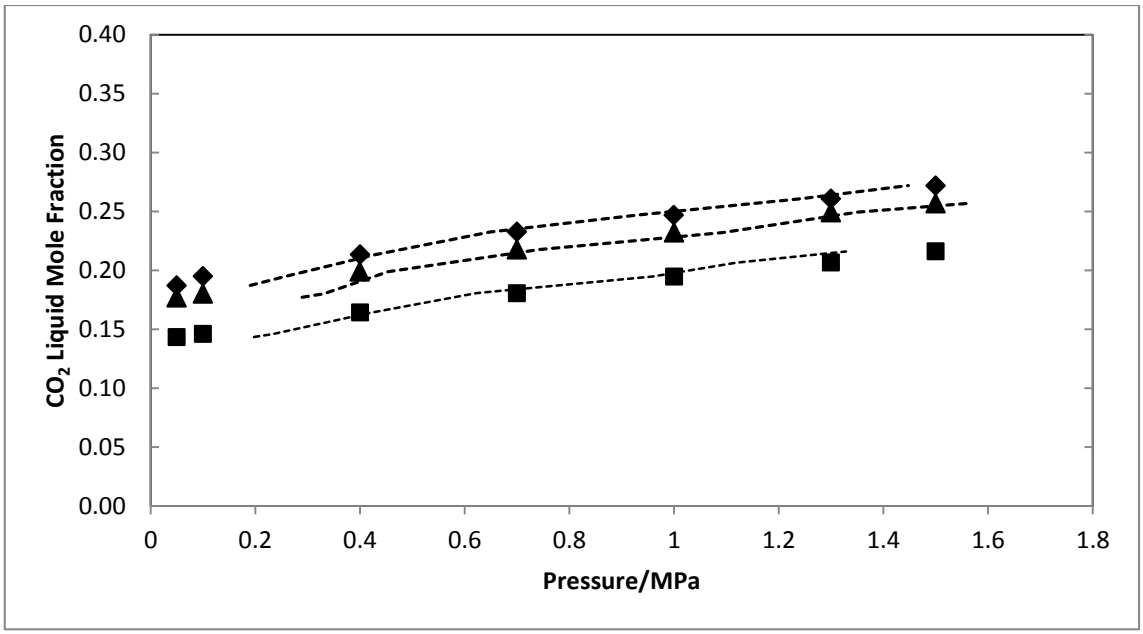

Figure 7-21: Experimental Results together with Posey-Tapperson-Rochelle and RK-EOS predictions for the System of CO_2 in in MEA:MDEA:[Bmim][BF_4] at 31.6:10.4:58 wt%. ■ – 303.15 K; ▲ – 313.15 K; ♦ - 323.15 K *Dotted lines indicate model predictions

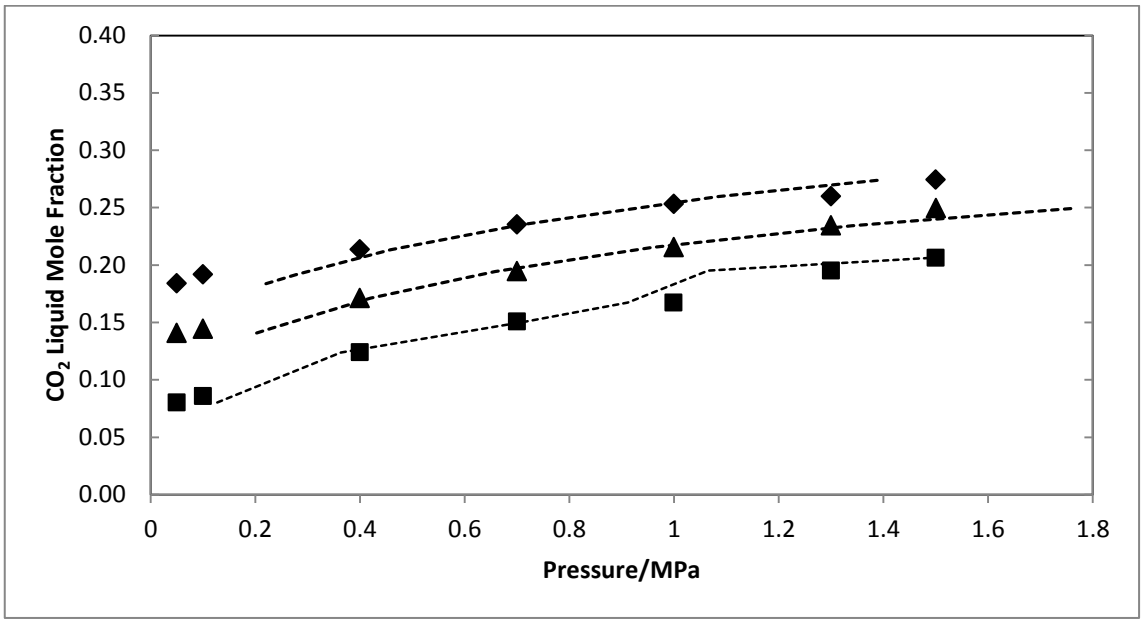

Figure 7-22: Experimental Results together with Posey-Tapperson-Rochelle and RK-EOS predictions for the System of CO_2 in in MEA:MDEA:[Bmim][BF_4] at 30.3:21.8:48 wt%. ■ – 303.15 K; ▲ – 313.15 K; ♦ - 323.15 K *Dotted lines indicate model predictions

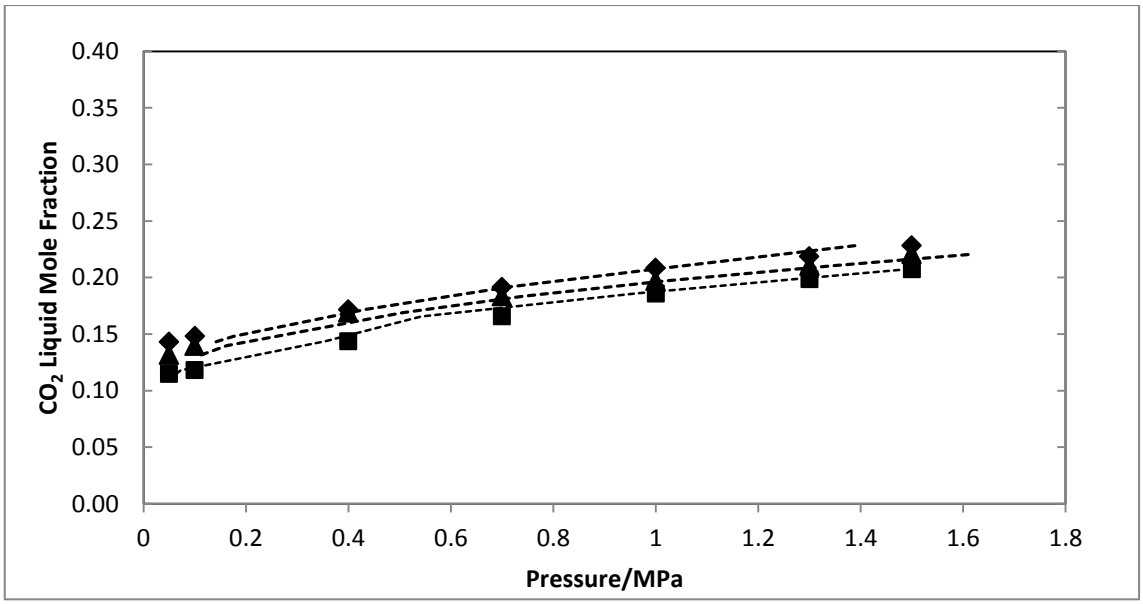

Figure 7-23: Experimental Results together with Posey-Tapperson-Rochelle and RK-EOS predictions for the System of CO_2 in in MEA:DEA:MDEA:[Bmim][BF_4] at 29.8:11.7:12.8:45.7 wt%. ■ – 303.15 K; ▲ – 313.15 K; ♦ - 323.15 K *Dotted lines indicate model predictions

Regressed RK-EOS parameters and Posey-Tapperson-Rochelle parameters for the systems above are presented in Table 7-5 below. Predicted data are presented alongside measured data in Tables A-10 to A-21 of Appendix A.

Table 7-5: Binary Interaction and Fitting Parameters for Predicting CO_2 Absorption in Hybrid Solvents using the Posey-Tapperson-Rochelle Model with RK-EOS

System	$ß_0$	$ß_1$	$ℓ_{12}$	$ℓ_{21}$	$τ_{12}$	m_{12}	A	B	C	D	Root* Mean Square Error (%)
CO_2 in [Bmim][BF_4] + MEA at 70.7:29.3 wt%	0.2935	-0.0563	3.92E+09	0.3843	114.2028	5.4496	14.3431	-1.53E+04	-4.79E+05	9.37E+03	6.898
CO_2 in MEA+DEA+[Bmim][BF_4] at 33:16.2:50.8 wt%	0.3221	-0.0685	1.8355	0.6412	1.52E+03	8.2411	-48.4584	-939.8185	-5.05E+05	1.11E+04	5.878
CO_2 in MEA+DEA+[Bmim][BF_4] at 31.8:12.1:56.1 wt%	0.293	-0.0564	1.3055	0.6216	490.9643	8.8182	-8.1056	-4.59E+03	-1.04E+05	3.79E+03	6.446
CO_2 in MEA+MDEA+[Bmim][BF_4] at 31.6:10.4:58 wt%	0.2567	-0.042	1.0011	0.9959	8.3398	874.5922	22.4223	-6.60E+03	-1.18E+03	689.2789	7.437
CO_2 in MEA+MDEA+[Bmim][BF_4] at 30.3:21.8:48 wt%	1.2752	-0.3841	0.2992	9.11E+12	-45.2823	7.0789	33.4778	-8.11E+03	3.05E+04	-264.418	7.729
CO_2 in MEA+DEA+MDEA+[Bmim][BF_4] at 29.8:11.7:12.8:45.7 wt%	-5.04E-06	1.23E-06	1.13E+13	21.3223	-184.5196	1.0698	-6.8937	-2.03E+03	-9.96E+04	3.04E+03	7.482
CO_2 in [Bmim][Tf_2N] + MEA at 32.8:67.2 wt%	0.9253	-0.161	0.5339	6.64E+13	886.1966	5.0691	-30.2665	-1.72E+03	-3.49E+05	7.93E+03	8.726
CO_2 in MEA+DEA+[Bmim][Tf_2N] at 32.6:21.3:46.2 wt%	0.1044	-0.0059	0.9994	1.0006	6.71E+03	-5.50E+03	171.4916	-9.20E+03	7.49E+05	-2.02E+04	7.638
CO_2 in MEA+DEA+[Bmim][Tf_2N] at 30.3:10.5:59.3 wt%	0.1303	-0.0134	1.3495	0.659	3.66E+03	6.4368	-39.8356	-6.27E+03	-2.58E+05	8.48E+03	8.186
CO_2 in MEA+MDEA+[Bmim][Tf_2N]] at 29.9:12.6:57.5 wt%	0.0337	-0.0022	-6.1595	2.53E+03	60.8871	1.1021	-0.7117	-2.00E+04	-2.02E+05	7.99E+03	9.109
CO_2 in MEA+MDEA+[Bmim][Tf_2N] at 30.4:19.3:50.3 wt%	-0.0258	0.013	-17.7076	3.27E+03	395.0809	1.062	28.9123	-1.16E+04	-1.04E+04	1.34E+03	9.645
CO_2 in MEA+DEA+MDEA+[Bmim][Tf_2N] at 29.1:10.1:12.5:48.3 wt%	0.1331	-0.021	0.9998	1	-3.12E+04	4.75E+04	8.727	-3.59E+03	1.38E+04	521.2345	8.826

**Root Mean Square Error for each system was calculated neglecting data measured at 0.05 and 0.1 MPa.*

Deviation in model predictions as root mean square errors were calculated using equations E4-1 and E4-2 above. However, it is important to note that model predictions for systems including hybrid solvents at low pressure of 0.05 and 0.1 MPa was highly inaccurate using the proposed models. This can be noted visually upon inspection of Figures 7-18 to 7-23, or by analysing predicted data in Tables A-10 to A-21. The inaccuracy in prediction was 50 to 128% for data measured at pressure of 0.05 and 0.1 MPa, indicating the failure of the combined RK-Posey-Tapperson-Rochelle model to predict the hybrid systems measured in this research at low pressure. Root mean square error as presented in Table 7-5 was thus calculated neglecting data measured at 0.05 and 0.1 MPa. n=15 for the root mean square errors presented.

The combining of alkanolamines and ionic liquids in the absence of water had a profound effect on CO_2 absorption at low pressure, which the RK-Posey-Tapperson-Rochelle model failed to predict, which is likely due to the lack of information on the chemistry of the hybrid systems. CO_2 absorption in conventional alkanolamine solvents diluted with water is usually very low at low pressure due to the high dilution of the alkanolamine with water. Water at the conditions studied in this research would not absorb CO_2 significantly. Moreover, while the ionic liquids in this research achieve good absorption of CO_2, the absorption achieved at low pressure is also very low, when the solvents are pure ionic liquids, as shown in Figures 7-12 to 7-17 above.

The magnitude of absorption achieved in this work at low pressure suggests that absorption is not occurring simply through absorption of CO_2 into the ionic liquids and alkanolamines separately. There has to be significant interaction and alternative reactions occurring between the alkanolamines, ionic liquid and CO_2. Although ionic liquids are known to be stable (Arshad, 2005), the high absorption achieved at low pressure indicate that at the very least, the ionic liquid is facilitating diffusion of CO_2 for the reaction with alkanolamines. Diffusion reactions are possibly occurring with superior kinetics to that of CO_2 with water.

The error achieved and presented in Table 7-5 indicate that even neglecting the data at low pressure, error of up to 9.645% was still noted. Aside from the lack of information regarding the chemistry of the systems, the limitations of the simple Posey-Tapperson-Rochelle model consistent with literature could still be observed.

Consider the systems containing [Bmim][BF_4] ionic liquid. Absorption in samples containing MEA only were less accurately modelled than systems containing MEA and DEA, especially the sample containing 33 wt% MEA with 16.2wt% DEA. This is consistent with literature which in the work of Posey et al. (1996), and Dicko et al. (2010), which showed better predictions for CO_2 in blends of MEA and DEA, than for systems containing only MEA.

The limitations of the model are highlighted for systems containing MDEA, which was the least accurately modelled. 7.4 to 7.7 % error was noted for systems containing MDEA, compared to 5.9 to 6.4 % for systems containing MEA and DEA. As explained in Section 2.4.1.1, the reaction mechanism between CO_2 and primary or secondary amines is the same, but with tertiary amines, the reaction mechanism is different. However, the Posey-Tapperson-Rochelle model does not account for the differing reaction mechanism between CO_2 and MDEA. A single reaction is assumed for all amines. Any combined model that includes the Posey-Tapperson-Rochelle model would not provide accurate prediction for CO_2 absorption in tertiary amines. This is also shown in Osman (2011) for systems containing differing concentrations of MDEA and DEA.

It is also noted that systems containing higher amounts of MDEA were less accurately modelled. The system containing MEA:DEA:MDEA:[Bmim][BF_4] at 29.8:11.7:12.8:45.7 wt% as shown in Figure 7-23 is more accurately modeled than the system containing MEA:MDEA:[Bmim][BF_4] at 30.3:21.8:48 wt% shown in Figure 7-22.

Figures 7-24 to 7-29 below show measured data and model predictions for systems containing [Bmim][Tf_2N].

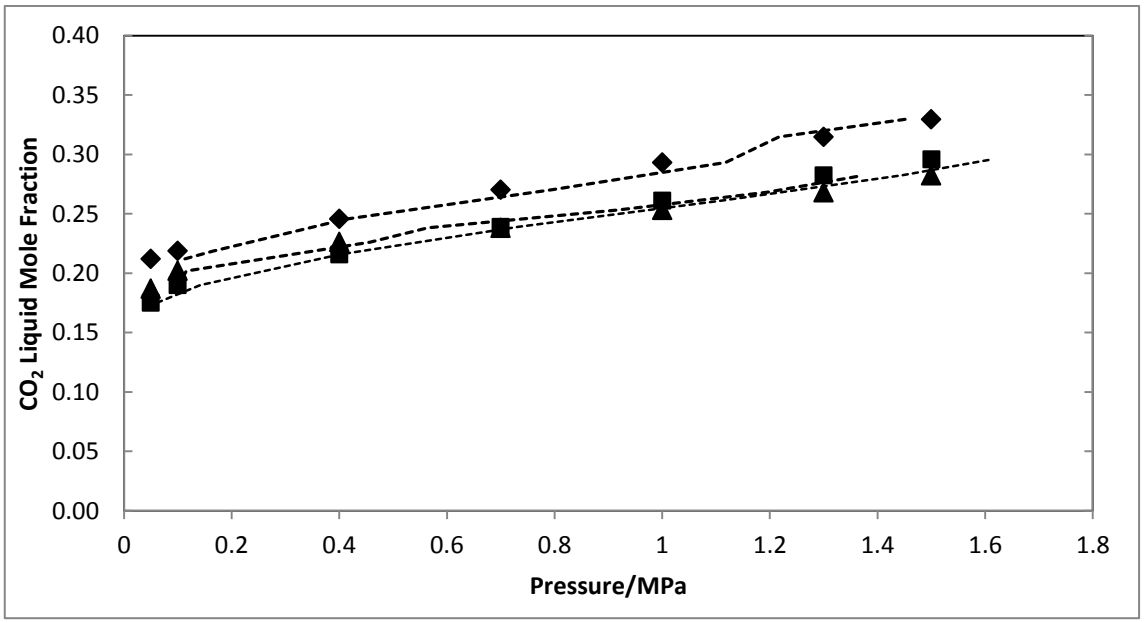

Figure 7-24: Experimental Results together with Posey-Tapperson-Rochelle and RK-EOS predictions for the System of CO_2 in in MEA:[Bmim][Tf_2N] at 32.8:67.2 wt%. ■ – 303.15 K; ▲ – 313.15 K; ♦ - 323.15 K *Dotted lines indicate model predictions

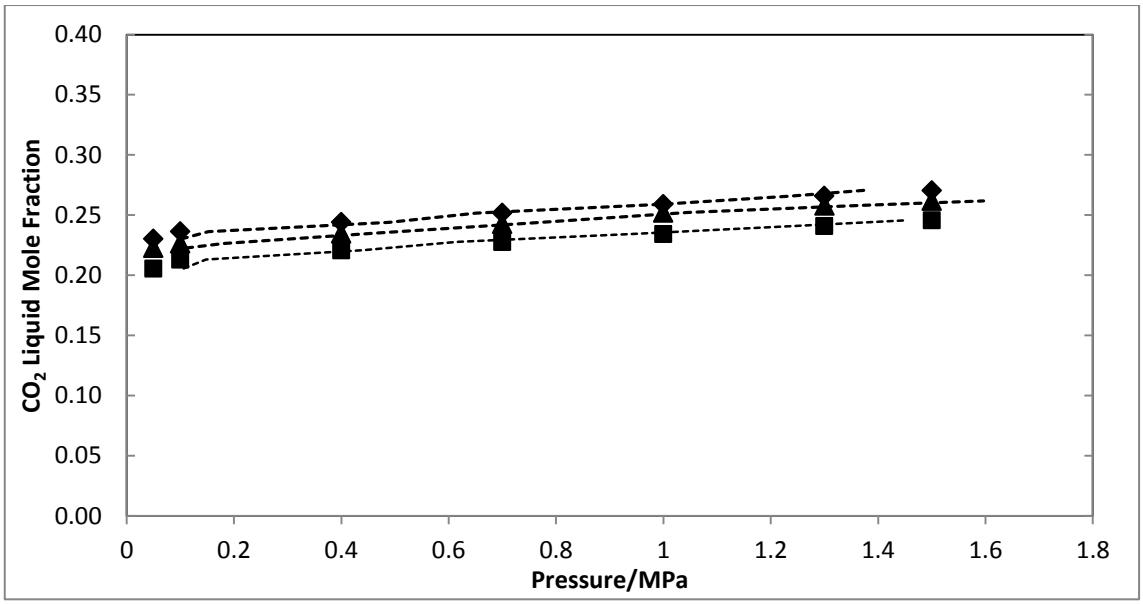

Figure 7-25: Experimental Results together with Posey-Tapperson-Rochelle and RK-EOS predictions for the System of CO_2 in in MEA:DEA:[Bmim][Tf_2N] at 32.6:21.3:46.2 wt%. ■ – 303.15 K; ▲ – 313.15 K; ♦ - 323.15 K *Dotted lines indicate model predictions

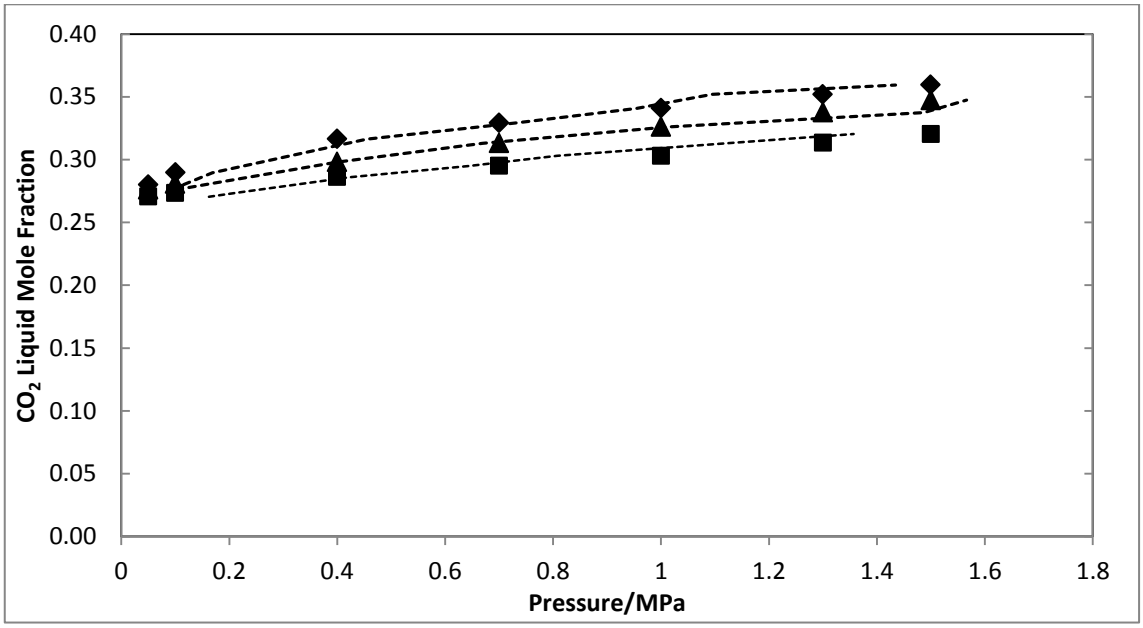

Figure 7-26: Experimental Results together with Posey-Tapperson-Rochelle and RK-EOS predictions for the System of CO_2 in in MEA:DEA:[Bmim][Tf_2N] at 30.3:10.5:59.3 wt%. ■ – 303.15 K; ▲ – 313.15 K; ♦ - 323.15 K *Dotted lines indicate model predictions

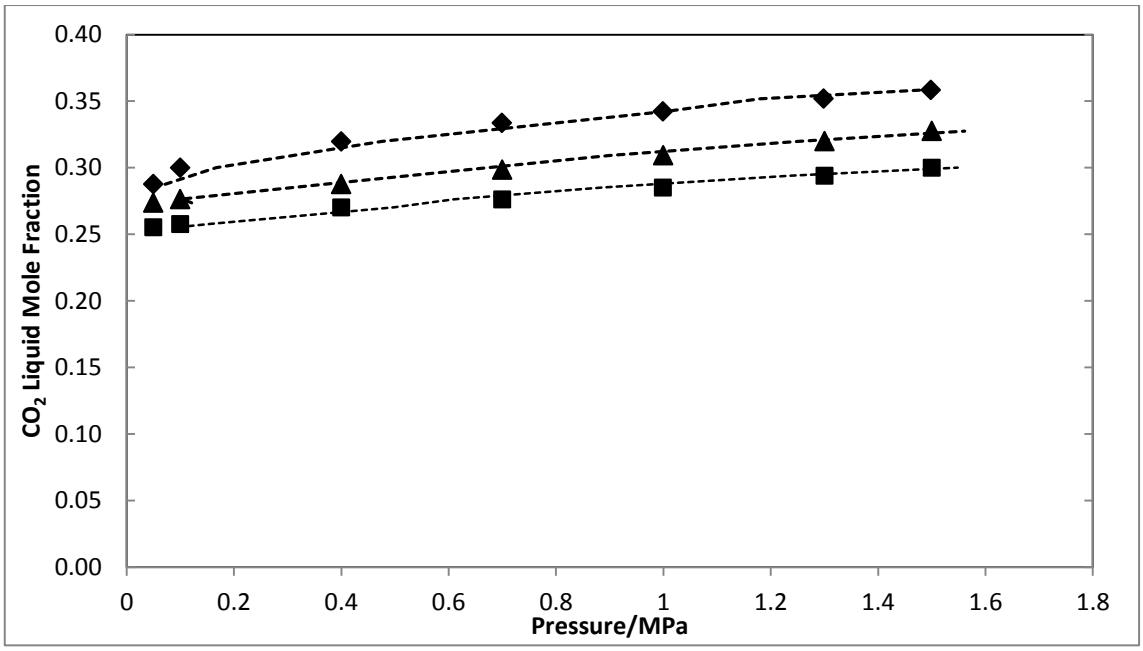

Figure 7-27: Experimental Results together with Posey-Tapperson-Rochelle and RK-EOS predictions for the System of CO_2 in in MEA:MDEA:[Bmim][Tf_2N] at 29.9:12.6:57.5 wt%. ■ – 303.15 K; ▲ – 313.15 K; ♦ - 323.15 K *Dotted lines indicate model predictions

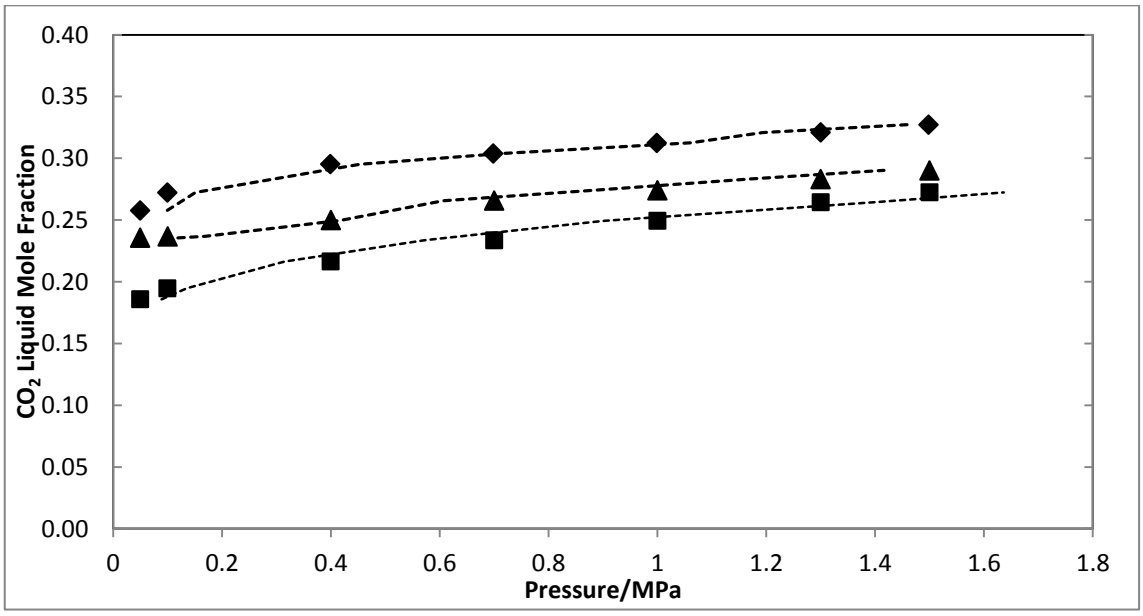

Figure 7-28: Experimental Results together with Posey-Tapperson-Rochelle and RK-EOS predictions for the System of CO_2 in in MEA:MDEA:[Bmim][Tf_2N] at 30.4:19.3:50.3 wt%. ■ – 303.15 K; ▲ – 313.15 K; ♦ - 323.15 K *Dotted lines indicate model predictions

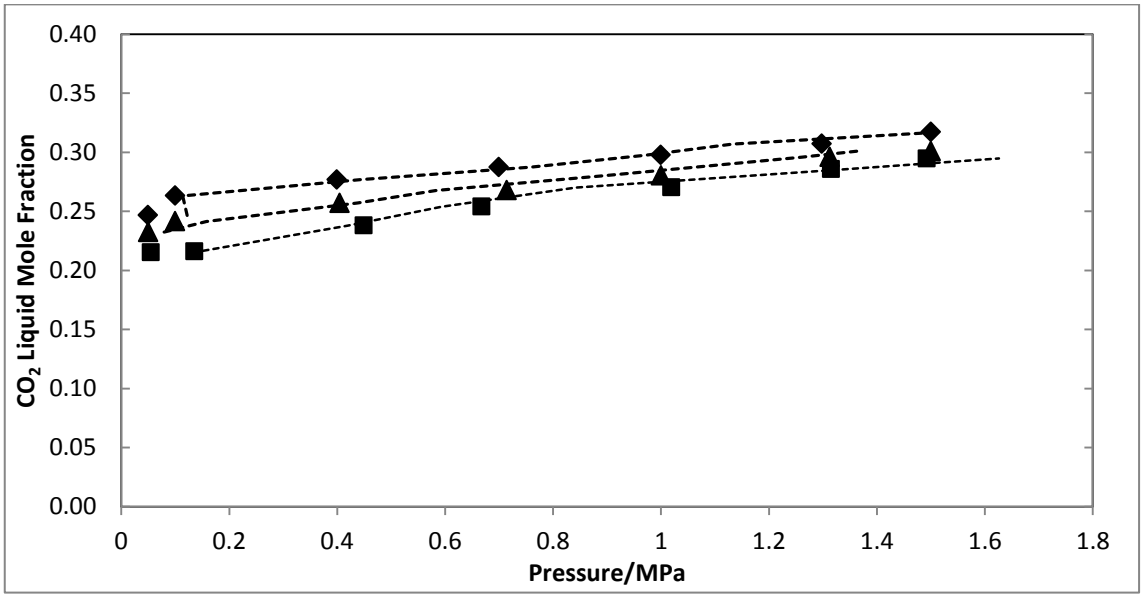

Figure 7-29: Experimental Results together with Posey-Tapperson-Rochelle and RK-EOS predictions for the System of CO_2 in in MEA:DEA:MDEA:[Bmim][Tf_2N] at 29.1:10.1:12.5:48.3 wt%. ■ – 303.15 K; ▲ – 313.15 K; ♦ - 323.15 K *Dotted lines indicate model predictions

Root mean square error is also computed and presented in Table 7-5. It is observable that systems with [Bmim][Tf_2N] were less accurately modelled than systems containing [Bmim][BF_4]. The accuracy regarding the effect of different alkanolamine compositions was found to be consistent with systems containing [Bmim][BF_4]. Systems containing MDEA were again less accurately predicted than systems without MDEA, with systems containing MEA and DEA blends being the most accurately predicted. Low pressure data of 0.05 and 0.1 MPa were again omitted due to highly erroneous predictions, which can be noted in Tables A-10 to A-21 of Appendix A.

A final observation is the high magnitude of the C and D parameters for the Posey-Tapperson-Rochelle model, indicating that the system is highly sensitive to alkanolamine concentration. This is contrast with results achieved by Osman (2011) which recorded very high values for the B parameter, which indicated very high temperature sensitivity for systems of MDEA:DEA:H_2O at various concentrations and at high temperatures of 383.15 and 410.15 K. This difference is possibly due to the alkanolamines being diluted with the ionic liquid instead of water.

The combined model investigated in this work, while sufficient to provide an initial estimate of CO_2 absorption in hybrid solvents in moderate to high pressure and moderate temperature,

would not suffice for use in process simulation. The model could be used to regress data over a smaller temperature range to provide a more accurate correlation. Isothermal regression can provide the most accurate results.

It is imperative however that the chemistry of such hybrid systems be better understood in order to determine accurate reaction mechanisms upon which reactions kinetics can be drawn. It is thus recommended that the FTIR Probe apparatus be modified as explained in Appendix F and Chapter 10 in order to grant greater insight and more accurate modelling of absorption data for process simulation.

CHAPTER 8: ASPEN SIMULATION OF CO_2 CAPTURE USING HYBRID AND CONVENTIONAL ALKANOLAMINE SOLVENTS

It is useful to simulate the process of CO_2 absorption using hybrid solvents in order to obtain at least a simple indication of the industrial implications of their use over conventional alkanolamine solvents.

While there are numerous sources in literature simulating absorption of CO_2 in conventional alkanolamines, relatively little study has been pursued in the simulation of CO_2 absorption using ionic liquids, particularly due to the lack of property data for most ionic liquids. Chang et al. (2007) simulated absorption using MEA and DGA in Aspen. Seven reactions were assumed to occur and the route for optimisation was determined. The RK-NRTL base method was used for vapour and liquid phase predictions. Different configurations of recycle between absorber and stripping columns were analysed. Mores et al. (2012) also conducted simulations of CO_2 absorption in MEA at 30 wt% concentration, using a packed absorber. The effect of reboiler temperature on CO_2 loading was studied.

The use of Aspen for data regression with systems containing alkanolamine solvents, and pure ionic liquid solvents, has been well practised by numerous sources. CO_2 and H_2S solubility in MDEA was modelled using the PC-SAFT model in Aspen by Zhang and Chen (2011). Data regression using the Peng-Robinson equation of state for CO_2 in ionic liquids containing the $[Tf_2N]$ anion, was achieved by Yazdizadeh et al. (2011). Similar approaches were achieved by Andreu and Vega (2007).

In this work, absorption was simulated using a Radfrac column model in Aspen Plus V8.0. Section 7.7 explains the success of hybrid solvents in achieving higher CO_2 absorption than that of pure ionic liquids and conventional amine solvents, through analysing measured absorption data. A hybrid solvent containing the ionic liquid $[Bmim][BF_4]$ was simulated for CO_2 absorption using Aspen Plus V.8.0. The lack of properties available for $[Bmim][Tf_2N]$ made simulation using this ionic liquid highly erroneous and incomplete.

A simple simulation was executed to provide a comparison of the absorption of CO_2 using a conventional MEA:H_2O solvent at 30:70% (by mass), to that of CO_2 absorption using MEA:DEA:$[Bmim][BF_4]$ at 31.8:12.1:56.1 wt%. This composition was tested as it achieved the highest CO_2 absorption of all hybrid solvents containing $[Bmim][BF_4]$, as shown by measurements.

Figure 8-1 below illustrates a simple absorption process without any recycle, which was used to benchmark the above mentioned solvent against the conventional amine solvent. The purpose of the simulation was to investigate the potential industrial implications of using hybrid solvents over conventional amine solvents. The comparison was made in terms of the extent of absorption achieved for CO_2 and other gases in the hybrid solvent and conventional amine solvent.

For both simulations, the Electrolyte Non-Random Two-Liquid-Redlich Kwong (ENRTL-RK) base method was used, which utilised the Redlich-Kwong equation of state to determine vapour phase properties, Henry's law for solubility of supercritical gases, and the unsymmetrical Electrolyte NRTL model for handling reaction mechanisms involving zwitterion formation as described in Section 2.4.1.1. Details regarding binary interaction parameters and expressions for Excess Gibbs energy (G^E) are available in the work of Osman (2011), in which the simulation of CO_2 absorption in blends of DEA and MDEA was successfully achieved.

Absorption data from Table A-12 of Appendix A were regressed and remaining properties were estimated for the hybrid and conventional solvent. The absorber and stripper contained 20 stages. The absorber contained bubble-cap trays, 1 m in diameter and 1m height for each stage. The stripper contained 15 mm ceramic Raschig rings as packing. The diameter of each stage was 1 m and the height of each stage was 1 m.

Flue gas was also kept consistent for both simulations. Flue gas occurred at 333.15 K and 0.17 MPa. Flue gas composition is available in Tables 8-1 and 8-3 below. Trace compounds commonly present in flue gas were neglected in order to simplify the simulation for the intended comparison. Both solvents were available at 303.15 K. After absorption, in each case the loaded solvent was heated to 363.15 K. The stripping column was operated at 0.1 MPa.

The following reversible reactions were assumed and applied from using the Aspen electrolyte database for the conventional amine and hybrid solvent processes:

$$HCO_3^- \leftrightarrow H^+ + CO_3^{2-} \quad \text{(R8-1)}$$

$$H_2O + CO_2 \leftrightarrow HCO_3^- + H^+ \quad \text{(R8-2)}$$

$$H_2O \leftrightarrow OH^- + H^+ \quad \text{(R8-3)}$$

$$MEACOO^- + H_2O \leftrightarrow HCO_3^- + MEA \quad \text{(R8-4)}$$

$$MEA^+ \leftrightarrow MEA + H^+ \quad \text{(R8-5)}$$

For the Hybrid solvent process, the following additional reactions were assumed:

$DEA^{+} \leftrightarrow H^{+} + DEA$……(R8-6)

$DEACOO^{-} + H_2O \leftrightarrow DEA + HCO_3^{-}$……(R8-7)

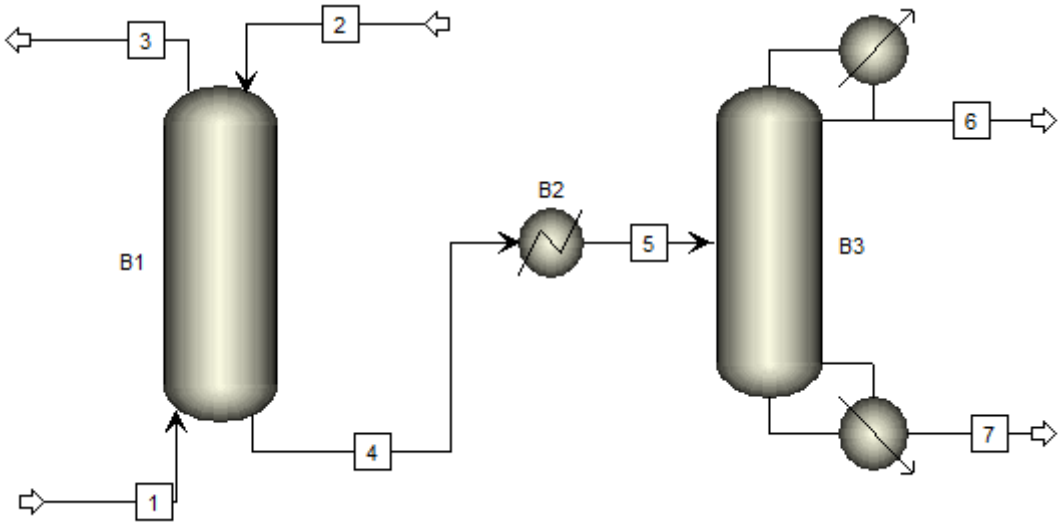

Stream	Description	Stream	Description
1	Flue gas	5	Loaded hot solvent
2	Solvent	6	CO_2 rich stream
3	Stack gas	7	Unloaded solvent
4	Loaded cold solvent		
Block	**Description**		
B1	Absorber		
B2	Heat Exchanger		
B3	Regenerator		

Figure 8-1: Once-Through Absorption and Regeneration Process Simulated using Aspen.

The Aspen simulation for the conventional amine absorption process is available electronically in the attached CD under the file name "MEASimulationSimple2.apwz", while the hybrid process is available under the file name "PhD_Hybrid_RegressionSimulation.apwz". Tables 8-1 and 8-3 below contain results for each stream for the conventional amine process, using MEA:H_2O at 30:70 wt%, and hybrid solvent process, using MEA:DEA:[Bmim][BF_4] at 31.8:12.1:56.1 wt%, respectively. Tables 8-2 and 8-4 below contain information pertaining to absorber and regenerator heat duties for the conventional and hybrid solvent processes respectively.

Table 8-1: Stream Results for Conventional Amine Absorption using the Solvent MEA:H_2O at 30:70 wt%

	Stream						
	1	2	3	4	5	6	7
Temperature/K	333.15	303.15	303.15	326.25	363.15	370.35	376.25
Pressure/MPa	0.17	0.17	0.17	0.17	0.1	0.1	0.1
Vapour Frac	0.725	0	1	0	< 0.001	0	0
Mole Flow/kmol·hr^{-1}	100	200	65.3	234.7	234.679	9.888	224.811
Mass Flow/kg·hr^{-1}	2607.58	4569.63	1981.98	5195.24	5195.236	178.717	5016.519
Volume Flow/m^3·hr^{-1}	1179.32	4.54	966.62	5.26	5.562	0.18	5.297
Mole Flow kmol/hr							
MEA	-	22.39	0.001	22.44	22.368	0.001	22.441
H_2O	36.11	177.51	1.432	212.234	212.2	9.864	202.37
CO_2	9.888	-	9.868	0.018	trace	0.02	trace
O_2	2.282	-	2.282	< 0.001	< 0.001	< 0.001	trace
N_2	51.721	-	51.718	0.003	0.003	0.003	trace
MEA^+	-	0.051	-	trace	0.054	trace	trace
H^+	< 0.001	trace	-	0.002	trace	trace	trace
$MEACOO^-$	-	-	-	0.002	0.02	trace	trace
OH^-	trace	0.051	-	trace	0.034	trace	trace
HCO_3^-	< 0.001	-	-	< 0.001	< 0.001	trace	trace
CO_3^{2-}	trace	-	-	trace	< 0.001	trace	trace

Table 8-2: Absorber, Heat Exchanger and Regenerator Results for Conventional Amine Absorption using the Solvent MEA:H_2O at 30:70 wt%

	Top of Absorber (B1)	Top of Regenerator (B3)
Temperature/K	303.16	380.53
Distillate rate/kmol·hr^{-1}	65.30	9.888
Heat duty/kW		-311.78
Reflux rate/kmol·hr^{-1}		9.888
Reflux ratio		1
	Bottom of Absorber (B1)	Bottom of Regenerator (B3)
Temperature/K	326.28	376.15
Bottoms rate/kmol·hr^{-1}	234.70	224.81
Heat duty/kW		339.88
Boilup rate/kmol·hr^{-1}		29.73
Boilup ratio		0.13
Heat Exchanger (B2) Duty/kW	200.07	

Table 8-3: Stream Results for Absorption using the Hybrid Solvent MEA:DEA:[Bmim][BF_4] at 31.8:12.1:56.1 wt%.

	Streams						
	1	2	3	4	5	6	7
Temperature/K	333.15	303.15	298.05	292.15	363.15	291.25	363.15
Pressure/MPa	0.17	0.17	0.17	0.17	0.1	0.1	0.1
Vapour Fraction	0.725	0	1	0	0.117	0	0
Mole Flow/kmol·hr^{-1}	100	100	62.98	162.42	159.048	10.747	148.1
Mass Flow/kg·hr^{-1}	2607.579	11313.59	2742.592	10984.81	10984.81	448.47	10351.7
Volume Flow/m^3·hr^{-1}	1179.342	10.803	667.897	< 0.001	501.618	1.116	6.14
Mole Flow kmol/hr							
MEA	-	58.898	2.341	2.293	0.001	-	0.001
DEA	-	13.021	2.417	trace	trace	-	-
CO_2	9.888	-	0.214	trace	10.361	9.767	0.393
O_2	2.282	-	2.208	0.074	0.074	0.07	0.004
N_2	51.721	-	51.161	0.001	0.001	0.001	trace
H_2O	36.11	-	0.97	trace	36.743	0.909	35.834
[Bmim][BF_4]	-	28.081	3.67	24.411	24.411	trace	24.411
MEA^+	-	-	-	13.73	16.519	trace	16.519
H^+	< 0.001	-	-	13.73	0.001	< 0.001	0.001
$MEACOO^-$	-	-	-	0.497	trace	trace	trace
OH^-	trace	-	-	13.73	trace	-	trace
HCO_3^-	< 0.001	-	-	23.014	< 0.001	< 0.001	< 0.001
CO_3^{2-}	trace	-	-	trace	trace	-	trace
DEA^+	-	-	-	57.207	44.057	-	44.057
$DEACOO^-$	-	-	-	13.73	26.88	-	26.88

Table 8-4: Absorber, Heat Exchanger and Regenerator Results for Absorption using the Hybrid Solvent MEA:DEA:[Bmim][BF_4] at 31.8:12.1:56.1 wt%.

	Top of Absorber (B1)	Top of Regenerator (B3)
Temperature/K	298.10	338.79
Distillate rate/kmol·hr^{-1}	56.48	9.89
Heat duty/kW		-1858.23
Reflux rate/kmol·hr^{-1}		9.89
Reflux ratio		1
	Bottom of Absorber (B1)	Bottom of Regenerator (B3)
Temperature/K	274.12	454.84
Bottoms rate/kmol·hr^{-1}	143.52	138.22
Heat duty/kW		4783.07
Boilup rate/kmol·hr^{-1}		23.40
Boilup ratio		0.17
Heat Exchanger (B2) Duty/kW	368.877	

Upon analysis of Tables 8-1 and 8-3 above, it is immediately observed that significantly higher CO_2 absorption occurred in the hybrid solvent process than in the conventional amine solvent process. The conventional amine solvent process achieved particularly poor CO_2 absorption due to the low operating pressure of the process. This reinforces the thermodynamic analysis conducted by Mamun (2005), Figueroa et al. (2007) and numerous other literature sources, that significant CO_2 absorption in conventional amine solvents requires very high pressure. In this study, 100 kmol/hr of solvent was fed to the absorber for the hybrid solvent process but 200 kmol/hr of solvent was fed in the case of the conventional amine solvent process. Yet, even despite doubling the molar flow of conventional amine solvent, the low operating pressure still greatly limited the absorption of CO_2. Only 2.02% of CO_2 was absorbed due to low flue gas pressure.

The hybrid solvent on the other hand was highly successful in absorbing CO_2. 97.8% of CO_2 in the flue gas was absorbed using the 100 kmol/hr hybrid solvent. This is due to the hybrid solvent's ability to effectively absorb CO_2 at low pressure. Figure 7-12 shows that the hybrid solvent studied in this simulation is capable of absorbing over 20 moles of CO_2 per 100 moles of solvent at the stated operating pressure. The simulation reflects this observation as well.

A discouraging result regarding the hybrid solvent is that 3% of O_2 gas was also absorbed from the flue gas. This is consistent with calculations of entropy of absorption found in Table E-1 of Appendix E, with shows entropy of absorption to be negative for all ionic liquids. This implies that O_2 absorption in the ionic liquid component of the hybrid solvent is not negligible, and the simulation confirms this.

By comparison no O_2 was absorbed by the conventional amine solvent. This result can be problematic when trying to isolate pure CO_2 for sequestration.

A potentially more problematic result was that the water vapour in the flue gas was also absorbed. This occurred for both processes. 3.2% of oxygen and 97% of H_2O was absorbed from the flue gas by the hybrid solvent. The conventional solvent did not absorb significant amounts of O_2 but absorbed 96% of H_2O from the flue gas. This is possibly due to the reaction mechanism between CO_2, MEA and DEA as shown in reactions R8-2, R8-3, R8-4 and R8-7 above, which includes dissociation reactions with water.

As Table 8-1 and 8-3 show, water from flue gas was absorbed and either existed as water in the loaded solvent in stream 4, or participated in dissociation reactions. In the case of the conventional amine solvent process, water existed as H_2O, because the solvent contains water anyway. But in the case of the hybrid solvent process, water was available only from the flue

gas and all of it participated in the reaction mechanism or was dissociated to H^+ and OH^- ions. Water is present in the CO_2 rich stream 6, reducing its purity.

An analysis of desorption streams 5, 6, and 7 in Table 8-1 and 8-3 show that the absorbed O_2 and most of the absorbed water was never recovered, which poses a problem for solvent recycling. If optimisation cannot rectify this problem, then it implies that ultimately the solvent will have to undergo further processing before being recycled to the absorber. Alternatively, a known hydrophobic ionic liquid may be combined instead of [Bmim][BF_4].

An analysis of Tables 8-2 and 8-4 show that the heat exchanger duty required to increase the solvent temperature for desorption is higher in the case of the hybrid solvent process. This is expected since the high molar mass of the ionic liquid resulted in comparatively high mass flows for a 100 kmol/hr solvent supply, in comparison to the conventional amine solvent. Mass flow of the hybrid solvent was over twice that of the conventional amine solvent mass flow. Despite the high mass flows, the duty required is less than twice that of the conventional amine solvent. Heat capacity of the ionic liquid was obtained from Arshad (2009).

Reboiler duty in the regenerator (B3) was perceived to be very high in the case of the hybrid solvent process, in comparison to the amine solvent process. This is due not only to the high mass flows of the hybrid solvent, but also the negligible vapour pressure of the ionic liquid results in the simulation of boilup in the regenerator being very difficult and requiring very large amounts of energy. The calculation of reboiler in a conventional setup of a distillation column is thus futile, since in practice it is well known that trying to boilup the ionic liquid would more likely decompose the ionic liquid rather than vapourise it. The regenerator process can rather be optimised with pump-around streams instead of a boil up stream to maintain good contact and ensure efficient desorption.

The limited database of properties for ionic liquids, including [Bmim][BF_4] resulted in the simulation reporting some errors. Ionic liquid viscosity, density and heat capacity was inserted manually into the simulation using information from Baltus et al. (2004) and Arshad (2009). Getting the ionic liquid structure correct on the Aspen simulation was difficult due to the structure of the ionic liquid being that of an anion with a cation. This resulted in charge imbalances especially when simulating the absorber and regenerator.

The negligible vapour pressure of the ionic liquid resulted in column convergence problems in the regenerator, and a relative error in mass balance of up to 1% of the feed stream for the absorber and 1.7% for the regenerator. Any further optimisation and the simulation of hybrid solvents containing [Bmim][Tf_2N] would require more comprehensive property databases. It is

thus recommended that simulation software and databases be upgraded to cater for ionic liquids in greater depth.

Despite these challenges, the most conclusive and important observation achieved by performing the simulation, was that the hybrid solvent achieved superior CO_2 absorption than the conventional amine solvent at a low pressure of 0.17 MPa. At the current flue gas temperature and pressure, the process would have to be significantly optimised for the conventional amine solvent to achieve the CO_2 absorption achieved by the hybrid solvent. This would entail significantly more stages and higher molar flows, with ultimately substantially higher mass flows. At current flue gas conditions, a definite increase in the scale of the conventional amine process will be necessary. A 4563.69 kg/hr mass flow rate of conventional amine solvent was used and absorbed 2.02% (by mole) of CO_2 from the flue gas. A 11313.59 kg/hr flow rate of hybrid solvent was used and it absorbed 97.8% (by mole) of CO_2 from the flue gas. If the flue gas pressure can be increased marginally or the flue gas temperature decreased, or if different packing and other mass contacting methods be investigated, potentially less hybrid solvent can be used to absorb higher amounts of CO_2, with a potential reduction in the scale of the process and also saving in material of construction due to operation at low pressure.

The addition of recycle loops between the regenerator and the absorber would ultimately be necessary to conserve the solvent. This is especially vital in the case of the ionic liquid, which is expected to be of higher cost than the amine solvent. The simulation neglects the circulation energy required. Further study would be necessary to ensure the economic advantage of utilising the hybrid solvent over the conventional solvent.

CHAPTER 9: CONCLUSIONS

Five CO_2 capture techniques were found to be abundantly researched, which have at least reached the pilot plant phase of research. Four new techniques were also found, which are currently researched independently by various institutions. The study found gas absorption using solvents to be the most developed and well understood CO_2 capture technique. This technique was found to currently have the most potential and likelihood for implementation in industry in the near future. The challenges of current CO_2 absorption using solvents were found to be low CO_2 absorption capacity, low CO_2 absorption rate, high regeneration energy requirements, and high corrosivity of conventional alkanolamine solvents, thereby requiring dilution with water. Ionic liquids were found to possess great potential in improving the technique of CO_2 absorption and were thus investigated experimentally in their pure state and in combination with conventional alkanolamine solvents.

Gravimetric analysis was found to be the most suitable measurement technique to investigate gas absorption in ionic liquids and hybrid solvents. The solvents that were studied were of very low volatility, which made gravimetric analysis applicable. Gravimetric analysis was advantageous since it utilised very low amounts of solvent (80 to 100 mg), was automated using software-controlled equipment, and produced relatively quick measurements, and at low cost, due to the small quantities of solvents loaded into the apparatus. Equilibrium mole fractions were measured at 303.15 K to 323.15 K, and pressure of 0.05 to 1.5 MPa.

Of the four ionic liquids studied, [MOA][Tf_2N] achieved the highest CO_2 absorption for the measured conditions, while [Bmim][$MeSO_4$] achieved the highest O_2 absorption and lowest CO_2 absorption. [Bmim][Tf_2N] and [Bmim][BF_4] were found to be the most CO_2 selective ionic liquids. While [MOA][Tf_2N] achieved the highest CO_2 absorption, it also achieved high O_2 absorption, resulting in lower CO_2 selectivity. Furthermore, it was proven that higher pressure, lower temperature, increased cation chain length and increased fluorination of the ionic liquid, facilitated higher gas absorption capacity. The use of imidazolium cations and fluorinated anions was found to increase CO_2 selectivity.

Due to their high CO_2 selectivity, [Bmim][BF_4] and [Bmim][Tf_2N] were combined with MEA, DEA, and MDEA at different compositions to create 14 hybrid solvents of varying ionic liquid and alkanolamine composition, and investigated for their CO_2 absorption capacity. Hybrid solvents achieved superior CO_2 absorption over conventional alkanolamine solvents as well as pure ionic liquids studied in this work and in other sources in the literature. Solvents containing [Bmim][Tf_2N] achieved higher CO_2 absorption than solvents containing [Bmim][BF_4], a trend consistent with pure ionic liquids of increasing anion fluorination.

Of all the hybrid solvents containing [Bmim][BF_4], the solvent containing MEA:DEA:[Bmim][BF_4] at 31.8:12.1:56.1 wt% achieved the highest CO_2 absorption. The solvent containing MEA:DEA:[Bmim][Tf_2N] at 30.18:10.53:59.2 wt% achieved the highest CO_2 absorption of all solvents studied. It was found that increasing the DEA and MDEA concentration above 10 wt% achieved lower CO_2 absorption. Enthalpy and entropy of absorption calculations showed that CO_2 absorption in solvents containing MDEA was found to decrease more significantly with increasing temperature.

P-T-x data for CO_2 and O_2 in all four ionic liquids were modelled using the RK-EOS. The deviation of model predictions was 0.04% of measured data, indicating a very good fit. While systems containing CO_2 could be regressed easily for all isotherms, the high temperature sensitivity of O_2 absorption required isothermal regression to be conducted. By comparison, modelling of CO_2 absorption in hybrid solvents was found to be challenging. The RK-Posey-Tapperson-Rochelle Model failed to model CO_2 absorption at pressure for systems of 0.1 MPa and lower, achieving inaccuracies in CO_2 partial pressure of 50 to 128% of measured data. Inaccuracy in model predictions, when neglecting points at low pressure, amount to 5.88-9.65% of measured CO_2 partial pressure, for pressures of 0.4 to 1.5 MPa. As with pure ionic liquids, hybrid systems containing [Bmim][Tf_2N] were less accurately modelled than systems containing [Bmim][BF_4]. Systems containing MEA and DEA were the most accurately modelled of all hybrid systems studied with a root mean square error of 5.878% for systems containing [Bmim][BF_4] and 7.638 for systems containing [Bmim][Tf_2N]. Systems containing only MEA as the alkanolamine component were less accurately modelled than systems containing MEA and DEA, while systems containing MDEA were the least accurately modelled.

Process simulations for CO_2 absorption and desorption were conducted in the engineering program Aspen Plus V. 8.0, for a conventional solvent containing MEA:H_2O at 30:70 wt% and for a hybrid solvent containing MEA:DEA:[Bmim][BF_4] at 31.8:12.1:56.1 wt%. It was found that when keeping flue gas conditions and process design parameters constant, the hybrid solvent achieved very high CO_2 absorption, capturing 97.8% of CO_2 from the flue gas. By contrast the low operating pressure of the process resulted in the conventional solvent only capturing 2.02% of CO_2 from the flue gas, indicating a very high dependence of absorption on increased system pressure.

CO_2 selectivity of both solvents was found to be poor. The hybrid solvent absorbed 3.2% of oxygen from the flue gas, and 97% of H_2O from the flue gas. The conventional solvent did not absorb significant amounts of O_2 but absorbed 96% of H_2O from the flue gas. Additionally, heat

exchanger and reboiler duties were significantly higher for the process using the hybrid solvent. Despite the above discouraging results, the high CO_2 absorption achieved by the hybrid solvent suggested that low pressure CO_2 capture is possible and the scale of the CO_2 capture process can be greatly reduced in comparison to processes utilising the conventional alkanolamine solvent.

CHAPTER 10: RECOMMENDATIONS

- It would be beneficial to conduct equilibrium absorption measurements at flue gas conditions close to that produced by IGCC power plants. As Section 2.1.2 showed, flue gas from IGCC power plants are emitted at conditions that are more favourable to efficient CO_2 capture. This may result in the solvents studied in this work achieving higher CO_2 absorption.
- In this work, relatively common ionic liquids containing [Bmim] cations, and $[Tf_2N]$ and $[BF_4]$ anions were tested for CO_2 absorption in their pure state and as hybrid solvents. However, there is great potential to expand the study of hybrid solvents by considering ionic liquids with higher cation chain lengths and more highly fluorinated anions, which may achieve higher CO_2 absorption when blended into a hybrid solvent with alkanolamines. More exotic TSILs may be investigated as well.
- The FTIR Probe apparatus at its current configuration was unsuccessful in achieving information regarding the chemistry of alkanolamine-ionic liquid-CO_2 systems, thereby disabling the application of more complex models such as the Deshmukh-Mather and Elec-NRTL models which might have provided more accurate predictions of CO_2 partial pressure in the hybrid systems. It is thus not only recommended, but imperative that this apparatus be upgraded to achieve Mid-infrared measurement as described in Section F2 of Appendix F. ATR or a high pressure circulating fluid cell accessories may be used to enable mid-infrared measurement, which will ensure composition analysis and identification of compounds associated with the reaction mechanism between undiluted hybrid solvents and CO_2.
- The lack of availability of property data for many ionic liquids posed an obstacle for accurate simulation of absorption processes, resulting in many errors in the simulation that would be redundant in practice. The main error in simulating CO_2 capture using solvents stemmed from the negligible vapour pressure of ionic liquids, which resulted in erroneous simulation of the stripping column. It is recommended that simulation software and databases be upgraded to cater for this relatively new class of chemicals called ionic liquids.
- This work focussed on the thermodynamic analysis of the CO_2 absorption capacity of various solvents. In order to provide a complete picture of CO_2 absorption, it is recommended that a kinetic study be conducted in order to ascertain the absorption rate of CO_2 in these solvents. Such an investigation would require more in-depth data collection and analysis using the gravimetric analyser. Such data would also provide for more accurate simulations of CO_2 capture using hybrid solvents.
- Simulation results of absorption using solvents can be improved by investigating the effect of different column heights, packing, heat integration and solvent recycle.

CHAPTER 11: REFERENCES

1. Abanades C., 2008, "Calcium sorbent cycling for simultaneous CO_2 capture and clinker production", Spanish National Research Council, National Coal Institute, Spain. Accessed 1/8/2011. http://gcep.stanford.edu/pdfs/2RK4ZjKBF2f71uM4uriP9g/Carlos_Abanades_Escritorio_CaOloopingStanford.pdf
2. Abdul-Sada A. K., Elaiwi A. E., Greenway A. M., Seddon K. R., 1997, "Letter: Evidence for the clustering of substituted imidazolium salts via hydrogen bonding under the conditions of fast atom bombardment mass spectrometry". European Journal of Mass Spectrometry, vol 3, pg. 245-247.
3. L'Agence de l'Environnement et de la Maîtrise de l'Energie (ADEME), 2010, "Panorama des voies de valorisation du CO_2", l'Agence de l'Environnement et de la Maîtrise de l'Energie (ADEME), France. Report made available by Dr. Christophe Coquelet of Mines-Paristech, France.
4. L'Agence de l'Environnement et de la Maîtrise de l'Energie (ADEME), 2007, "CO_2 capture and storage in the subsurface: A technological pathway for combating climate change", Co-edited and published by Charbonnages de France, the Paris School of Mines and BRGM, France. ISBN: 978-2-7159-2438
5. Alvarez, V. H.; Valderrama, J. O., 2004, "A modified Lydersen-Joback-Reid method to estimate the critical properties of biomolecules". Alimentaria, 254, 55–66.
6. Anderson J.L., Dixon J.K., Muldoon M.J., Brennecke J.F., and Maginn E.J., 2007, "Ionic liquids as CO_2 capture media", University of Notre Dame Energy Centre, Notre Dame, USA. Accessed 7/3/2011. www.chem.queensu.ca/Conferences/CHEMRAWN/Anderson_54.ppt
7. Anderson J.L., Dixon J.K., Brennecke J.F., 2007, "Solubility of CO_2, CH_4, C_2H_6,C_2H_4, O_2, and N_2 in 1-hexyl-3-methylpyridinium bis(trifluoromethylsulfonyl)imide: Comparison to other ionic liquids", Acc. Chem. Res., Vol. 40, Pg. 1208–1216.
8. Andreu J.S., Vega R.F., 2007, "Modeling the Solubility Behavior of CO_2, H_2, and Xe in [Cn-mim][Tf_2N] Ionic Liquids", J. Phys. Chem. B,112, 15398–15406.
9. Archane, L. Gicquel, E. Provost, W. Fu¨ rst, 2008 "Effect of methanol addition on water–CO_2–diethanolamine system: Influence on CO_2 solubility and on liquid phase speciation", Chem. Eng. Res. Des. 86, 592–599
10. Arshad M.W., 2009, "CO_2 capture using Ionic Liquids", Department of Chemical and Biochemical Engineering, Technical University of Denmark. Accessed 28/3/2011. http://docs.google.com/viewer?a=v&q=cache:uF9eKE4Xeg0J:orbit.dtu.dk/getResource%3F

recordId%3D240068%26objectId%3D1%26versionId%3D1+Non+fluorinated+Ionic+Liquids+%2B+CO2+capture&hl=en&pid=bl&srcid=ADGEESg9aXin_GbLKmM6LyI0ZwZISYo9jdm6WoHXOZShMxVHKwcdqJ9348xr_ET4DibAHbAcF09sbUcIgJSDpEtHdGpt8LdGo4lv02MgmONX0xD9Dj8r9vXvxaAYZI1cbkOF3ovX0axf&sig=AHIEtbRXq7UJoi74_T-CVBR3d5zuDcG5EQ

11. Austgen D.M., Rochelle G.T., Chen C.C., 1991, "Model of vapour-liquid equilibria for aqueous acid gas-alkanolamine systems. 2. Representation of H_2S and CO_2 solubility in aqueous MDEA and CO_2 solubility in aqueous mixtures of MDEA with MEA or DEA", Industrial and Engineering Chemistry Research, 30, pg 543-555
12. Austgen D.M., Rochelle G.T., Peng X., Chen C.C., 1989, "Model of vapor-liquid equilibria for aqueous acid gas-alkanolamine systems using the electrolyte-NRTL equation". Ind. Eng. Chem. Res, vol 28, pg. 1060-1073
13. Austgen D.M., Rochelle G.T., Chen C.C., 1991, "Model of vapour-liquid equilibria for aqueous acid gas-alkanolamine systems. 2. Representation of H_2S and CO_2 solubility in aqueous MDEA and CO_2 solubility in aqueous mixtures of MDEA with MEA or DEA", Industrial and Engineering Chemistry Research, 30, pg 543-555
14. Baltus R.E., Culbertson B.H., Dai S., Luo H., and DePaoli D.W., 2004, "Low-pressure solubility of carbon dioxide in room-temperature ionic liquids measured with a quartz crystal microbalance", J. Phys. Chem. B, Vol. 108, pg. 721-727.
15. Baltusa R.E., Counceb R.M., Culbertsonb B.H., Luoc H., DePaolic D.W., Daid S., Duckworthd D.C., 2005, "Examination of the potential of ionic liquids for gas separations", Separation Science and Technology, Vol. 40, pg. 525-541.
16. Bara J.E., Lessmann S., Gabriel C.J., Hatakeyama E.S., Noble R.D., and Gin D.L., 2007, "Synthesis and Performance of Polymerizable Room-Temperature Ionic Liquids as Gas Separation Membranes", Ind. Eng. Chem. Res., Vol. 46, pg. 5397-5404
17. Bara, J. E.; Kaminski, A. K.; Noble, R. D.; Gin, D. L., 2007, " Influence of Nanostructure on Light Gas Separations in Cross-Linked Lyotropic Liquid Crystal Membranes". J. Membr. Sci., Vol. 288, pg. 13-19.
18. Bara G.E., Camper D.E., Gin D.L., and Noble R.D., 2010, "Room temperature ionic liquids and composite materials: Platform technologies for CO_2 capture". Accounts of Chemical Research, Vol. 53 Pg., 152-159.
19. Bates E.D., Mayton R.D., Ntai I., and Davis J.H., 2002, "CO_2 capture by a task-specific ionic liquid", American Chemical Society Journal, Vol. 124, No. 6, Pg. 926-927.
20. Benamor A., and Aroua M.K., 2005, "Modelling of CO_2 solubility and carbamate concentration in DEA, MDEA and their mixtures using the Deshmukh–Mather model", Fluid Phase Equilibria 231, pg 150-162.

21. Brennecke J.F. and Gurkan B.E., 2010, "Ionic liquids for CO_2 capture and emission reduction", J. Phys. Chem. Lett., Vol. 1, Pg.3459–3464.
22. Burt S., Baxter A., and Baxter L., 2009, "Cryogenic CO_2 Capture to Control Climate Change Emissions", Brigham Young University, Utah, U.S.A.. Accessed 21/06/2011. http://www.sustainablees.com/documents/Clearwater.pdf
23. Cadena C., Anthony J.L., Shah J.K., Morrow T.I., Brennecke J.F., and Maginn E.J., 2004, "Why Is CO_2 So Soluble in Imidazolium-Based Ionic Liquids?", J. Am. Chem. Soc., vol. 126, pg. 5300-5308.
24. Camper D., Bara J.E., Gin D.L., Noble R.D., 2008, "Room-Temperature Ionic Liquid-Amine Solutions: Tunable Solvents for Efficient and Reversible Capture of CO_2", Ind. Eng. Chem. Res. 47, 8496–8498.
25. Carbon Monitoring for Action (CARMA), 2007, "Top 30 CO_2-emitting power plants in the world", CARMA - a division of the Centre for Global Development, U.S.A. Accessed 4 July, 2011. www.carma.org.
26. Carbon Monitoring for Action (CARMA), 2011, "The 10 largest CO_2 emitting power sectors in Africa by country", CARMA - a division of the Centre for Global Development, U.S.A. Accessed 4 July, 2011. www.carma.org.
27. Carbon Monitoring for Action (CARMA), 2011, "The 10 largest CO_2 emitting power sectors in the world by country", CARMA - a division of the Centre for Global Development, U.S.A. Accessed 4 July, 2011. www.carma.org.
28. Carroll J.J., Mather A.E., 1992, "The System Carbon Dioxide-Water and the Krichevski-Kasarnovski Equation", J. Sol. Chem., 21, 607-621.
29. Chakravarti S., Gupta A., Hunek B., 2001, "Advanced technology for the capture of carbon dioxide from flue gases", Praxair, Inc. Process & Systems R&D, CO_2 Technology, USA
30. Chang H, Shih C., 2007, "Simulation and Optimization for Power Plant Flue Gas CO_2 Absorption-Stripping Systems", Sep. Sci. Tech., 40, 877-909.
31. Chatti I., Delahaye A., Fournaison L., Petitet J.P., 2005, "Benefits and drawbacks of clathrate hydrates: a review of the areas of interest", Energy Conversion and Management Vol. 46, pg. 1333–1343
32. Chemicalbook, 2013, "1-Butyl-3-Methyl Imidazolium Methyl Sulfate", Chemical Book Inc., 2008, U.S.A. [Accessed July 2013]
33. Chemicalbook, 2013, "Methyl Trioctyl ammonium bis(Trifluorosulfonyl)imide", Chemical Book Inc., 2008, U.S.A. [Accessed July 2013]
34. Chen C., Evans L. B., 1986, "A local composition model for the excess gibbs energy of aqueous electrolyte system". AIChE Journal, Vol. 32, 444−454

35. Chen Y., Zhang S., Yuan X., Zhang Y., Zhang X., Dai W., Mori R., 2006, "Solubility of CO_2 in imidazolium-based tetrafluoroborate ionic liquids", Thermochimica Acta, vol. 441, 42-44.
36. Chen Q., Yong Y., Zeng P., Yang W., Liang Q., Peng X, Liu Y., Hu Y., 2008, "Effect of 1-butyl 3-methylimidazolium tetrafluoroborate on the formation rate of CO_2 hydrate", Journal of Natural Gas Chemistry, vol. 17, pg. 264-267
37. Chen H., Zhao C., Chen M., Li Y., and Chen X., 2011, "CO_2 uptake of modified calcium-based sorbents in a pressurized carbonation–calcination looping", Fuel Processing Technology, Vol. 92, pg 1144-1151.
38. Chen H., Zhao C., Duan L., Liang C., Liu D., Chen X., 2011, "Enhancement of reactivity in surfactant-modified sorbent for CO_2 capture in pressurized carbonation", Fuel Processing Technology, Vol. 92, pg. 493-499.
39. Chenga M., Caparangaa A.R., Sorianoa A.N., Li M., 2010, "Solubility of CO_2 in the solvent system (water + monoethanolamine + triethanolamine)", J. Chem. Therm. 42, 342–347.
40. Clodic D., Hitti R., Younes M., Bill A. and Casier F., 2005, "CO_2 capture by anti-sublimation: thermo-economic process evaluation", 4th Annual Conference on Carbon Capture and Sequestration, U.S.A.
41. Cloete M., 2010, "Atlas on geological storage of carbon dioxide in South Africa", Council for Geoscience, Department of Energy, South Africa. Accessed 30 June 2011. http://www.sacccs.org.za/wp-content/uploads/2010/11/Atlas.pdf
42. Condemarin R., Scovazzo P., 2009, "Gas permeabilities, solubilities, diffusivities, and diffusivity correlations for ammonium-based room temperature ionic liquids with comparison to imidazolium and phosphonium RTIL data", Chemical Engineering Journal, Vol. 147, Pg. 51–57.
43. Coquelet C., Richon D., 2007, "Chapter 14: Solubility of BTEX and Acid Gases in Alkanolamine Solutions in Relation to the Environment", from the book: "Developments and applications of solubility", RSC, Cambridge, UK
44. Cserjesi P., Nemestothy N., Belafi-Bako K., 2010, "Gas separation properties of supported liquid membranes prepared with unconventional ionic liquids", Journal of Membrane Science, vol. 349, pg. 6-11.
45. Danckwerts P.V., 1965, "The Absorption of Gases in Liquids", Department of Chemical Engineering, University of Cambridge, UK. pp 625-642
46. Davison J., 2007, "Performance and costs of power plants with capture and storage of CO_2", Energy Vol. 32, pg 1163–1176
47. Deenadayalu, N.; Bahadur, I.; Hofman, T., 2010 Ternary excess molar volumes of {methyltrioctylammonium bis(trifluoromethylsulfonyl)imide + ethanol + methyl acetate, or

ethyl acetate} systems at T = (298.15, 303.15, and 313.15) K. J. Chem. Thermodyn. 42, 726–733.

48. Descamps C, Bouallou C, Kanniche M, 2008, "Efficiency of an integrated gasification combined cycle (IGCC) power plant including CO_2 removal.", Energy 33, pg 874-881.
49. Dholabhal P.D., Kalogerakis N., Bishnol P.R., 1993, "Evaluation of gas hydrate formation and deposition in condensate pipelines: Pilot plant studies", Society of Petroleum Engineers, Dallas, U.S.A. Accessed 29/07/2011. ftp://78.39.200.210/FTP%20server/Teacher/montazere/Gas%20Condensate%20Papers/SPE/00022829.pdf
50. Diab F, Provost E., Laloué N., Alix P., Souchon V., Delpoux O., Fürst W., 2012, "Quantitative analysis of the liquid phase by FTIR spectroscopy in the system CO_2/Diethanolamine (DEA)/H_2O", Fluid Phase Equilibria, 325, pg. 90-99.
51. Dias J.T., Oliveira N.S., 2010, "polymeric membranes and ionic liquids for CO_2 capture and sequestration technologies", Instituto Politécnico de Leiria, Portugal. Accessed 1/4/2011. http://eventos.ipleiria.pt/gecamb2010/PT/POLYMERIC_MEMBRANES_AND_IONIC_LIQUIDS_FOR_CO_2_Dias_Oliveira_4thGECAMB.pdf
52. DiGuillo R.M., Lee R., Schaeffer S.T., Brasher L.L., and Tela A.S., 1992, "Densities and Viscosities of the Ethanolamines", J. Chem. Eng. Data, 37, 239-242.
53. Duc N.H., Chauvy F and Herri J.M., 2007, "CO_2 capture by hydrate crystallization – a potential solution for gas emission of steelmaking industry", Energy Conversion and Management, Vol 48, pg 1313-1322
54. Eskom Ltd., 2011, "Eskom coal power animation", Eskom Holdings Ltd., South Africa. Accessed 25/05/2011. http://www.eskom.co.za/content/Coal.swf
55. Eskom Power Generation, 2011, "Eskom – Coal Power", Eskom Holdings Ltd., South Africa. Accessed 28/02/2011. http://www.eskom.co.za/live/content.php?Item_ID=279
56. Eskom Holdings Ltd., 2011, "Annual Report for 2011", Eskom Holdings Ltd., South Africa. Accessed 26/09/2011. http://financialresults.co.za/2011/eskom_ar2011/profile_key_facts.php
57. Fang H., Haibin L., and Zengli Z., 2009, "Advancements in development of chemical-looping combustion: A Review", International Journal of Chemical Engineering, Vol. 2009, pg. 1-16.
58. Ferna´ndez J., Gonza´lez F., Pesquera C., Blanco C., and Renedo M.J., 2010, "Study of the CO_2/sorbent interaction in sorbents prepared with mesoporous supports and calcium compounds", Ind. Eng. Chem. Res., Vol. 49, pg. 2986-2991.

59. Figueroa J.D., Fout T, Plasynski S., McIlvried H. and Srivastava R.D., 2008, "Advances in CO_2 capture technology—The U.S. department of energy's carbon sequestration program", International Journal of Greenhouse Gas Control, Vo. 2, pg 9—20
60. Font O., Querol X., Plana F., Coca P., Burgos S., Garcıa-Pena F., 2006, "Condensing species from flue gas in Puertollano gasification power plant, Spain", Fuel 85, 2229–2242.
61. Fredlake C.P., Crosthwaite J.M., Hert D.G., Aki S.N.V.K., and Brennecke J.F., 2004, "Thermophysical Properties of Imidazolium-Based Ionic Liquids", J. Chem. Eng. Data, Vol. 49,Pg. 954-964.
62. Gan Q., Rooney D., Xue M., Thompson G., Zou Y., 2006, "An experimental study of gas transport and separation properties of ionic liquids supported on nanofiltration membranes", Journal of Membrane Science, vol. 280, pg. 948-956.
63. Ge J.J., Cowan R.M., Tu C.K., McGregor M.L., Trachtenburg M.C., 2002, "Enzyme-based CO_2 capture for ALS", Carbozyme Ltd., U.S.A.. Accessed 4/08/2011. http://www.carbozyme.us/publications/P5.pdf
64. Gielen D., 2003, "The energy policy consequences of future CO_2 capture and sequestration technologies", International Energy Agency, France. Accessed 19 February 2009. http://www.resourcemodels.org/pap060503.pdf
65. Gnanendran N, and Amin R., 2004, "Modelling hydrate formation kinetics of a hydrate promoter–water–natural gas system in a semi-batch spray reactor", Chemical Engineering Science, Vol. 59, pg. 3849-3863.
66. Gonzalez M.M., Palomar J., Omar S., and Rodriguez F., 2011, "CO_2/N_2 Selectivity Prediction in Supported Ionic Liquid Membranes (SILMs) by COSMO-RS", Ind. Eng. Chem. Res., Volume and page numbers not available presently. Accessed 1/4/2011.
67. Gottlicher G. And Pruschek R., 1997, "Comparison of CO_2 removal systems for fossil-fuelled power plant processes", Energy Conversion Management, vol. 38, pg. 173-178.
68. GovMonitor, 2010, "DOE Invests $67 Million For Carbon Capture Development", GovMonitor Public Sector News and Information, U.S.A. Accessed 10/3/2011. http://www.thegovmonitor.com/world_news/united_states/doe-invests-67-million-for-carbon-capture-development-35077.html
69. Gas Processors Association (GPA), 2004. "GPSA Engineering Data Book: Section 21 – Hydrocarbon Treating", 12th Edition, published by GPA. Accessed 12 April 2011. http://www.gasprocessors.com/gpsa_book.html#About
70. Gray M.L., Soong Y., Champagne K.J., Pennline H., Baltrus J., Stevens Jr. R.W., Khatri R., Chuang S.S.C., and Filburn T., 2004, "Improved immobilized carbon dioxide capture sorbents", Prepr. Pap.-Am. Chem. Soc. Div. Fuel Chem., Vol. 49, pg. 257-258.

71. Green D.A., Turk B.S., Portzer J.W., Gupta R.P., McMichael W.J, Nelson T., Gangwal S., Liang Y, Moore T., Williams M., Harrison D.P., 2004, "Carbon dioxide capture from flue gas using dry regenerable sorbents", Topical report for the U.S. Department of Energy, NETL, Pittsburgh
72. Griffiths J., 2008, "Lose the carbon, not the capacity.", TCE Magazine, issue 810. December 2008/January 2009, Pg. 43. www.tcetoday.com
73. Gurkan B.E., Fuente J.C., Mindrup E.M., Ficke L.E., Goodrich B.F., Price E.A., Schneider W.F., Maginn E., and Brennecke J.F., 2010, "Chemically complexing ionic liquids for post-combustion CO_2 capture", Department of Chemical and Biomolecular Engineering, University of Notre Dame, USA. Accessed 9/3/2011. http://www.nd.edu/~wschnei1/papers/2010_Gurkan_CCC.pdf
74. Hanioka S., Maruyama T., Sotani T., Teramoto M., Matsuyama H., Nakashima K., Hanaki M., Kubota F., Goto M., 2008, "CO_2 separation facilitated by task-specific ionic liquids using a supported liquid membrane", Journal of Membrane Science, vol. 314, pg. 1-4.
75. Hasib-ur-Rahman M., Siaj M., Larachi F., 2010, "Ionic liquids for CO_2 capture—Development and progress", Chemical Engineering and Processing, Vol. 49, Pg. 313–322.
76. Heintz Y.J., Sehabiague L., Morsi B.I., Jones K.L., Luebke D.R., and Pennline H.W., 2009, "Hydrogen sulfide and carbon dioxide removal from dry fuel gas streams using an ionic liquid as a physical solvent", Energy Fuels, Vol. 23, Pg. 4822–4830.
77. Holbrey J.D. and Seddon K.R., 1999, "The phase behaviour of 1-alkyl-3-methylimidazolium tetrafluoroborates; ionic liquids and ionic liquid crystals", J. Chem. Soc., Dalton Trans., 2133–2139.
78. Huang J. and Rüther T., 2009, "Why are ionic liquids attractive for CO_2 absorption? An overview", Aust. J. Chem., vol. 62, pg. 298-308.
79. Huang, X.; Margulis, C. J.; Li, Y.; Berne, B. J., 2005, "Why is the Partial Molar Volume of CO_2 So Small When Dissolved in a Room Temperature Ionic Liquid? Structure and Dynamics of CO_2 Dissolved in $[Bmim]^+[PF6]^-$". J. Am. Chem. Soc., 127, 17842–17851.
80. Ibrahim H., 2011. Personal correspondence with Mr. Hamisu Ibrahim, School of Chemistry, University of KwaZulu Natal, South Africa.
81. Intergovernmental Panel on Climate Change, 2013, "Climate Change 2013, The Phyical Science Basis – Summary for Policy Makers ", IPCC, http://www.climatechange2013.org/images/uploads/WGIAR5-SPM_Approved27Sep2013.pdf
82. International Energy Agency (IEA), 2004, "Prospects for CO_2 capture and storage", Paris Cedex, France. Accessed 5 March 2009. http://www.iea.org/textbase/nppdf/free/2004/prospects.pdf

83. International Energy Agency (IEA), 2007, "CO_2 Capture Ready Plants", United Kingdom: Organisation for Economic Cooperation and Development, Greenhouse Gas R&D Programme. http://www.iea.org/Textbase/Papers/2007/CO2_Capture_Ready_Plants.pdf.
84. International Energy Agency (IEA), 2007, "Capturing CO_2", Separations Research Programme, Texas. Accessed 29 January 2009 http://www.ieagreen.org.uk/glossies/co2capture.pdf
85. International Energy Agency (IEA), 2010, "Key World Energy Statistics – 2010", International Energy Agency, Paris Cedex, France.
86. Ignat'ev N.V., Welz-Biermann U., Kucheryna A., Bissky G., Willner H., 2005, "New ionic liquids with tris(perfluoroalkyl)trifluorophosphate (FAP) anions", Journal of Fluorine Chemistry, Vol. 126, pg. 1150-1159.
87. Intergovernmental Panel on Climate Change (IPCC), 2005. "Carbon Dioxide Capture and Storage: Summary for Policy Makers and Technical Summary". Accessed 26 January 2011 http://www.climnet.org/EUenergy/IPCC_CCS_0905.pdf
88. Jadhawar P., Mohammadi A.H., Yang J., Tohidi B., 2006, "Subsurface carbon dioxide storage through clathrate hydrate formation", Institute of Petroleum Engineering, Heriot-Watt University, Edinburgh, United Kingdom
89. Jacquemin, J.; Husson, P.; Padua, A. A. H.; Majer, V., 2006, "Density and viscosity of several pure and water-saturated ionic liquids". Green Chem. 8, 172–180.
90. Jayarathna S.A., Lie B., Melaaen M.C., 2013, "Dynamic modelling of the absorber of a post-combustion CO_2 capture plant: Modelling and simulations", Comp. Chem. Eng., Vol 53, pg. 178-189
91. Jayarathna, S. A., Lie, B., & Melaaen, M. C., 2011. "NEQ rate based modeling of an absorption column for post combustion CO_2 capturing". Energy Procedia, 4, 1797–1804.
92. Jones D., Bhattacharyya D., Turton R., Zitney S.E., 2011, "Optimal design and integration of an air separation unit (ASU) for an integrated gasification combined cycle (IGCC) power plant with CO_2 capture", Fuel Processing Technology. Article in press.
93. Jou F., Otto F.D., Mather A.E., 1994, "Vapor-Liquid Equilibrium of Carbon Dioxide in Aqueous Mixtures of Monoethanolamine and Methyldiethanolamine", Ind. Eng. Chem. Res.,33, 2002-2005.
94. Kanniche M., Bouallou C., 2007, "CO_2 capture study in advanced integrated gasification combined cycle", Applied Thermal Engineering Vol. 27, pg. 2693-2702
95. Karmarkar M., Griffiths J., Russell A., Allen R., Austell M., Trusler M., 2009, "Industrial and utility scale IGSC coal power stations", Department of Energy and Climate Change, U.S.A.. Accessed 3/08/2011. http://webarchive.nationalarchives.gov.uk/+/http://www.berr.gov.uk/files/file52638.pdf

96. Kent R., 2009, “New Power Cycles with Carbon Capture and Sequestration”, Sempra Energy Utilities, Waste Management Association, U.S.A.. Accessed 3/08/2011. http://www.wcsawma.org/sitebuildercontent/sitebuilderfiles/34.pdf
97. Knudsen J.N., Vilhelmsin P.J., Jensen J.N and Biede O., 2008, “Performance review of Castor pilot plant at Esbjerg”. Published by Dong Energy, Austria
98. Knuutila H., Hallvard F. Svendsen, and Mikko Anttila, 2008, “CO_2 capture from coal-fired power plants based on sodium carbonate slurry; a systems feasibility and sensitivity study”, International Journal of Greenhouse Gas Control, Vol 3, pg 143-151.
99. Kock D., 2013. Personal correspondence with Dr. David Kock of the Nuclear Energy Corporation of South Africa (NECSA), Pretoria
100. Krichevski I.R., Kasarnovski J.S., 1935, “Thermodynamical Calculations of Solubilities of Nitrogen and Hydrogen in Water at High Pressures”,J. Am. Chem. Soc., 57, 2168.
101. Kroon M.C., Karakatsani E.K., Economou I.G., Witkamp G., Peters C.J., 2006, “Modeling of the Carbon Dioxide Solubility in Imidazolium-Based Ionic Liquids with the tPC-PSAFT Equation of State”, J. Phys. Chem. B, 110, 9262-9269.
102. Kumelan J., Tuma D., Kamps A.P.S., and Maurer G., 2010, “Solubility of the Single Gases Carbon Dioxide and Hydrogen in the Ionic Liquid [bmpy][Tf_2N]”, J. Chem. Eng. Data, 55, 165–172
103. Lee J.B., Ryu C.K., Baek J., Lee J.H., Eom T.H., Kim S.H., 2008, “Sodium based dry regenerable sorbent for carbon dioxide capture from power plant flue gas”, Ind. Eng. Chem Vol. 47, pg. 4465-4472
104. Lee H.S., Seo M.D., Kang J.W., and Yang D.R., 2012, “Measurement and Correlation of the Solubility of Carbon Dioxide in the Mixtures of Aqueous Monoethanolamine Solution and Benzoic Acid”, J. Chem. Eng. Data, 57, 3744−3750
105. Lewis W.K., Whitman W.G., 1924, “Principles of Gas Absorption”, Ind. Eng. Chem., Vol 16, pp 1215-1220.
106. Linga P., Kumar R., Englezos P., 2007, “The clathrate hydrate process for post and pre combustion capture of carbon dioxide”, Journal of Hazardous Materials 149, pg. 625–629.
107. Liu H., Huang J., Pendleton P.,2011, “Experimental and modelling study of CO_2 absorption in ionic liquids containing Zn (II) ions”, Energy Procedia, vol. 4, pg. 59-66.
108. Long J., 2010, “New metal organic frameworks in action for capturing carbon dioxide”, The Green Optimistic, U.S.A.. Accessed 4/08/2011. http://www.greenoptimistic.com/2010/06/02/metal-organic-frameworks-carbon-dioxide-capture/

109. Lozano L.J., Godínez C., Ríos A.P., Hernández-Fernández F.J., Sánchez-Segado S., Alguacil F.J., 2011, "Recent advances in supported ionic liquid membrane technology", Journal of Membrane Science, newly accepted manuscript.

110. Lu D.Y., Hughes R.W., Anthony E.J., 2008, "Ca-based sorbent looping combustion for CO_2 capture in pilot-scale dual fluidized beds" Fuel Process Technol Vol. 89, pg. 1386-1395.

111. Luebke D., Ilconich J.B., Myers C., and Pennline H.W., 2007, "Carbon Dioxide Separation with Supported Ionic Liquid Membranes", Department of Energy (DOE), Office of Scientific and Technical Information (OSTI), U.S.A. Accessed 1/4/2011. http://www.osti.gov/bridge/purl.cover.jsp?purl=/913401-BW53PD/

112. Luis P., Neves L.A., Afonso C.A.M., Coelhoso I.M., Crespo J.G., Garea A., Irabien A., 2009, "Facilitated transport of CO_2 and SO_2 through Supported Ionic Liquid Membranes (SILMs)"Desalination, Vol. 245, pg. 485-493.

113. Ma J., Zhou Z., Zhang F., Fang C., Wu Y., Zhang Z., Li A., 2011, "Ditetraalkylammonium Amino Acid Ionic Liquids as CO_2 Absorbents of High Capacity", Environ. Sci. Technol. 45, 10627–10633.

114. Maginn E.J., 2005, "Design and evaluation of ionic liquids as novel CO_2 absorbents", Department of Energy (DOE), University of Notre Dame, Notre Dame, USA. Accessed 7/3/2011.
http://www.osti.gov/bridge/purl.cover.jsp?purl=/841006-AL0CWm/native/

115. Ma'mun S., Nilsen R. and Svendsen H.F., 2005, "Solubility of carbon dioxide in 30 mass % monoethanolamine and 50 mass % methyldiethanol amine solutions", Journal of Chemical Engineering Data, vol. 50, page 630-634

116. Ma'mun S, Svendsen HF, Hoff K.A. and Juliussen O, 2006, "Selection of new absorbents for carbon dioxide capture", Energy Conversion and Management, Vol. 48, pg 251-258.

117. Ma'mun S., 2005, "Selection and characterisation of new absorbents for carbon dioxide capture", Faculty of Natural Science and Technology, Department of Chemical Engineering, NTNU, Norway

118. Manovic V., Anthony E.J., Lu D.Y., 2008, "Sulphation and carbonation properties of hydrated sorbents from a fluidized bed CO_2 looping cycle reactor", Fuel, Vol. 87, pg. 2923-2931.

119. Manuel A., Pacheco T. and Rochelle G.T., 1998, "Rate-based modelling of reactive absorption of CO_2 and H_2S into aqueous methyldiethanolamine", Ind. Eng. Chem. Res. Vol. 37, pg. 4107-4117

120. Mattisson T. and Lyngfelt A., 2001, "Applications of chemical-looping combustion with capture of CO_2", Department of Energy Conversion, Chalmers University of Technology, Sweden. Accessed 8/08/2011. http://www.entek.chalmers.se/~anly/symp/01mattisson.pdf

121. Mattisson T., 2007, "Chemical looping combustion using gaseous and solid fuels", International Energy Agency (IEA) Greenhouse Gas R&D Programme, Sweden. Accessed 8/08/2011. http://www.co2captureandstorage.info/docs/oxyfuel/MTG2Presentations/Session%2006/22%20-%20T.%20Mattisson%20(Chalmers%20University).pdf

122. MacColl B., 2011, "Carbon capture and storage (CCS) – Strategic considerations for Eskom", South African Centre for Carbon Capture and Storage. [updated 2011, cited 8 August 2013].

123. McGalliard R.L. and Larrabee G.W., 1980, "Method for cryogenic separation of carbon dioxide from hydrocarbons", Standard Oil Company, U.S. patent 4,185,978.

124. Meisen A, Shuai X., 1997, "Research and development issues in CO_2 capture", Energy Conversion and Management Vol. 38, pg. S37-S42.

125. Mores P., Scenna N, Mussati S., 2012 "CO_2 capture using monoethanolamine (MEA) aqueous solution: Modeling and optimization of the solvent regeneration and CO_2 desorption process", Energy 45, pg. 1-17.

126. Muldoon M.J., Aki S.N.V.K, Anderson J.L., Dixon J.K., and Brennecke J.F., 2007, "Improving carbon dioxide solubility in ionic liquids", J. Phys. Chem. B , Vol. 111,Pg. 9001-9009.

127. Najibi H., Maleki N., 2013, "Equilibrium solubility of carbon dioxide in N-methyldiethanolamine+piperazine aqueous solution: Experimental measurement and prediction:, Fluid Phase Equilibria, 354, 298–303.

128. National Treasury, 2013. "Carbon Tax Policy Paper - Reducing greenhouse gas emissions and facilitating the transition to a green economy. Discussion paper for public comment", Department of National Treasury, South Africa; [updated 2013; cited 7/08/2013]; http://www.treasury.gov.za/public%20comments/Discussion%20Paper%20Carbon%20Taxes%2081210.pdf

129. National Treasury, 2010, "Reducing Greenhouse Gas Emissions: The Carbon Tax Option. Discussion Paper for Public Comment", Department of National Treasury, South Africa. Accessed 5/09/2011. http://www.treasury.gov.za/public%20comments/Discussion%20Paper%20Carbon%20Taxes%2081210.pdf

130. National Energy Technology Laboratory (NETL), 2007, “Chemical looping process in a coal to liquids configuration”, published by Department of Energy, accessed 29 January 2009, http://www.netl.doe.gov/energy-analyses/pubs/DOE%20Report%20on%20OSU%20Looping%20final.pdf

131. National Energy Technology Laboratory (NETL), 2010, “Doe/Netl Advanced Carbon Dioxide Capture R&D Program: Technology Update”, NETL, U.S.A. Accessed 25/5/2011. http://www.netl.doe.gov/technologies/coalpower/ewr/pubs/CO2%20Capture%20Tech%20Update%20Final.pdf

132. Nerula S.C. and Ashraf M., 1987, “Carbon dioxide separation”, Process Economics Program, S.R.I International, California, USA

133. Nishi N., Kawakami T., Shigematsu F., Yamamoto M. and Kakiuchi T., 2006, “Fluorine-free and hydrophobic room-temperature ionic liquids, tetraalkylammonium bis(2-ethylhexyl)sulfosuccinates, and their ionic liquid–water two-phase properties”, Green Chemistry, Vol 8, pg. 349-355.

134. Osman K., 2011, “Carbon dioxide capture methods for industrial sources: A literature review, energy efficiency and feasibility study”, University of KwaZulu Natal, South Africa

135. Osman K., Coquelet C., Ramjugernath D., 2012, “Absorption Data and Modeling of Carbon Dioxide in Aqueous Blends of Bis(2-hydroxyethyl)methylamine (MDEA) and 2,2-Iminodiethanol (DEA): 25 % MDEA + 25 % DEA and 30 % MDEA + 20 % DEA”, J. Chem. Eng. Data, Vol. 57, pg. 1607-1620

136. Othmer K., 2008, “Ionic liquids”, Encyclopedia of Chemical Technology, Vol. 26, pg. 836-920. Accessed 1/6/2011.http://mrw.interscience.wiley.com/emrw/9780471238966/home/

137. Palgunadi J., Kang J.E., Cheong M., Kim H., Lee H., and Kim H.S., 2009. “Fluorine-free imidazolium-based ionic liquids with a phosphorous-containing anion as potential CO_2 absorbents”, Bull. Korean Chem. Soc., Vol. 30, pg. 1749-1754.

138. Park S.H., Lee K.B., Hyun J.C., and Kim S.H., 2002 “Correlation and Prediction of the Solubility of Carbon Dioxide in Aqueous Alkanolamine and Mixed Alkanolamine Solutions”, Ind. Eng. Chem. Res., 41, pg. 1658-1665.

139. Park J., Seo Y.T, Lee J.W., Lee H., 2006, “Spectroscopic analysis of carbon dioxide and nitrogen mixed gas hydrates in silica gel for CO_2 separation”, Catalysis Today Vol. 115, pg. 279-282

140. Park Y., Kim B., Byun Y., Lee S., Lee E., Lee J., 2009, “Preparation of supported ionic liquid membranes (SILMs) for the removal of acidic gases from crude natural gas”, Desalination, vol. 236, pg. 342-348.

141. Pereiro, A. B.; Verdı´a, P.; Tojo, E.; Rodrı´guez, 2007, “A. Physical Properties of 1-Butyl-3-methylimidazolium Methyl Sulfate as a Function of Temperature”. J. Chem. Eng. Data, 52, 377–380.

142. Plasynski S., Lang D.A., and Richard W., 2008, “Carbon dioxide separation with novel microporous metal organic frameworks”, National Energy Technology Laboratory (NETL), U.S.A.. Accessed 4/07/2011. http://www.netl.doe.gov/publications/factsheets/project/Proj315.pdf

143. Prausnitz J.M., Lichtenthaler R.N., Azevedo E.G., 1999, “Molecular Thermodynamics of Fluid Phase Equilibria”, 3rd Edition, Prentice Hall, U.S.A.

144. Raynal L., Alixa P., Bouillona P., Gomeza A., de Naillya M.F., Jacquina M., Kittela J., di Lellab A., Mougin P., Trapy J., 2011, “The DMX™ process : an original solution for lowering the cost of post-combustion carbon capture”, Energy Procedia 4, 779–786.

145. Richon D., Antoine P., and Renon H., 1980, “Infinite Dilution Activity Coefficients of Linear and Branched Alkanes from C, to C9 in n-Hexadecane by Inert Gas Stripping”, Ind. Eng. Chem. Process Des. Dev. 1980, 19, 144-147

146. Richon D., 2011, “New equipment and new technique for measuring activity coefficients and Henry’s constants at infinite dilution”, Review of Scientific Instruments, Vol. 82., pg. 1-8.

147. Ritter J.A. and Armin D.E., and Reynolds S.P. and Du H., 2006, “New adsorption cycles for carbon dioxide capture and concentration”, Department of Chemical Engineering, University of South Carolina, Columbia.

148. Rodríguez, H.; Brennecke, J. F., 2006, “Temperature and composition dependence of the density and viscosity of binary mixtures of water + ionic liquid”. J. Chem. Eng. Data, 51, 2145–2155.

149. Scovazzo P., Havard D., McShea M., Mixon S., Morgan D., 2009, “Long-term, continuous mixed-gas dry fed CO_2/CH_4 and CO_2/N_2 separation performance and selectivities for room temperature ionic liquid membranes”, Journal of Membrane Science, vol. 327, pg. 41-48.

150. Scovazzo P., 2009, “Determination of the upper limits, benchmarks, and critical properties for gas separations using stabilized room temperature ionic liquid membranes (SILMs) for the purpose of guiding future research”, Journal of Membrane Science, vol. 343, pg. 199-211.

151. Scovazzo, P.; Camper, D.; Kieft, J.; Poshusta, J.; Koval, C.; Noble, R. D., 2004, “ Regular solution theory and CO_2 gas solubility in room temperature ionic liquids”. Ind. Eng. Chem. Res. 43, 6855–6860.

152. Seeberger A., Kern C., Uerdingen M., Jess A., 2007, "Gas separation by supported ionic liquid membranes", DGMK Conference, Hamburg, Germany. Accessed 1/4/2011. http://www.dgmk.de/petrochemistry/abstracts_content15/Seeeberger.pdf

153. Shannon, M. S.; Tedstone, J. M.; Danielsen, S. P. O.; Hindman, M.S.; Irvin, A. C.; Bara, J. E., 2012, "Fractional Free Volume as the Basis of Gas Solubility & Selectivity in Imidazolium-based Ionic Liquids. Ind. Eng. Chem. Res., 51, 5565–5576.

154. Shiflett M.B. and Yokozeki A., 2005, "Solubilities and diffusivities of carbon dioxide in ionic liquids:[bmim][PF_6] and [bmim][BF_4]", Ind. Eng. Chem. Res. , Vol. 44, Pg. 4453-4464.

155. Shiflett M. B., Yokozeki A., 2007, "Solubility of CO_2 in Room Temperature Ionic Liquid [hmim][Tf_2N]". J. Phys. Chem. B, 111, 2070–2074.

156. Shokouhi M., Adibi M., Jalili A.H., Hosseini-Jenab M., and Mehdizadeh A., 2010, "Solubility and diffusion of H_2S and CO_2 in the ionic liquid 1-(2-hydroxyethyl)-3-methylimidazolium tetrafluoroborate", J. Chem. Eng. Data, Vol. 55, Pg. 1663–1668.

157. Simmons J.M., Wu H., Zhou W., Yildirima T., 2011, "Carbon capture in metal-organic frameworks – A comparative study", Energy and Environmental Science, Vol. 4, pg. 2177-2185.

158. Smiths Ltd., 2013, "Specac Product Catalogue", Smiths Technology, United Kingdom. Information provided by Mr. Kevin Wickee of Shimadzu.

159. Steeneveldt R., Berger B. and Torp. T.A., 2006, "CO_2 capture and storage. Closing the knowing-doing gap", Chemical Engineering Research and Design Vol. 84, pg 739-763.

160. Su. C., Ran X., Hu. J., Shao C., "Photocatalytic Process of Simultaneous Desulfurization and Denitrification of Flue Gas by TiO_2–Polyacrylonitrile Nanofibers", Environ. Sci. Technol., 47 (20), pp 11562–11568

161. SuoJiang Z., XiangPing Z., YanSong Z., GuoYing Z., XiaoQian Y., and HongWei Y., 2010, "A novel ionic liquids-based scrubbing process for efficient CO_2 capture", Science China Chemistry, Vol.53, Pg. 1549-1553.

162. Surridge T., 2005, "South African activities related to carbon capture and storage – September 2005", Department of Minerals and Energy, South Africa, Carbon Sequestration Leadership Forum, accessed 28 January 2009 http://www.cslforum.org/documents/pg_RomeMinutespublic.pdf.

163. Surridge T., 2011. Personal correspondence with Dr. Tony Surridge, South African National Energy Research Institute (SANERI), and Head of the South African Centre for Carbon Capture and Storage (SACCCS), South Africa.

164. SuoJiang Z., XiangPing Z., YanSong Z., GuoYing Z., XiaoQian Y., HongWei Y., 2010, "A novel ionic liquids-based scrubbing process for efficient CO_2 capture Sci China Chem Vol.53 Pg. 1549-1543.

165. Tam S.S., Stanton M.E., Ghose S., Deppe G., Spencer D.F., Currier R.P., Young J.S., Anderson G.K., Le L.A., and Devlin D.J., 2000, "A High Pressure Carbon Dioxide Separation Process for IGCC Plants", National Energy Technology Laboratory, Department of Energy, U.S.A. Accessed 29/07/2011. http://www.netl.doe.gov/publications/proceedings/01/carbon_seq/1b4.pdf.

166. Tang, S.; Baker, G. A.; Zhao, H., 2012, "Ether- and alcohol-functionalized task-specific ionic liquids: attractive properties and applications". Chem. Soc. Rev., 41, 4030–4066.

167. Tariq M., Forte P.A.S., Gomes M.F.C., Lopes J.N.C., Rebelo L.P.N., 2009, "Densities and refractive indices of imidazolium- and phosphonium-based ionic liquids: Effect of temperature, alkyl chain length, and anion", J. Chem. Therm., 41, pg. 790-798

168. Thermo Nicolet Corporation, 2001, "Introduction to Fourier Transform Infrared Spectrometry", Thermo Nicolet, U.S.A.

169. Teng F. and Tondeur D., 2006, "Efficiency of carbon storage with leakage: physical and economical approaches", Energy Vol. 32, pg. 540-548

170. Tillner-Roth, R.; Friend, D. G. 1998, "A Helmholtz free-energy formulation of the thermodynamic properties of the mixture (water+ ammonia)". J. Phys. Chem. Ref. Data, 27, 63-96.

171. Trachtenberg M.C., Cowan R.M., Smith D.A., Horazak D.A., Jensen M.D., Laumb J.D., Vucelic A.P., Chen H., Wang L., Wu X., 2009, "Membrane-based, enzyme-facilitated, efficient carbon dioxide capture", Energy Procedia, Vol. 1, pg. 353-360.

172. Trachtenberg M.C., Tu C.K., Landers R.A., Willson R.C., McGregor M.L., Laipis P.J., Kennedy J.F., Paterson M., Silverman D.N., Thomas D., Smith R.L., Rudolph F.B., 1999, "Carbon dioxide transport by proteic and facilitated transport membranes", International Journal of Earth Space, Vol. 6, pg. 293-302.

173. Treybal R.E., 1981, "Mass Transfer Operations", 3rd Edition, McGraw-Hill Book Company. Printed in Singapore.

174. Valderrama, J. O.; Robles, P. A. Critical properties, normal boiling temperatures, and acentric factors of fifty ionic liquids. Ind. Eng. Chem. Res. 2007, 46, 1338–1344.

175. Vahidi M., Zoghi A.T., Moshtari B., Nonahal B., 2013, "Equilibrium Solubility of Carbon Dioxide in an Aqueous Mixture of N‑Methyldiethanolamine and Diisopropanolamine: An Experimental and Modeling Study", J. Chem. Eng. Data, 58, 1963−1968

176. Valencia J.A. and Victory D.J., 1990, “Method and apparatus for cryogenic separation of carbon dioxide and other acid gases from methane”, Exxon Production Research Company, U.S. patent 4,923,493.

177. Vierde Nationaal Symposium (VNS) CCS, 2008, “CATO CO_2 Catcher, A CO_2 Capture Plant Treating Real Flue Gas”, Published by EON Ltd. Accessed 12 February 2011. http://www.co2-cato.nl/modules.php?name= CATO&page =79& symposium=true

178. Wall T. and Liu Y., 2008, “Chemical looping combustion and CO_2 capture: Status and developments”, Co-operative Research Centre for Coal in Sustainable Development (CCSD), University of Newcastle, Australia. Accessed 8/08/2011. http://www.ccsd.biz/publications/files/TN/TN%2032%20Chem%20looping%20updated_web.pdf

179. Wang S., Wang G., Jiang F., Luo M. and Li H., 2010, “Chemical looping combustion of coke oven gas by using Fe_2O_3/CuO with $MgAl_2O_4$ as oxygen carrier”, Energy and Environmental Science, Vol. 3, pg. 1353-1360.

180. Wappel D., Gronald G., Kalb R., and Draxlar J., 2009, “Ionic liquids for post-combustion CO_2 absorption”, International Post-Combustion CO_2 Capture Network, Austrian Energy and Environment, Austria. Presentation in Canada. Accessed 7/3/2011. http://www.co2captureandstorage.info/networks/cap12pdf/2-5.pdf

181. Welton, T., 1999, “Room temperature ionic liquids. solvents for synthesis and catalysis”, Chem.Rev., vol. 99, pg. 2071-2084.

182. Weast R.C., Astle M.J., Beyer W. H., 1984, “Handbook of Chemistry and Physics”, 64th Edition, CRC Press, Florida.

183. Wickee K., 2013, Personal correspondence with Mr. Kevin Wickee of Shimadzu Ltd., South Africa.

184. Wilkes J.S., 2004, “Properties of ionic liquids for catalysis”, Journal of Molecular Catalysis A: Chemical, Vol. 214, pg. 11-17.

185. Yazaydın A.O., Snurr Q., Park T.H., Koh K., Liu J., LeVan M.D., Benin A.I., Jakubczak P., Lanuza M., Galloway D.B., Low J.J., and Willis R.R., 2009, “Screening of metal-organic frameworks for carbon dioxide capture from flue gas using a combined experimental and modelling approach”, J. Am. Chem. Soc., Vol. 131, pg. 18198-18199.

186. Yazdizadeh M., Rahmani F., Forghani A.A., 2011, “Thermodynamic modeling of CO_2 solubility in ionic liquid ([Cn-mim] [Tf_2N]; n=2, 4, 6, 8) with using Wong-Sandler mixing rule, Peng-Robinson equation of state (EOS) and differential evolution (DE) method”, Korean J. Chem. Eng., 28, 246-251

187. Yi C., Jo S., Seo Y., Lee J., Ryu C., 2007, “Continuous operation of the potassium-based dry sorbent CO_2 capture process with two fluidized-bed reactors”, International Journal of Greenhouse Gas Control, Vol. 1, pg. 31-36.

188. Yokozeki, A., 2005, “Theoretical performance of various refrigerant-absorbent pairs in a vapor-absorption refrigeration cycle by the use of equation of state”. Appl. Energy, 80, 383-399

189. Yokozeki A. 2001, “Solubility of refrigerants in various lubricants.”, Int. J. Thermophys., 22, 1057-1071.

190. Zhang S., Sun N., He X., Lu X., and Zhang X., 2006, “Physical properties of ionic liquids: Database and evaluation”, J. Phys. Chem. Ref. Data, Vol. 35, pg. 1475-1517.

191. Zhang Y., Zhang S., Lu X., Zhou Q., Fan W., and Zhang X., 2009, “Dual amino-functionalised phosphonium ionic liquids for CO_2 capture”, Chem. Eur. J., Vol. 15, pg. 3003-3011.

192. Zhang Y. and Chen C., 2011, “Modeling Gas Solubilities in the Aqueous Solution of Methyldiethanolamine”, Ind. Eng. Chem. Res., 50, 6436–6446

193. Zhao H., Xia S., and Ma P., 2005, “Use of ionic liquids as ‘green’ solvents for extractions”, J. Chem. Technol. Biotechnol. Vol. 80, Pg. 1089-1096.

194. Zhao C., Chen X., Zhao Ch., Liu Y., 2008, “Carbonation and hydration characteristics of dry potassium-based sorbents for CO_2 capture”, Energy and Fuels Journal 2008, Thermoenergy Engineering Research Institute, China.

195. Zhao Y., Zhang X., Zhen Y., Dong H, Zhao G., Zeng S., Tian X, Zhang S, 2011, “Novel alcamines ionic liquids based solvents: Preparation, characterization and applications in carbon dioxide capture”, International Journal of Greenhouse Gas Control 5, 367–373

196. Zhou, L.; Fan, J.; Shang, X.; Wang, J., 2013, “Solubilities of CO_2, H_2, N_2 and O_2 in ionic liquid 1-n-butyl-3-methylimidazolium heptafluorobutyrate”. J. Chem. Thermodyn., 59, 28–34.

197. Zoghi A.T., Feyzi F., Zarrinpashneh S., 2012, “Equilibrium solubility of carbon dioxide in a 30 wt.% aqueous solution of 2-((2-aminoethyl)amino)ethanol at pressures between atmospheric and 4400 kPa: An experimental and modelling study”, J. Chem. Therm., 44, 66–74.

APPENDIX A: MEASURED AND CALCULATED ABSORPTION DATA

Table A-1: Measured Absorption and Desorption Data of CO_2 in [MOA][Tf_2N]

P_{meas}/MPa	T/K	x_{CO2}	P_{meas}/MPa	T/K	x_{CO2}	*P_{calc}/MPa
Absorption			Desorption			
0.0499	303.18	0.017	0.0499	303.17	0.017	0.0500
0.1000	303.21	0.031	0.0998	303.15	0.035	0.1000
0.3998	303.18	0.122	0.3998	303.21	0.138	0.4003
0.7000	303.18	0.198	0.7000	303.15	0.197	0.7005
1.0000	303.18	0.263	0.9998	303.05	0.280	1.0000
1.2999	303.17	0.319	1.2997	303.17	0.323	1.3000
1.4999	303.23	0.343	1.4999	303.23	0.344	1.5011
0.0499	313.25	0.019	0.0500	313.14	0.013	0.0500
0.1000	313.09	0.027	0.0998	313.13	0.030	0.0999
0.4000	313.13	0.104	0.3998	313.07	0.110	0.3999
0.6999	313.15	0.173	0.7000	313.10	0.187	0.6999
0.9997	313.13	0.235	0.9999	313.12	0.235	0.9993
1.2999	313.16	0.287	1.2998	313.07	0.293	1.2989
1.4996	313.17	0.313	1.4996	313.17	0.314	1.4992
0.0500	323.26	0.0143	0.0499	323.16	0.010	0.0500
0.1000	323.18	0.0215	0.0998	323.10	0.022	0.0999
0.4001	323.14	0.0886	0.3998	323.22	0.094	0.3997
0.7000	323.20	0.1511	0.6999	323.07	0.154	0.6999
0.9999	323.19	0.1981	1.0000	323.19	0.212	0.9999
1.3000	323.17	0.2493	1.3000	323.05	0.260	1.2993
1.5000	323.15	0.2820	1.5000	323.15	0.282	1.4992

Uncertainty: T = ±0.01 K; P = 1x10^{-6} MPa; x = ±0.00005

*P_{Calc} *obtained using RK-EOS with regressed parameters*

Table A-2: Measured Absorption and Desorption Data of CO_2 in [Bmim][Tf_2N]

P_{meas}/MPa	T/K	x_{CO2}	P_{meas}/MPa	T/K	x_{CO2}	*P_{calc}/MPa
Absorption			Desorption			
0.0499	303.22	0.016	0.0499	303.17	0.014	0.0504
0.1000	303.16	0.027	0.0999	303.13	0.028	0.0996
0.4000	303.18	0.096	0.3998	303.14	0.104	0.3996
0.7000	303.18	0.158	0.6994	303.06	0.165	0.7000
0.9998	303.25	0.202	0.9996	303.06	0.219	1.0009
1.3001	303.20	0.260	1.2996	303.10	0.263	1.3013
1.4999	303.22	0.283	1.4999	303.22	0.283	1.5021
0.0499	313.28	0.015	0.0499	313.17	0.008	0.0503
0.1000	313.19	0.020	0.0998	313.15	0.024	0.0984
0.4001	313.13	0.077	0.3998	313.10	0.083	0.3993

Table A-2 (Contd.): Measured Absorption and Desorption Data of CO_2 in [Bmim][Tf_2N]

P_{meas}/MPa	T/K	x_{CO2}	P_{meas}/MPa	T/K	x_{CO2}	*P_{calc}/MPa
Absorption			Desorption			
0.7001	313.18	0.131	0.6997	313.05	0.135	0.6996
1.0001	313.14	0.178	0.9995	313.07	0.182	0.9996
1.2998	313.14	0.216	1.2999	313.12	0.223	1.299
1.5000	313.11	0.245	1.5000	313.11	0.245	1.4977
0.0500	323.27	0.011	0.0499	323.15	0.005	0.0501
0.1000	323.22	0.016	0.0998	323.15	0.013	0.1019
0.3999	323.20	0.064	0.3997	323.09	0.051	0.3992
0.7000	323.14	0.108	0.6998	323.12	0.098	0.6994
1.0000	323.24	0.147	0.9997	323.17	0.140	1.0000
1.3000	323.09	0.186	1.2999	323.10	0.179	1.2985
1.5000	323.17	0.210	1.5000	323.17	0.210	1.4974

P_{Calc} obtained using RK-EOS with regressed parameters

Table A-3: Measured Absorption and Desorption Data of CO_2 in [Bmim][$MeSO_4$]

P_{meas}/MPa	T/K	x_{CO2}	P_{meas}/MPa	T/K	x_{CO2}	*P_{calc}/MPa
Absorption			Desorption			
0.0499	303.18	0.005	0.0505	303.18	0.008	0.0500
0.1000	303.20	0.010	0.1001	303.19	0.015	0.1000
0.3997	303.16	0.045	0.4011	303.16	0.048	0.4000
0.7001	303.09	0.084	0.7003	303.09	0.085	0.6998
1.0001	303.20	0.104	0.9996	303.10	0.106	1.0006
1.3001	303.17	0.130	1.3001	303.09	0.132	1.3003
1.5000	303.17	0.138	1.5000	303.17	0.140	1.5012
0.0506	313.25	0.008	0.0509	313.15	0.007	0.0500
0.0998	313.20	0.010	0.1005	313.14	0.013	0.1000
0.4005	313.13	0.038	0.4000	313.06	0.040	0.3998
0.6998	313.11	0.074	0.6999	313.17	0.071	0.6994
1.0000	313.14	0.096	0.9995	313.05	0.097	0.9994
1.3000	313.16	0.118	1.2999	313.11	0.117	1.2989
1.5000	313.16	0.129	1.5000	313.16	0.129	1.4988
0.0507	323.23	0.007	0.0502	323.14	0.003	0.0500
0.1003	323.11	0.007	0.1004	323.11	0.007	0.1000
0.4000	323.15	0.035	0.4004	323.19	0.035	0.3997
0.7001	323.19	0.058	0.7001	323.08	0.058	0.6998
1.0001	323.24	0.078	1.0001	323.15	0.077	1.0001
1.2999	323.23	0.097	1.3000	323.21	0.099	1.3004
1.4999	323.13	0.112	1.4999	323.13	0.109	1.4991

P_{Calc} obtained using RK-EOS with regressed parameters

Table A-4: Measured Absorption and Desorption Data of CO_2 in [Bmim][BF_4]

P_{meas}/MPa	T/K	x_{CO2}	P_{meas}/MPa	T/K	x_{CO2}	*P_{calc}/MPa
Absorption			Desorption			
0.0499	303.41	0.0228	0.0497	303.14	0.0218	0.0890
0.0999	303.17	0.0200	0.0999	303.20	0.0190	0.0653
0.3999	303.16	0.0585	0.3999	303.23	0.0555	0.3674
0.6999	303.17	0.0969	0.7000	303.13	0.0939	0.6994
1.0000	303.17	0.1328	1.0000	303.11	0.1268	1.0212
1.2998	303.16	0.1642	1.2999	303.20	0.1623	1.3071
1.5001	303.18	0.1835	1.4998	303.17	0.1844	1.4859
0.0497	313.25	0.0140	0.0498	313.05	0.0138	0.0850
0.0996	313.09	0.0140	0.0999	313.24	0.0138	0.0851
0.3999	313.16	0.0472	0.3996	313.23	0.0442	0.3987
0.6999	313.14	0.0784	0.7000	313.23	0.0744	0.7075
0.9999	313.15	0.1081	1.0000	313.08	0.1051	1.0173
1.3000	313.10	0.1351	1.3000	313.03	0.1341	1.3018
1.5001	313.13	0.1522	1.5000	313.13	0.1502	1.4845
0.0498	323.25	0.0100	0.0498	323.06	0.0090	0.0831
0.0999	323.17	0.0095	0.0999	323.23	0.0095	0.0780
0.3996	323.13	0.0353	0.3996	323.25	0.0350	0.3628
0.7000	323.11	0.0671	0.7000	323.23	0.0668	0.7267
1.0000	323.21	0.0869	1.0000	323.09	0.0861	0.9600
1.3000	323.14	0.1174	1.3000	323.08	0.1166	1.3248
1.5000	323.18	0.1316	1.5000	323.15	0.1301	1.4976

**P_{Calc} obtained using RK-EOS with regressed parameters*

Table A-5: Measured Absorption and Desorption Data of O_2 in [MOA][Tf_2N]

P_{meas}/MPa	T/K	x_{O2}	P_{meas}/MPa	T/K	x_{O2}	*P_{calc}/MPa	x_{CO2}/x_{O2}
Absorption			Desorption				
0.0499	303.11	0.004	0.0498	303.17	0.003	0.0499	3.97
0.0999	303.19	0.008	0.0999	303.11	0.008	0.0999	3.80
0.3997	303.15	0.016	0.3997	303.11	0.016	0.3997	7.47
0.6998	303.15	0.023	0.6998	303.15	0.024	0.6998	8.45
0.0498	313.31	0.002	0.0498	313.14	0.001	0.0511	12.07
0.0999	313.11	0.004	0.0999	313.10	0.002	0.1012	7.07
0.3997	313.21	0.013	0.3998	313.07	0.012	0.3996	8.01
0.7000	313.17	0.020	0.7000	313.17	0.021	0.7000	8.47
0.0498	323.25	0.000	0.0498	323.13	0.000	0.0499	67.68
0.0999	323.18	0.001	0.0999	323.23	0.002	0.0999	14.84
0.3999	323.24	0.008	0.3998	323.16	0.007	0.3999	11.75
0.6999	323.15	0.013	0.6999	323.15	0.013	0.6999	11.95

**P_{Calc} obtained using RK-EOS with regressed parameters*

Table A-6: Measured Absorption and Desorption Data of O_2 in [Bmim][Tf_2N]

P_{meas}/MPa	T/K	x_{O2}	P_{meas}/MPa	T/K	x_{O2}	*P_{calc}/MPa	x_{CO2}/x_{O2}
Absorption			Desorption				
0.0498	303.19	0.001	0.050	303.162	0.001	0.05	10.58
0.0999	303.17	0.002	0.100	303.071	0.002	0.0999	12.54
0.3999	303.22	0.006	0.400	303.109	0.005	0.3999	16.97
0.7000	303.25	0.006	0.700	303.248	0.006	0.7	25.00
0.0498	313.29	0.001	0.050	313.154	0.001	0.05	12.44
0.0999	313.12	0.002	0.100	313.059	0.001	0.0999	11.64
0.3999	313.12	0.004	0.400	313.054	0.004	0.3999	19.63
0.7001	313.20	0.005	0.700	313.197	0.005	0.7001	24.36
0.0499	323.27	0.000	0.050	323.143	0.001	0.05	29.89
0.0998	323.09	0.001	0.100	323.220	0.001	0.0999	15.35
0.3998	323.24	0.003	0.400	323.138	0.003	0.3998	21.17
0.6999	323.23	0.005	0.700	323.234	0.004	0.6999	23.84

**P_{Calc} obtained using RK-EOS with regressed parameters*

Table A-7: Measured Absorption and Desorption Data of O_2 in [Bmim][$MeSO_4$]

P_{meas}/MPa	T/K	x_{O2}	P_{meas}/MPa	T/K	x_{O2}	*P_{calc}/MPa	x_{CO2}/x_{O2}
Absorption			Desorption				
0.0495	303.18	0.007	0.0495	303.19	0.007	0.0500	0.70
0.0994	303.15	0.008	0.0996	303.06	0.008	0.0999	1.27
0.3994	303.22	0.012	0.3994	303.11	0.012	0.3989	3.72
0.6995	303.06	0.013	0.6995	303.06	0.013	0.6997	6.37
0.0496	313.30	0.007	0.0495	313.14	0.007	0.0486	1.22
0.0994	313.15	0.007	0.0996	313.06	0.007	0.0973	1.37
0.3995	313.08	0.011	0.3995	313.04	0.011	0.3942	3.51
0.6995	313.15	0.012	0.6995	313.15	0.012	0.7000	6.13
0.0495	323.33	0.006	0.0496	323.14	0.005	0.0496	1.29
0.0993	323.11	0.007	0.0996	323.16	0.007	0.0999	1.09
0.3993	323.20	0.009	0.3996	323.17	0.009	0.3992	4.16
0.6995	323.23	0.010	0.6995	323.23	0.010	0.6995	6.04

**P_{Calc} obtained using RK-EOS with regressed parameters*

Table A-8: Measured Absorption and Desorption Data of O_2 in [Bmim][BF_4]

P_{meas}/MPa	T/K	x_{O2}	P_{meas}/MPa	T/K	x_{O2}	*P_{calc}/MPa	x_{CO2}/x_{O2}
Absorption			Desorption				
0.0498	303.23	0.0010	0.0499	303.17	0.0011	0.0500	23.91
0.0999	303.15	0.0016	0.0999	303.13	0.0016	0.0999	12.51
0.1999	303.23	0.0022	0.1997	303.06	0.0022	0.1999	-
0.3997	303.23	0.0026	0.3996	303.06	0.0026	0.3997	22.50
0.7000	303.13	0.0030	0.7000	303.13	0.0030	0.7000	32.31
0.0499	313.29	0.0003	0.0499	313.14	0.0003	0.0496	43.67

Table A-8 (Contd.): Measured Absorption and Desorption Data of O_2 in [Bmim][BF_4]							
P_{meas}/MPa	T/K	x_{O2}	P_{meas}/MPa	T/K	x_{O2}	*P_{calc}/MPa	x_{CO2}/x_{O2}
Absorption			Desorption				
0.1000	313.14	0.0006	0.0999	313.07	0.0005	0.0979	21.91
0.1999	313.19	0.0009	0.1998	313.07	0.0009	0.1899	-
0.3998	313.14	0.0012	0.4000	313.07	0.0011	0.3512	39.34
0.6999	313.10	0.0015	0.6999	313.10	0.0015	0.5228	53.44
0.0499	323.30	0.0001	0.0497	323.24	0.0000	0.0489	77.30
0.0999	323.19	0.0002	0.0999	323.15	0.0002	0.0958	45.38
0.1999	323.24	0.0005	0.1998	323.24	0.0005	0.1890	-
0.3999	323.19	0.0008	0.3998	323.24	0.0007	0.3850	43.53
0.6999	323.19	0.0010	0.6999	323.19	0.0010	0.7706	66.45

P_{Calc} obtained using RK-EOS with regressed parameters

Table A-9: Henry's Law Constants of CO_2 and O_2 (K_{HCO2} and K_{HO2}) in [MOA][Tf_2N], [Bmim][Tf_2N], [Bmim][$MeSO_4$] and [Bmim][BF_4] Estimated from Absorption Data

T/K	[MOA][Tf_2N]	[Bmim][Tf_2N]	[Bmim][$MeSO_4$]	[Bmim][BF_4]
	K_{HCO2}/MPa			
303.15	3.00	3.71	8.91	5.48
313.15	3.17	4.88	9.67	7.43
323.15	4.03	6.09	12.68	10.64
	K_{HO2}/MPa			
303.15	11.14	35.07	26.63	50.88
313.15	25.23	53.31	28.92	153.13
323.15	67.88	91.08	36.06	434.15

Table A-10: Measured and Modelled Absorption and Desorption Data of CO_2 in MEA:[Bmim][BF_4] at 29.3:70.7 wt%

P_{meas}/MPa	T/K	x_{CO2}	P_{meas}/MPa	T/K	x_{CO2}	*P_{calc}/MPa
Absorption			**Desorption**			
0.0498	303.74	0.142	0.0496	303.18	0.140	0.1125
0.1000	303.18	0.159	0.0996	303.20	0.157	0.1685
0.3999	303.17	0.182	0.3993	303.23	0.182	0.4531
0.6997	303.18	0.200	0.6996	303.21	0.199	0.7362
1.0001	303.20	0.217	0.9995	303.21	0.215	1.0641
1.2998	303.11	0.232	1.2977	303.23	0.228	1.2596
1.5001	303.17	0.242	1.4999	303.18	0.241	1.4053
0.0498	313.16	0.122	0.0499	313.22	0.122	0.1176
0.1000	313.15	0.126	0.0999	313.08	0.126	0.1816
0.3999	313.12	0.142	0.4048	313.25	0.142	0.3894

Table A-10 (Contd.): Measured and Modelled Absorption and Desorption Data of CO_2 in MEA:[Bmim][BF_4] at 29.3:70.7 wt%

P_{meas}/MPa	T/K	x_{CO2}	P_{meas}/MPa	T/K	x_{CO2}	*P_{calc}/MPa
Absorption			**Desorption**			
0.6998	313.11	0.156	0.7144	313.24	0.156	0.6965
1.0001	313.17	0.170	0.9999	313.22	0.170	0.9361
1.3000	313.15	0.184	1.3127	313.25	0.184	1.1369
1.5000	313.12	0.192	1.5003	313.25	0.192	1.3069
0.0498	313.18	0.079	0.0545	323.27	0.079	0.0197
0.0998	323.15	0.087	0.1351	323.22	0.087	0.0463
0.3999	323.11	0.124	0.4489	323.20	0.124	0.4290
0.7000	323.13	0.138	0.6675	323.14	0.138	0.6661
1.0000	323.21	0.151	1.0188	323.24	0.151	1.1265
1.3000	323.23	0.160	1.3150	323.09	0.160	1.2381
1.5001	323.13	0.171	1.4925	323.17	0.171	1.5705

**P_{Calc} obtained using RK-EOS and Posey-Tapperson-Rochelle model with regressed parameters*

Table A-11: Measured and Modelled Absorption and Desorption Data of CO_2 in MEA:DEA:[Bmim][BF_4] at 33:16.2:50.8 wt%

P_{meas}/MPa	T/K	x_{CO2}	P_{meas}/MPa	T/K	x_{CO2}	*P_{calc}/MPa
Absorption			**Desorption**			
0.0498	303.16	0.100	0.0498	303.17	0.100	0.0833
0.1000	303.17	0.104	0.0995	303.18	0.102	0.1472
0.3999	303.20	0.121	0.3991	303.20	0.120	0.3973
0.6999	303.18	0.137	0.6983	303.17	0.133	0.7008
0.9999	303.19	0.153	0.9988	303.16	0.151	1.0652
1.3000	303.17	0.166	1.2999	303.17	0.166	1.3398
1.5001	303.21	0.170	1.4985	303.20	0.170	1.3653
0.0497	313.20	0.100	0.0498	313.15	0.101	0.1107
0.0999	313.10	0.103	0.0999	313.09	0.103	0.1632
0.3999	313.14	0.115	0.3999	313.16	0.114	0.3344
0.6999	313.20	0.131	0.7000	313.14	0.129	0.6877
0.9999	313.11	0.144	0.9999	313.15	0.143	1.0127
1.2999	313.15	0.158	1.3000	313.10	0.158	1.4052
1.4999	313.10	0.162	1.5000	313.13	0.161	1.4535
0.0498	323.14	0.096	0.0498	323.13	0.098	0.0850
0.0999	323.16	0.098	0.0998	323.16	0.101	0.1193
0.3999	323.13	0.112	0.3993	323.12	0.109	0.3439
0.7000	323.16	0.125	0.7000	323.13	0.127	0.6012
0.9999	323.20	0.139	0.9999	323.17	0.141	1.0734
1.2998	323.21	0.149	1.2999	323.12	0.152	1.2938
1.5000	323.15	0.155	1.4999	323.16	0.154	1.4657

**P_{Calc} obtained using RK-EOS and Posey-Tapperson-Rochelle model with regressed parameters*

Table A-12: Measured and Modelled Absorption and Desorption Data of CO_2 in MEA:DEA:[Bmim][BF_4] at 31.8:12.1:56.1 wt%

P_{meas}/MPa	T/K	x_{CO2}	P_{meas}/MPa	T/K	x_{CO2}	*P_{calc}/MPa
Absorption			**Desorption**			
0.0499	303.16	0.210	0.0498	303.21	0.208	0.1157
0.0999	303.19	0.214	0.1000	303.12	0.210	0.1853
0.3999	303.17	0.229	0.3999	303.14	0.225	0.4003
0.6999	303.18	0.245	0.6999	303.17	0.240	0.7090
1.0000	303.14	0.257	0.9999	303.25	0.254	1.0251
1.3000	303.17	0.270	1.2999	303.21	0.267	1.3782
1.5000	303.23	0.273	1.4999	303.20	0.273	1.3842
0.0498	313.07	0.196	0.0497	313.28	0.192	0.1072
0.0999	313.13	0.200	0.1000	313.05	0.203	0.1639
0.3999	313.17	0.219	0.3999	313.23	0.215	0.4194
0.6999	313.15	0.229	0.6999	313.25	0.224	0.7122
1.0000	313.23	0.238	1.0000	313.08	0.234	0.8860
1.3000	313.15	0.248	1.3001	313.11	0.245	1.1213
1.5000	313.21	0.252	1.5000	313.15	0.253	1.2930
0.0498	323.14	0.172	0.0497	323.27	0.168	0.0745
0.0999	323.11	0.174	0.0999	323.22	0.169	0.0975
0.3998	323.13	0.194	0.3999	323.20	0.190	0.3916
0.6999	323.12	0.212	0.6999	323.14	0.208	0.6549
1.0001	323.14	0.226	1.0001	323.24	0.222	0.9096
1.2999	323.18	0.240	1.3000	323.09	0.245	1.3182
1.4999	323.10	0.249	1.5000	323.17	0.250	1.7179

**P_{Calc} obtained using RK-EOS and Posey-Tapperson-Rochelle model with regressed parameters*

Table A-13: Measured and Modelled Absorption and Desorption Data of CO_2 in MEA:MDEA:[Bmim][BF_4] at 31.6:10.4:58 wt%

P_{meas}/MPa	T/K	x_{CO2}	P_{meas}/MPa	T/K	x_{CO2}	*P_{calc}/MPa
Absorption			**Desorption**			
0.0498	303.15	0.187	0.0498	303.18	0.189	0.1902
0.0999	303.15	0.195	0.0998	303.20	0.197	0.2571
0.4000	303.19	0.213	0.3993	303.23	0.216	0.4288
0.6997	303.17	0.233	0.7000	303.21	0.235	0.6489
0.9998	303.25	0.247	0.9999	303.21	0.249	0.9309
1.3000	303.18	0.261	1.2999	303.23	0.261	1.2431
1.5001	303.14	0.272	1.4999	303.18	0.272	1.4478
0.0499	313.16	0.177	0.0499	313.15	0.179	0.2892
0.0999	313.18	0.180	0.0999	313.09	0.183	0.3309
0.3997	313.14	0.199	0.4048	313.16	0.202	0.4535
0.6999	313.15	0.218	0.7144	313.14	0.221	0.7421
1.0001	313.13	0.232	0.9999	313.15	0.231	1.0920
1.2998	313.17	0.249	1.3127	313.10	0.249	1.3510

Table A-13 (Contd.): Measured and Modelled Absorption and Desorption Data of CO_2 in MEA:MDEA:[Bmim][BF_4] at 31.6:10.4:58 wt%

P_{meas}/MPa	T/K	x_{CO2}	P_{meas}/MPa	T/K	x_{CO2}	*P_{calc}/MPa
Absorption			**Desorption**			
1.5001	313.15	0.257	1.5003	313.13	0.257	1.5597
0.0498	323.13	0.143	0.0499	313.27	0.145	0.1978
0.0999	323.16	0.146	0.1000	323.14	0.148	0.2328
0.4000	323.12	0.164	0.4000	323.16	0.166	0.4211
0.6999	323.13	0.181	0.7000	323.25	0.183	0.6226
1.0000	323.17	0.195	1.0000	323.22	0.197	0.9594
1.2999	323.12	0.206	1.3000	323.23	0.206	1.1188
1.5001	323.16	0.216	1.4999	323.10	0.216	1.3285

P_{Calc} obtained using RK-EOS and Posey-Tapperson-Rochelle model with regressed parameters

Table A-14: Measured and Modelled Absorption and Desorption Data of CO_2 in MEA:MDEA:[Bmim][BF_4] at 30.3:21.8:48 wt%

P_{meas}/MPa	T/K	x_{CO2}	P_{meas}/MPa	T/K	x_{CO2}	*P_{calc}/MPa
Absorption			**Desorption**			
0.0498	303.25	0.184	0.0499	303.74	0.186	0.2204
0.0999	303.19	0.192	0.1000	303.18	0.194	0.2773
0.3998	303.17	0.213	0.4000	303.17	0.216	0.4580
0.6999	303.19	0.235	0.7000	303.18	0.238	0.7069
0.9999	303.21	0.253	1.0000	303.20	0.256	0.9809
1.2999	303.24	0.260	1.3000	303.11	0.264	1.0830
1.5001	303.19	0.274	1.4999	303.17	0.277	1.3943
0.0498	313.16	0.141	0.0499	313.07	0.143	0.2024
0.0999	313.17	0.144	0.1000	313.13	0.146	0.2274
0.3999	313.12	0.171	0.4000	313.17	0.173	0.4202
0.6999	313.17	0.194	0.7000	313.15	0.196	0.6578
0.9999	313.15	0.215	0.9998	313.23	0.213	0.9566
1.2999	313.14	0.234	1.3001	313.15	0.237	1.3392
1.5002	313.05	0.249	1.4999	313.21	0.246	1.7603
0.0498	323.13	0.080	0.0498	323.13	0.080	0.1272
0.0999	323.15	0.086	0.0999	323.16	0.087	0.1558
0.3999	323.14	0.124	0.3999	323.12	0.125	0.3631
0.6999	326.53	0.151	0.7000	323.13	0.154	0.7171
0.9992	325.56	0.167	0.9999	323.17	0.170	0.9110
1.3000	320.47	0.195	1.3000	323.12	0.193	1.0656
1.4999	323.07	0.206	1.5000	323.16	0.204	1.4933

P_{Calc} obtained using RK-EOS and Posey-Tapperson-Rochelle model with regressed parameters

Table A-15: Measured and Modelled Absorption and Desorption Data of CO_2 in MEA:DEA:MDEA:[Bmim][BF_4] at 29.8:11.7:12.8:45.7 wt%

P_{meas}/MPa	T/K	x_{CO2}	P_{meas}/MPa	T/K	x_{CO2}	*P_{calc}/MPa
Absorption			**Desorption**			
0.0498	303.19	0.143	0.0498	303.21	0.142	0.1410
0.1000	303.18	0.148	0.1000	303.12	0.147	0.1757
0.3999	303.16	0.172	0.3999	303.14	0.171	0.4329
0.6999	303.18	0.191	0.6997	303.17	0.190	0.7120
0.9999	303.17	0.208	1.0001	303.25	0.205	1.0146
1.2999	303.24	0.219	1.2998	303.21	0.216	1.2066
1.4999	303.20	0.228	1.5001	303.20	0.231	1.3930
0.0498	313.15	0.132	0.0498	313.15	0.132	0.1122
0.0999	313.14	0.140	0.0999	313.09	0.141	0.1626
0.3999	313.16	0.169	0.3999	313.16	0.169	0.5062
0.6998	313.14	0.183	0.6999	313.14	0.182	0.7397
0.9999	313.16	0.197	0.9999	313.15	0.199	1.0174
1.3000	313.18	0.211	1.2999	313.10	0.213	1.3487
1.4995	313.14	0.221	1.5002	313.13	0.221	1.6216
0.0498	323.13	0.115	0.0499	323.23	0.113	0.0640
0.0999	323.13	0.118	0.0999	323.12	0.117	0.0726
0.3999	323.15	0.144	0.3999	323.12	0.145	0.3555
0.6999	323.15	0.166	0.6999	323.11	0.167	0.5417
1.0001	323.15	0.186	1.0000	323.11	0.184	0.9613
1.3000	323.21	0.199	1.3000	323.10	0.202	1.2671
1.5000	323.18	0.207	1.5000	323.10	0.205	1.4935

**P_{Calc} obtained using RK-EOS and Posey-Tapperson-Rochelle model with regressed parameters*

Table A-16: Measured and Modelled Absorption and Desorption Data of CO_2 in MEA:[Bmim][Tf_2N] at 32.8:67.2 wt%

P_{meas}/MPa	T/K	x_{CO2}	P_{meas}/MPa	T/K	x_{CO2}	*P_{calc}/MPa
Absorption			**Desorption**			
0.0498	303.17	0.212	0.0498	303.16	0.210	0.1130
0.0999	303.16	0.219	0.0998	303.19	0.216	0.1647
0.4000	303.24	0.245	0.3999	303.17	0.250	0.4116
0.6999	303.24	0.270	0.7000	303.18	0.267	0.7954
1.0000	303.25	0.293	1.0000	303.14	0.298	1.1177
1.2998	303.17	0.315	1.3000	303.17	0.315	1.2169
1.4997	303.25	0.329	1.5001	303.23	0.329	1.4520
0.0499	313.29	0.187	0.0498	313.34	0.189	0.0991
0.1000	313.19	0.202	0.0999	313.21	0.200	0.1154
0.4000	313.23	0.226	0.3999	313.17	0.222	0.4567
0.7000	313.26	0.238	0.7000	313.24	0.238	0.5647
1.0000	313.23	0.253	0.9999	313.22	0.253	0.9195
1.3000	313.25	0.268	1.3000	313.21	0.272	1.1942

Table A-16 (Contd.): Measured and Modelled Absorption and Desorption Data of CO_2 in MEA:[Bmim][Tf_2N] at 32.8:67.2 wt%

P_{meas}/MPa	T/K	x_{CO2}	P_{meas}/MPa	T/K	x_{CO2}	*P_{calc}/MPa
Absorption			**Desorption**			
1.4999	313.12	0.282	1.5000	313.13	0.282	1.3709
0.0499	323.27	0.175	0.0499	323.14	0.177	0.0617
0.1001	323.14	0.190	0.0999	323.16	0.188	0.1415
0.4000	323.16	0.216	0.3997	323.13	0.220	0.4018
0.7000	323.25	0.239	0.6999	323.16	0.241	0.7326
1.0000	323.22	0.261	1.0001	323.20	0.261	1.1107
1.2999	323.23	0.282	1.2998	323.21	0.285	1.4455
1.5001	323.10	0.296	1.5001	323.15	0.293	1.6102

**P_{Calc} obtained using RK-EOS and Posey-Tapperson-Rochelle model with regressed parameters*

Table A-17: Measured and Modelled Absorption and Desorption Data of CO_2 in MEA:DEA:[Bmim][Tf_2N] at 32.6:21.3:46.2 wt%

P_{meas}/MPa	T/K	x_{CO2}	P_{meas}/MPa	T/K	x_{CO2}	*P_{calc}/MPa
Absorption			**Desorption**			
0.0498	303.18	0.230	0.0498	303.19	0.230	0.1012
0.1000	303.20	0.236	0.0999	303.18	0.239	0.1521
0.3999	303.23	0.244	0.3999	303.16	0.248	0.4885
0.6999	303.21	0.252	0.6999	303.18	0.254	0.6520
0.9999	303.21	0.259	0.9992	303.17	0.262	0.9914
1.3000	303.23	0.266	1.3000	303.24	0.268	1.2365
1.5000	303.18	0.270	1.4999	303.20	0.273	1.3734
0.0497	303.28	0.223	0.0498	313.16	0.225	0.1110
0.1000	313.05	0.227	0.0998	313.17	0.229	0.1807
0.3999	313.23	0.235	0.3993	313.12	0.237	0.4596
0.6999	313.25	0.243	0.7000	313.17	0.245	0.7358
1.0000	313.08	0.252	0.9999	313.15	0.255	1.0462
1.3001	313.11	0.258	1.2999	313.14	0.261	1.3677
1.5000	313.15	0.262	1.4999	313.05	0.265	1.5965
0.0496	313.26	0.206	0.0498	313.27	0.208	0.1063
0.1001	323.12	0.213	0.1000	323.22	0.215	0.1480
0.4000	323.24	0.221	0.3999	323.20	0.223	0.4398
0.6999	323.23	0.228	0.6999	323.14	0.230	0.6149
0.9999	323.22	0.234	0.9999	323.24	0.237	0.9451
1.3000	323.21	0.241	1.2999	323.09	0.243	1.2479
1.5000	323.12	0.246	1.4999	323.17	0.248	1.4474

**P_{Calc} obtained using RK-EOS and Posey-Tapperson-Rochelle model with regressed parameters*

Table A-18: Measured and Modelled Absorption and Desorption Data of CO_2 in MEA:DEA:[Bmim][Tf_2N] at 30.3:10.5:59.2 wt%

P_{meas}/MPa	T/K	x_{CO2}	P_{meas}/MPa	T/K	x_{CO2}	*P_{calc}/MPa
Absorption			**Desorption**			
0.0500	302.31	0.280	0.0500	303.22	0.276	0.1157
0.1001	300.22	0.290	0.1000	303.16	0.285	0.1690
0.3998	303.23	0.316	0.3999	303.18	0.320	0.4549
0.6998	303.10	0.329	0.7000	303.18	0.332	0.7330
0.9999	303.16	0.341	1.0000	303.25	0.341	0.9544
1.2993	303.18	0.352	1.3000	303.20	0.355	1.0946
1.4992	303.14	0.359	1.5000	303.22	0.356	1.4345
0.0500	313.34	0.276	0.0498	313.07	0.281	0.1019
0.1000	313.21	0.281	0.0998	313.13	0.284	0.1661
0.3999	313.17	0.298	0.3993	313.17	0.298	0.3989
0.6999	313.24	0.313	0.7000	313.15	0.316	0.6697
0.9999	313.22	0.326	0.9999	313.23	0.327	1.0118
1.3001	313.21	0.338	1.2999	313.15	0.341	1.4872
1.5000	313.13	0.347	1.4999	313.21	0.344	1.5664
0.0499	323.23	0.270	0.0498	323.13	0.270	0.1625
0.0999	323.12	0.273	0.0999	323.15	0.276	0.2117
0.4000	323.12	0.286	0.4000	323.14	0.286	0.4226
0.6999	323.11	0.295	0.6999	326.53	0.290	0.6435
0.9999	323.11	0.303	1.0000	325.56	0.297	0.8073
1.3001	323.10	0.313	1.2998	320.47	0.318	1.1368
1.5000	323.10	0.320	1.4997	323.07	0.320	1.3568

**P_{Calc} obtained using RK-EOS and Posey-Tapperson-Rochelle model with regressed parameters*

Table A-19: Measured and Modelled Absorption and Desorption Data of CO_2 in MEA:MDEA:[Bmim][Tf_2N] at 29.9:12.6:57.5 wt%

P_{meas}/MPa	T/K	x_{CO2}	P_{meas}/MPa	T/K	x_{CO2}	*P_{calc}/MPa
Absorption			**Desorption**			
0.0499	303.21	0.288	0.0498	303.17	0.291	0.0716
0.0998	303.12	0.300	0.1000	303.16	0.305	0.1672
0.3997	303.14	0.320	0.3999	303.24	0.323	0.4759
0.6992	303.17	0.334	0.6999	303.24	0.339	0.8027
0.9990	303.25	0.342	0.9999	303.25	0.346	1.0064
1.2988	303.21	0.352	1.2999	303.17	0.358	1.1798
1.4983	303.20	0.359	1.4999	303.25	0.359	1.4886
0.0499	313.22	0.274	0.0498	313.15	0.278	0.1209
0.0999	313.08	0.277	0.0999	313.14	0.279	0.1031
0.3999	313.25	0.288	0.3999	313.16	0.293	0.3680
0.6999	313.24	0.298	0.6999	313.14	0.304	0.6319
0.9998	313.22	0.309	0.9992	313.16	0.314	0.8999
1.3001	313.25	0.320	1.3000	313.18	0.324	1.2509

Table A-19 (Contd.): Measured and Modelled Absorption and Desorption Data of CO_2 in MEA:MDEA:[Bmim][Tf_2N] at 29.9:12.6:57.5 wt%

P_{meas}/MPa	T/K	x_{CO2}	P_{meas}/MPa	T/K	x_{CO2}	*P_{calc}/MPa
Absorption			**Desorption**			
1.5000	313.25	0.328	1.4999	313.14	0.333	1.5613
0.0499	323.21	0.255	0.0499	323.14	0.259	0.0958
0.0999	323.16	0.258	0.0999	323.16	0.260	0.1543
0.3998	323.10	0.270	0.4048	323.13	0.273	0.4982
0.6996	323.16	0.276	0.7144	323.16	0.281	0.6097
0.9993	323.16	0.285	0.9999	323.20	0.288	0.8868
1.3001	323.21	0.294	1.3127	323.21	0.298	1.2386
1.5000	323.24	0.300	1.5003	323.15	0.303	1.5482

**P_{Calc} obtained using RK-EOS and Posey-Tapperson-Rochelle model with regressed parameters*

Table A-20: Measured and Modelled Absorption and Desorption Data of CO_2 in MEA:MDEA:[Bmim][Tf_2N] at 30.4:19.3:50.3 wt%

P_{meas}/MPa	T/K	x_{CO2}	P_{meas}/MPa	T/K	x_{CO2}	*P_{calc}/MPa
Absorption			**Desorption**			
0.0498	303.19	0.258	0.0499	303.19	0.260	0.0993
0.0995	303.18	0.272	0.0999	303.18	0.276	0.1512
0.3991	303.17	0.295	0.3999	303.16	0.300	0.4532
0.6983	303.24	0.304	0.6999	303.18	0.307	0.7179
0.9988	303.22	0.312	1.0000	303.17	0.318	1.0608
1.2999	303.25	0.321	1.2998	303.24	0.324	1.1936
1.4985	303.22	0.327	1.5001	303.20	0.333	1.4630
0.0498	313.26	0.236	0.0498	313.34	0.238	0.1186
0.0999	313.17	0.237	0.0999	313.21	0.240	0.1695
0.3999	313.24	0.250	0.4000	313.17	0.254	0.4184
0.7000	313.14	0.266	0.6999	313.24	0.268	0.6064
0.9999	313.18	0.274	1.0000	313.22	0.279	0.8853
1.3000	313.21	0.283	1.2999	313.21	0.286	1.1701
1.5000	313.16	0.290	1.5001	313.13	0.295	1.4160
0.0498	323.25	0.186	0.0498	323.27	0.188	0.0889
0.0998	323.19	0.195	0.0999	323.14	0.197	0.1359
0.3993	323.17	0.216	0.4000	323.16	0.220	0.3143
0.7000	323.21	0.234	0.6999	323.25	0.236	0.5733
0.9999	323.12	0.249	1.0000	323.22	0.254	0.8997
1.2999	323.20	0.264	1.2998	323.23	0.267	1.4040
1.4999	323.17	0.272	1.4997	323.10	0.277	1.6362

**P_{Calc} obtained using RK-EOS and Posey-Tapperson-Rochelle model with regressed parameters*

Table A-21: Measured and Modelled Absorption and Desorption Data of CO_2 in MEA:DEA:MDEA:[Bmim][Tf_2N] at 29.1:10.1:12.5:48.3 wt%

P_{meas}/Mpa	T/K	x_{CO2}	P_{meas}/Mpa	T/K	x_{CO2}	*P_{calc}/MPa
Absorption			**Desorption**			
0.0496	303.09	0.247	0.0499	303.17	0.249	0.1220
0.0996	303.14	0.263	0.1001	303.16	0.260	0.1134
0.3993	303.17	0.277	0.4000	303.24	0.277	0.4439
0.6996	303.25	0.287	0.7000	303.24	0.290	0.7597
0.9995	303.25	0.297	1.0000	303.25	0.300	0.9708
1.2977	303.24	0.307	1.2999	303.17	0.310	1.1332
1.4998	303.24	0.317	1.5001	303.25	0.314	1.5143
0.0499	313.18	0.232	0.0499	313.15	0.232	0.0790
0.0999	313.21	0.241	0.0999	313.14	0.244	0.1578
0.4048	313.24	0.257	0.3999	313.16	0.260	0.4382
0.7144	313.24	0.268	0.6999	313.14	0.265	0.5837
0.9999	313.26	0.280	1.0000	313.16	0.283	0.8936
1.3127	313.19	0.296	1.3000	313.18	0.293	1.2605
1.5003	313.23	0.301	1.5000	313.14	0.304	1.3642
0.0545	313.31	0.215	0.0498	323.14	0.213	0.1331
0.1351	323.15	0.216	0.0998	323.16	0.214	0.1425
0.4489	323.23	0.238	0.3999	323.13	0.240	0.4192
0.6675	323.17	0.254	0.7000	323.16	0.251	0.5931
1.0188	323.24	0.270	1.0000	323.20	0.267	0.8420
1.3150	323.23	0.286	1.3000	323.21	0.288	1.3387
1.4925	323.21	0.295	1.5001	323.15	0.298	1.6263

**P_{Calc} obtained using RK-EOS and Posey-Tapperson-Rochelle model with regressed parameters*

APPENDIX B: PROPERTIES OF IONIC LIQUIDS AND ALKANOLAMINES

Table B-1: Properties of Ionic Liquids

	Molar Mass (g/mol)	T_b (K)	T_C (K)	P_C (bar)	V_C (cm^3/mol)	ω
[Bmim][Tf_2N]	419.37	784.6	1133.41	25.69	956.02	0.3526
[MOA][Tf_2N]	648.85	1190.0	1447.35	10.31	2002.30	1.0096
[Bmim][BF_4]	226.02	391.0	523.25	18.88	645.61	0.6234
[Bmim][$MeSO_4$]	250.32	595.0	877.42	35.51	663.94	0.3913

APPENDIX C: BOUYANCY AND LIQUID MOLE FRACTION CALCULATION

As mentioned in Section 5.7 of Chapter 5 and Section 7.3 of Chapter 7, the weight reading produced by the gravimetric analyser is given by the following equation:

$$W = g[m_s + m_a - m_c + m_I - m_{II} - \rho_f(V_{as} + V_I - V_{II} - V_c)] \quad \text{(E-C1)}$$

Where:

W = weight reading [N],

g = acceleration due to gravity in [$m \cdot s^{-2}$]

ρ_f = density of the absorbing gas [$g \cdot cm^{-3}$].

m_s = dry sample mass[g]

m_a = mass of absorbed gas [g]

m_c = mass of counterweight [g]

m_I = mass of hook and chain on sample side [g]

m_{II} = mass of hook and chain on counterweight side [g]

V_I = volume of hook and chain on sample side [cm^{-1}]

V_{II} = volume of hook and chain on counterweight side [cm^{-1}]

V_C = volume of counterweight [cm^{-1}]

V_{as} = volume of sample and absorbed gas [cm^{-1}]

For systems measured using non absorbing gas such as nitrogen use in this work, the weight reading is expressed in E-C2 below. N_2 gas was used as the non absorbing gas for buoyancy correction.

$$W = g[m_s + m_{a,N2} - m_c + m_I - m_{II} - \rho_{N2}(V_{N2} + V_I - V_{II} - V_c)] \quad \text{(E-C2)}$$

where $m_{a,N2}$ is the mass of absorbed nitrogen. $m_{a,N2}$ = 0 g.

V_{N2} is the volume of sample and absorbed nitrogen.

The data obtained from absorption measurements using nitrogen is available in Tables D-1 to D-3 of Appendix D for pure ionic liquids and for hybrid solvents. The data for pure [Bmim][BF_4] at 303.15 K has been plotted below in Figure C-1 simply for illustration of the buoyancy effect. Another illustration for MEA:[Bmim][Tf_2N] at 32.8:67.2 wt% at 313.15 K can be found in Figure 7-1 in Section 7.3 of Chapter 7.

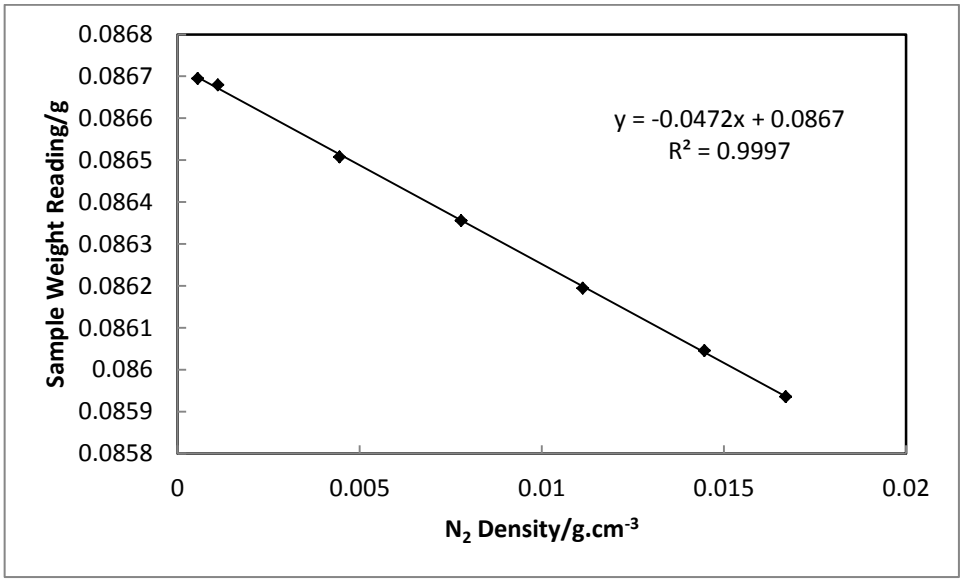

Figure C-1: Bouyancy Measurements using N_2 gas for [Bmim][BF_4] at 303.15 K

Equation (E-C2) may be rearranged to form the following linear equation:

$$\frac{W}{g} = -\rho_{N_2}(V_{N_2} + A) + C \quad \text{.....(E-C3)}$$

Where constants $A = V_I - V_{II} - V_C$ and $C = m_S + m_{a,N_2} - m_C + m_I + m_{II}$

$m_{a,N2}$ = 0 since absorption of N_2 in the solvents studied in this work is negligible.

A plot of weight reading W against nitrogen density ρ_{N_2} such as those shown in Figure C-1 and Figure 7-1 of Chapter 7 was drawn for each system and the gradient of the plot was found in order to obtain V_{N_2}.

It can be assumed that V_{as} from Equation (E-C1) is equal to V_{N2} in Equation (E-C2) (Macedonia et al., 2000). This assumption is theoretically valid in simulating the buoyancy effect on the solvent without absorption actually occurring between N_2 and the solvent. N_2 is negligibly soluble in the samples in this work and possesses a molecular mass more comparable to CO_2 than the use of helium gas, thus increasing the accuracy of the assumption of $V_{as} = V_{N2}$.

Thus, V_{as} is substituted for V_{N2} in Equation (E-C1) to accurately calculate the mass of gas absorbed (m_a) in systems containing CO_2 and O_2.

$$m_a = \frac{W}{g} - m_s + \rho_{CO_2}\left(C + V_{as}\right) \text{.....(E-C4)}$$

Where $V_{as} = V_{N2}$

The equilibrium mole fraction x_{CO2} is found by the following:

$$x_{CO_2} = \frac{\frac{m_a}{MM_{CO_2}}}{\frac{m_a}{MM_{CO_2}} + \frac{m_s}{MM_s}} \text{.....(E-C5)}$$

Where MM_{CO2} and MMs are the molar masses of CO_2 and the solvent respectively. The same calculation was be applied for systems containing O_2.

For hybrid solvents, the moles of each component in the hybrid solvent are calculated since the the composition and mass quantity of each component is predetermined during the combining of the solvent.

APPENDIX D: BOUYANCY DATA FOR ALL ABSORPTION MEASUREMENTS

Table D-1: Bouyancy Data Using Nitrogen Gas for [MOA][Tf_2N] and [Bmim][Tf_2N] Ionic liquids

P/MPa	Weight/g	N_2 Density/g·cm^{-3}	P/MPa	Weight/g	N_2 Density/g·cm^{-3}
	[MOA][Tf_2N]			[Bmim][Tf_2N]	
	303.15 K			303.15 K	
0.0498	0.08463	0.0006	0.0499	0.08338	0.0006
0.1000	0.08461	0.0011	0.1000	0.08336	0.0011
0.4001	0.08444	0.0044	0.4001	0.08326	0.0044
0.7000	0.08426	0.0078	0.6999	0.08316	0.0078
1.0000	0.08409	0.0111	1.0001	0.08305	0.0111
1.2998	0.08392	0.0145	1.2998	0.08295	0.0145
1.5001	0.08381	0.0167	1.5001	0.08288	0.0167
	313.15 K			313.15 K	
0.0499	0.08464	0.0005	0.0499	0.08338	0.0005
0.1000	0.08460	0.0011	0.1000	0.08336	0.0011
0.4000	0.08444	0.0043	0.4000	0.08328	0.0043
0.7000	0.08430	0.0075	0.6999	0.08320	0.0075
1.0000	0.08414	0.0108	1.0000	0.08311	0.0108
1.3001	0.08399	0.0140	1.2996	0.08303	0.0140
1.4998	0.08389	0.0162	1.4999	0.08296	0.0162
	323.15 K			323.15 K	
0.0499	0.08464	0.0005	0.0500	0.08339	0.0005
0.1000	0.08460	0.0010	0.1000	0.08336	0.0010
0.4000	0.08447	0.0042	0.3998	0.08330	0.0042
0.6999	0.08434	0.0073	0.7000	0.08322	0.0073
0.9999	0.08419	0.0104	0.9995	0.08314	0.0104
1.3000	0.08406	0.0136	1.3000	0.08307	0.0136
1.5000	0.08398	0.0156	1.4999	0.08303	0.0156

Table D-2: Bouyancy Data Using Nitrogen Gas for [Bmim][BF_4] and [Bmim][$MeSO_4$] Ionic Liquids

P/MPa	Weight/g	N_2 Density/g·cm^{-3}	P/MPa	Weight/g	N_2 Density/g·cm^{-3}
	[Bmim][BF_4]			[Bmim][$MeSO_4$]	
	303.15 K			303.15 K	
0.0499	0.08669	0.0006	0.0502	0.06918	0.0006
0.0998	0.08668	0.0011	0.1005	0.06916	0.0011
0.3999	0.08651	0.0044	0.4000	0.06904	0.0044
0.6997	0.08636	0.0078	0.7000	0.06894	0.0078
1.0000	0.08619	0.0111	0.9987	0.06883	0.0111
1.2999	0.08605	0.0145	1.3000	0.06871	0.0145
1.5001	0.08594	0.0167	1.5144	0.06862	0.0167

Table D-2: Bouyancy Data Using Nitrogen Gas for [Bmim][BF_4] and [Bmim][$MeSO_4$] Ionic Liquids

P/MPa	Weight/g	N_2 Density/g·cm^{-3}	P/MPa	Weight/g	N_2 Density/g·cm^{-3}
	[Bmim][BF_4]			[Bmim][$MeSO_4$]	
	313.15 K			313.15 K	
0.0502	0.08678	0.0005	0.0502	0.06918	0.0005
0.0998	0.08664	0.0011	0.1009	0.06918	0.0011
0.3999	0.08650	0.0043	0.3999	0.06905	0.0043
0.6999	0.08637	0.0075	0.7004	0.06897	0.0075
0.9998	0.08623	0.0108	0.9999	0.06886	0.0108
1.2994	0.08609	0.0140	1.2999	0.06875	0.0140
1.5000	0.08599	0.0162	1.4999	0.06865	0.0156
	323.15 K			323.15 K	
0.0499	0.08667	0.0005	0.0499	0.06919	0.0005
0.0999	0.08666	0.0010	0.1005	0.06915	0.0010
0.3999	0.08651	0.0042	0.4001	0.06907	0.0042
0.6998	0.08639	0.0073	0.7000	0.06901	0.0073
0.9998	0.08626	0.0104	0.9999	0.06890	0.0104
1.3000	0.08613	0.0136	1.2998	0.06881	0.0136
1.5000	0.08604	0.0156	1.4999	0.06870	0.0156

Table D-3: Bouyancy Data Using Nitrogen Gas for Hybrid Solvents

P/MPa	Weight/g	N_2 Density/g·cm^{-3}	P/MPa	Weight/g	N_2 Density/g·cm^{-3}
MEA:[Bmim][BF_4] at 29.3:70.7 wt%			MEA:DEA:[Bmim][BF_4] at 33:16.2:50.8 wt%		
	303.15 K			303.15 K	
0.1506	0.08026	0.0017	0.1499	0.08780	0.0017
0.1999	0.07967	0.0022	0.2000	0.08719	0.0022
0.3998	0.07958	0.0044	0.4000	0.08706	0.0044
0.6999	0.07942	0.0078	0.7000	0.08687	0.0078
0.9999	0.07925	0.0111	0.9999	0.08667	0.0111
1.3000	0.07907	0.0145	1.3000	0.08646	0.0145
1.5001	0.07895	0.0167	1.5002	0.08631	0.0167
	313.15K			313.15K	
0.1500	0.07661	0.0016	0.1500	0.08450	0.0016
0.1998	0.07583	0.0022	0.2000	0.08379	0.0022
0.3999	0.07573	0.0043	0.4000	0.08367	0.0043
0.6999	0.07558	0.0075	0.6999	0.08349	0.0075
0.9999	0.07540	0.0108	1.0000	0.08329	0.0108
1.3001	0.07523	0.0140	1.3000	0.08309	0.0140
1.5001	0.07510	0.0162	1.5001	0.08294	0.0162
	323.15 K			323.15 K	
0.1503	0.07100	0.0016	0.1500	0.08092	0.0016
0.2000	0.07050	0.0021	0.1998	0.07995	0.0021
0.4000	0.07027	0.0042	0.3999	0.07898	0.0042
0.7000	0.07010	0.0073	0.6999	0.07850	0.0073
0.9999	0.06993	0.0104	0.9999	0.07795	0.0104
1.3001	0.06978	0.0136	1.3000	0.07776	0.0136
1.5001	0.06960	0.0156	1.5001	0.07730	0.0156

Table D-3 (Contd.): Bouyancy Data Using Nitrogen Gas for Hybrid Solvents

P/MPa	Weight/g	N_2 Density/g·cm^{-3}	P/MPa	Weight/g	N_2 Density/g·cm^{-3}
MEA:DEA:[Bmim][BF_4] at 31.8:12.1:56.1 wt%			MEA:MDEA:[Bmim][BF_4] at 31.6:10.4:58 wt%		
	303.15 K			303.15 K	
0.1500	0.08804	0.0017	0.1499	0.08137	0.0017
0.1999	0.08740	0.0022	0.1999	0.08103	0.0022
0.4000	0.08728	0.0044	0.4000	0.08093	0.0044
0.6998	0.08709	0.0078	0.7000	0.08077	0.0078
1.0000	0.08689	0.0111	1.0000	0.08058	0.0111
1.3000	0.08668	0.0145	1.3001	0.08042	0.0145
1.5002	0.08653	0.0167	1.5001	0.08029	0.0167
	313.15K			313.15K	
0.1500	0.08459	0.0016	0.1501	0.08034	0.0016
0.1998	0.08384	0.0022	0.2000	0.07937	0.0022
0.3999	0.08372	0.0043	0.4000	0.07924	0.0043
0.7000	0.08355	0.0075	0.7000	0.07906	0.0075
0.9999	0.08335	0.0108	0.9999	0.07887	0.0108
1.3001	0.08315	0.0140	1.3001	0.07869	0.0140
1.5000	0.08300	0.0162	1.5000	0.07856	0.0162
	323.15 K			323.15 K	
0.1501	0.07822	0.0016	0.1500	0.07248	0.0016
0.1998	0.07728	0.0021	0.1998	0.07060	0.0021
0.4000	0.07717	0.0042	0.4000	0.07034	0.0042
0.7000	0.07626	0.0073	0.6999	0.07020	0.0073
0.9998	0.07608	0.0104	0.9999	0.07002	0.0104
1.2997	0.07590	0.0136	1.3000	0.06983	0.0136
1.4945	0.07574	0.0156	1.4996	0.06967	0.0156

Table D-3 (Contd.): Bouyancy Data Using Nitrogen Gas for Hybrid Solvents

P/MPa	Weight/g	N_2 Density/g·cm^{-3}	P/MPa	Weight/g	N_2 Density/g·cm^{-3}
MEA:MDEA:[Bmim][BF_4] at 30.3:21.8:48 wt%			MEA:DEA:MDEA:[Bmim][BF_4] at 29.8:11.7:12.8:45.7 wt%		
	303.15 K			303.15 K	
0.1499	0.09789	0.0017	0.1499	0.08057	0.0017
0.1999	0.09741	0.0022	0.2000	0.08013	0.0022
0.3998	0.09727	0.0044	0.3999	0.08003	0.0044
0.7000	0.09704	0.0078	0.6999	0.07986	0.0078
0.9999	0.09681	0.0111	1.0000	0.07968	0.0111
1.3000	0.09658	0.0145	1.3001	0.07951	0.0145
1.5000	0.09642	0.0167	1.5001	0.07939	0.0167
	313.15K			313.15K	
0.1499	0.09671	0.0016	0.1501	0.07933	0.0016

Table D-3 (Contd.): Bouyancy Data Using Nitrogen Gas for Hybrid Solvents

P/MPa	Weight/g	N_2 Density/g·cm^{-3}	P/MPa	Weight/g	N_2 Density/g·cm^{-3}
MEA:MDEA:[Bmim][BF_4] at 30.3:21.8:48 wt%			MEA:DEA:MDEA:[Bmim][BF_4] at 29.8:11.7:12.8:45.7 wt%		
0.1999	0.09533	0.0022	0.2003	0.07836	0.0022
0.3999	0.09517	0.0043	0.4001	0.07825	0.0043
0.6999	0.09493	0.0075	0.7000	0.07808	0.0075
1.0000	0.09467	0.0108	0.9999	0.07790	0.0108
1.2998	0.09443	0.0140	1.3000	0.07771	0.0140
1.5001	0.09424	0.0162	1.5001	0.07758	0.0162
	323.15 K			323.15 K	
0.1502	0.09384	0.0016	0.1498	0.07726	0.0016
0.1999	0.09222	0.0021	0.1998	0.07599	0.0021
0.3999	0.09097	0.0042	0.4001	0.07587	0.0042
0.6999	0.09073	0.0073	0.7000	0.07567	0.0073
0.9999	0.09048	0.0104	1.0000	0.07546	0.0104
1.3001	0.09026	0.0136	1.3000	0.07473	0.0136
1.5001	0.09006	0.0156	1.5001	0.07461	0.0156

Table D-3 (Contd.): Bouyancy Data Using Nitrogen Gas for Hybrid Solvents

P/MPa	Weight/g	N_2 Density/g·cm^{-3}	P/MPa	Weight/g	N_2 Density/g·cm^{-3}
MEA:[Bmim][Tf_2N] at 32.8:67.2 wt%			MEA:DEA:[Bmim][Tf_2N] at 32.6:21.3:46.2 wt%		
	303.15 K			303.15 K	
0.1499	0.05993	0.0017	0.1500	0.08641	0.0017
0.1993	0.05984	0.0022	0.1999	0.08589	0.0022
0.3999	0.05978	0.0044	0.4000	0.08578	0.0044
0.6999	0.05955	0.0078	0.7000	0.08562	0.0078
1.0000	0.05922	0.0111	0.9998	0.08545	0.0111
1.2998	0.05902	0.0145	1.3001	0.08527	0.0145
1.5007	0.05895	0.0167	1.4997	0.08514	0.0167
	313.15 K			313.15 K	
0.1500	0.05878	0.0016	0.1499	0.08487	0.0016
0.1999	0.05787	0.0022	0.1999	0.08367	0.0022
0.4000	0.05779	0.0043	0.3998	0.08355	0.0043
0.6999	0.05770	0.0075	0.6999	0.08337	0.0075
1.0000	0.05759	0.0108	0.9999	0.08319	0.0108
1.3000	0.05749	0.0140	1.3001	0.08301	0.0140
1.5000	0.05742	0.0162	1.5000	0.08288	0.0162
	323.15 K			323.15 K	
0.1499	0.05661	0.0016	0.1500	0.08236	0.0016
0.1998	0.05457	0.0021	0.1999	0.08089	0.0021
0.4000	0.05440	0.0042	0.3999	0.07971	0.0042
0.7000	0.05422	0.0073	0.7000	0.07955	0.0073
0.9998	0.05372	0.0104	1.0000	0.07934	0.0104
1.3012	0.05360	0.0140	1.3000	0.07915	0.0136
1.5002	0.05355	0.0156	1.5002	0.07899	0.0156

Table D-3 (Contd.): Bouyancy Data Using Nitrogen Gas for Hybrid Solvents

P/MPa	Weight/g	N_2 Density/g·cm^{-3}	P/MPa	Weight/g	N_2 Density/g·cm^{-3}
MEA:DEA:[Bmim][Tf_2N] at 30.3:10.5:59.2 wt%			MEA:MDEA:[Bmim][Tf_2N] at 29.9:12.6:57.5 wt%		
	303.15 K			303.15 K	
0.1997	0.08308	0.0022	0.1500	0.08559	0.0017
0.3997	0.08306	0.0044	0.2000	0.08561	0.0022
0.6992	0.08298	0.0078	0.3997	0.08557	0.0044
0.9991	0.08286	0.0111	0.7016	0.08547	0.0078
1.2978	0.08273	0.0145	0.9952	0.08534	0.0111
1.5000	0.08263	0.0167	1.3001	0.08519	0.0145
	313.15 K		1.5065	0.08508	0.0167
0.1994	0.07995	0.0022		313.15 K	
0.3995	0.07985	0.0043	0.1500	0.08350	0.0016
0.6998	0.07971	0.0075	0.2000	0.08311	0.0022
0.9986	0.07954	0.0108	0.3998	0.08302	0.0043
1.2997	0.07937	0.0140	0.6999	0.08270	0.0075
1.4987	0.07922	0.0162	0.9999	0.08227	0.0108
	323.15 K		1.2989	0.08211	0.0140
0.1997	0.07647	0.0021	1.4988	0.08199	0.0162
0.3991	0.07536	0.0042		323.15 K	
0.6978	0.07524	0.0073	0.1500	0.06043	0.0016
0.9983	0.07506	0.0104	0.2000	0.06030	0.0021
1.2981	0.07488	0.0136	0.3998	0.06010	0.0042
1.4991	0.07472	0.0156	0.7000	0.06003	0.0073
			0.9994	0.05992	0.0104
			1.2993	0.05961	0.0136
			1.5001	0.05942	0.0156

Table D-3 (Contd.): Bouyancy Data Using Nitrogen Gas for Hybrid Solvents

P/MPa	Weight/g	N_2 Density/g·cm^{-3}	P/MPa	Weight/g	N_2 Density/g·cm^{-3}
MEA:MDEA:[Bmim][Tf_2N] at 30.4:19.3:50.3 wt%			MEA:DEA:MDEA:[Bmim][Tf_2N] at 29.1:10.1:12.5:48.3 wt%		
	303.15 K			303.15 K	
0.1500	0.06972	0.0017	0.1497	0.09030	0.0017
0.2000	0.06906	0.0022	0.1998	0.09019	0.0022
0.3998	0.06898	0.0044	0.3994	0.09010	0.0044
0.6999	0.06887	0.0078	0.7000	0.08996	0.0078
0.9999	0.06874	0.0111	0.9998	0.08980	0.0111
1.2998	0.06860	0.0145	1.2994	0.08963	0.0145
1.4998	0.06849	0.0167	1.4995	0.08950	0.0167
	313.15 K			313.15 K	
0.1499	0.08480	0.0016	0.1498	0.08620	0.0016

Table D-3 (Contd.): Bouyancy Data Using Nitrogen Gas for Hybrid Solvents					
P/MPa	Weight/g	N_2 Density/g·cm^{-3}	P/MPa	Weight/g	N_2 Density/g·cm^{-3}
MEA:MDEA:[Bmim][Tf_2N] at 30.4:19.3:50.3 wt%			MEA:DEA:MDEA:[Bmim][Tf_2N] at 29.1:10.1:12.5:48.3 wt%		
0.2000	0.08457	0.0022	0.1997	0.08612	0.0022
0.3998	0.08451	0.0043	0.3990	0.08600	0.0043
0.7000	0.08440	0.0075	0.6999	0.08585	0.0075
0.9999	0.08427	0.0108	0.9998	0.08568	0.0108
1.3000	0.08414	0.0140	1.2986	0.08551	0.0140
1.4999	0.08404	0.0162	1.4996	0.08538	0.0162
	323.15 K			323.15 K	
0.1499	0.08090	0.0016	0.1497	0.08337	0.0016
0.2000	0.08076	0.0021	0.1998	0.08234	0.0021
0.3999	0.08066	0.0042	0.3999	0.08124	0.0042
0.7000	0.08050	0.0073	0.7000	0.08108	0.0073
0.9995	0.08033	0.0104	0.9991	0.08073	0.0104
1.2985	0.08015	0.0136	1.2994	0.08057	0.0136
1.5000	0.08004	0.0156	1.5000	0.08031	0.0156

APPENDIX E: ENTHALPY AND ENTROPY OF ABSORPTION DATA

Table E-1: Enthalpy and Entropy of Absorption for CO_2 and O_2 in the Ionic Liquids Studied in this Work

	[Bmim][Tf_2N]	[MOA][Tf_2N]	[Bmim][BF_4]	[Bmim][$MeSO_4$]
	$\Delta h/kJ \cdot mol^{-1}$			
CO_2	-13.46 ± 1.8	-10.46 ± 1.8	-14.88 ± 2.9	-18.15 ± 4.46
O_2	-26.80 ± 2.32	-25.53 ± 3.45	-46.46 ± 2.49	-9.25 ± 3.29
	$\Delta S/J \cdot mol^{-1} \cdot K^{-1}$			
CO_2	-45.30 ± 5.74	-34.27 ± 4.96	-42.81 ± 4.89	-47.52 ± 5.47
O_2	-79.12 ± 19.07	-81.80 ± 11.02	-148.26 ± 7.92	-35.62 ± 2.61

Table E-2: Enthalpy and Entropy of Absorption of CO_2 in all Hybrid Solvents

Solvent	$\Delta h/kJ \cdot mol^{-1}$	$\Delta S/J \cdot mol^{-1} \cdot K^{-1}$
[Bmim][BF_4] + MEA at 70.7:29.3 wt%	-14.9 ± 0.4	-48.2 ± 1.8
MEA+DEA+[Bmim][BF_4] at 33:16.2:50.8 wt%	-3.9 ± 0.4	-12.4 ± 1.4
MEA+DEA+[Bmim][BF_4] at 31.8:12.1:56.1 wt%	-5.4 ± 1.1	-17.1 ± 3.6
MEA+MDEA+[Bmim][BF_4] at 31.6:10.4:58 wt%	-9.9 ± 0.6	-31.6 ± 1.8
MEA+MDEA+[Bmim][BF_4] at 30.3:21.8:48 wt%	-15.9 ± 4.5	-50.9 ± 14.4
MEA+DEA+MDEA+[Bmim][BF_4] at 29.8:11.7:12.8:45.7 wt%	-5.1 ± 1.4	-16.4 ± 4.5
[Bmim][Tf_2N] + MEA at 32.8:67.2 wt%	-4.8 ± 0.3	-15.4 ± 1.2
MEA+DEA+[Bmim][Tf_2N] at 32.6:21.3:46.2 wt%	-4.0 ± 0.1	-12.9 ± 0.2
MEA+DEA+[Bmim][Tf_2N] at 30.3:10.5:59.3 wt%	-4.6 ± 0.3	-14.6 ± 0.9
MEA+MDEA+[Bmim][Tf_2N]] at 29.9:12.6:57.5 wt%	-7.3 ± 0.3	-23.4 ± 1.0
MEA+MDEA+[Bmim][Tf_2N] at 30.4:19.3:50.3 wt%	-9.6 ± 2.1	-30.7 ± 6.8
MEA+DEA+MDEA+[Bmim][Tf_2N] at 29.1:10.1:12.5:48.3 wt%	-4.2 ± 1.4	-13.5 ± 4.4

Appendix F: LIQUID PHASE COMPOSITION MEASUREMENT USING A FOURIER TRANSFORM INFRARED PROBE APPARATUS

It was desirable to determine the chemistry and reaction mechanism between CO_2 and undiluted alkanolamines present in the alkanolamine-ionic liquid hybrid solvents, in order to employ more complex and accurate models for regression of measured data. The concentration of intermediate species could theoretically have been obtained.

As mentioned in Chapters 3 and 6, it was proposed to conduct absorption measurements using FTIR spectroscopy on the systems described in Table 6-3 at the prescribed isotherms and gas partial pressures in order to identify and quantify the concentration of intermediate species in the reaction mechanism between CO_2 and the alkanolamine components of each hybrid solvent.

Below is a description of the equipment that was developed and a discussion of preliminary absorption results, including the limitations of the apparatus for the systems investigated in this research.

F1 Apparatus construction and operation

A near infrared (NIR) probe and spectrophotometer was purchased prior to this project and part of this project entailed construction and setup of an apparatus to use the infrared probe to achieve in-situ composition measurement at the desired pressure and temperature for the systems described in Table 6-3. It was desired to obtain accurate P-T-x data of each species in the CO_2-loaded solvent, including different species associated with the reaction mechanisms between CO_2 and primary, secondary, and tertiary alkanolamines as described in reactions R2-4 to 2-12 in Section 2.4.1.1. Figure F-1 below shows a setup of the apparatus.

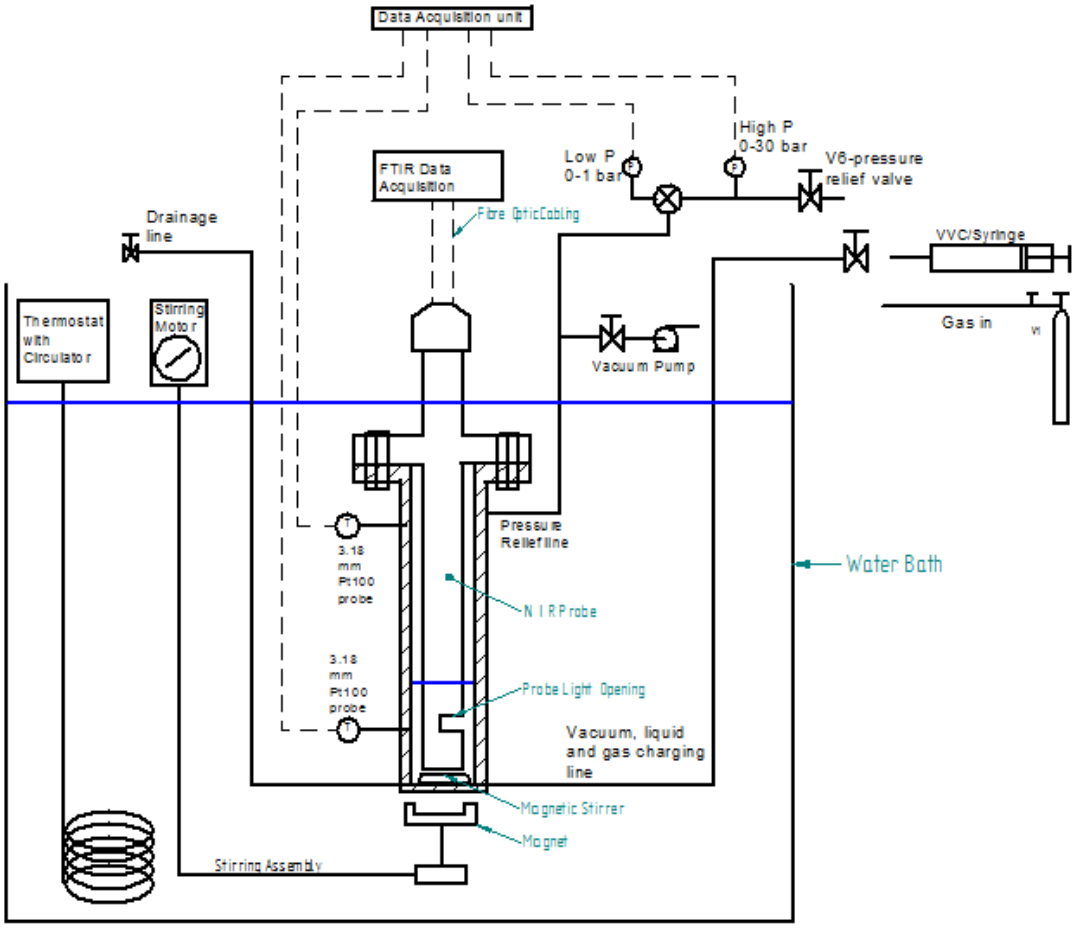

Figure F-1: Fourier Transform Infrared Probe Apparatus

The cell is composed of 316 stainless steel and has a thickness of 8mm on the sides and bottom, with an 18 mm thickness at the top due to the probe construction. The cell has a 42mm internal diameter and is 218 mm in depth internally. A near infrared (NIR) probe is connected and sealed to the cell using rubber gaskets and a flange. The probe is constructed by Hellma Analytical Ltd and is 25mm in diameter. An opening to allow suspension of the solvent is located 25mm from the bottom of the probe.

The probe is connected to a Shimadzu IR Prestige-21 spectrophotometer via fibre optic cabling, which transfers infrared light between the spectrophotometer and the probe. The spectrophotometer is connected to a PC for data display, study, and manipulation of infrared spectra.

The cell has a pressure relief valve which limits the operating pressure of the apparatus to 2.5 MPa, the operating limit of the probe. Two Wika P-10 pressure transmitters are located off a pressure relief line connected towards the top of the cell, one for accurate pressure measurement for a range of 0-2.5 MPa, and one for accurate measurement of vacuum conditions (0-0.1 MPa).

The accuracy of pressure measurement is ±1 kPa for the 0-3 MPa transmitter and ±1 Pa for the 0-0.1 MPa transmitter. The 0-2.5 MPa transmitter recorded gauge pressure. This transmitter was calibrated using Wika 0-1.6 and 0-10 MPa pressure standards. Pressure transmitters were kept in a constant temperature aluminium block environment. Temperature was maintained at 313.15 K using a Chuan HSIN viriac.

An Edwards-3 vacuum pump is also connected to the pressure relief line to establish vacuum in the cell before liquid and gas loading. The vacuum achieved was 0.4 kPa.

Temperature probes are located 35 mm from the bottom and 45 mm from the top of the cell, fixed through the side wall of the cell. Cell temperature was measured using two 3.18 mm Pt100 Wika temperature probes calibrated using a Wika standard. The accuracy in temperature measurement was ±0.1 K, while the temperature differential between the bottom and top of the cell was 0.5 K. Temperature was controlled by submerging the cell in a 500 mm x 400 mm x 400 mm deep water bath containing water as the controlling medium. Temperature was maintained a Grant GR-150 thermostat and circulator. An additional Ebmpapst M2E068 circulator was later installed for quicker circulation. A Polyscience KR-80A cold finger was available for low temperature applications.

Temperature probes and pressure transmitters were connected to an Agilent 34972A data acquisition unit, which was connected to a PC for data recording.

An inlet line is located at the bottom of the cell for liquid and gas loading. Solvents mass was measured using a Mettler Balance and 60 ml of solvent was loaded into the cell using a 70ml syringe, which was adequate to submerge the opening of the NIR probe. Gas loading occurred after liquid loading.

A drainage line is also located at the bottom of the cell to expel solvent under pressure. The solvent was continuously stirred using a magnetic stirrer controlled by a Heidolph RZR 2041 stirrer with stirring mechanism.

For each solvent and gas loading, the cell was first evacuated. Thereafter, a known mass of solvent is introduced into the cell and its IR spectrum was read using the IR probe. Thereafter, CO_2 gas was loaded into the cell, the stirrer was switched on and the apparatus was allowed time to reach equilibrium at specific CO_2 partial pressures and system temperatures. Once equilibrium was established, the IR spectrum was read again to establish the amount of CO_2 absorbed in the solvent.

The experiment could be run on a single solvent charge and multiple gas charges at different pressure. Once the first liquid and gas charge had reached equilibrium and the composition of the solvent is read, more gas could be added into the cell to reach equilibrium at a higher CO_2 partial pressure.

Once all measurements were completed, the cell contents were removed under pressure. The cell was cleaned using distilled water and thereafter acetone, and evacuated for the next measurement.

F2 Absorption analyses attempted using the apparatus

Absorption measurements were attempted using an infrared probe which measured an infrared spectrum exclusively in the Near-Infrared (NIR) region. The infrared spectrum is divided into near, mid and far infrared regions. The far infrared region (wavenumbers below 400 cm^{-1}) detects molecular rotational vibrations, while the mid-infared region (wavenumbers of 400 to 4000 cm^{-1}) detects linear molecular vibrations and rotation. The near infrared region (wavenumbers greater than 4000 cm^{-1}) however, detects only combination bands and overtones, which are secondary vibrations produced by X-H stretching in some molecules.

A consequence of this is that the NIR region could not be used to identify compounds, since the overtones produced by molecules are not unique (Thermo Nicolet, 2001). The use of the NIR region was thus limited to a few types of organic molecules associated mainly with the food and agricultural industry.

Tests using pure CO_2 with no liquid in the cell were initially encouraging. Figure F-2 below shows the absorbance of infrared light through CO_2 at 0.5, 1, and 1.4 MPa.

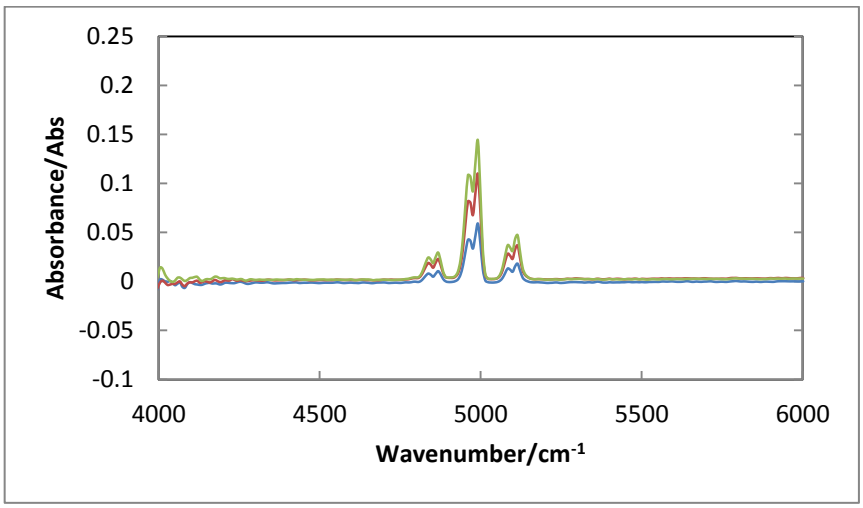

Figure F-2: Absorption Spectra of CO_2 at 0.5 to 1.4 MPa. Blue - 0.5 MPa; Red - 1 MPa; Green - 1.4 MPa.

The absorbance consistently increases with increasing CO_2 pressure, and the spectra could thus be calibrated for pressure. CO_2 overtones were detected by 3 peaks from 4800 to 5130 cm^{-1}.

It was thereafter attempted to calibrate the absorption spectra for measuring CO_2 mole fraction. Spectra were recorded at various partial pressures from 0.1 to 1.4 MPA and at 313.15 and 333.15 K. in an attempt to match the conditions to that of Jou et al. (1994), in order to calibrate the absorption spectra with the CO_2 loading achieved. However, the measurements were unsuccessful. Figure F-3 below shows an absorption spectrum for MEA:H_2O at 30:70 wt%.

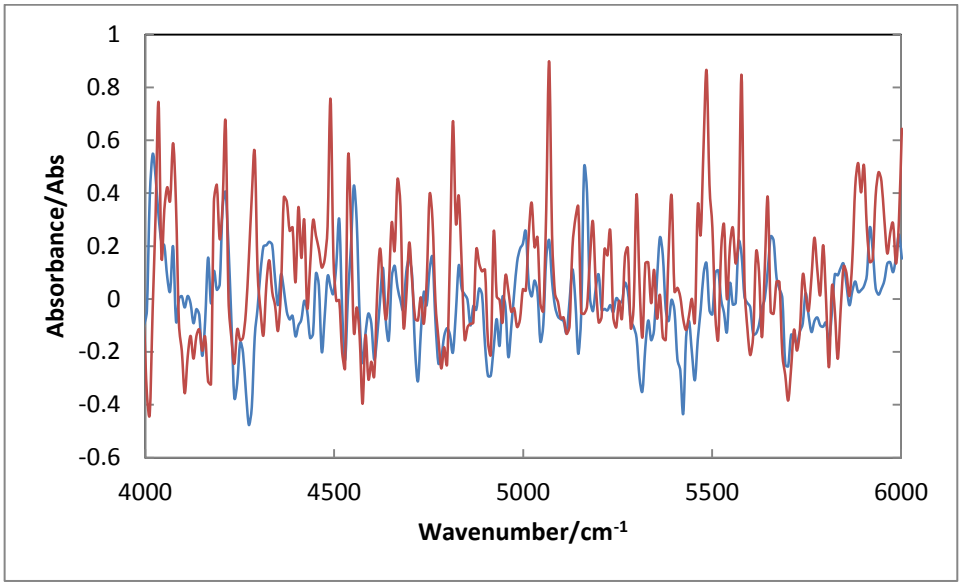

Figure F-3: Absorption Spectra for Unloaded and Loaded MEA:H_2O Solvent at 30:70 wt%. Blue - Unloaded MEA Solvent; Red - MEA Solvent with CO_2 at 0.4 MPa.

As Figure F-3 shows, the spectra suffered from interference and noise. Moreover, the region where CO_2 bands are found was masked by overtones generated by the unloaded solvent itself. Performing a background scan did not help, as shown in the spectrum of MEA loaded with CO_2. Various spectra of this nature taken at different equilibrium conditions showed no consistency or direct correlation with the actual CO_2 loading achieved. Thus, no accurate calibration between spectra and CO_2 loading could be achieved

Moreover, other components associated with reaction mechanism between CO_2 and MEA could not be detected, due to the probe operating only in the NIR region. Lack of overtone and combination band information in the literature also made various peaks unlinked to any particular component or functional group. Thus, the chemistry of chemical absorption could not be ascertained. Different functional groups could not be identified.

While the current setup of the apparatus employing an NIR probe was proven unsuitable for the desired purpose, other configurations and accessories were found using the MIR region. Kock (2013) and Wickee (2013) proposed the use of the MIR region and establishing a circulation loop between the equilibrium cell and the spectrometer, using a high pressure cell with sampling windows and an electric heating jacket to maintain equilibrium temperature conditions (Smiths, 2013). Such configurations have proven successful in the work of Archane et al. (2008). Measurements using an Attenuated total reflectance (ATR) accessory were also successfully applied in the work of Diab et al. (2012), though at more limited pressure conditions. Composition analysis using FTIR spectroscopy has been abundantly achieved using the MIR region. There is abundant data available for comparison and identification of compounds. As mentioned in Chapter 3, Zhao et al. (2011) and Austgen and Rochelle (1991) also successfully utilised FTIR spectroscopy for absorption measurements in the MIR region.

Further investigating into the procurement and application of these configurations are thus recommended.